

## Analysis of ISIS data - how to deal with density - porosity - thickness

at different temperatures and for different deposition times

### Temperature dependent density of ASW

Dohmálek et al. 2003

J. Chem. Phys., Vol. 118, No. 1, 1 January 2003

The deposition of amorphous solid water films

369

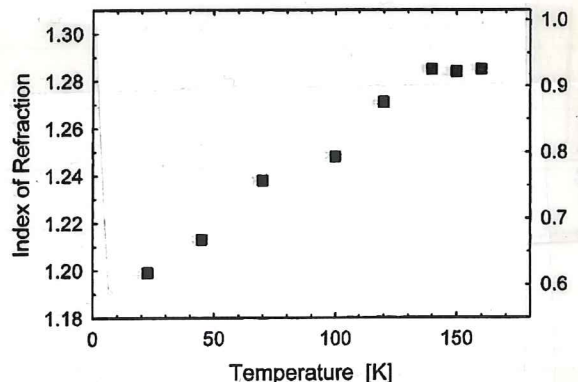


FIG. 8. The index of refraction and density of films deposited from background H<sub>2</sub>O vapor as a function of deposition temperature.

Brown et al. 1996

4994 J. Phys. Chem., Vol. 100, No. 12, 1996

H<sub>2</sub>O condensation coefficient and  
Refractive Index for Vapour-Deposited  
ice from Molecular Beam and  
Optical Interference Measurements

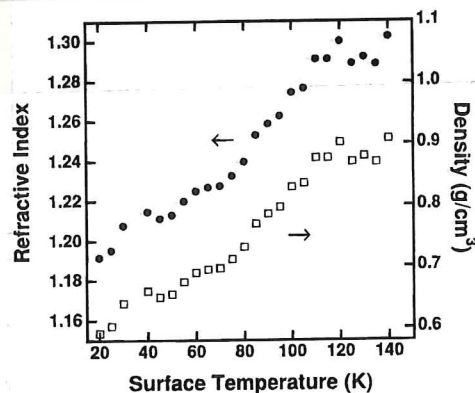


Figure 10. Reevaluation of previous optical interference measurements (ref 1) to determine the refractive index (solid circles) and density (open squares) of vapor-deposited ice versus surface temperature. This reinterpretation assumed  $S = \alpha = 1$  and a refractive index of  $n = 1.27$  and a density of  $\rho = 0.82 \text{ g/cm}^3$  at 90 K.

dense ASW:  $\rho = 0.94 \text{ g/cm}^3$

dense crystalline ice:  $\rho = 0.93 \text{ g/cm}^3$

Both plots show the overall density (including pores),  
NOT the bulk density!

They assume the bulk density to constant for the different temperatures and apparently also for ASW and crystalline ice. From the derived overall densities, they calculate the porosities.

Since the porosity depends a lot on deposition conditions and heating path, I would use a constant density and use the tweak factor in badrun to account for pores.

~~Thickness of the samples: stop 2121 to rejustify~~

We know that at the ~~highest~~ measured temperatures the pores have collapsed  $\rightarrow$  no porosity.

Therefore, we should use a ~~tweak~~ factor of 1 for those samples. We can assume the density to be  $0,93 - 0,94 \text{ g/cm}^3$  ( $\rightarrow$  check which value to use).

Knowing the ~~tweak~~ factor and the density, we can use Badman to determine the thickness of the sample as it was after deposition & heating.

How does thickness change during deposition and heating?

Dohnálek 2003:

$$z = \bar{d} \cdot t$$
$$\bar{d} = \frac{HS \sin \theta}{g N_A}$$

That means,  $z$  is  $\sim \frac{1}{g}$ !

$$\bar{d} = \frac{HS \sin \theta}{N_A} \Rightarrow d = \frac{\bar{d}}{S}$$

$$\Rightarrow z = \frac{\bar{d} \cdot t}{S}$$

$z$ : film thickness

$\bar{d}$ : deposition rate

$t$ : deposition time

$H$ : molecular weight of deposited material

$S$ : condensation coefficient

$J_{\text{in}}$ : molecular beam flux

$\theta$ : angle of incidence of molecular beam

$N_A$ : Avogadro's number

$g$ : overall density

$s_i$ : bulk density

$x$ : tweak factor

The density can be expressed by the Porosity  $\equiv 1 - x$ , bulk density and the tweak factor

$$g = s_i \cdot x \Rightarrow z = \frac{\bar{d} \cdot t}{s_i \cdot x}$$

Assuming a constant deposition rate  $\bar{d}$  (which is probably wrong) and a constant bulk density, we expect the following changes:

Thickness is proportional to deposition time.

Thickness changes during heating because porosity changes.

Problem: How do we determine  $z$  and  $x$  at the same time?

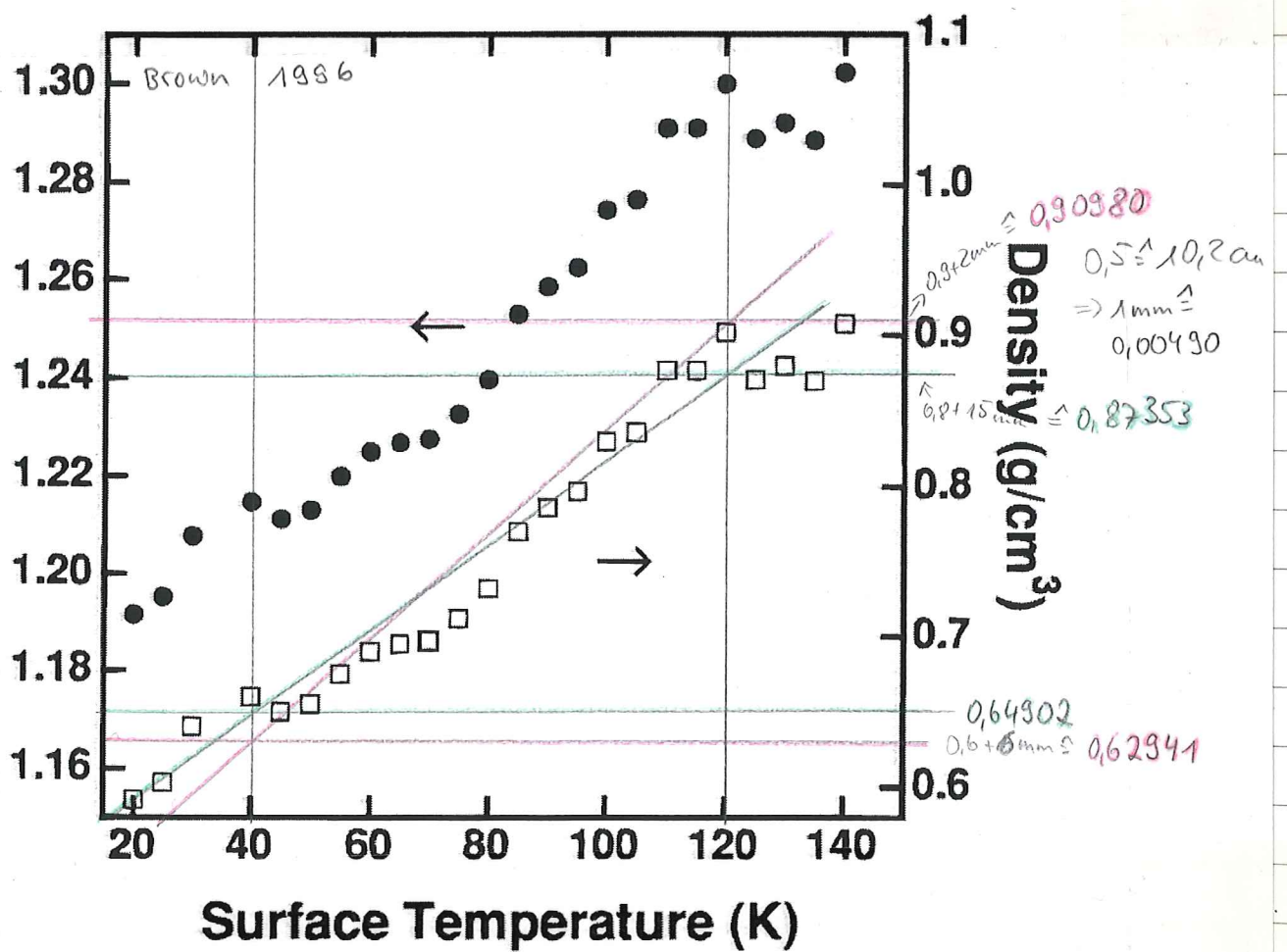
→ Had a chat with Catherine: Basically we can't

Suggestion: Use constant bulk density and adjust weak factor to match porosities stated in literature  
→ work out thickness that way for different  $T$ .

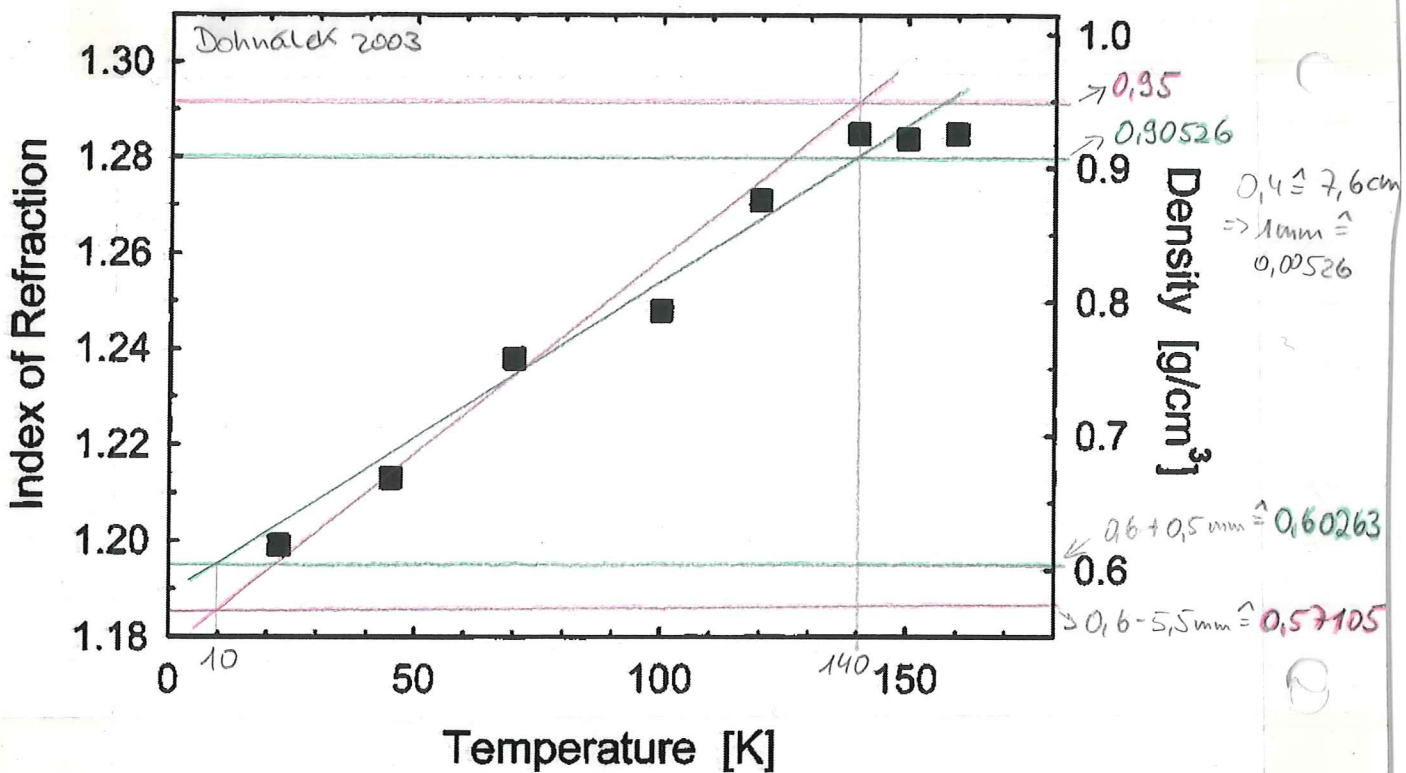
Alternatively, we could do what Catherine did before: keep weak factor at 1 and use literature overall densities instead of bulk densities.

27.07.2015

Refractive Index



$$S(T) = 0,003156 \frac{\text{g}}{\text{cm}^3 \text{K}} \cdot T + 0,51299 \frac{\text{g}}{\text{cm}^3}$$



$$S(T) = 0,002621 \frac{\text{g}}{\text{cm}^3 \text{K}} \cdot T + 0,560625 \frac{\text{g}}{\text{cm}^3}$$

Both averaged lead to :  $S(T) = 0,002889 \frac{\text{g}}{\text{cm}^3 \text{K}} \cdot T + 0,536808$

$$y = a \cdot x + b$$

$$y_1 = ax_1 + b$$

$$y_2 = ax_2 + y_1 - ax_1$$

$$y_2 - y_1 = a(x_2 - x_1)$$

$$\Rightarrow a = \frac{y_2 - y_1}{x_2 - x_1}$$

$$b = \frac{y_1 x_2 - y_1 x_1}{x_2 - x_1} - \frac{y_2 x_1 - y_1 x_1}{x_2 - x_1}$$

$$= \frac{y_1 x_2 - y_2 x_1}{x_2 - x_1}$$

$\hat{C}$  for  $T < 137,8523 \text{ K}$

for higher  $T$ ,  $S = 0,935 \frac{\text{g}}{\text{cm}^3}$   
(average)

$$y = a \cdot x + b$$

$$\Rightarrow x = \frac{y - b}{a}$$

$$y = 0,935$$

$$\Rightarrow x = 137,8523$$

Analysis of ISIS data - how to deal with  
density - porosity - thickness  
at different temperatures and for different  
deposition times

Porosity: determine tweak factor for different temperatures:

$$g = s_i \cdot x$$

$$s: \text{density} \rightarrow s(T)$$

$$\Rightarrow x(T) = \frac{s(T)}{s_i}$$

$$s_i: \text{bulk density} \rightarrow \text{const}$$

$$x: \text{tweak factor} \rightarrow x(T)$$

$$\Rightarrow x(T) = \begin{cases} 0,003089 \frac{1}{K} \cdot T + 0,574126 & , T \leq 137,8523 \\ 1 & , T > 137,8523 \end{cases}$$

28.07.2015

When I analyse the heating data that way, the  
thickness results all go through a maximum  $\rightarrow$  odd

(except the 50K)

18 K deposition		isothermal steps during heating		
file_start	file_end	total_thick	tweak_fact	temperatures
35022	35036	0.005392	0.63	18
35039	35041	0.006717	0.636	20
35049	35051	0.005848	0.667	30
35059	35061	0.007056	0.698	40
35069	35078	0.007324	0.729	50
35086	35095	0.00739	0.759	60
35103	35112	0.007478	0.79	70
35120	35129	0.007516	0.821	80
35137	35146	0.007546	0.852	90
35154	35163	0.007372	0.883	100
35171	35180	0.007173	0.914	110
35188	35197	0.006735	0.945	120
35205	35214	0.006365	0.976	130
35222	35231	0.005823	1	140
35239	35248	0.005206	1	150
35256	35265	0.005165	1	160
35273	35282	0.004482	1	170
35290	35299	0.003415	1	180

30 K deposition      isothermal steps during heating

file_start	file_end	total_thick	tweak_fact	temperatures
35892	35899	0.004717	0.667	30
35907	35919	0.004547	0.698	40
35927	35936	0.005702	0.729	50
35944	35953	0.005507	0.759	60
35961	35970	0.005447	0.79	70
35978	35987	0.005447	0.821	80
35995	36004	0.005387	0.852	90
36012	36021	0.005225	0.883	100
36029	36038	0.005183	0.914	110
36046	36055	0.004945	0.945	120
36063	36072	0.004712	0.976	130
36080	36089	0.004317	1	140
36097	36106	0.003789	1	150

121

39-1

These three samples

should all have

the same

thickness, i.e.

1/2 of the 18K

deposition thickness.

1308

→ works roughly

for 50 and 80

K but not at

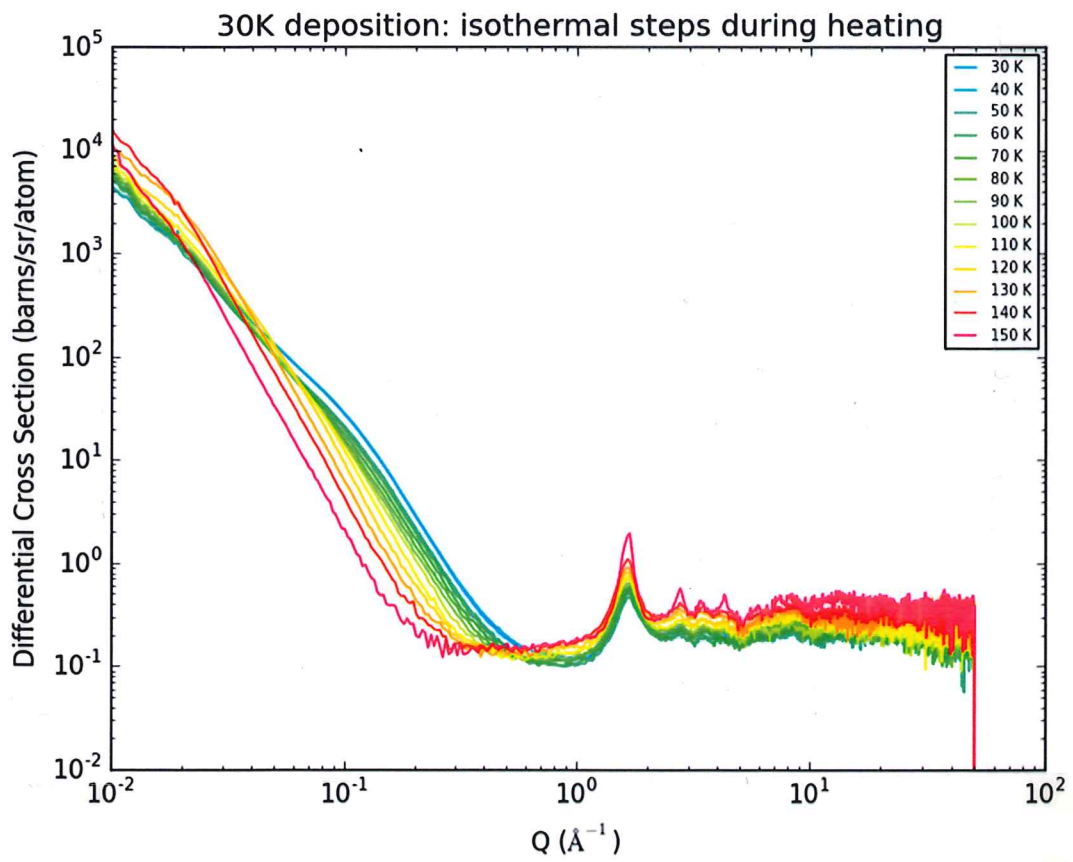
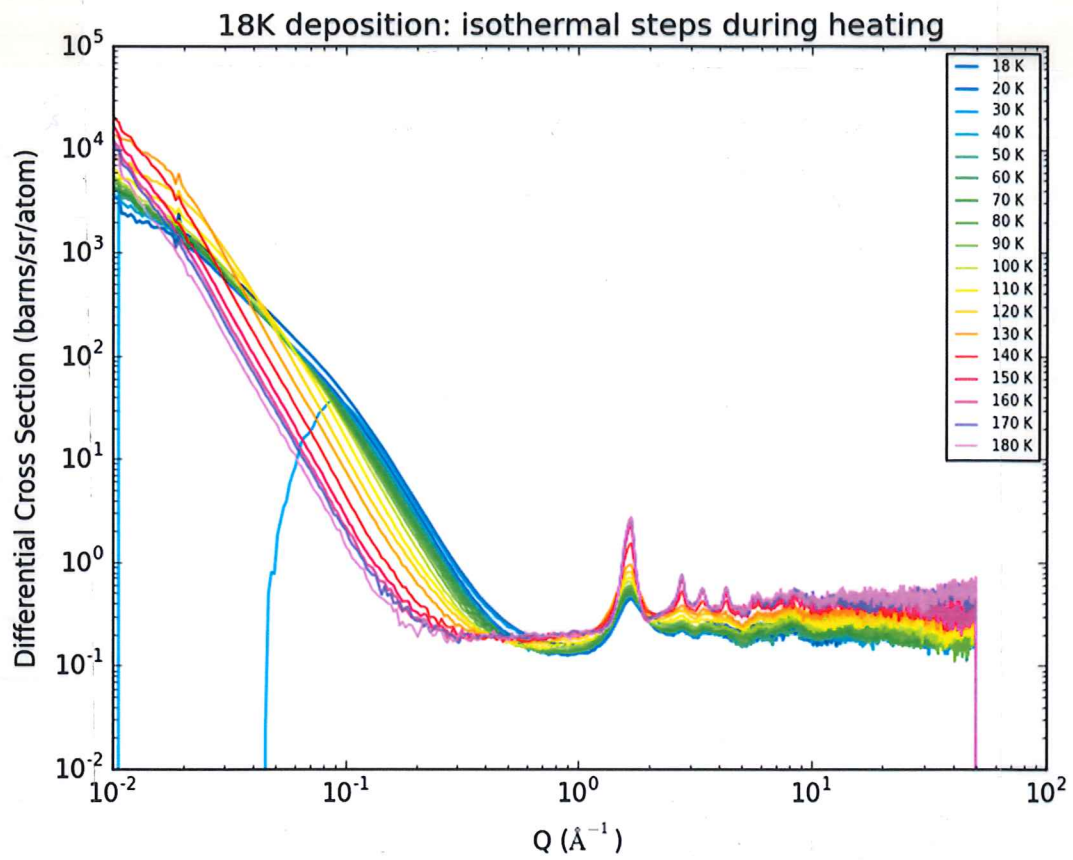
all for 30 K.

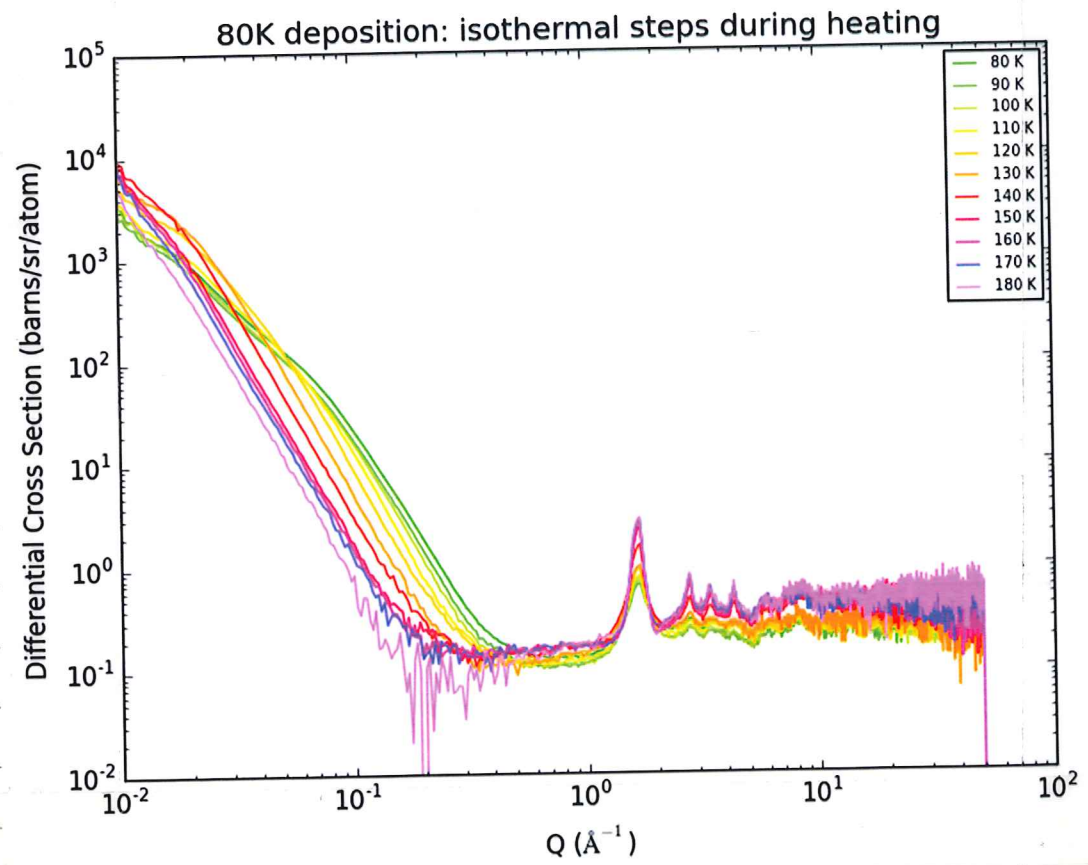
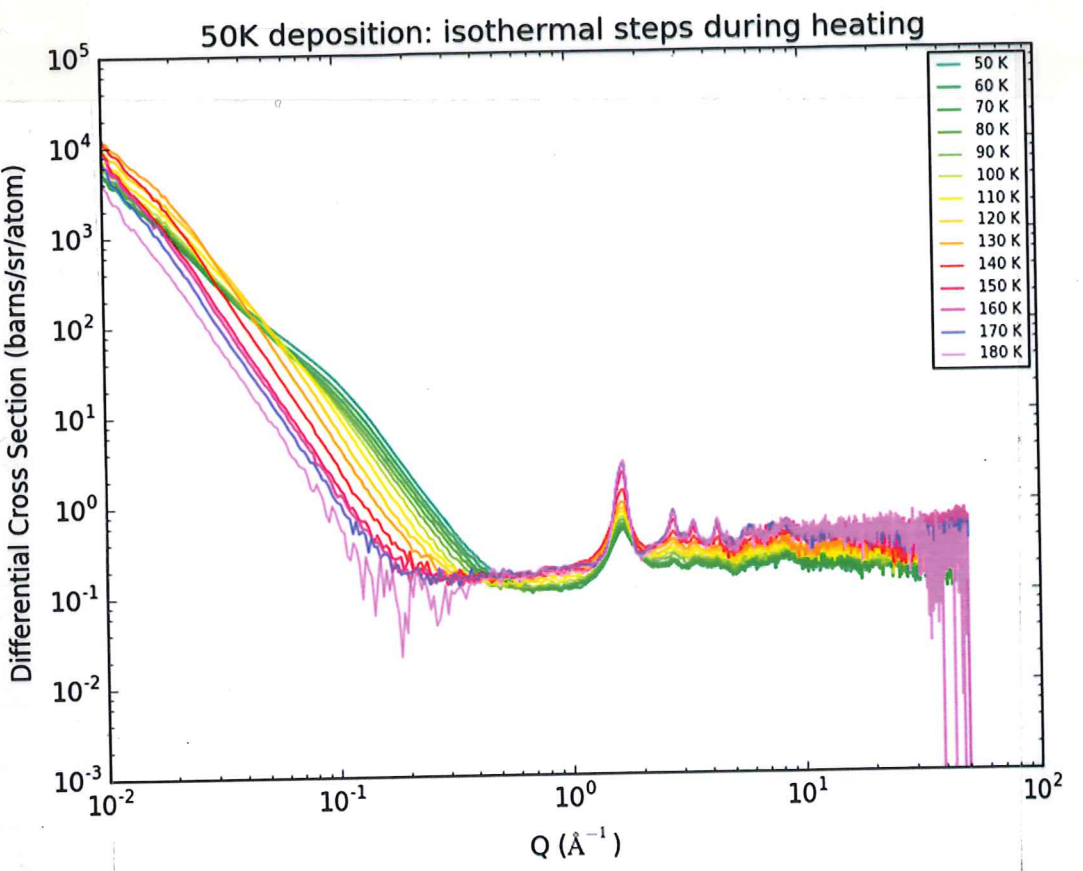
50 K deposition      isothermal steps during heating

file_start	file_end	total_thick	tweak_fact	temperatures
35365	35368	0.005071	0.729	50
35376	35385	0.005496	0.759	60
35393	35402	0.005386	0.79	70
35410	35419	0.005283	0.821	80
35427	35436	0.005156	0.852	90
35444	35453	0.005028	0.883	100
35461	35470	0.004796	0.914	110
35478	35487	0.004619	0.945	120
35495	35504	0.004383	0.976	130
35512	35521	0.00401	1	140
35529	35538	0.003573	1	150
35546	35555	0.003277	1	160
35563	35572	0.003018	1	170
35580	35589	0.001855	1	180

80 K deposition      isothermal steps during heating

file_start	file_end	total_thick	tweak_fact	temperatures
35646	35657	0.004501	0.821	80
35666	35675	0.005521	0.852	90
35683	35692	0.005471	0.883	100
35700	35709	0.005334	0.914	110
35717	35726	0.004816	0.945	120
35734	35743	0.004975	0.976	130
35751	35760	0.003962	1	140
35768	35777	0.003595	1	150
35785	35794	0.003386	1	160
35802	35811	0.002837	1	170
35819	35828	0.0017	1	180





## PDRA Meeting

ISIS Dec. analysis:

✓ concentrate on good blue and red

maybe also quick scattering paper from long run.

assign peaks in high-Q-range

→ work out fraction of hexagonal/cubic ice

→ paper Salzmann UCL PCCP 2012/13

coexistence of both crystalline forms

✓ Tom and Tristan will do direct broad analysis

→ ask them about that (different angle defector banks)

✓ Porod analysis on slope in Pow-Q

→ SSA,  $\alpha$ -factor,  $\beta$  (surface roughness)

$s$ -factor (Porod constant → spherical grains)

as function of T

start with isothermal data ( $1/2$  h averages)

(maybe later also the heating data)

✓ Kinetic experiment: time dependent analysis

(Porod, 1h averages)

22.12.2015

Comments:  $s$ -parameter (for shape) and  $\alpha$ -parameter

(for surface roughness) can only be determined

for pores (from Scimier-Porod analysis)

I assume this  $\alpha$ -parameter is the  $\beta$  from above.

need to find out what  $\alpha$ -factor is.

↪  $\alpha$ -parameter is  $\beta$  (→ porod slope)

05.01.2016

→ run separate fit to determine actual slope

(Porod analysis assume it to be  $\alpha^4$ )

→ tells about surface roughness

06.01.2016

## topics for tomorrow's meeting:

### -Presentation-topics at upcoming meetings:

#### \* 22.01: UKPF early career

talk or poster: collision stuff "if time allows I'll talk about ISIS stuff"

#### \* 01.-02.02.: Water in the inner solar system

poster only (missed deadline) : Dec ISIS staff talk to Nakic about poster company

#### \* 09.-09.03: Duisburg, Planet formation

talk or poster: collision and ISIS dec send abstract comet (to all co-authors before hand)

### -data analysis:

#### \* cold dust: look at modified COR plots

look at mixed out come analysis (notebook)

#### \* ISIS dec: look at plots so far

how to tell surface roughness from  $\beta$

does my fit routine for  $\beta$  / Porod-const. make sense?

how to calculate useful uncertainties for  $\beta$  yes

### - Calendar staff:

#### \* schedule next ISIS runs

#### \* any other facility runs?

#### \* working from home in may?

$$\beta = 2 + \frac{1}{h}, \text{ roughness exponent } h$$

$h=0 \rightarrow$  very rough,  $h=1 \rightarrow$  very smooth

$h=\frac{1}{2}$  (Porod case)  $\rightarrow$  random walk fluctuations

$\hookrightarrow$  what does that mean?

## PDR A Meeting

ISIS dec:

✓ peak assignment: ask for meeting with Daniel to do it

cubic - hexagonal phase transition  $\approx 180-200\text{ K}$

{ d-spacings: separates out cubic and hexagonal paper by Saltzmann<sup>(UCL)</sup> on coexistence of both phases  
gffs-filters: O-H, H-H, O-O bond distances

→ any stress or strain in the lattice

✓ directionality: Heller will look for Tom's email on that.

✓ check Endrun user manual

✓ Sample 2: check all the scans beyond 250

for melting effects. (liquid layers)

Search literature for liquid water spectrum

✓ individual scans: throw out all data that has

less than 3 min → see how much is left

check outliers, maybe tweak factor went stupid  
or something like that

✓ SSA: 0 → box indicating our detection limit

(from error bars)

✓ mid Q-range: ask Daniel why signal increases with temperature

✓ SSA: make estimate of expected SSA from particle size and filling factor

tweak factor: maybe phase change also changes density  
→ wrong tweak factors.

✓ surface roughness : do this on individual scars as well

compared red and blue: is loss of crystalline phases different  
(to explain difference in  $\lambda/\beta$ )

✓ kinetic experiment: work out time constant

11.01.2016

Topics for next meeting:

~~3 min presentation at Department Research Day~~  
~~talk title~~ (I'll be at ISIS)

✓ go to ISIS for data analysis discussion:  
(26<sup>th</sup> to 29<sup>th</sup> Jan) 27<sup>th</sup>

✓ Astrodrum board game? Maybe online printable version  
Ask Andrew Norton and Joe what they think about it.  
email Averil Macdonald about amount of money  
and who has to submit proposal

Find out who is IP officer at OU to find out who has  
which IP on current game

Maybe Natalia

✓ 60s adventures: print start certificate from AMS for signature

14.01.2015

## PDR A Meeting

ISIS dec analysis:

✓ tweak factor: fit temp dependence only  
(no time dependence)

✓ make summary PDF for Sunday:  
bullet points on differences we see  
questions we have, ...

topics for tomorrow's meeting:

10.02.2015

- Parabolic flight proposal

- data analysis:

\* cold dust: look at modified COR plots  
look at mixed outcome analysis  
(notebook)

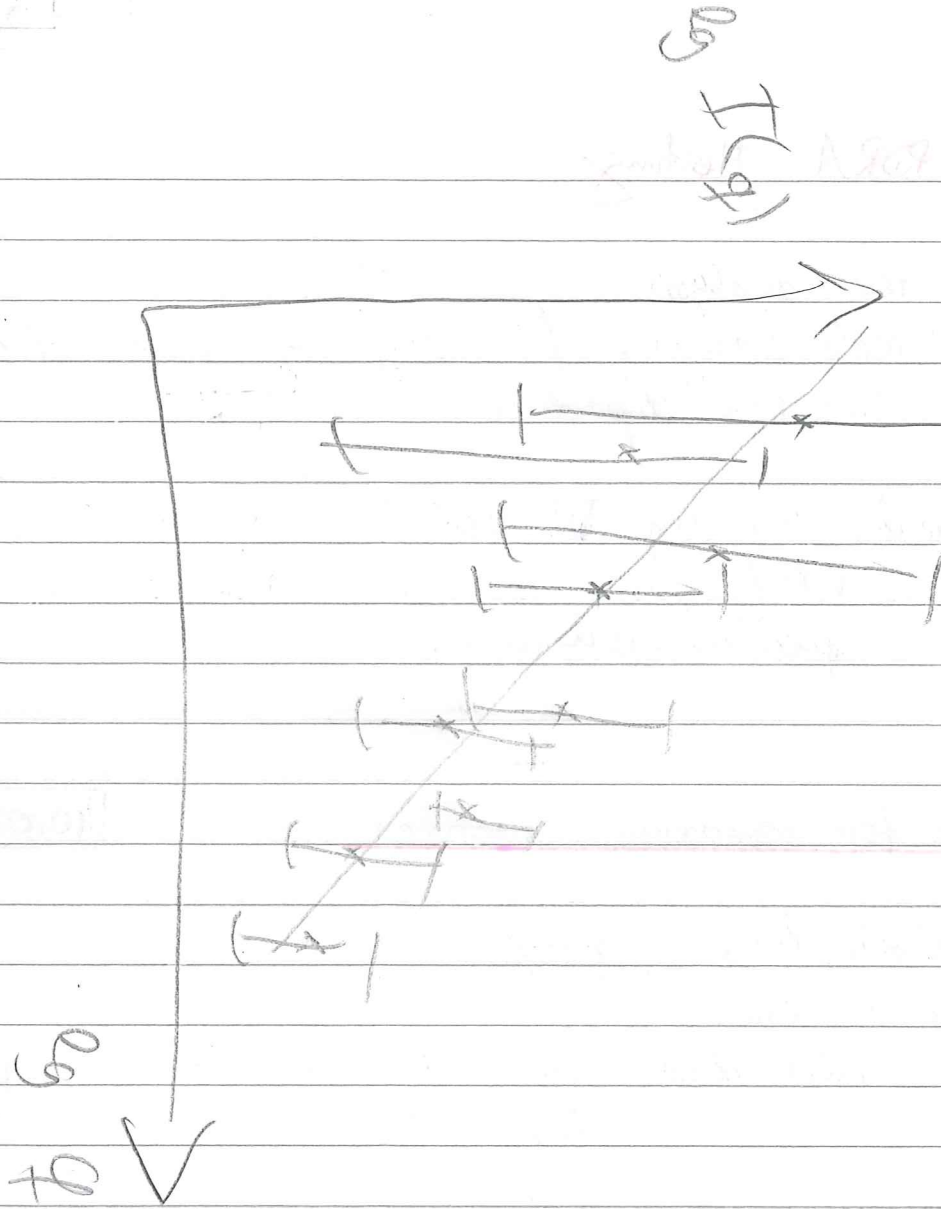
\* ISIS Dec: • tweak factor: 1 h averages scatter  
• background shift in mint filters as well  
• how to do uncertainties for  $\beta$ ?  
• fit-limits for  $\beta$ ? (model dependent)

- Conference: DPS in Pasadena (16.-21.10.2016)?  
papers more important  $\rightarrow$  no for now

11.02.2015

ISIS analysis: • use constant tweak factor for  
final analysis

- send background plot to ISIS people (mint)
- try weighted fit  $\rightarrow$  should include data  
uncertainties for uncertainties of fit parameters
- manually fit stupid data sets



maybe they can arrange for me  
 → to have half a day with  
 SANS people and discuss what I did

- $\beta$ -range  $\rightarrow$  ask ISIS people  
 look for book on Helen's shelf or papers on  
 glass / soft condensed matter
- fit range for  $\beta$ -fit  $\rightarrow$  plot numbers of range  
 borders vs temperature (maybe Porod region  
 is moving) do same for Porod range

Collisions: split data up for papers binary first  
 papers multiple comparison with warm  
 second paper (warm only qualitatively)

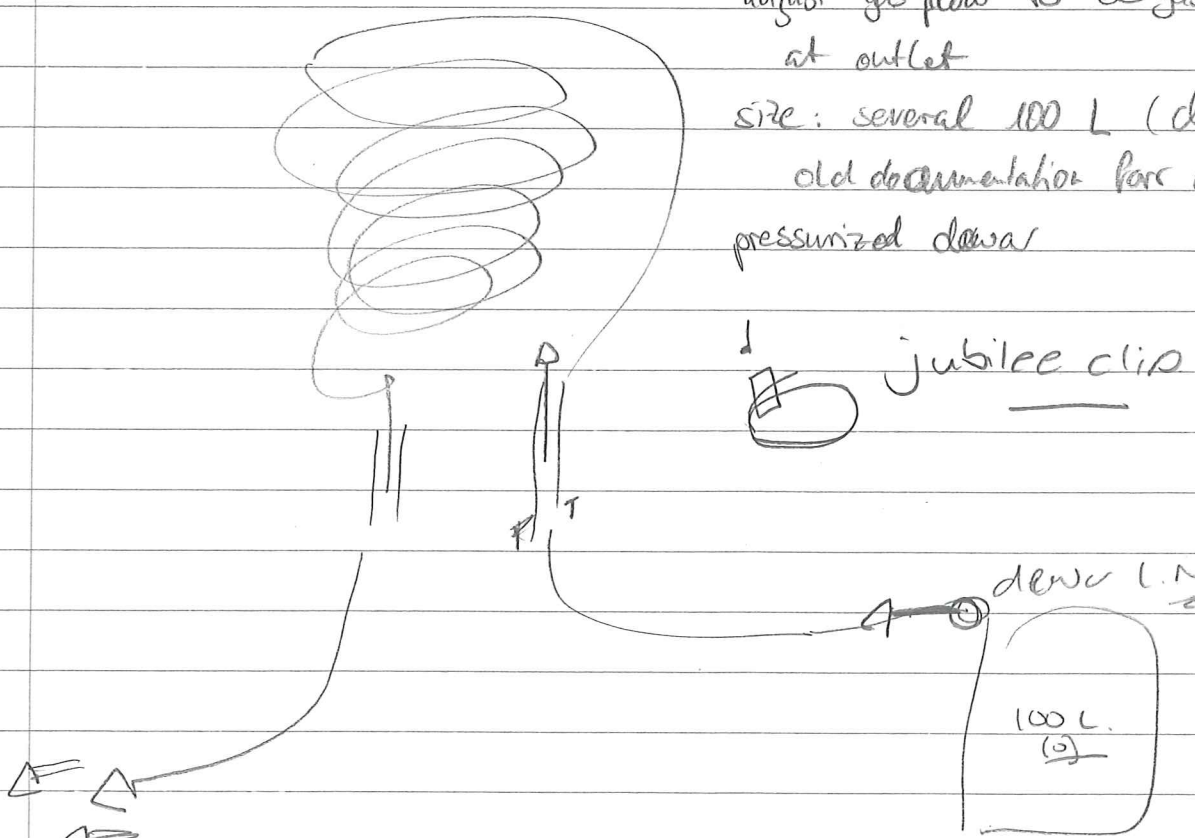
## PDRA Meeting

topics for next meeting:

- ISIS<sup>dec</sup> data: - new bump in latest sample 4 plots
  - ↳ Tristan says: bad statistics, use molcs files
  - crystalline peak intensities → don't match theory
  
- PF experiment:
  - how to use cooling time?
  - which freezer can I use?
  - EPOS specifications      ↳ fill container
  - What size and type of dewar do we need (pressurized)?

adjust gas flow to be gaseous at outlet

size: several 100 L (check old documentation for order pressurized dewar)



3.3.

arrange meeting with everyone at ISIS on thursday ( )

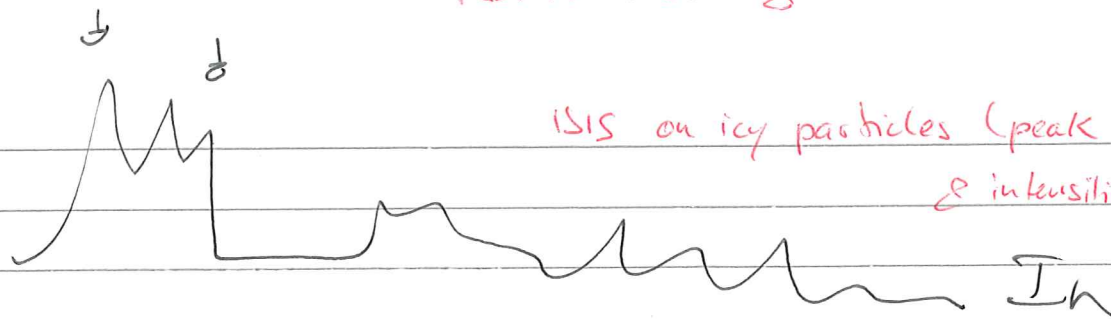
ISIS data: when we're coasting cubic ice, we're  
not gaining hexagonal ice

fit all intensities

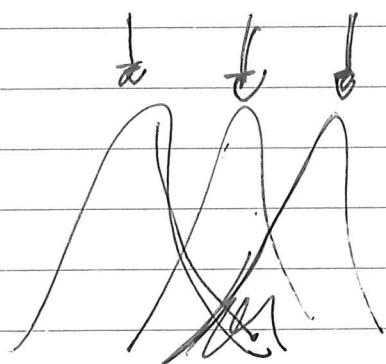
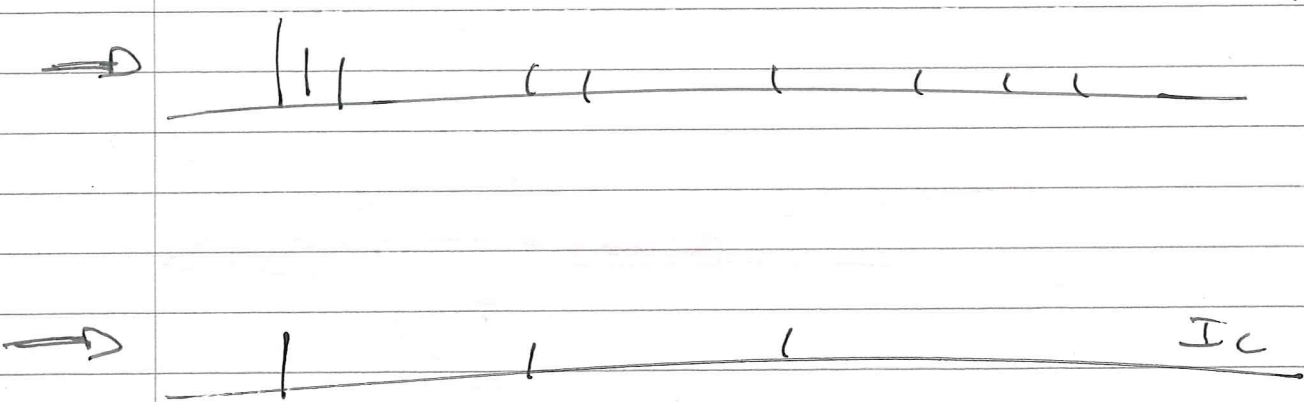
look at error bars

plot 250 points

03.03.2016

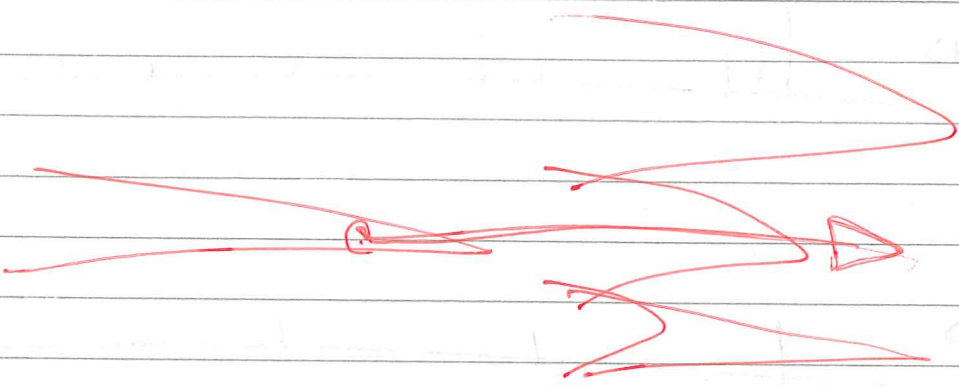


ISIS on icy particles (peak positions  
& intensities)



2.1                    0.65°  
1.8                    1.65°                    0.75°

0.5°



# Data analysis ASW ISIS (June '15 + April '16)

## Guinier-Porod-Analysis:

(from : [www.ncnr.nist.gov/summerschool/ss06/SANS\\_and\\_USANS\\_Analysis.pdf](http://www.ncnr.nist.gov/summerschool/ss06/SANS_and_USANS_Analysis.pdf))

$$I(Q) \approx I(0) \cdot e^{-\frac{1}{3} R_g^2 Q^2} \quad (\text{Guinier Approximation})$$

(from Catherine's python script)

$$I(Q) = \begin{cases} G \cdot Q^s \cdot e^{-\frac{Q^2 R_g^2}{3-s}} & , Q \leq \frac{1}{R_g} \cdot \sqrt{\frac{(d-s)(3-s)}{2}} \\ A \cdot Q^{-d} & , Q > \frac{1}{R_g} \cdot \sqrt{\frac{(d-s)(3-s)}{2}} \end{cases}$$

$$[ d \stackrel{\wedge}{=} \beta ]$$

$$\frac{1}{R_g} \cdot \sqrt{\frac{(d-s)(3-s)}{2}}$$

must be the bump position, i.e.  
 $\overline{z''}$   
 periodic spacing

(from : [www.ncnr.nist.gov/staff/hammonda/publications/2010hammonda-j-app-cryst.pdf](http://www.ncnr.nist.gov/staff/hammonda/publications/2010hammonda-j-app-cryst.pdf))

spheres:

$$I(Q) = \begin{cases} G \cdot e^{-\frac{Q^2 R_g^2}{3}} & , Q \leq \frac{1}{R_g} \cdot \sqrt{\frac{3d}{2}} \\ D \cdot Q^{-d} & , Q > \frac{1}{R_g} \cdot \sqrt{\frac{3d}{2}} \end{cases}$$

general model: same equation as Catherine used

⇒ See notes in PDRA meeting (05.05.2016)

22.07.2016

Estimate SSA for compact sample

(See Estimate-Ice Amount From Deposition\_Gas\_Flow.xls)

If we had deposited all gas used from the bottles (i.e. ignore pumps) we would expect

$$\text{SSA} \approx 0.2 \frac{\text{m}^2}{\text{cm}^3}$$

(ignoring ice-vanadium interfaces)

For sample 1 (40K deposition) we observe at 40K:  $\text{SSA} \approx 170 \frac{\text{m}^2}{\text{cm}^3}$

Guinier-Porod analysis

Idea: for low T ( $\leq 120\text{K}$ ) use double Guinier-Porod:

Note: this definition does not reproduce two-bump structure

$$I(Q) = \begin{cases} G_1 \cdot Q^{-s_1} \cdot e^{-\frac{Q^2 \cdot R_g^2}{3-s_1}} & , Q \leq Q_1 \\ G_2 \cdot Q^{-s_2} \cdot e^{-\frac{Q^2 \cdot R_g^2}{3-s_2}} & , Q_1 < Q \leq Q_2 \\ A \cdot Q^{-d} & , Q_2 < Q \end{cases}$$

$$Q_2 = \frac{1}{R_g} \cdot \sqrt{\frac{(d-s_2) \cdot (3-s_2)}{2}}, Q_1 = ?$$

Function and first derivative must be continuous at  $Q_1$  and  $Q_2$ :

$$\frac{d}{dQ} \left( G \cdot Q^{-s} \cdot e^{-\frac{Q^2 \cdot R_g^2}{3-s}} \right) = G \cdot \left( -s \cdot Q^{-(s+1)} \cdot e^{-\frac{Q^2 \cdot R_g^2}{3-s}} + Q^{-s} \cdot \left( -\frac{2Q \cdot R_g^2}{3-s} \right) \cdot e^{-\frac{Q^2 \cdot R_g^2}{3-s}} \right)$$

$$= G \cdot Q^{-s} \cdot e^{-\frac{Q^2 \cdot R_g^2}{3-s}} \cdot \left( -s \cdot Q^{-1} - 2 \frac{Q \cdot R_g^2}{3-s} \right)$$

$$\frac{d}{dQ} (A \cdot Q^{-d}) = -Ad \cdot Q^{-(d+1)}$$

Continue with ISIS ASW analysis (June '15 + April '16)

confirm definition of  $Q_2$ :

$$G_2 \cdot Q_2^{-s_2} \cdot e^{-\frac{Q_2^2 \cdot R_{g2}^2}{3-s_2}} \stackrel{(1)}{=} A \cdot Q_2^{-d} \wedge \text{Ad}Q = G_2 Q_2^{-s_2} \cdot e^{-\frac{d-1}{3-s_2} \cdot (s_2 Q_2^{-1} + 2 \frac{Q_2^2 R_{g2}^2}{3-s_2})}$$

$$\stackrel{(2)}{\Rightarrow} \text{Ad}Q_2^{-d-1} = A Q_2^{-d} \cdot (s_2 Q_2^{-1} + 2 \frac{Q_2^2 R_{g2}^2}{3-s_2}) \quad | \cdot Q/A^{d+1}$$

$$\Rightarrow d = Q_2 \cdot (s_2 Q_2^{-1} + 2 \frac{Q_2^2 R_{g2}^2}{3-s_2}) = s_2 + 2 \frac{R_{g2}^2}{3-s_2} Q_2^2$$

$$\Rightarrow Q_2^2 = \frac{(d-s_2)(3-s_2)}{2 R_{g2}^2} \Rightarrow Q_2 = \frac{1}{R_{g2}} \cdot \sqrt{\frac{(d-s_2)(3-s_2)}{2}}$$

Actually, now  $A$  could be derived as well.

q.read

For some reason this is fitted separately  $\rightarrow$  strange, violates continuity of  $I(Q)$

derive  $Q_1$ :

$$G_2 Q_1^{-s_2} \cdot e^{-\frac{Q_1^2 R_{g1}^2}{3-s_2}} \stackrel{(1)}{=} G_1 Q_1^{-s_1} \cdot e^{-\frac{Q_1^2 R_{g1}^2}{3-s_1}} \wedge G_2 Q_1^{-s_2} \cdot e^{-\frac{Q_1^2 R_{g1}^2}{3-s_2}} \cdot (s_2 Q_1^{-1} + 2 \frac{Q_1^2 R_{g1}^2}{3-s_2}) \stackrel{(2)}{=} G_1 Q_1^{-s_1} \cdot e^{-\frac{Q_1^2 R_{g1}^2}{3-s_1}} \cdot (s_1 Q_1^{-1} + 2 \frac{Q_1^2 R_{g1}^2}{3-s_1})$$

$$\stackrel{(1)}{\Rightarrow} s_2 Q_1^{-1} + 2 \frac{Q_1^2 R_{g1}^2}{3-s_2} = s_1 Q_1^{-1} + 2 \frac{Q_1^2 R_{g1}^2}{3-s_1} \quad | \cdot Q_1$$

$$\Rightarrow Q_1^2 \left( \frac{2 R_{g1}^2}{3-s_2} - \frac{2 R_{g1}^2}{3-s_1} \right) = s_1 - s_2$$

$$\Rightarrow Q_1^2 \left( \frac{(3-s_1) R_{g1}^2 - (3-s_2) R_{g1}^2}{(3-s_2)(3-s_1)} \right) = \frac{s_1 - s_2}{2}$$

$$\Rightarrow Q_1 = \sqrt{\frac{s_1 - s_2}{2} \cdot \frac{(3-s_1)(3-s_2)}{(3-s_1) R_{g1}^2 - (3-s_2) R_{g1}^2}}$$

**⚠** The fit routine often returns functions that are not continuous  $\rightarrow$  that doesn't make sense  
 $\Rightarrow$  calculate  $A \leftrightarrow G_1 \leftrightarrow G_2$  relations as well.

$$\Rightarrow Q_1 = \frac{3-s_1}{2\sqrt{2}} \frac{Rg_2}{Rg_1^2} \frac{d}{\sqrt{(d-s_2)(3-s_2)}} + \left[ \frac{(3-s_1)^2 Rg_2^2 d^2}{4 \cdot 2 Rg_1^4 (d-s_2)(3-s_2)} - \frac{Rg_2 s_1 (3-s_1)}{Rg_1^2 \sqrt{(d-s_2)(3-s_2)}} \right]$$

$$= \frac{3-s_1}{2\sqrt{2}} \frac{Rg_2}{Rg_1^2} \frac{d}{\sqrt{(d-s_2)(3-s_2)}} + \frac{(3-s_1)^2 Rg_2^2 d^2 - Rg_2 s_1 (3-s_1) Rg_1^2 \cdot 4}{4 \cdot 2 Rg_1^4 (d-s_2)(3-s_2)}$$

$$\Rightarrow Q_1 = \frac{(3-s_1) Rg_2 \cdot d}{(4 \cdot 2 Rg_1^2 (d-s_2)(3-s_2)) \cdot \sqrt{(3-s_1)^2 Rg_2^2 d^2 - (3-s_1) s_1 Rg_1^2 Rg_2 \cdot 4 (d-s_2)(3-s_2)}}$$

derive  $G_2$  (based on  $G_1$ ):

$$\underline{\underline{G_2 = G_1 \cdot Q_1^{s_2-s_1} \cdot e^{\frac{Q_1^2 Rg_2^2}{3-s_2} - \frac{Q_1^2 Rg_1^2}{3-s_1}}}} = \underline{\underline{G_1 \cdot Q_1^{s_2-s_1} \cdot e^{\frac{(3-s_1) Rg_2^2 - (3-s_2) Rg_1^2}{(3-s_2)(3-s_1)}}}}$$

(I'm not substituting  $Q_1$  as that wouldn't simplify the expression)

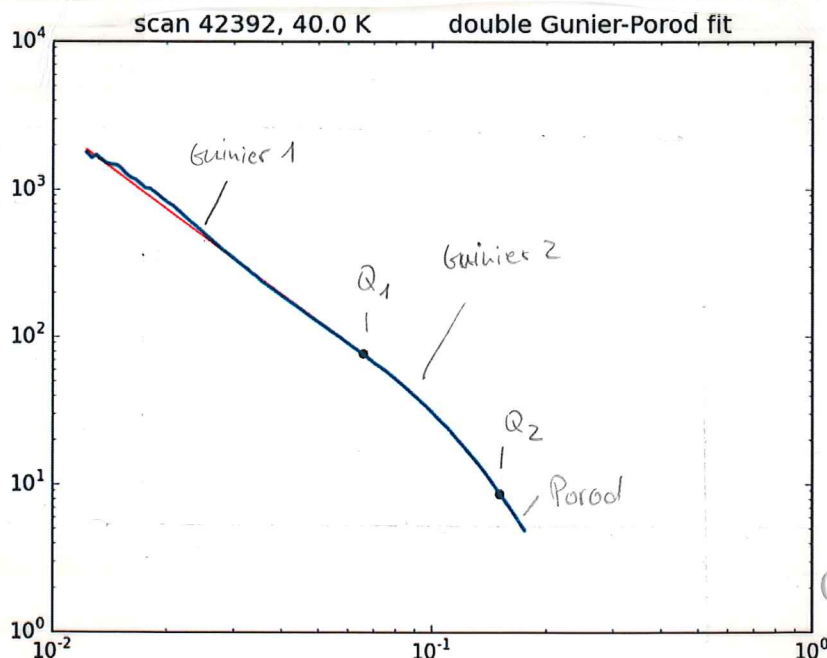
derive  $A$  (based on  $G_2$ )

$$\underline{\underline{A = G_2 Q_2^{d-s_2} e^{-\frac{Q_2^2 Rg_2^2}{3-s_2}}}}$$

Now the fit is working, but it's not able to reproduce both bumps

$\Rightarrow$  I probably need to really split the data in half and do two independent Gunier-Porod fits

$\Rightarrow$  Or introduce a power-law interval between the two bumps



# double Guinier-Porod analysis

Idea: insert power-law interval between the 2 Guinier intervals

$$I(Q) = \begin{cases} G_1 \cdot Q^{-s_1} \cdot e^{-\frac{Q^2 R_{g1}^2}{3-s_1}}, & Q \leq Q_1 \\ A_1 \cdot Q^{-d_1}, & Q_1 < Q \leq Q_2 \\ G_2 \cdot Q^{-s_2} \cdot e^{-\frac{Q^2 R_{g2}^2}{3-s_2}}, & Q_2 < Q \leq Q_3 \\ A_2 \cdot Q^{-d_2}, & Q_3 < Q \end{cases}$$

$I(Q)$  and first derivative must be continuous:

Positions:

$$Q_1 = \frac{1}{R_{g1}} \sqrt{\frac{(d_1 - s_1) \cdot (3 - s_1)}{2}}$$

$$Q_3 = \frac{1}{R_{g2}} \sqrt{\frac{(d_2 - s_2) \cdot (3 - s_2)}{2}}$$

$$Q_2: A_1 \cdot Q_2^{-d_1} = G_2 \cdot Q_2^{-s_2} \cdot e^{-\frac{Q_2^2 R_{g2}^2}{3-s_2}}$$

$$\Rightarrow Q_2 = \frac{1}{R_{g2}} \sqrt{\frac{(d_1 - s_2) \cdot (3 - s_2)}{2}}$$

Factors:

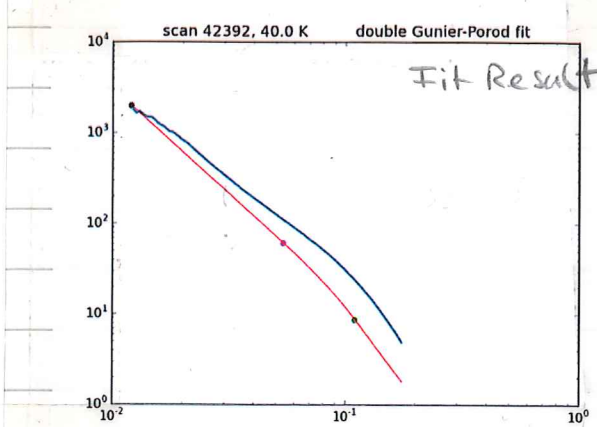
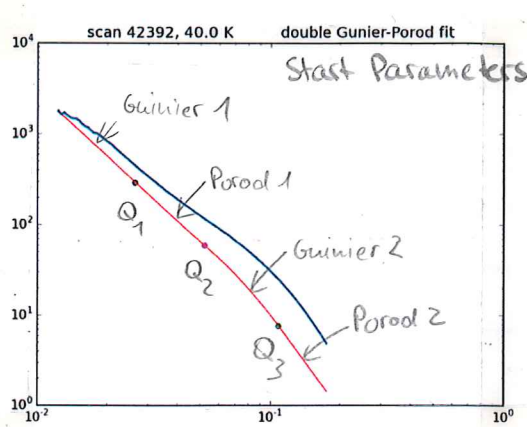
$$Q_1: A_1 Q_1^{-d_1} = G_1 Q_1^{-s_1} e^{-\frac{Q_1^2 R_{g1}^2}{3-s_1}} \Rightarrow A_1 = G_1 Q_1^{d_1 - s_1} e^{-\frac{Q_1^2 R_{g1}^2}{3-s_1}}$$

$$Q_2: G_2 = A_1 Q_2^{s_2 - d_1} \cdot e^{-\frac{Q_2^2 R_{g2}^2}{3-s_2}}$$

$$Q_3: A_2 = G_2 Q_3^{d_2 - s_2} e^{-\frac{Q_3^2 R_{g2}^2}{3-s_2}}$$

Maybe that could produce something useful at some point,  
but for now I can't figure out any good start parameters.

The fit always runs into some curves that don't look like  
what I want.

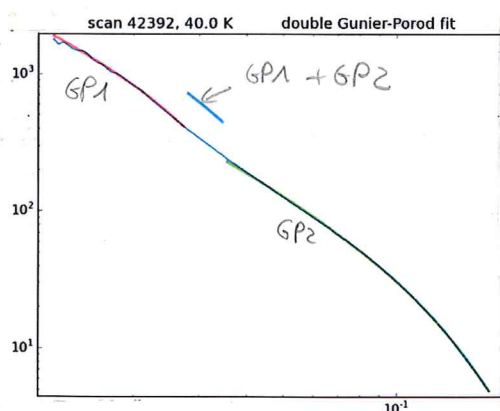


For now: Try splitting data in half (at manually chosen  $Q (= Q_2)$ ) and run two separate Guinier-Porod fits on both intervals

26.07.2016

That nicely fits both bumps, but the area in between does not really fit  
=> I had to leave a gap between both GP fits. This seemed to have a slope in between that of GP1 and GP2

=> I plotted the sum of both in this area  
=> seems to have the right slope



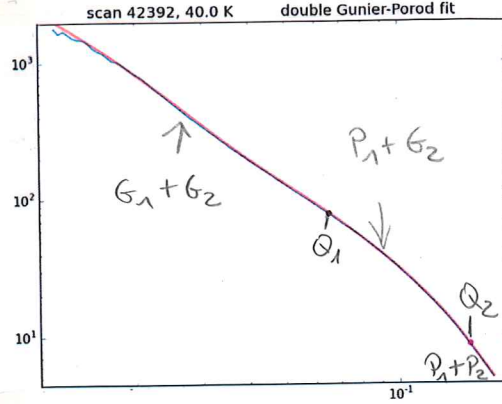
=> Instead of splitting the function into 4 intervals, I probably need to fit a sum of two GP functions

This works, but it looks as if I could do with only one Porod interval

⇒ Try

(\*)

$$I(Q) = \begin{cases} G_1(Q) + G_2(Q), & Q \leq Q_1 \\ P(Q), & Q_1 < Q \end{cases}$$



$$G_i(Q) = G_i \cdot Q^{-\frac{s_i}{3-s_i}} - \frac{Q^2 R_{gi}^2}{3-s_i}$$

$$P(Q) = A \cdot Q^{-d}$$

~~Double Guinier - Porod fit~~ not done, see next page for  $I(Q)$

$$\Rightarrow Q_1: A \cdot Q_1^{-d} = G_1 Q_1^{-\frac{s_1}{3-s_1}} - \frac{Q_1^2 R_{g1}^2}{3-s_1} + G_2 Q_1^{-\frac{s_2}{3-s_2}} - \frac{Q_1^2 R_{g2}^2}{3-s_2} \quad (1)$$

$$\wedge A d \cdot Q_1^{-d-1} = G_1 Q_1^{-\frac{s_1}{3-s_1}} - \frac{Q_1^2 R_{g1}^2}{3-s_1} \left( s_1 Q_1^{-1} + 2 \frac{Q_1 R_{g1}^2}{3-s_1} \right) \quad (2)$$

$$+ G_2 Q_1^{-\frac{s_2}{3-s_2}} - \frac{Q_1^2 R_{g2}^2}{3-s_2} \left( s_2 Q_1^{-1} + 2 \frac{Q_1 R_{g2}^2}{3-s_2} \right)$$

$$(2) \cdot \frac{Q_1}{d}: A Q_1^{-d} = G_1 Q_1^{-\frac{s_1}{3-s_1}} - \frac{Q_1^2 R_{g1}^2}{3-s_1} \left( s_1 + 2 \frac{Q_1^2 R_{g1}^2}{3-s_1} \right) \quad (2')$$

$$+ G_2 Q_1^{-\frac{s_2}{3-s_2}} - \frac{Q_1^2 R_{g2}^2}{3-s_2} \left( s_2 + 2 \frac{Q_1^2 R_{g2}^2}{3-s_2} \right)$$

$$(2) - (1) 0 = G_1 Q_1^{-\frac{s_1}{3-s_1}} - \frac{Q_1^2 R_{g1}^2}{3-s_1} \left( s_1 - 1 + 2 \frac{Q_1^2 R_{g1}^2}{3-s_1} \right) + G_2 Q_1^{-\frac{s_2}{3-s_2}} - \frac{Q_1^2 R_{g2}^2}{3-s_2} \left( s_2 - 1 + 2 \frac{Q_1^2 R_{g2}^2}{3-s_2} \right)$$

$$\cdot \frac{Q_1}{G_1} e^{\frac{Q_1^2 R_{g1}^2}{3-s_1}}: 0 = s_1 - 1 + 2 \frac{Q_1^2 R_{g1}^2}{3-s_1} + \frac{G_2}{G_1} Q_1^{\frac{s_1-s_2}{3-s_1}} e^{\frac{Q_1^2 R_{g1}^2}{3-s_1} - \frac{Q_1^2 R_{g2}^2}{3-s_2}} \left( s_2 - 1 + 2 \frac{Q_1^2 R_{g2}^2}{3-s_2} \right)$$

$$0 = \frac{(3-s_1)(s_1-1) + 2 Q_1^2 R_{g1}^2}{3-s_1} + \frac{G_2}{G_1} Q_1^{\frac{s_1-s_2}{3-s_1}} e^{\frac{Q_1^2 R_{g1}^2}{3-s_1} - \frac{Q_1^2 R_{g2}^2}{3-s_2}} \cdot \frac{3s_2 - 4 - s_2^2 + s_2^2 + 2}{3-s_2}$$

$$\cdot \frac{3-s_2}{-s_2^2 + 4s_2 - 2 + 2 Q_1^2 R_{g2}^2}: 0 = \frac{2 Q_1^2 R_{g1}^2 - s_1^2 + 4s_1 - 2}{2 Q_1^2 R_{g2}^2 - s_2^2 + 4s_2 - 2} + \frac{G_2}{G_1} Q_1^{\frac{s_1-s_2}{3-s_1}} e^{\frac{Q_1^2 R_{g1}^2}{3-s_1} - \frac{Q_1^2 R_{g2}^2}{3-s_2}}$$

→ This is getting too complicated.

∴ Use above double GP instead (\*)



This fit only produces useful results when experimental uncertainties are ignored and  $\ln(I)$  is fitted to  $\ln(I_0)$  data.

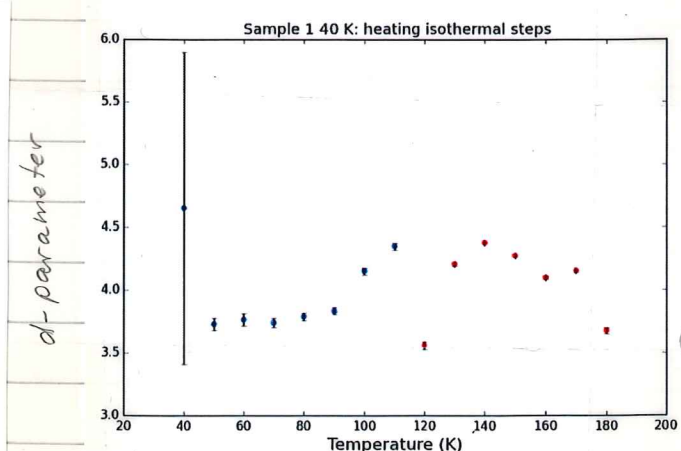
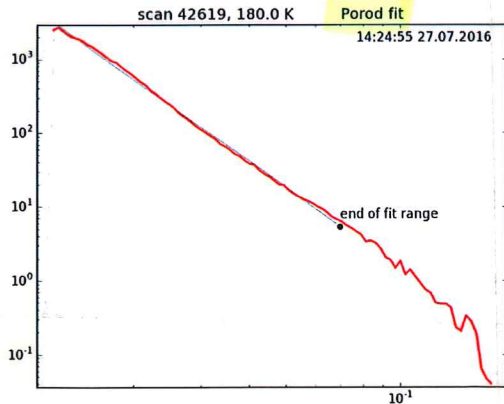
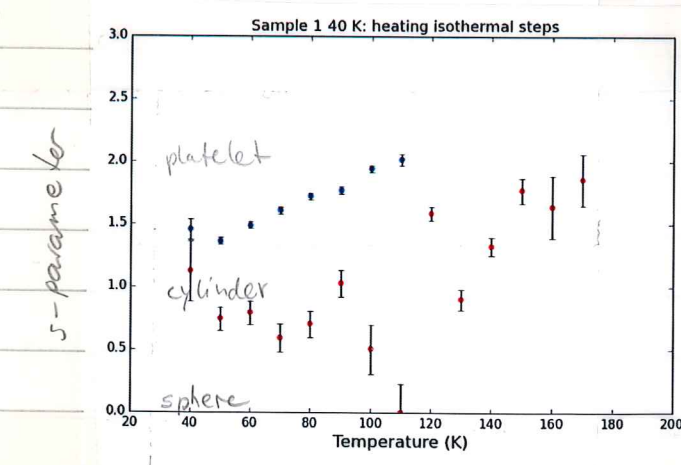
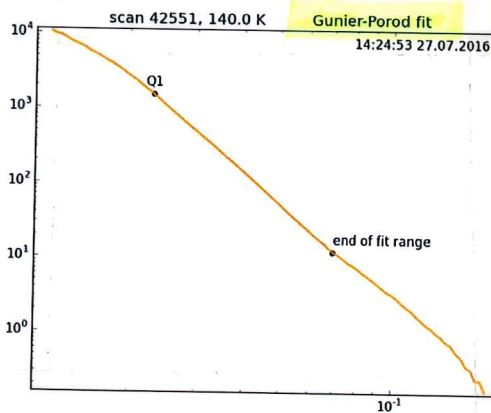
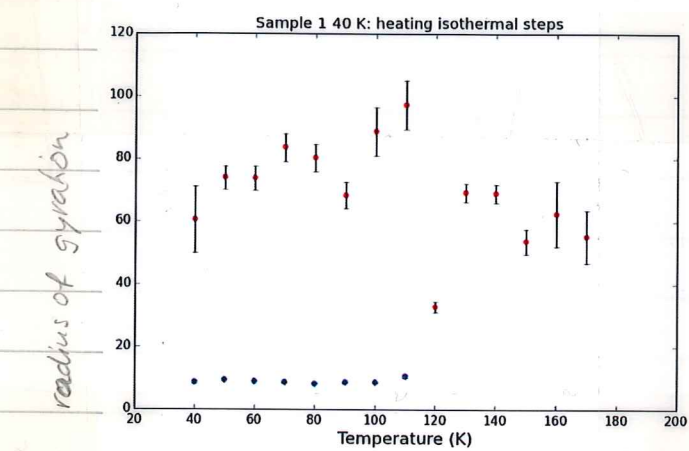
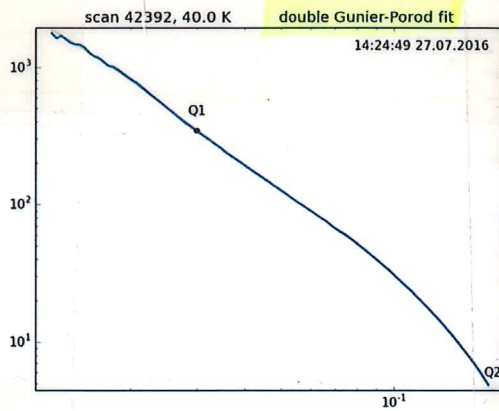
27.07.2016

I realised that  $d_1$  and  $d_2$  get fitted with very similar values  $\Rightarrow$  replaced them by  $d$ .

$$GP_i(Q) = \begin{cases} G_i \cdot Q^{-s_i} \cdot e^{-\frac{Q^2 Rg_i^2}{3s_i}}, & Q \leq Q_i = \frac{1}{Rg_i} \sqrt{\frac{(d - s_i)(3s_i)}{2}} \\ A_i \cdot Q^{-d}, & Q > Q_i \end{cases}$$

$$I(Q) = GP_1(Q) + GP_2(Q)$$

Double Guinier-Porod fit



Strey et al. 1991

Small-Angle Neutron Scattering from Diffuse Interfaces.1. Mono- and Bilayers in the Water-Octane - C<sub>12</sub>E<sub>5</sub> SystemExperiment:

They mix water, oil and surfactant (= Tensid).  $\rightarrow$  Determine surfactant layer thickness from SANS experiments.

Theoretical Considerations:

Assume that all surfactant molecules aggregate to form internal surface per unit Volume:  $A = \frac{s}{V}$

surface:  $A = v a_s \frac{\phi_s}{2V_s}$ ,  $v = \begin{cases} 1 & \text{for bilayer} \Rightarrow \frac{2}{v} = 2 \\ 2 & \text{for monolayer} \Rightarrow \frac{2}{v} = 1 \end{cases}$

surfactant volume fraction (compared to total sample)  $\phi_s = \frac{v_s N_s}{V_s}$   
 surfactant surface  $s = \frac{v a_s N_s}{2}$

$v_s \approx \frac{M}{S_s N_A}$  g/mol  
 density · molecules/mol =  $\frac{\text{g}}{\text{molecul}\cdot\text{cm}^3}$   
 volume per molecule =  $\frac{\text{cm}^3}{\text{molecul}}$

$a_s$  = effective area per surfactant molecule

(effective)  
 thickness of the surface:  $s = \frac{\phi_s}{A}$

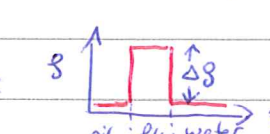
$$V = \frac{v_s N_s}{\phi_s} \Rightarrow A = \frac{s}{V} = \frac{v a_s N_s}{2} \frac{\phi_s}{v_s N_s} = \frac{v a_s \phi_s}{2 v_s}$$

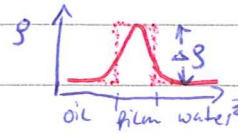
$$s = \frac{\phi_s}{A} = \frac{\phi_s \cdot 2 v_s}{v a_s \phi_s} = \frac{2}{v} \cdot \frac{v_s}{a_s} = \text{number of layers} \cdot \frac{\text{volume per molecule}}{\text{area per molecule}}$$

= number of layers · thickness per molecule

Contrast matching: match contrast of water and oil  $\Rightarrow$  get only

SANS signal from film

scattering density profile:   $\Rightarrow$  sharp (step function) transitions

 instead smooth transition  $\Leftarrow$  observed

$\hookrightarrow$  physically caused by thermal disorder and penetration of oil/water molecules into film of surfactant

Scattering from a diffuse 2-D film:  $I(q) = \frac{4\pi}{\lambda} \phi_s \frac{v_s}{a_s} \frac{(\Delta S)^2}{q^2} e^{-q^2 t^2}$

$t$  = thickness parameter

(for contrast matching only!)

Porod limit of a diffuse interface: assume scattering length densities of water and oil to be different.  $\Rightarrow$  smooth transition of  $g$  across the interface.  $\Rightarrow$  convolute step profile with Gaussian smoothing function.

$$\Rightarrow I(q) = 2\pi \phi_s \frac{as}{vs} \frac{(\Delta g)^2}{q^4} e^{-q^2 t^2}$$

$t$ : thickness parameter

in the case of an abrupt change in  $g$  (no diffuse interface)  
 $(t \rightarrow 0)$  this yields the porod limit  $I(q) \sim q^{-4}$ .

Empirically observed functional forms:

$b$ : mostly incoherent background

$$I(q) = c q^{-4} e^{-q^2 t^2} + b$$

$$\phi_s \frac{as}{vs} \approx A \Rightarrow I(q) = 2\pi \cdot A \cdot \frac{(\Delta g)^2}{q^4} e^{-q^2 t^2} + b$$

$$c = 2\pi \cdot A \cdot (\Delta g)^2 \approx \text{Porod constant}$$

$$\Rightarrow A = \frac{c}{2\pi (\Delta g)^2} = \text{SSA} \quad (\text{specific surface area})$$

$\Rightarrow$  I could probably derive SSA and particle interface thickness from fitting the icy particles data with

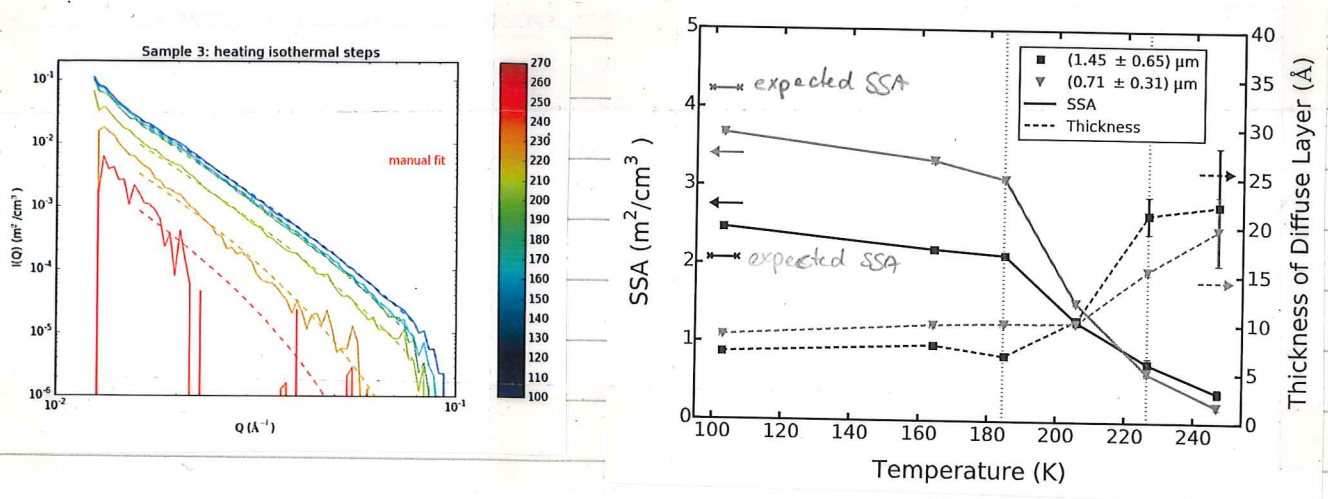
$$I(q) = 2\pi \cdot (\Delta g)^2 \cdot \text{SSA} \cdot q^{-4} e^{-q^2 t^2} + \text{background}$$

$\Rightarrow$  check with Tom!

27.07.2016

Tom agrees, but suggests to use .min+01 files so that no background term is required.

This fit is working nicely for most scans and produces more reasonable SSA results.



Träser et al. 2001

28.07.2016

## Thermal desorption of water ice in the interstellar medium

Thermal desorption of thin (vapour deposited) H<sub>2</sub>O films is found to occur with zeroth-order kinetics

- surface binding energy  $E_{\text{des}} = 5773 \pm 60 \text{ K} \cdot \text{K}_B$  (crystalline ice)  
(on gold substrate)  $\approx 5600 \text{ K} \cdot \text{K}_B$  (amorphous ice)
- pre-exponential factor  $A = 10^{30 \pm 2} \frac{\text{molecules}}{\text{cm}^2 \cdot \text{s}}$  (cryst. & amorph. ice)

Experiment: base pressure  $6 \cdot 10^{-11} \text{ torr} = 8 \cdot 10^{-11} \text{ mbar}$

primary vacuum constituent (>50%) : H<sub>2</sub>

effusive gas deposition system

quadrupole mass spectrometer (QMS)  $\Rightarrow$  TPD

Fourier Transform Infrared (FTIR) spectrometer  $\Rightarrow$  RAIRS

quartz crystal microbalance (QCM)  $\Rightarrow$  <sup>thin film mass</sup> determination

grain mimic : uncharacterised gold film surface on 7K

cold head (precision of control 0.5K)

radiative heating by halogen bulb from reverse

temperature measurement: thermocouples (Ni-Cr alloy, ~~Fe~~ type)

precision of measurement 0.25K

Deposition: 3 freeze thaw cycles (better than  $10^{-7}$  torr)

deposition rate:  $10^{10}$  molecules/s

must be  $T_c$  according to Petranko + Whitworth (p. 278, fig. 11.15)

temperature: 10 K (amorphous) / 130 K (crystalline)

quasi-effusive molecular beam directed at surface normal ( $5^\circ\text{C}$ )

~ ballistic deposition  $\Rightarrow$  high density amorphous ice (H<sub>2</sub>O)

film thickness:  $\approx 0.03 \mu\text{m}$

TPD: desorption rate:  $R = -\frac{dN_s}{dt}$   $N_s$  = number of molecules adsorbed on the surface

$$= k_d N_s^m$$

$m$  = order of reaction

rate constant:  $k_d = A \cdot e^{-\frac{E_{des}}{k_B T}}$

heating rate:  $\beta = \frac{dT}{dt}$

$$\Rightarrow -\frac{dN_s}{dT} > k_d \frac{N_s^m}{\beta}$$

position of TPD peak maximum  $T_d$ :  $\frac{d^2N_s}{dT^2} = 0$

$$\Rightarrow \frac{E_{des}}{k_B T_d^2} = \frac{A}{\beta} m N_s^{m-1} e^{-\frac{E_{des}}{k_B T_d}}$$

Calculate desorption temperature at a given pressure:

desorption rate:  $-\frac{dN_s}{dt} = N_s^m \cdot A \cdot e^{-\frac{E_{des}}{k_B T}}$

adsorption rate:  $\frac{dN_s}{dt} = \mu \cdot S$

$S$  = sticking coefficient  
 $\mu$  = arrival rate ( $\frac{\text{particles}}{\text{cm}^2 \text{s}}$ )

$\Rightarrow$  equilibrium:  $\mu S = N_s^m \cdot A \cdot e^{-\frac{E_{des}}{k_B T}}$

for water ice:  $m = 0 \Rightarrow \frac{\mu S}{A} = e^{-\frac{E_{des}}{k_B T}}$

Problem:  $\mu$  could be calculated from  $T$  and  $p$ , but  $S$  apparently needs to be determined experimentally (dependent on  $T, p, \text{substrate}$ )

Batista et al 2005: What determines the sticking probability of water molecules on ice?

→ Sticking probability = 1 for impact energies (0.5–1.5 eV) at normal incidence, decreasing for higher energies and increasing angles (w.r.t. surface normal)

$$\text{impact energy: } \frac{1}{2} m_{H_2O} v^2 = \frac{3}{2} k_B T$$

$$\text{e.g. } 250 \text{ K: } 0.03 \text{ eV}$$

Let's assume that under our experimental conditions (100–250 K, background deposition) the sticking probability is 1.

$$\Rightarrow \frac{\mu}{A} = e^{-\frac{E_{\text{kin}}}{k_B T}}$$

Derive  $\mu$ : We have  $N_g$  molecules in the gas phase inside a volume  $V$  at a temperature  $T$  moving with average velocity  $v = \sqrt{3 m_{H_2O}^{-1/2} k_B T}$ .

The icy particles have a specific surface area of

$$\text{SSA} = \frac{A_{\text{sample}}}{V_{\text{sample}}} \Rightarrow \text{The gas molecules see an area } A + 6L^2.$$

Assume:  $V = L^3 \Rightarrow$  Molecules will travel from one "wall" to the other in  $t = \frac{L}{v}$ .

$$\Rightarrow \text{Impact rate per wall area: } N_g \cdot \frac{V}{L} \cdot \frac{1}{6L^2} = \frac{1}{6} \frac{V}{L} \cdot N_g$$

$$\rightarrow \text{Impact rate on the sample: } N_g \cdot \frac{1}{6} \cdot \frac{V}{L} \cdot A_{\text{sample}} = \frac{1}{6} N_g \cdot V \cdot \text{SSA} \cdot V$$

$$\text{sample volume} \approx (4 \cdot 10^{-2})^2 \cdot 2 \cdot 10^{-3} \text{ m}^3 = 8.2 \cdot 10^{-4} \cdot 10^{-3} \text{ m}^3 = 1.6 \cdot 10^{-6} \text{ m}^3$$

$$\text{container (gas) volume} \approx (\frac{1}{2})^2 \cdot 1 \text{ m}^3 = \frac{1}{4} \text{ m}^3$$

$$\Rightarrow \frac{V_{\text{sample}}}{V} \approx 4 \cdot 1.6 \cdot 10^{-6}, \text{ SSA} \approx 3 \frac{\text{m}^2}{\text{cm}^3}$$

09.08.16:

$$\mu = N_g \frac{1}{6} \frac{V}{V}$$

$$= \frac{k_B T}{p \cdot V} \cdot \sqrt{\frac{k_B T}{m_{H_2O}}} \frac{1}{V}$$

$$= \frac{k_B T}{p \cdot V^2} \cdot \sqrt{3 \frac{k_B T}{m_{H_2O}}}$$

$$\Rightarrow \mu \approx N_g \cdot V \cdot 3.2 \cdot 10^{-6} \frac{\text{m}^2}{\text{cm}^3} = N_g \cdot V \cdot d$$

$$p \cdot V = N_g k_B T \Rightarrow N_g = \frac{k_B T}{p \cdot V}$$

$$\Rightarrow \mu \approx \frac{k_B T}{p \cdot V} \cdot \sqrt{3 m_{H_2O}^{-1} k_B T} \cdot d = \text{const.} \cdot T^{3/2}$$

$$09.08.16: \text{check units: } [pV] = [k_B T] = \frac{\text{m}^2 \text{kg}}{\text{s}^2} \quad [\sqrt{\text{m}^{-1} \text{kg}}] = \frac{\text{kg}}{\text{s}} \quad [d] = \frac{1}{\text{m}} \Rightarrow [\mu] = \frac{\text{kg}}{\text{s}} \neq \frac{\text{particles}}{\text{cm}^2 \cdot \text{s}}$$

$$[\sqrt{\text{m}^{-1} \text{kg}}] = \frac{\text{m}}{\text{s}} \Rightarrow [\mu] = \frac{1}{\text{s}} \rightarrow \text{still wrong} \Rightarrow \text{something is wrong}$$

$$\Rightarrow \text{const. } T^{3/2} = e^{-\frac{E_{\text{des}}}{k_B T}}$$

$$\Rightarrow \text{Wolfram alpha : } a x^{3/2} = e^{-b/x}$$

$$\Rightarrow x = -\frac{25}{3W(-\frac{2}{3}a^{2/3}b)}$$

$$W(z) = \sum_{m=1}^{\infty} \frac{(-m)}{m!} z^m = 1 \text{ for } z \geq 1$$

09.08.2016      in our case:  $a = \frac{\text{const}}{A} = \frac{\alpha k_B}{\rho V} \cdot \frac{\sqrt{3m_D^{-1}k_B^{-1}}}{A}$        $\rho = 3.2 \cdot 10^{-6} \frac{\text{m}^2}{\text{cm}^3}$

$$A = 10^{30} \frac{\text{molecules}}{\text{cm}^2 \text{s}}, \rho = 30 \text{ mbar} = 3 \cdot 10^3 \text{ Pa} = 3 \cdot 10^3 \frac{\text{kg}}{\text{m} \cdot \text{s}^2}, V = \frac{1}{4} \text{ m}^3$$

$$k_B = 1.38 \cdot 10^{-23} \frac{\text{J}}{\text{K}}, m_{D_2O} \approx 20 \text{ u} = 20 \cdot 1.66 \cdot 10^{-27} \text{ kg} = 3.32 \cdot 10^{-26} \text{ kg}$$

$$\Rightarrow a = \frac{3.2 \cdot 10^{-6} \frac{\text{m}}{\text{cm}^3} \cdot 1.38 \cdot 10^{-23} \frac{\text{J}}{\text{K}} \cdot \sqrt{3 \cdot 3.32 \cdot 10^{-26} \text{ kg}} \cdot 1.38 \cdot 10^{-23} \frac{\text{J}}{\text{K}}}{3 \cdot 10^3 \frac{\text{kg}}{\text{m} \cdot \text{s}^2} \cdot \frac{1}{4} \text{ m}^3 \cdot 10^{30} \frac{1}{\text{cm}^2 \text{s}}} = 3.2 \cdot 1.38 \cdot \sqrt{3 \cdot 3.32 \cdot 1.38} \cdot 10^{-23 - \frac{26+23}{2}} \cdot \frac{\text{m}^{2+2+1} \cdot \text{kg}}{\text{cm}^3 \text{s}^{2+1} \text{K}^{1.5}}$$

$$= 21.8 \cdot 10^{1/2} \cdot 10^{-23 - \frac{48}{2} - 33} \cdot \frac{\text{m}^5 \cdot \text{kg}^2}{\text{cm}^3 \text{s}^3 \text{K}^{1.5}} \cdot \frac{\text{cm}^2 \text{s}^3}{\text{kg} \cdot \text{m}^2}$$

$$= 68.9 \cdot 10^{-86} \cdot \frac{\text{m}^3 \text{kg}}{10^{-2} \text{mK}} = 6.89 \cdot 10^{-83} \cdot \frac{\text{m}^2 \text{kg}}{\text{K}^{1.5}}$$

$$b = \frac{E_{\text{des}}}{k_B} = \begin{cases} 5773 \text{ K} & I_C \\ 5600 \text{ K} & I_{\text{dis}} \end{cases}$$

$$\Rightarrow -\frac{2}{3} a^{2/3} b = -\frac{2}{3} \cdot 3.62 \cdot 10^{-83 \frac{2}{3}} \cdot \frac{\text{m}^{4/3} \text{kg}^{2/3}}{\text{K}}$$

$$a = \frac{\text{const}}{A} = \frac{k_B}{p \cdot V^2} \sqrt{\frac{3k_B}{m_{\text{D}_2\text{O}}}} \cdot \frac{1}{A}, m_{\text{D}_2\text{O}} = 3,32 \cdot 10^{-26} \text{ kg}$$

$$A = 10^{30} \frac{1}{\text{cm}^2 \text{s}} + p = 3 \cdot 10^3 \frac{\text{kg}}{\text{m}^2 \text{s}^2}, V = \frac{1}{4} \text{m}^3, k_B = 1,38 \cdot 10^{-23} \frac{\text{m}^2 \text{kg}}{\text{s}^2 \text{K}}$$

$$\Rightarrow a = \frac{1,38 \cdot 10^{-23} \frac{\text{m}^2 \text{kg}}{\text{s}^2 \text{K}}}{3 \cdot 10^3 \frac{\text{kg}}{\text{m}^2 \text{s}^2} \cdot \frac{1}{16} \text{m}^6 \cdot 10^{30} \frac{1}{\text{cm}^2 \text{s}}} \cdot \sqrt{\frac{3 \cdot 1,38 \cdot 10^{-23} \frac{\text{m}^2 \text{kg}}{\text{s}^2 \text{K}}}{3,32 \cdot 10^{-26} \text{kg}}}$$

$$= \frac{16 \cdot 1,38}{3} \cdot 10^{-23-33} \frac{\text{m}^2 \text{kg} \text{m}^2 \text{s}^2 \text{cm}^2 \text{s}}{\text{kg} \text{m}^6 \text{s}^2 \text{K}} \cdot \sqrt{\frac{3 \cdot 1,38 \cdot 10}{3,32} \cdot 10 \cdot 10 \frac{\text{m}}{\text{s}^2 \text{K}}}$$

$$= 26 \cdot 10^{-55} \cdot 10^{-4} \text{ K} = 2,6 \cdot 10^{-58} \text{ K}$$

$$b = \frac{E_{\text{des}}}{k_B} = \begin{cases} 5773 \text{ K} & I_c \\ 5600 \text{ K} & I_{\text{dis}} \end{cases}$$

$$-\frac{2}{3} a^{2/3} = -\frac{2}{3} \cdot 1,83 \cdot 10^{-38} \cdot 10^{-2/3} \frac{1}{\text{K}} = -0,27 \cdot 10^{-38} \frac{1}{\text{K}} = -2,7 \cdot 10^{-39} \frac{1}{\text{K}}$$

$$\Rightarrow -\frac{2}{3} a^{2/3} b = \begin{cases} -1,5587 \cdot 10^{-35} & I_c \\ -1,5120 \cdot 10^{-35} & I_{\text{dis}} \end{cases}$$

$W(-\frac{2}{3} a^{2/3} b) =$  can't get that out of Wolfram alpha

$$\rightarrow \text{input } 2,6 \cdot 10^{-58} \cdot x^{3/2} = e^{-\frac{5773}{x}} \text{ instead}$$

$$\Rightarrow x = 44,8243 \text{ or } 3,84615 \cdot 10^{57}$$

$$2,6 \cdot 10^{-58} \cdot x^{3/2} = e^{-\frac{5600}{x}}$$

$$\Rightarrow x = 43,4707 \text{ or } 3,84615 \cdot 10^{57}$$

$$\Rightarrow \text{Desorption temperatures would be: } T_{\text{des}} = \begin{cases} 44,82 \text{ K}, I_c \\ 43,47 \text{ K}, I_{\text{dis}} \end{cases}$$

These values appear very low and we see  $I_c$  before  $I_{\text{dis}}$ , not the other way around.  $\Rightarrow$  Ask Helen. (changing A by  $10^2$  changes T by 1K)

Continue with ISIS ASW analysis (June '15 + April '16)

### Double Guinier-Porod fits:

For the lowest (40 K) T and around the transition to normal GP fb (100-120 K), the python fits go a bit weird.

⇒ I've implemented the possibility for manual fitting in the program. That kind-of works.

However, there are so many fit parameters (7) that it is impossible to find the best fit via eye. Many different combinations of the parameters lead to very similar results.

⇒ Try to introduce minimum precision for fit into routine; maybe that helps to force python into the best fit instead of a reasonably good one.

can't figure out how to do that, but choosing different start parameters seems to help a bit.

11.08.2016

12.08.2016

Tom suggested to:

- \* as a first approach fit only the higher Q-Sump, to have the results comparable with the previous papers.

- I want to do the full and proper analysis now and not something quick and dirty and then do it all over again later.

- \* Tom recommends to include experimental uncertainties in the fit

- I stopped doing that, because the fits were going really weird, maybe investigate later

- check at which point exp uncertainties become very high (towards low-Q) and truncate data there.

- \* He pointed out that the Hammouda 2014 GP paper also states a model with two Guinier and one Porod region(s)

- try that one on my data

## Gaussian-Gaussian-Porod fit

(Hammonda 2010)

$$I(Q) = \begin{cases} \frac{G_2}{Q^{S_2}} e^{-\frac{Q^2 R_{g2}^2}{3-S_2}}, & Q \leq Q_2 \\ \frac{G_1}{Q^{S_1}} e^{-\frac{Q^2 R_{g1}^2}{3-S_1}}, & Q_2 \leq Q \leq Q_1 \\ \frac{D}{Q^2}, & Q_1 \leq Q \end{cases}$$

$$Q_1 = \frac{1}{R_{g1}} \sqrt{\frac{(d-S_1)(3-S_1)}{2}}, \quad Q_2 = \sqrt{\left( \frac{2}{3-S_2} R_{g2}^2 - \frac{2}{3-S_1} R_{g1}^2 \right)}$$

$$D = G_1 e^{-\frac{Q_1^2 R_{g1}^2}{3-S_1}} \quad Q_1, \quad G_2 = G_1 e^{-\frac{d-S_1}{Q_2}}$$

16.09.2016

## ASW - double GP fit

Beaucage  
1996 J. Appl. Cryst.

Beaucage  
1994-1996

Tom will send link

12.10.2016

## Double GP fit (GP1 + GP2):

works ok for 40 K and 120 K deposition, although 120 K individual scans lead to very different results. 100 K individual scans do not fit automatically, would have to do most of them manually. Isothermal averages do not fit terribly well automatically, but still better than individual scans.

13.10.2016

60 K deposition: I have to do most of the isothermal average fits manually. For the individual scans that's the same → stop it for now.

19.10.2016 Solution to fitting problems: \* make sure start parameter for S is  $\leq 1.95$

21.10.2016 remaining q-split from double GP fit much better! [adjust q-split for each sample (& T\_Porod)]

*shape*

## lamellar

Lyotropic lamellar phase with uniform SLD and random distribution

Parameter	Description	Units	Default value
scale	Source intensity	None	1
background	Source background	cm <sup>-1</sup>	0.001
thickness	total layer thickness	Å	50
sld	Layer scattering length density	10 <sup>-6</sup> Å <sup>-2</sup>	1
sld_solvent	Solvent scattering length density	10 <sup>-6</sup> Å <sup>-2</sup>	6

The returned value is scaled to units of cm<sup>-1</sup> sr<sup>-1</sup>, absolute scale.

Polydispersity in the bilayer thickness can be applied from the GUI.

**Definition**

*dilute = distance >> thickness ?  
would this be pores or ASW? ————— ↓*

The scattering intensity  $|I(q)|$  for dilute, randomly oriented, "infinitely large" sheets or lamellae is

$$|I(q) = \text{scale} \frac{2\pi P(q)}{q^2 \Delta} + \text{background}|$$

The form factor is

$$P(q) = \frac{2\Delta \rho^2}{q^2} (1 - \cos(q\Delta)) = \frac{4\Delta \rho^2}{q^2} \sin^2 \left( \frac{q\Delta}{2} \right)$$

where  $(\Delta)$  is the total layer thickness and  $(\Delta\rho)$  is the scattering length density difference.

This is the limiting form for a spherical shell of infinitely large radius. Note that the division by  $(\Delta)$  means that  $(\text{scale})$  in sasview is the volume fraction of sheet,  $(\phi = S/\Delta)$  where  $(S)$  is the area of sheet per unit volume.  $(S)$  is half the Porod surface area per unit volume of a thicker layer (as that would include both faces of the sheet).

The 2D scattering intensity is calculated in the same way as 1D, where the  $(q)$  vector is defined as

$$|q = \sqrt{q_x^2 + q_y^2}|$$

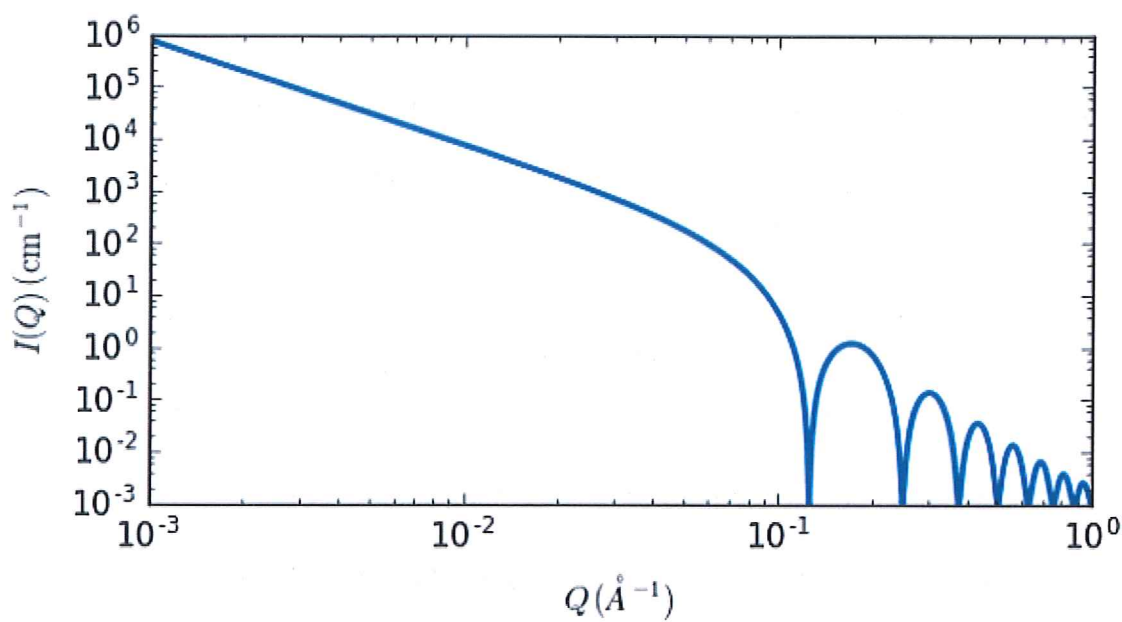


Fig. 40 1D plot corresponding to the default parameters of the model.

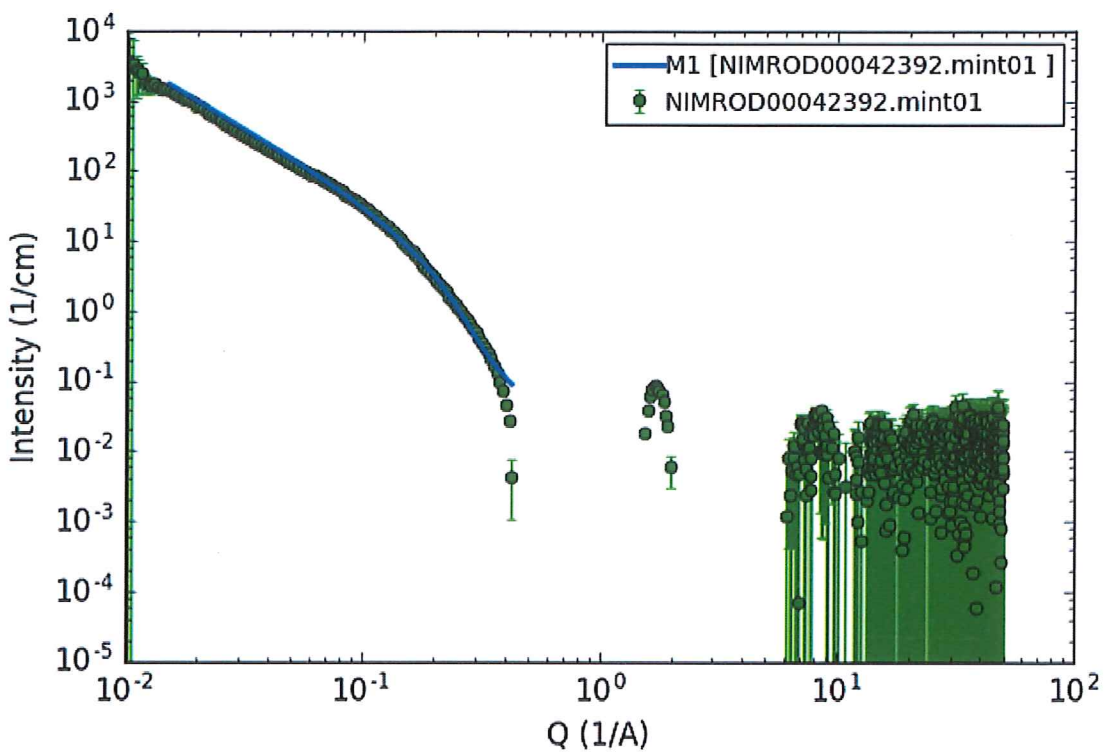
## References

F Nallet, R Laversanne, and D Roux, J. Phys. II France, 3, (1993) 487-502

also in J. Phys. Chem. B, 105, (2001) 11081-11088

Shape

Lamellar



Category  Shapes  Description

Model Parameters

Model Parameter	Value	Error	Min	Max	[Units]
scale	0.00015079	+/- 8.8556e-05	0	inf	1/cm
background	2.0404e-05	+/- 1e-08	0	inf	1/cm
thickness	16.788	+/- 0.0098739	0	inf	Ang
std	135.23	+/- 47.806	-inf	inf	1e-6/Ang^2
std_solvent	-359.85	+/- 118.43	-inf	inf	1e-6/Ang^2

lamellar

Polydispersity and Orientational Distribution

On  Off

PD[ratio]  +/-  Min  Max  Npts  Function

Fitting

Set Instrumental Smearing

None  Use dQ Data  Custom Pinhole Smear  Custom Slit Smear

No smearing is selected...

Set Weighting by Selecting dI Source

No Weighting  Use dI Data  Use[sqrt(|Data|)]  Use[|Data|]

Q range   Masking(2D)

# shape

## ellipsoid

Ellipsoid of revolution with uniform scattering length density.

Parameter	Description	Units	Default value
scale	Source intensity	None	1
background	Source background	$\text{cm}^{-1}$	0.001
sld	Ellipsoid scattering length density	$10^{-6} \text{\AA}^{-2}$	4
sld_solvent	Solvent scattering length density	$10^{-6} \text{\AA}^{-2}$	1
radius_polar	Polar radius	$\text{\AA}$	20
radius_equatorial	Equatorial radius	$\text{\AA}$	400
theta	In plane angle	degree	60
phi	Out of plane angle	degree	60

The returned value is scaled to units of  $\text{cm}^{-1} \text{ sr}^{-1}$ , absolute scale.

The form factor is normalized by the particle volume

**Definition**      *What does "2D" mean?*

The output of the 2D scattering intensity function for oriented ellipsoids is given by (Feigin, 1987)

$$P(q, \alpha) = \frac{\text{scale}}{V} F^2(q, \alpha) + \text{background}$$

where

$$F(q, \alpha) = \frac{3\Delta\rho V(\sin[qr(R_p, R_e, \alpha)] - \cos[qr(R_p, R_e, \alpha)])}{[qr(R_p, R_e, \alpha)]^3}$$

and

$$r(R_p, R_e, \alpha) = [R_e^2 \sin^2 \alpha + R_p^2 \cos^2 \alpha]^{1/2}$$

$\alpha$  is the angle between the axis of the ellipsoid and  $\vec{q}$ ,  $V = (4/3)\pi R_p R_e^2$  is the volume of the ellipsoid,  $R_p$  is the polar radius along the rotational axis of the ellipsoid,  $R_e$  is the equatorial radius perpendicular to the rotational axis of the ellipsoid and  $\Delta\rho$  (contrast) is the scattering length density difference between the scatterer and the solvent.

To provide easy access to the orientation of the ellipsoid, we define the rotation axis of the ellipsoid using two angles  $\theta$  and  $\phi$ . These angles are defined in the cylinder orientation figure. For the ellipsoid,  $\theta$  is the angle between the rotational axis and the  $z$ -axis.

NB: The 2nd virial coefficient of the solid ellipsoid is calculated based on the  $R_p$  and  $R_e$  values, and used as the effective radius for  $S(q)$  when  $P(q) \cdot S(q)$  is applied.

The  $\theta$  and  $\phi$  parameters are not used for the 1D output.

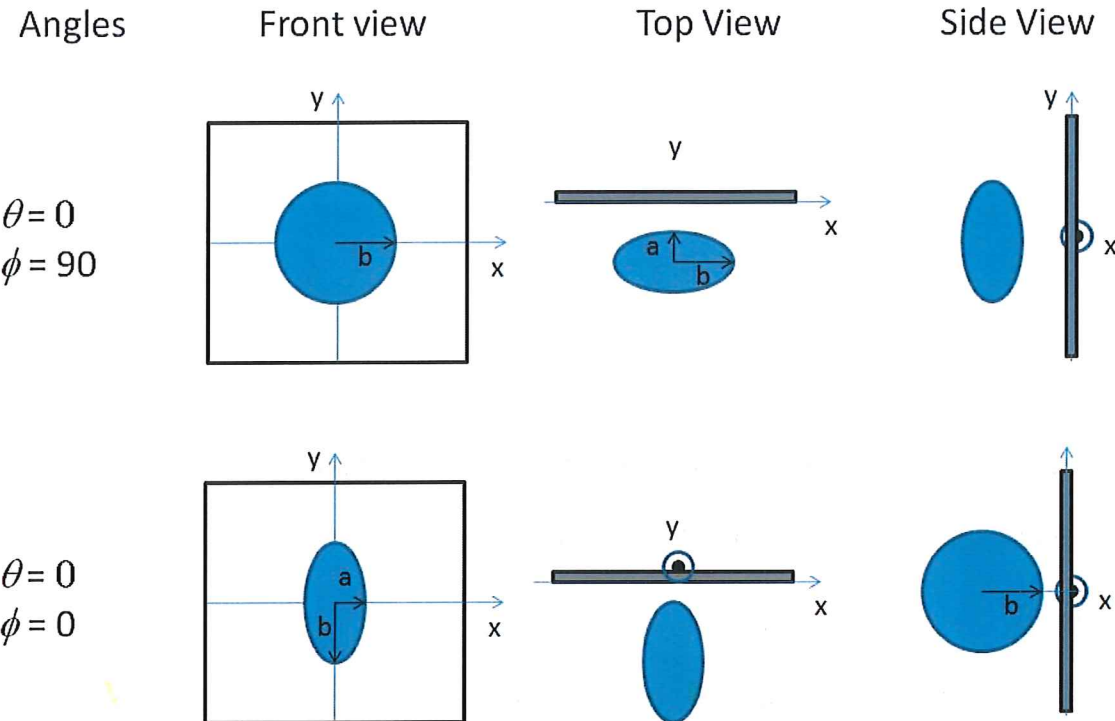


*Fig. 34* The angles for oriented ellipsoid, shown here as oblate,  $a = R_p$  and  $b = R_e$

## Validation

Validation of the code was done by comparing the output of the 1D model to the output of the software provided by the NIST (Kline, 2006).

The implementation of the intensity for fully oriented ellipsoids was validated by averaging the 2D output using a uniform distribution  $p(\theta, \phi) = 1.0$  and comparing with the output of the 1D calculation.

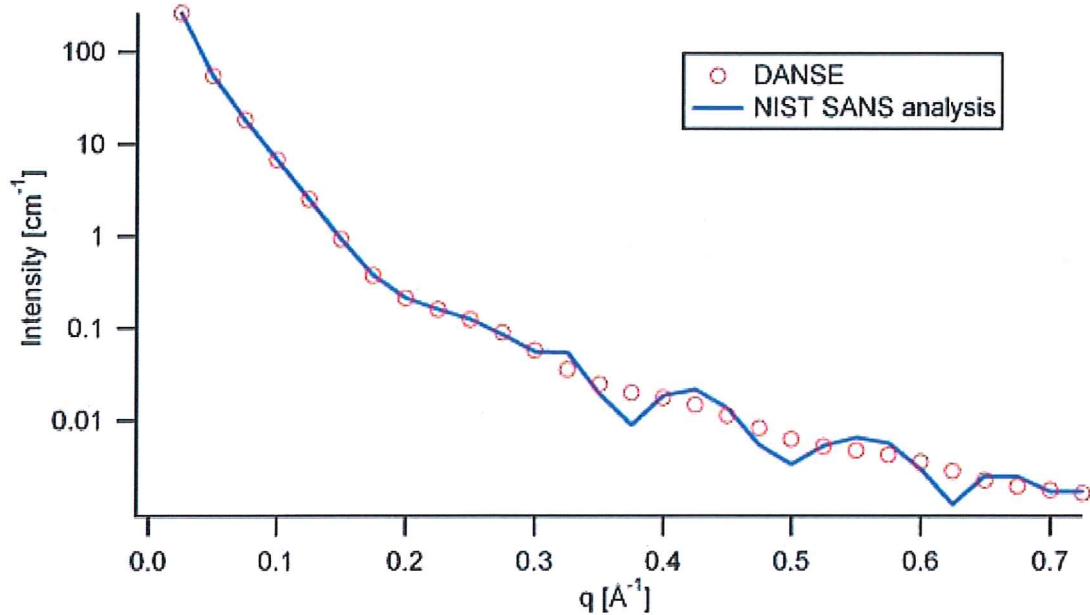
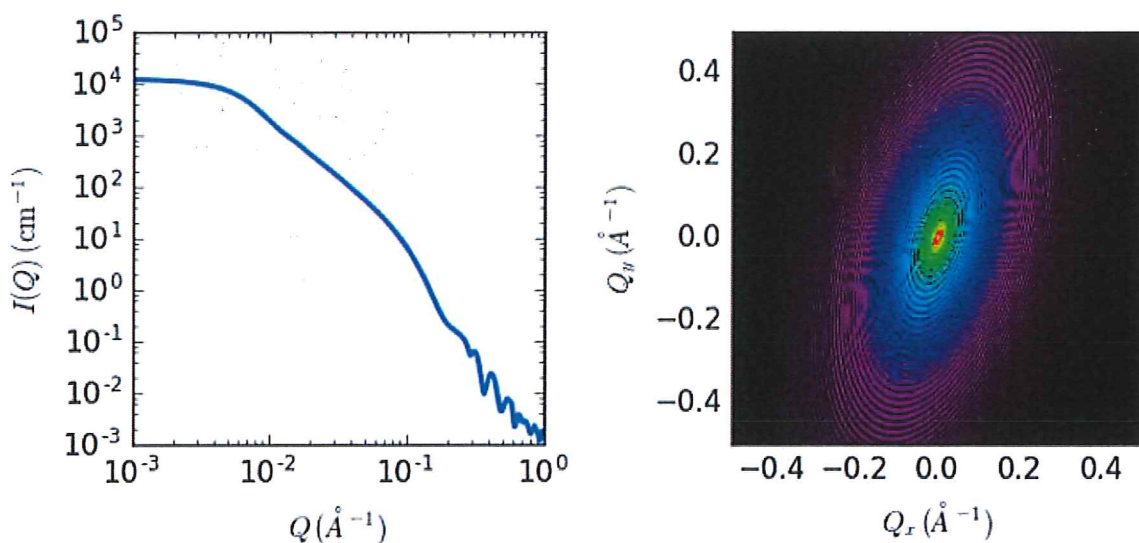


Fig. 35 Comparison of the intensity for uniformly distributed ellipsoids calculated from our 2D model and the intensity from the NIST SANS analysis software. The parameters used were: `scale` = 1.0, `radius_polar` = 20 Å, `radius_equatorial` = 400 Å, `contrast` = 3e-6 Å<sup>-2</sup>, and `background` = 0.0 cm<sup>-1</sup>.

The discrepancy above  $q = 0.3$  cm<sup>-1</sup> is due to the way the form factors are calculated in the c-library provided by NIST. A numerical integration has to be performed to obtain  $P(q)$  for randomly oriented particles. The NIST software performs that integration with a 76-point Gaussian quadrature rule, which will become imprecise at high  $q$  where the amplitude varies quickly as a function of  $q$ . The SasView result shown has been obtained by summing over 501 equidistant points. Our result was found to be stable over the range of  $q$  shown for a number of points higher than 500.

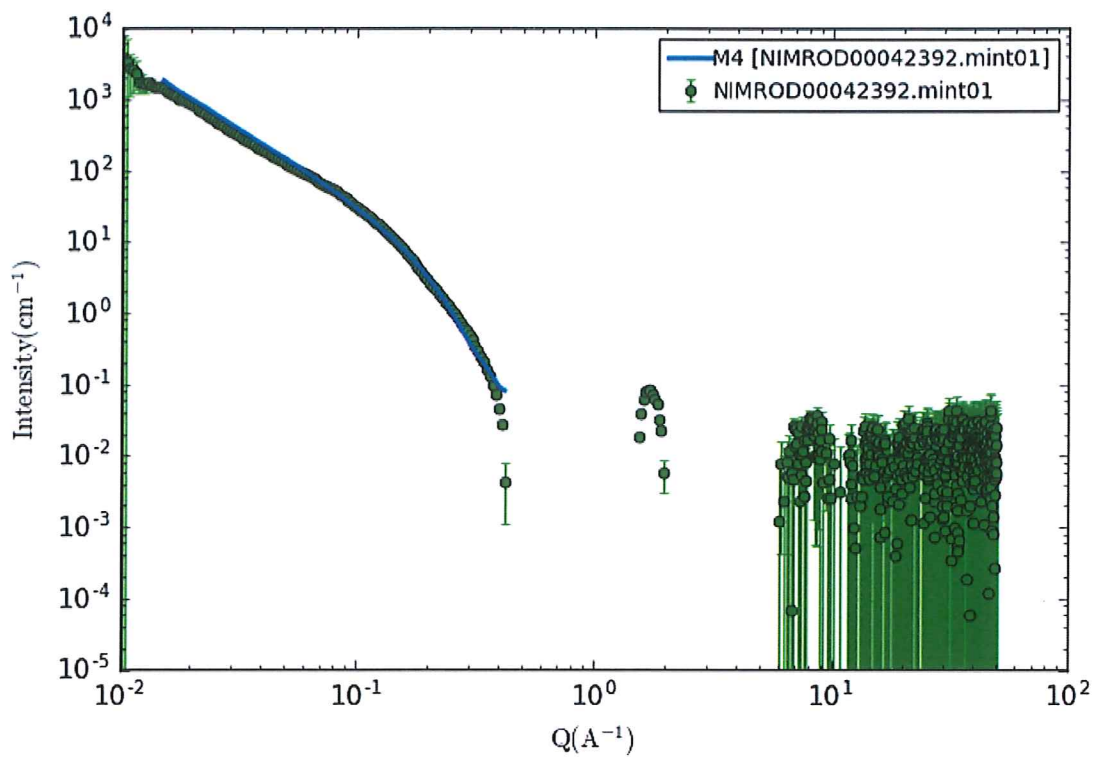


*Fig. 36* 1D and 2D plots corresponding to the default parameters of the model.

## References

L A Feigin and D I Svergun. *Structure Analysis by Small-Angle X-Ray and Neutron Scattering*, Plenum Press, New York, 1987.

Shape  
ellipsoid



Model Parameters						
	Value	Error	Min	Max	[Units]	
<input checked="" type="checkbox"/> Select All	0.00015054	+/- 2.2053e-05	0	inf		
<input checked="" type="checkbox"/> scale	0.00032377	+/- 0.00042032	0	inf	1/cm	
<input checked="" type="checkbox"/> background	119.77	+/- 9.4408	-inf	inf	1e-6/Ang^2	
<input checked="" type="checkbox"/> sld	-376.13	+/- 30.356	-inf	inf	1e-6/Ang^2	
<input checked="" type="checkbox"/> sld_solvent	10.763	+/- 0.0095077	0	inf	Ang	
<input checked="" type="checkbox"/> radius_polar	302.63	+/- 0.98912	0	inf	Ang	
<input checked="" type="checkbox"/> radius_equatorial	302.63	+/- 0.98912	0	inf	Ang	

Polydispersity and Orientational Distribution

On     Off    [?](#)

PD[ratio]	Min	Max	Npts	Nsig	Function
-0.16699	+/- 0.0022636		35	3	gaussian <a href="#">▼</a>
-0.033111	+/- 0.0029951		35	3	gaussian <a href="#">▼</a>

Fitting

Set Instrumental Smearing

None     Use dQ Data     Custom Pinhole Smear     Custom Slit Smear    [?](#)

No smearing is selected...

Set Weighting by Selecting dI Source

No Weighting     Use dI Data     Use |sqrt(I|Data)|     Use ||Data|

Q range	Min[1/A]	Max[1/A]	Masking[2D]
0.015	0.43		<a href="#">Editor</a>

[Reset](#)

*shape-independent*

# gel\_fit

Fitting using fine-scale polymer distribution in a gel.

Parameter	Description	Units	Default value
scale	Source intensity	None	1
background	Source background	cm <sup>-1</sup>	0.001
guinier_scale	Guinier length scale	cm <sup>-1</sup>	1.7
lorentz_scale	Lorentzian length scale	cm <sup>-1</sup>	3.5
rg	Radius of gyration	Å	104
fractal_dim	Fractal exponent	None	2
cor_length	Correlation length	Å	16

The returned value is scaled to units of cm<sup>-1</sup> sr<sup>-1</sup>, absolute scale.

*This model was implemented by an interested user!*

*I guess this doesn't make sense then?*

Unlike a concentrated polymer solution, the **fine-scale polymer distribution** in a gel involves at least two characteristic length scales, a shorter correlation length ( $a_1$ ) to describe the rapid fluctuations in the position of the polymer chains that ensure thermodynamic equilibrium, and a longer distance (denoted here as  $a_2$ ) needed to account for the static accumulations of polymer pinned down by junction points or clusters of such points. The latter is derived from a simple Guinier function. Compare also the gauss\_lorentz\_gel model.

## Definition

The scattered intensity  $I(q)$  is calculated as

$$I(Q) = I(0)_L \frac{1}{\left(1 + \left[((D + 1/3)Q^2 a_1^2)\right]^{D/2}\right)} + I(0)_G \exp(-Q^2 a_2^2) + B$$

where

$$a_2^2 \approx \frac{R_g^2}{3}$$

Note that the first term reduces to the Ornstein-Zernicke equation when  $D = 2$ ; ie, when the Flory exponent is 0.5 (theta conditions). In gels with significant hydrogen bonding  $D$  has been reported to be ~2.6 to 2.8.

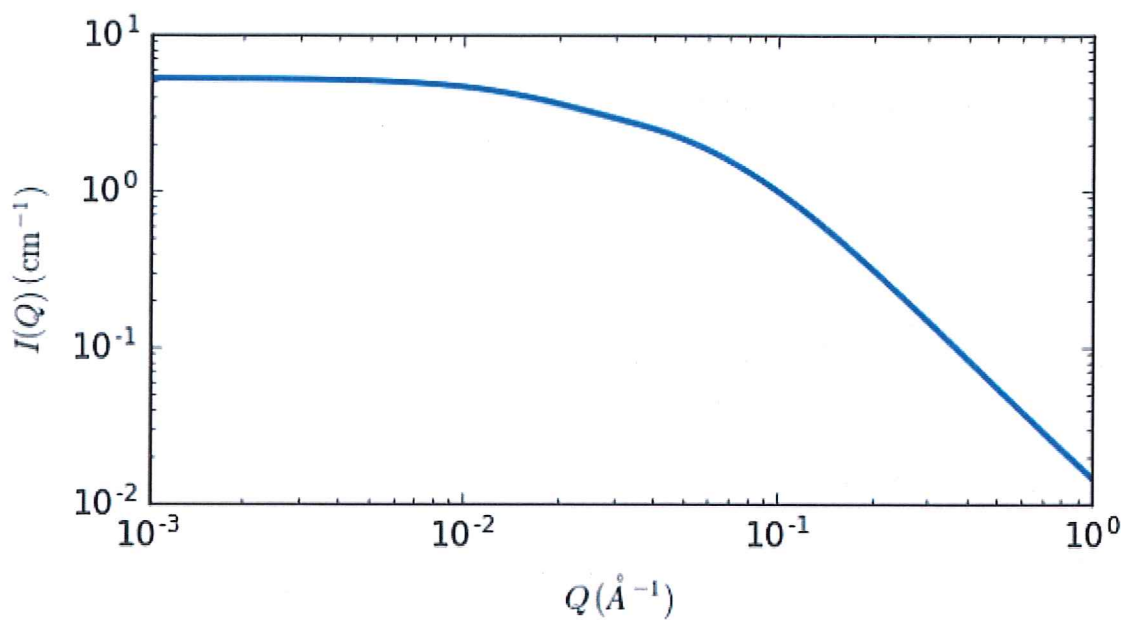


Fig. 89 1D plot corresponding to the default parameters of the model.

## References

Mitsuhiko Shibayama, Toyoichi Tanaka, Charles C Han, *J. Chem. Phys.* 1992, 97 (9), 6829-6841

Simon Mallam, Ferenc Horkay, Anne-Marie Hecht, Adrian R Rennie, Erik Geissler, *Macromolecules* 1991, 24, 543-548

shape-independent

gel fit

Shape-Independent ▾

Modify

Description

Help

gel\_fit

Model Parameters

<input checked="" type="checkbox"/> Select All	Value	Error	Min	Max	[Units]
<input checked="" type="checkbox"/> scale	12.709	+/- 11.145	0	inf	
<input checked="" type="checkbox"/> background	1.2664e-05	+/- 1e+08	0	inf	1/cm
<input checked="" type="checkbox"/> guinier_scale	59.377	+/- 52.185	-inf	inf	cm^-1
<input checked="" type="checkbox"/> lorentz_scale	13.83	+/- 12.13	-inf	inf	cm^-1
<input checked="" type="checkbox"/> rg	65.34	+/- 0.2556	2	inf	Ang
<input checked="" type="checkbox"/> fractal_dim	5.4401	+/- 0.0093189	0	inf	
<input checked="" type="checkbox"/> cor_length	6.4137	+/- 0.019972	0	inf	Ang

Polydispersity and Orientational Distribution

On     Off    [?](#)

No polydispersity available for this model

Fitting

Set Instrumental Smearing

None  Use dQ Data  Custom Pinhole Smear  Custom Slit Smear [?](#)

No smearing is selected...

Set Weighting by Selecting dI Source

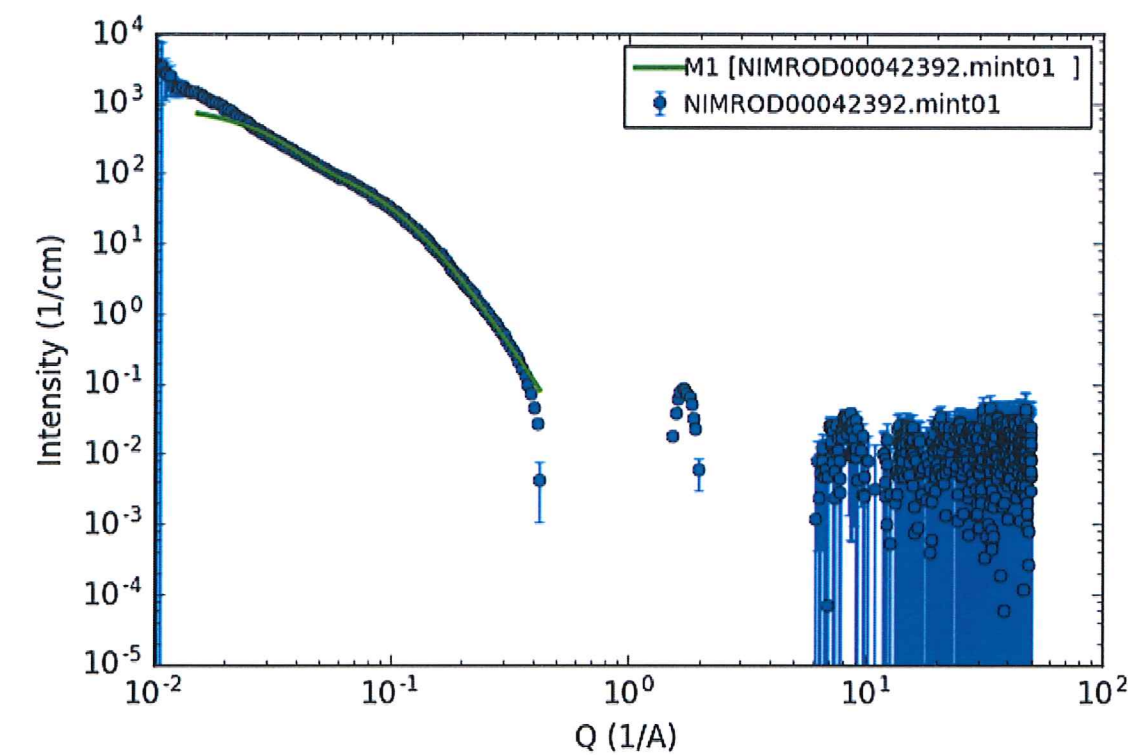
No Weighting  Use dI Data  Use [sqrt(I) Data]  Use [I] Data

Q range    Min[1/A]    Max[1/A]    Masking(2D)

Reset

0.015

0.43



## *shape-independent* fractal\_core\_shell

Parameter	Description	Units	Default value
scale	Source intensity	None	1
background	Source background	cm <sup>-1</sup>	0.001
radius	Sphere core radius	Å	60
thickness	Sphere shell thickness	Å	10
sld_core	Sphere core scattering length density	10 <sup>-6</sup> Å <sup>-2</sup>	1
sld_shell	Sphere shell scattering length density	10 <sup>-6</sup> Å <sup>-2</sup>	2
sld_solvent	Solvent scattering length density	10 <sup>-6</sup> Å <sup>-2</sup>	3
volfraction	Volume fraction of building block spheres	None	1
fractal_dim	Fractal dimension	None	2
cor_length	Correlation length of fractal-like aggregates	Å	100

The returned value is scaled to units of cm<sup>-1</sup> sr<sup>-1</sup>, absolute scale.

Calculates the scattering from a fractal structure with a primary building block of core-shell spheres, as opposed to just homogeneous spheres in the fractal model. This model could find use for aggregates of coated particles, or aggregates of vesicles. ← Could this be translated to "islands/grains of porous ice"?

### Definition

$$I(q) = \text{background} + P(q)S(q)$$

The form factor  $P(q)$  is that from core\_shell model with  $bkg = 0$

$$P(q) = \frac{\text{scale}}{V_s} \left[ 3V_c(\rho_c - \rho_s) \frac{\sin(qr_c) - qr_c \cos(qr_c)}{(qr_c)^3} + 3V_s(\rho_s - \rho_{\text{solv}}) \frac{\sin(qr_s) - qr_s \cos(qr_s)}{(qr_s)^3} \right]^2$$

while the fractal structure factor  $S(q)$  is

$$S(q) = \frac{D_f \Gamma(D_f - 1) \sin((D_f - 1) \tan^{-1}(q\xi))}{(qr_c)^{D_f} \left(1 + \frac{1}{q^2 \xi^2}\right)^{\frac{D_f - 1}{2}}}$$

where  $D_f$  = fractal\_dim,  $\xi$  = cor\_length,  $r_c$  = (core) radius, and  $scale$  = volume fraction.

The fractal structure is as documented in the fractal model. Polydispersity of radius and thickness is provided for.

For 2D data: The 2D scattering intensity is calculated in the same way as 1D, where the  $q$  vector is defined as

$$q = \sqrt{q_x^2 + q_y^2}$$

File failed to load: <https://cdn.mathjax.org/mathjax/contrib/a11y/accessibility-menu.js>

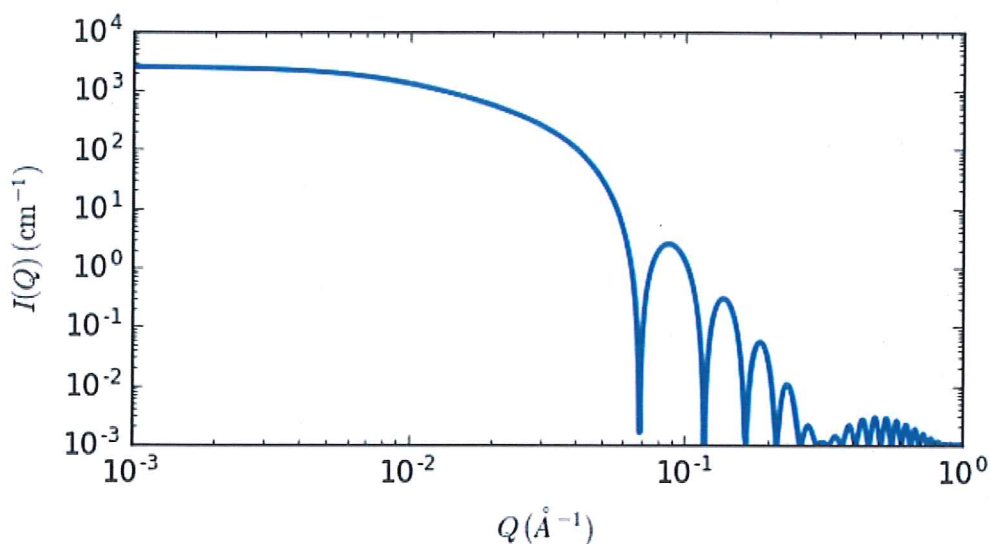


*Fig. 86* 1D plot corresponding to the default parameters of the model.

## References

See the core\_shell and fractal model descriptions

shape-independent  
fractal-core-shell

fractal\_core\_shell

P(Q)S(Q)

None

Model Parameters

<input checked="" type="checkbox"/> Select All	Value	Error	Min	Max	[Units]
<input checked="" type="checkbox"/> scale	2.6219	+/- 0.36105	0	inf	
<input checked="" type="checkbox"/> background	0.0018803	+/- 0.0016996	0	inf	1/cm
<input checked="" type="checkbox"/> radius	246.72	+/- 0.063045	0	inf	Ang
<input checked="" type="checkbox"/> thickness	15.321	+/- 0.038899	0	inf	Ang
<input checked="" type="checkbox"/> sld_core	8.7492	+/- 0.53093	-inf	inf	1e-6/Ang^2
<input checked="" type="checkbox"/> sld_shell	-5.6273	+/- 0.61472	-inf	inf	1e-6/Ang^2
<input checked="" type="checkbox"/> sld_solvent	7.9615	+/- 0.49028	-inf	inf	1e-6/Ang^2
<input checked="" type="checkbox"/> volfraction	0.45775	+/- 0.052516	0	inf	
<input checked="" type="checkbox"/> fractal_dim	0.9039	+/- 0.14853	-inf	inf	
<input checked="" type="checkbox"/> cor_length	3.6011	+/- 0.81379	0	inf	Ang

Polydispersity and Orientational Distribution

On     Off   

	PD[ratio]		Min	Max	Npts	Nsigs	Function
<input checked="" type="checkbox"/> Distribution of radius	0.2271	+/- 0.000352C		35	3		gaussian ▾
<input checked="" type="checkbox"/> Distribution of thickness	-0.31806	+/- 0.0031851		35	3		gaussian ▾

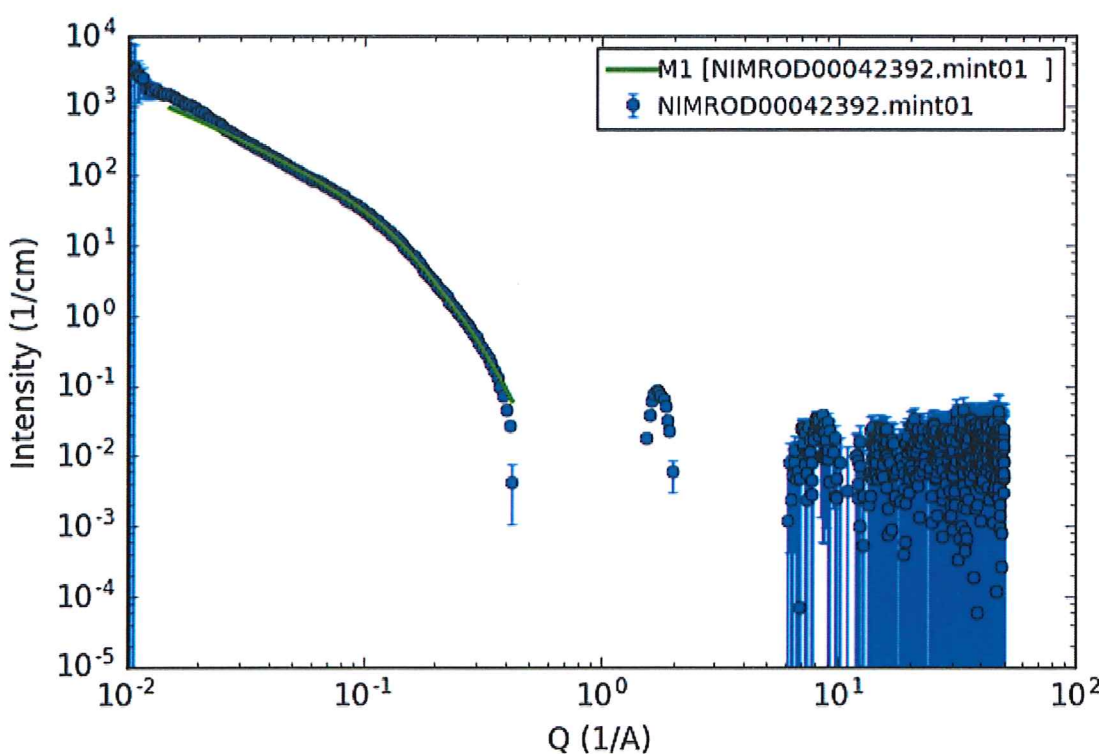
Fitting

Set Instrumental Smearing

None     Use dQ Data     Custom Pinhole Smear     Custom Slit Smear   

No smearing is selected...

Set Weighting by Selecting all Source



*shape-independent*

# adsorbed\_layer

Scattering from an adsorbed layer on particles

Parameter	Description	Units	Default value
scale	Source intensity	None	1
background	Source background	cm <sup>-1</sup>	0.001
second_moment	Second moment of polymer distribution	Å	23
adsorbed_amount	Adsorbed amount of polymer	mg·m <sup>-2</sup>	1.9
density_shell	Bulk density of polymer in the shell	g·cm <sup>-3</sup>	0.7
radius	Core particle radius	Å	500
volfraction	Core particle volume fraction	None	0.14
sld_shell	Polymer shell SLD	10 <sup>-6</sup> Å <sup>-2</sup>	1.5
sld_solvent	Solvent SLD	10 <sup>-6</sup> Å <sup>-2</sup>	6.3

The returned value is scaled to units of cm<sup>-1</sup> sr<sup>-1</sup>, absolute scale.

This model describes the scattering from a layer of surfactant or polymer adsorbed on large, smooth, notionally spherical particles under the conditions that (i) the particles (cores) are contrast-matched to the dispersion medium, (ii)  $S(Q) \sim 1$  (ie, the particle volume fraction is dilute), (iii) the particle radius is  $\gg$  layer thickness (ie, the interface is locally flat), and (iv) scattering from excess unadsorbed adsorbate in the bulk medium is absent or has been corrected for.

*I guess this doesn't make sense for ASW?*

Unlike many other core-shell models, this model does not assume any form for the density distribution of the adsorbed species normal to the interface (cf, a core-shell model normally assumes the density distribution to be a homogeneous step-function). For comparison, if the thickness of a (traditional core-shell like) step function distribution is  $t$ , the second moment about the mean of the density distribution (ie, the distance of the centre-of-mass of the distribution from the interface),  $\sigma = \sqrt{t^2/12}$ .

## Definition

$$I(q) = \text{scale} \cdot (\rho_{\text{poly}} - \rho_{\text{solvent}})^2 \left[ \frac{6\pi\phi_{\text{core}}}{Q^2} \frac{\Gamma^2}{\delta_{\text{poly}}^2 R_{\text{core}}} \exp(-Q^2\sigma^2) \right] + \text{background}$$

where *scale* is a scale factor,  $\rho_{\text{poly}}$  is the sld of the polymer (or surfactant) layer,  $\rho_{\text{solvent}}$  is the sld of the solvent/medium and cores,  $\phi_{\text{core}}$  is the volume fraction of the core particles,  $\delta_{\text{poly}}$  is the bulk density of the polymer,  $\Gamma$  is the adsorbed amount, and  $\sigma$  is the second moment of the thickness distribution.

Note that all parameters except  $\sigma$  are correlated so fitting more than one of these

parameters will generally fail. Also note that unlike other shape models, no volume normalization is applied to this model (the calculation is exact).

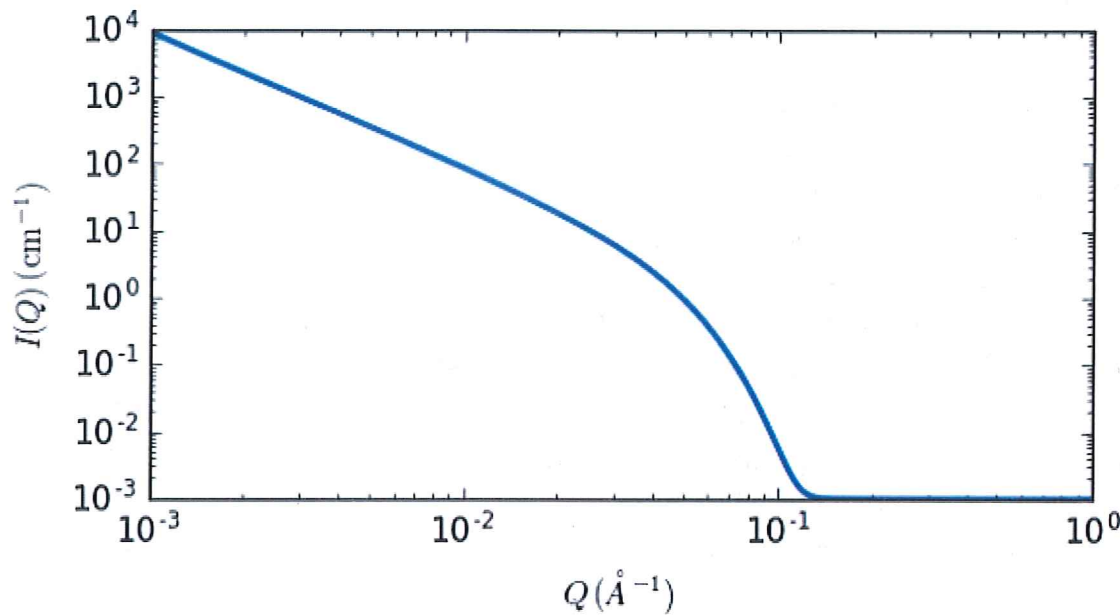
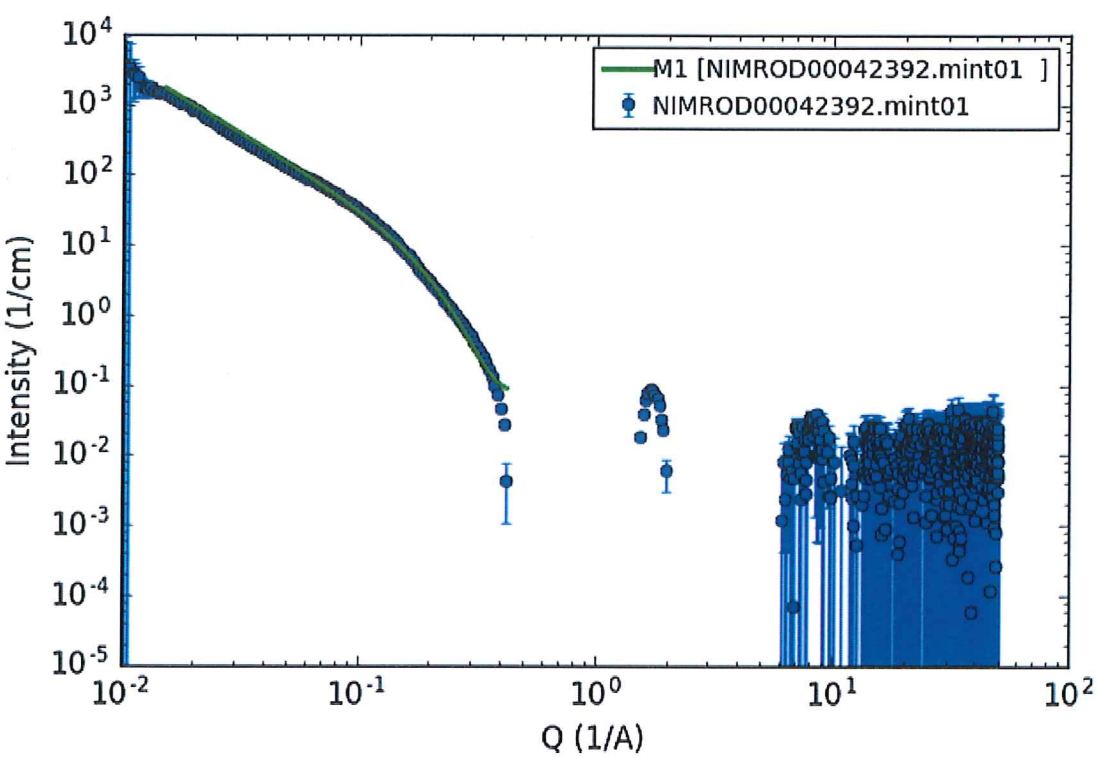


Fig. 62 1D plot corresponding to the default parameters of the model.

## References

S King, P Griffiths, J Hone, and T Cosgrove, *SANS from Adsorbed Polymer Layers*, *Macromol. Symp.*, 190 (2002) 33-42.

shape-independent  
adsorbed\_layer



adsorbed\_layer ▾

Polydispersity and Orientational Distribution					
<input checked="" type="radio"/> On	<input type="radio"/> Off	<a href="#">?</a>			
No polydispersity available for this model					
<b>Fitting</b>					
Set Instrumental Smearing					
<input checked="" type="radio"/> None <input type="radio"/> Use dQ Data <input type="radio"/> Custom Pinhole Smear <input type="radio"/> Custom Slit Smear <a href="#">?</a>					
No smearing is selected...					
Set Weighting by Selecting dI/Source					
<input type="radio"/> No Weighting <input checked="" type="radio"/> Use dI Data <input type="radio"/> Use  sqrt(I)  Data   <input type="radio"/> Use   I  Data					
Q Range	Min[1/Å]	Max[1/Å]	Masking(2D)		
<a href="#">Reset</a>	0.015	0.43	<a href="#">Editor</a>		

Model Parameters					
	Value	Error	Min	Max	[Units]
<input checked="" type="checkbox"/> Select All	1.9643	+/- 57562	0	inf	
<input checked="" type="checkbox"/> scale	0.077542	+/- 0.0012116	0	inf	1/cm
<input checked="" type="checkbox"/> background	5.4267	+/- 0.0034654	0	inf	Ang
<input checked="" type="checkbox"/> second_moment	2.6369	+/- NaN	0	inf	mg/m^2
<input checked="" type="checkbox"/> adsorbed_amount	0.4966	+/- 15148	0	inf	g/cm^3
<input checked="" type="checkbox"/> radius	248.64	+/- 1.2418e+0	0	inf	Ang
<input checked="" type="checkbox"/> volffraction	0.3432	+/- NaN	0	inf	None
<input checked="" type="checkbox"/> sld_shell	3.823	+/- NaN	-inf	inf	1e-6/Ang^2
<input checked="" type="checkbox"/> sld_solvent	9.0098	+/- NaN	-inf	inf	1e-6/Ang^2

$$\Delta \bar{x} = \sqrt{\frac{1}{m \cdot (m-1)} \sum_{i=1}^m (\bar{x} - x_i)^2} \quad | m=2$$

$$\Rightarrow \Delta \bar{x} = \sqrt{\frac{1}{2 \cdot 1} \cdot \left[ (\bar{x} - x_1)^2 + (\bar{x} - x_2)^2 \right]}$$
$$= \sqrt{\frac{1}{2} \cdot \left[ \left( \frac{x_1+x_2}{2} - x_1 \right)^2 + \left( \frac{x_1+x_2}{2} - x_2 \right)^2 \right]}$$
$$= \sqrt{\frac{1}{2} \cdot \left[ \left( \frac{x_2-x_1}{2} \right)^2 + \left( \frac{x_1-x_2}{2} \right)^2 \right]}$$
$$= \sqrt{\frac{1}{2} \cdot \left( \frac{1}{2} \right)^2 \cdot 2 \cdot (x_1 - x_2)^2}$$
$$= \left| \frac{1}{2} (x_1 - x_2) \right| = \left| \frac{x_1 - x_2}{2} \right|$$

130.01.2017

$$f(x) = off + \frac{int}{\sqrt{2\pi s^2}} \cdot e^{-\frac{(x-t_0)^2}{2s^2}}$$

$$\Delta f = \left[ \left( \frac{\partial f}{\partial x} \cdot \Delta x \right)^2 + \left( \frac{\partial f}{\partial off} \cdot \Delta off \right)^2 + \left( \frac{\partial f}{\partial int} \cdot \Delta int \right)^2 + \left( \frac{\partial f}{\partial s} \cdot \Delta s \right)^2 + \left( \frac{\partial f}{\partial b} \cdot \Delta b \right)^2 \right]^{0.5}$$

$$\frac{\partial f}{\partial x} = \left( \frac{f - off}{int} \right) \left( -\frac{2(x-t_0)}{2s^2} \right)$$

$$\frac{\partial f}{\partial s} = \left( \frac{f - off}{int} \right) + \frac{2(x-t_0)^2}{2s^3}$$

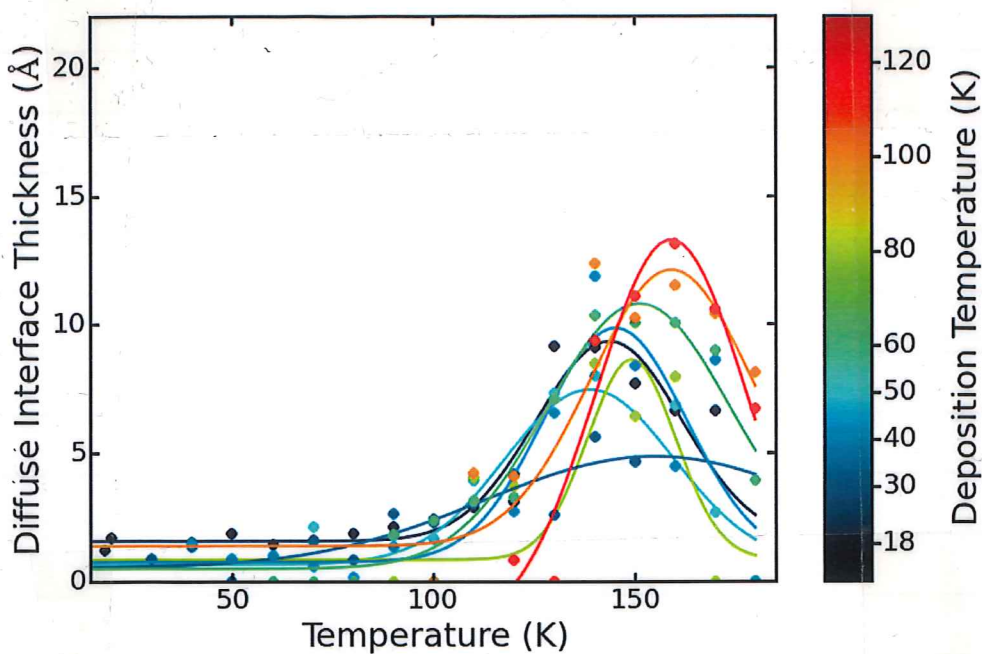
$$\frac{\partial f}{\partial int} = \left( \frac{f - off}{int} \right) \cdot \left( +\frac{2(x-t_0)}{2s^2} \right)$$

continue with: ISIS on ASW - Data Analysis

C

### Diffuse Interface Thickness

fitted with Gaussian to  
get Temperature ( $t_0$ )  
& Thickness of  
Maximum



$$f(x) = off + \frac{int}{\sqrt{2\pi}s} \cdot e^{-\frac{(x-t_0)^2}{2s^2}}$$

$$\frac{\partial f}{\partial x} = \frac{int}{\sqrt{2\pi}s} \cdot e^{-\frac{(x-t_0)^2}{2s^2}} \cdot \left( -\frac{2(x-t_0)}{2s^2} \right) = -\frac{int}{\sqrt{2\pi}s} \cdot e^{-\frac{(x-t_0)^2}{2s^2}} \cdot \frac{x-t_0}{s^2}$$

$$\frac{\partial f}{\partial off} = 1$$

$$\frac{\partial f}{\partial int} = \frac{1}{\sqrt{2\pi}s} \cdot e^{-\frac{(x-t_0)^2}{2s^2}}$$

$$\frac{\partial f}{\partial s} = \frac{int}{\sqrt{2\pi}s} \cdot e^{-\frac{(x-t_0)^2}{2s^2}} \cdot \left( +\frac{2(x-t_0)^2}{2s^3} \right) + \left( -\frac{int}{\sqrt{2\pi}s^2} \cdot e^{-\frac{(x-t_0)^2}{2s^2}} \right)$$

$$= \frac{int}{\sqrt{2\pi}s} \cdot e^{-\frac{(x-t_0)^2}{2s^2}} \cdot \left( \frac{(x-t_0)^2}{s^3} - \frac{1}{s} \right)$$

$$\frac{\partial f}{\partial t_0} = \frac{int}{\sqrt{2\pi}s} \cdot e^{-\frac{(x-t_0)^2}{2s^2}} \cdot \frac{x-t_0}{s^2}$$

$$\Rightarrow \Delta f = \left[ (\Delta off)^2 + \left( \frac{int}{\sqrt{2\pi}s} e^{-\frac{(x-t_0)^2}{2s^2}} \right)^2 \right] \cdot \left\{ \left( \frac{\Delta int}{int} \right)^2 + \left( \Delta x \cdot \frac{x-t_0}{s^2} \right)^2 + \left( \Delta t_0 \cdot \frac{x-t_0}{s^2} \right)^2 + \left( \left( \frac{(x-t_0)^2}{s^3} - \frac{1}{s} \right) \cdot \Delta s \right)^2 \right\}$$

Problem:  $x=t_0 \Rightarrow$  these terms vanish ( $x-t_0=0$ )  $\Rightarrow$  look at  $f(t_0 - \Delta t_0)$  instead

$$\Rightarrow \Delta f = \left[ (\Delta off)^2 + \left( \frac{\Delta int}{\sqrt{2\pi} s} \right)^2 + \left( \frac{\Delta int \Delta s}{\sqrt{2\pi} s^2} \right)^2 + \left( \frac{\Delta int}{\sqrt{2\pi} s} \cdot \left( 1 - e^{-\frac{(\Delta t_0)^2}{2s^2}} \right) \right)^2 \right]^{0.5}$$

$$= \left[ (\Delta off)^2 + \left( \frac{\Delta int}{\sqrt{2\pi} s} \right)^2 \cdot \left\{ \left( \frac{\Delta int}{\Delta int} \right)^2 + \left( \frac{\Delta s}{s} \right)^2 + \left( 1 - e^{-\frac{(\Delta t_0)^2}{2s^2}} \right)^2 \right\} \right]^{0.5}$$

$\Rightarrow$  error propagation from the fit produces huge uncertainties, because  $int \& s$  come out with  $> 100\%$  uncertainties from the fits

$\Rightarrow$  estimate uncertainty in max thickness to be maximum standard deviation of the mean from averaging thickness of individual samples at each  $T$

31.01.2017

**Fit SSA decay:** Onset looks linear, then turn over to ?exponential?

$$\Rightarrow SSA(T) = \begin{cases} off_s_1 + \text{grad. } T & , T \leq T_1 \quad \Leftarrow f_1(T) \\ off_s_2 + \text{int. } e^{-\frac{T}{\tau}} & , T_1 < T \quad \Leftarrow f_2(T) \end{cases}$$

$$f_1(T_1) = f_2(T_1) \Rightarrow off_s_1 + \text{grad. } T_1 = off_s_2 + \text{int. } e^{-\frac{T_1}{\tau}}$$

$$f'_1(T_1) = f'_2(T_1) \Rightarrow \left\{ \text{grad} = -\frac{\text{int}}{\tau} e^{-\frac{T_1}{\tau}} \right\} (*)$$

$$\Rightarrow off_s_1 + \left( -\frac{\text{int}}{\tau} e^{-\frac{T_1}{\tau}} \right) \cdot T = off_s_2 + \text{int. } e^{-\frac{T_1}{\tau}}$$

$$\Rightarrow off_s_1 - off_s_2 = \text{int. } e^{-\frac{T_1}{\tau}} \cdot \left( 1 + \frac{T_1}{\tau} \right)$$

$$\Rightarrow \text{int. } = \frac{off_s_1 - off_s_2}{1 + \frac{T_1}{\tau}} \cdot e^{\frac{T_1}{\tau}} \quad (**)$$

$$16.02.2017 \quad (*) \Rightarrow -\frac{\text{grad. } \tau}{\text{int. }} = e^{-\frac{T_1}{\tau}} \Rightarrow -\frac{T_1}{\tau} = \ln \left( -\frac{\text{grad. } \tau}{\text{int. }} \right) \Rightarrow T_1 = -\tau \cdot \ln \left( \frac{-\text{grad. } \tau}{\text{int. }} \right)$$

$$(**) \Rightarrow \text{int. } = \frac{off_s_1 - off_s_2}{1 - \ln \left( \frac{-\text{grad. } \tau}{\text{int. }} \right)} \cdot e^{-\ln \left( \frac{-\text{grad. } \tau}{\text{int. }} \right)} = \frac{off_s_1 - off_s_2}{1 - \ln \left( \frac{-\text{grad. } \tau}{\text{int. }} \right)} \cdot \frac{\text{int. }}{-\text{grad. } \tau}$$

$$\Rightarrow 1 - \ln \left( \frac{-\text{grad. } \tau}{\text{int. }} \right) = -\frac{off_s_1 - off_s_2}{\text{grad. } \tau} \Rightarrow \ln \left( \frac{-\text{grad. } \tau}{\text{int. }} \right) = 1 + \frac{off_s_1 - off_s_2}{\text{grad. } \tau}$$

$$\Rightarrow -\frac{\text{grad. } \tau}{\text{int. }} = e^{1 + \frac{off_s_1 - off_s_2}{\text{grad. } \tau}} \Rightarrow \text{int. } = -\text{grad. } \tau \cdot e^{-\left( 1 + \frac{off_s_1 - off_s_2}{\text{grad. } \tau} \right)}$$

Günier - Porod fits:

Radius of gyration: sphere ( $s=0$ ):  $R_g = R \cdot \sqrt{\frac{3}{5}}$ ,  $R$  = radius of sphere

cylinder ( $s=1$ ):  $R_g = R \cdot \sqrt{\frac{1}{2}}$ ,  $R$  = radius of cylinder

lamella ( $s=2$ ):  $R_g = T \cdot \sqrt{\frac{1}{12}}$ ,  $T$  = thickness of lamella

Pore dimensions: assume  $s$  to linearly change ( $1 \rightarrow 2$ )

for transition (cylinder  $\rightarrow$  disk)

swap  $\rightarrow$  see 3.8.17

$$\begin{aligned} \Rightarrow R_g &= (s-1) \cdot R \cdot \sqrt{\frac{1}{2}} + (2-s) \cdot T \cdot \sqrt{\frac{1}{12}} \quad | \quad T = \alpha \cdot R \\ &= (s-1) \cdot R \cdot \sqrt{\frac{1}{2}} + (2-s) \cdot \alpha \cdot R \cdot \sqrt{\frac{1}{12}} \\ &= R \cdot ((s-1) \sqrt{\frac{1}{2}} + \alpha(2-s) \cdot \sqrt{\frac{1}{12}}) \end{aligned}$$

$\Rightarrow$  need function  $\alpha(s)$  to move on  $\Rightarrow$  continue 24.03.2017

Uncertainties for SSA decay fit:

20.02.2017

$$\frac{\partial \text{int}}{\partial \text{grad}} = -\tau \cdot e - (1 + \frac{\text{off}_1 - \text{off}_2}{\text{grad} \cdot \tau}) + \text{grad} \cdot \tau \cdot e - (1 + \frac{\text{off}_1 - \text{off}_2}{\text{grad} \cdot \tau}) \cdot (1) \cdot \frac{\text{off}_1 - \text{off}_2}{\text{grad}^2 \cdot \tau}$$

$$= \text{int} \cdot \left( \frac{\text{off}_1 - \text{off}_2}{\text{grad} \cdot \tau} - \frac{1}{\text{grad}} \right) = \frac{\text{int}}{\text{grad}} \cdot \left( \frac{\text{off}_1 - \text{off}_2}{\text{grad} \cdot \tau} - 1 \right)$$

$$\frac{\partial \text{int}}{\partial \tau} = \frac{\text{int}}{\tau} \cdot \left( \frac{\text{off}_1 - \text{off}_2}{\text{grad} \cdot \tau} - 1 \right)$$

$$\frac{\partial \text{int}}{\partial \text{off}_1} = \frac{\text{int}}{\text{grad} \cdot \tau}$$

$$\frac{\partial \text{int}}{\partial \text{off}_2} = \frac{\text{int}}{\text{grad} \cdot \tau}$$

$$\Rightarrow \Delta \text{int} = \text{int} \cdot \left\{ \left[ \left( \frac{\Delta \text{grad}}{\text{grad}} \right)^2 + \left( \frac{\Delta \tau}{\tau} \right)^2 \right] \cdot \left( \frac{\text{off}_1 - \text{off}_2}{\text{grad} \cdot \tau} - 1 \right)^2 + \left( \frac{\Delta \text{off}_1}{\text{grad} \cdot \tau} \right)^2 + \left( \frac{\Delta \text{off}_2}{\text{grad} \cdot \tau} \right)^2 \right\}^{0.5}$$

$$\frac{\partial T_1}{\partial \text{grad}} = +\tau \cdot \frac{\text{int}}{\text{grad} \cdot \tau} \cdot \frac{\tau}{\text{int}} = \frac{\tau}{\text{grad}} \quad | \quad \frac{\partial T_1}{\partial \text{int}} = -\tau \cdot \frac{\text{int}}{\text{grad} \cdot \tau} \cdot \frac{\text{grad} \cdot \tau}{\text{int}^2} = -\frac{\tau}{\text{int}}$$

$$\left( \frac{T_1}{\Delta \tau} \right) = -\ln \left( \frac{-\text{grad} \cdot \tau}{\text{int}} \right) + \tau \cdot \frac{\text{int}}{\text{grad} \cdot \tau} \cdot \frac{\text{grad}}{\text{int}} = 1 - \ln \left( \frac{-\text{grad} \cdot \tau}{\text{int}} \right)$$

$$\Rightarrow \Delta T_1 = \left\{ \left[ \left( \frac{\Delta \text{grad}}{\text{grad}} \right)^2 + \left( \frac{\Delta \text{int}}{\text{int}} \right)^2 \right] \cdot \tau^2 + (\Delta \tau)^2 \cdot \left( 1 - \ln \left( \frac{-\text{grad} \cdot \tau}{\text{int}} \right) \right)^2 \right\}^{0.5}$$

20.03.2017

## Ornstein-Zernike Analysis:

$$S(Q) = \frac{S_0}{1 + S_0 \xi_0^2 Q^2}$$

$$\Rightarrow \ln(S(Q)) = \ln(S_0) - \ln(1 + S_0 \xi_0^2 Q^2)$$

assume  $S_0 \xi_0^2 \cdot Q^2 \gg 1$  :  $\Leftarrow$  high-Q

$$\begin{aligned} \Rightarrow \ln(S(Q)) &\approx \ln(S_0) - \ln(S_0 \xi_0^2 Q^2) \\ &= -\ln(\xi_0^2) - 2 \cdot \ln(Q) \end{aligned}$$

$\Rightarrow$  straight line with slope -2

$\rightsquigarrow$  need to not have  $S_0 \xi_0^2 Q^2 \gg 1$

$$Q \approx \frac{1}{10} \Rightarrow S_0 \xi_0^2 \approx 10$$

$$S_0 = \frac{1}{100} \Rightarrow \xi_0^2 \approx 1000 \Rightarrow \xi_0 \approx 30$$

assume  $S_0 \xi_0^2 Q^2 \ll 1$  :  $\Leftarrow$  low-Q

$$\ln(S(Q)) = \ln(S_0) \Rightarrow \text{constant}$$

$\Rightarrow$  this function will turn from a constant at low Q  
to straight line with slope -2 at high Q (in log-log-plot)  
 $S_0$  &  $\xi_0$  determine the low Q value and the turning point.  
 $\Rightarrow$  No way to make that fit our data

530

# MODELS OF DISORDER:

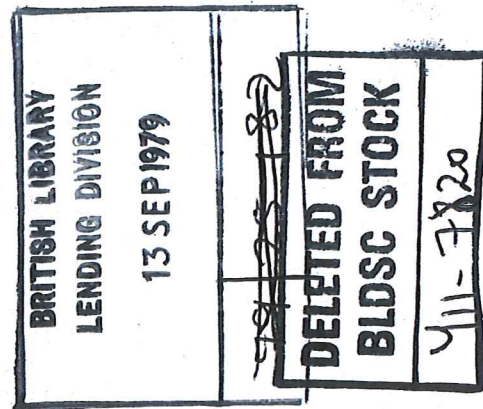
*The theoretical physics of homogeneous  
disordered systems*

2 7  
J. M. ZIMAN, FRS

H. O. WILLS PROFESSOR OF PHYSICS IN THE  
UNIVERSITY OF BRISTOL

'The whole world is in a state of chassis!'

Sean O'Casey



6 7  
CUP 1979

DELETED FROM  
BLDSG STOCK  
411-7120  
CAMBRIDGE UNIVERSITY PRESS

CAMBRIDGE

LONDON · NEW YORK · MELBOURNE

this into a formal language we should consider transitions between neutron states of different frequencies (i.e. energies)  $\Omega$  and  $\Omega'$ . In place of (4.2) we may write

$$\langle \mathbf{Q}', \Omega' | \mathcal{U} | \mathbf{Q}, \Omega \rangle = \frac{1}{V} \int \mathcal{U}(\mathbf{R}, t) e^{i(\omega t - \mathbf{q} \cdot \mathbf{R})} d^3 \mathbf{R} dt, \quad (4.17)$$

where  $\omega = \Omega' - \Omega$  is the change of energy in the diffraction process. In effect, this matrix element is proportional to the Fourier transform  $n(\mathbf{q}, \omega)$  of the *density operator*

$$n(\mathbf{R}, t) = \frac{1}{V} \sum_i \delta(\mathbf{R} - \mathbf{R}_i(t)) \quad (4.18)$$

for the positions  $\mathbf{R}_i(t)$  of the atomic nuclei as functions of time. But without knowledge of the phases of the scattered radiation we cannot go back from the inelastic diffraction intensity  $I(\mathbf{q}, \omega)$  to this density function. The generalized structure factor  $S(\mathbf{q}, \omega)$  is a spectral density function in both space and time: by the Wiener-Kintchine theorem (3.8) it must be the Fourier transform of the *van Hove correlation function* (cf. (3.4))

$$\Gamma(\mathbf{R}, t) = \langle n^*(\mathbf{R}', t') n(\mathbf{R} + \mathbf{R}', t + t') \rangle. \quad (4.19)$$

In principle, this is all that we can learn from this sort of experiment.

Inelastic neutron diffraction thus provides valuable evidence concerning the *dynamics* of our system. But it is almost impossible to unscramble the information provided by  $S(\mathbf{q}, \omega)$  or  $\Gamma(\mathbf{R}, t)$  without a theoretical model for comparison. For a crystal we interpret the observations quite easily (and to very good effect) in the phonon representation; for a glass or liquid the problem of representing the vibrational modes is much more complicated (see § 11.1) and most attempts to describe the *diffusive* motion of the atoms are frankly phenomenological.

But information about the static structure of the system is given by  $\Gamma(\mathbf{R}, 0)$  whose Fourier representation contains an integral of  $S(\mathbf{q}, \omega)$  over all frequencies. The *static structure factor* that we should use in any formula such as (4.10) is given by

$$S(\mathbf{q}) = \int_{-\infty}^{\infty} S(\mathbf{q}, \omega) d\omega. \quad (4.20)$$

Unfortunately, for elementary geometrical reasons, this integration is not quite the same as the experimental result one would obtain by the simple device of collecting all neutrons diffracted into a given *direction*, regardless of energy. Corrections for this effect are again part of the standard technique of structure determination by neutron diffraction. Neutrons are sensitive, through their intrinsic spin, to the magnetization

### 4.3 Structure determination by X-rays

X-ray diffraction differs from neutron diffraction in two main respects. On the one hand, the effects of inelasticity of scattering can be ignored. The energy of X-rays of a given wavelength is much higher than that of neutrons. The small change of energy in the diffraction process produces a negligible relative change in the momentum, so that the integration (4.20) for the structure factor is accurately achieved by collecting all the radiation scattered in a given direction.

On the other hand, X-rays are scattered by the *electrons* in an atom or solid, so that the atomic potential  $u(\mathbf{R})$  cannot be considered as concentrated at the nucleus. The atomic form factor for X-rays is, in fact, the Fourier transform of the *electron density*  $\rho(\mathbf{R})$  in an atom and is not, therefore, independent of the momentum transfer  $\mathbf{q}$ . To determine the structure factor we must follow (4.7) and divide the observed diffraction intensity by this form factor – usually obtained by independent diffraction measurements on a gas of free atoms. But this begs the question whether the actual electron density in the condensed phase can be represented, as in (4.6), as a superposition of free atom densities. In principle, there should be some redistribution of charge in the interstitial regions. By very careful measurements this effect can be observed in some semiconductor crystals but is, of course, entirely masked by the general disorder in a glass or liquid.

### 4.4 Small-angle scattering

The diffraction of X-rays with a small scattering vector – i.e. through a small angle from the incident beam – provides information about the state of the specimen over distances larger than a few atomic diameters. Near a phase transition, where the range of order becomes large (§ 1.7), this information can become significant (§ 5.12). The behaviour of  $S(q)$  for small  $q$  is also important in some theoretical formulae for the electrical properties of liquid metals, etc. (§ 10.1).

The limiting value of the structure factor as  $q \rightarrow 0$  simply measures the macroscopic variance of the density of the medium. Starting from the Fourier integral (4.11) we return to the definitions of the distribution

functions in § 2.7; the integral over the pair distribution function is then thought of as an ensemble expectation of the *square* of the number of atoms in a volume – remembering that the atom at the origin is not counted again. Thus (Green 1952; Hill 1956)

$$\begin{aligned} S(0) &= 1 + n \int \{g(\mathbf{R}) - 1\} d^3\mathbf{R} \\ &= 1 + \frac{1}{\langle N \rangle} \iint \{n(1, 2) - n(1)n(2)\} d\mathbf{l}_1 d\mathbf{l}_2 \\ &= [\langle N^2 \rangle - \langle \langle N \rangle \rangle^2] \langle \langle N \rangle \rangle. \end{aligned} \quad (4.21)$$

But the amplitude of fluctuations of macroscopic density is calculable by thermodynamics being simply proportional to the *isothermal compressibility*  $\kappa_r$ . In general, therefore, for a thermodynamic system such as liquid or crystal, we have

$$S(0) = n\kappa_r T \kappa_r. \quad (4.22)$$

Under ordinary circumstances this is all that we need to know: as  $q$  decreases,  $S(q)$  falls quickly from its main peak to a value near  $S(0)$ , where it stays nearly constant as  $q \rightarrow 0$ . In other words, the density fluctuations reach their thermodynamic amplitude for regions of only a few dozen atoms and are then more or less uncorrelated. For most liquids, in fact, this limiting value of  $S(0)$  is a few per cent. It is interesting to note that the variance of the cell volume of an RCP model of hard spheres (Finney 1970; see fig. 2.42) is only 0.0016, which is much smaller than the thermodynamic variance. In other words, ideal hard-sphere packing is much more uniform in density than is required by the thermal fluctuations in an actual liquid. Notice, however, that a glass is not in thermodynamic equilibrium so that there is nothing to prevent large fluctuations of density having been frozen in without having to satisfy (4.22) for the compressibility in the rigid phase.

The reference to density fluctuations in (4.21) strongly suggests that we should think about small-angle X-ray scattering (SAXS) as a *continuum effect*, without regard to the contributions of the individual atoms. Following (4.19), for example, and smoothing the sum in (4.18) into a continuous density variable  $n(\mathbf{R}, t)$ , we see that  $S(q)$  for small  $q$  is nothing more than the spectral function (3.8) for variations of ‘local’ density, about the mean value  $n$ . The variable

$$\Delta n(\mathbf{R}, t) = n(\mathbf{R}, t) - n \quad (4.23)$$

is a random field of continuum disorder, of the kind discussed in chapter 3.

This provides a very simple model for the analogous phenomenon of *optical scattering* (see e.g. McIntyre & Sengers 1968) by fluids and glasses.

#### We simply assume that the local refractive index, $\epsilon(\mathbf{R})$ , varies from place to place by an amount proportional to the local density, i.e.

$$\Delta\epsilon(\mathbf{R}) = \gamma \Delta n(\mathbf{R}) \quad (4.24)$$

(with time variation as well, if necessary). This variation will appear in the wave equation for light propagation in this medium as a small perturbation term, which gives rise to transitions between the incident and scattered beams (cf. § 10.1). The argument is no deeper than the Born approximation: it is very easy to show that the intensity of the scattered radiation for a change of wave vector  $\mathbf{q}$  is proportional to  $q^2$  and to the spectral function  $S(q)$  of the density field  $n(\mathbf{R})$ . Inelastic diffraction due to time variation of the density is also accounted for, exactly as in (4.17). Optical scattering may have technical advantages, especially for measurements of small momentum transfer and small changes of energy, but it responds to precisely the same structural features as small-angle X-ray scattering.

But (4.22) only tells us the limiting value of the structure factor: it does not tell us the form of the spectrum for non-zero values of  $q$ . In the neighbourhood of a *critical point* the compressibility of a fluid can become very large, so that the behaviour of  $S(q)$  between  $S(0)$  and the main peak comes into question. This point was discussed long ago in the famous paper by Ornstein & Zernike (1914). Notice the very simple relation (4.14) between the Fourier representation of the direct correlation function  $c(q)$  and the structure factor. Evidently, if  $S(q)$  becomes large near  $q = 0$  then  $c(q)$  tends to a value near unity:

$$c(0) = 1 - 1/S(0). \quad (4.25)$$

On the other hand, when  $S(q)$  rises rapidly and exceeds unity near the main peak,  $c(q)$  behaves quite normally: this is the basic principle of the PY equation (2.44). The assumption is, therefore, that  $c(q)$  is well behaved throughout this range, and may be expanded as a power series in  $q^2$  (remember that  $q$  is the modulus of a vector quantity  $\mathbf{q}$ ) near the limiting value (4.25). We thus write

$$c(q) \approx c(0) - \xi_0^2 q^2, \quad (4.26)$$

with  $\xi_0$  to be determined. Putting this into (4.14) we have

$$\begin{aligned} S(q) &= \frac{1}{\{1 - c(0)\} + \xi_0^2 q^2} \\ &= \frac{S(0)}{1 + S(0) \xi_0^2 q^2} \end{aligned} \quad (4.27)$$

The Ornstein–Zernike spectrum of the density fluctuations is evidently

Lorentzian (as in (3.27)) in this approximation. Applying the Wiener-Kintchine formula (2.8) we obtain the density-density correlation function in the medium, in the form

$$\Gamma(R) \sim \frac{1}{R} e^{-R/\xi_1} \quad (4.28)$$

for large values of  $R$ . This is of the form (1.37), with the correlation length

$$\xi_1 = \{S(0)\}^{1/4} \xi_0. \quad (4.29)$$

The basic physical assumption of the Ornstein-Zernike theory is that the parameter  $\xi_0$  is governed by the local structural order in the fluid and is not, therefore, strongly influenced by the proximity of the critical point. Approaching this point, however,  $S(0)$  can vary rapidly with temperature and become very large; the high compressibility of the medium is associated with long-wave *critical fluctuations* of density. The *critical opalescence* observed optically yields sensitive evidence concerning, for example, the exponent of the temperature variation of the long-range order parameter under these conditions (cf. Stanley 1971). The range of order in a liquid crystal above the critical temperature can also be studied by this method (Stinson & Littser 1973). It is evident, however, from the form of (4.28) that the disorder observed over distances greater than  $\xi_1$  is best considered as a macroscopic *inhomogeneity* present in a large specimen whose local fluid structure is given, as a function of local density, by the usual statistical arguments.

In view of the heuristic assumptions in the Ornstein-Zernike formula (4.27), it is interesting to note that the exponent of  $q$  in the observed spectrum is actually quite close to 2. But model calculations for two-dimensional systems give results that are quite different from (4.27).

In the present section, our main aim is to draw attention to the information concerning large-scale disorder that can be obtained by small-angle X-ray and optical scattering. From the general argument of § 3.3, however, it is clear that an observed structure factor cannot be interpreted unambiguously as evidence for a particular type of density variation in the medium. The dynamical theory of critical fluctuations proves that these must satisfy the conditions for Gaussian disorder (cf. §§ 1.8, 3.3); but a Lorentzian spectrum such as (4.27) could equally well be characteristic of a 'step surface' model as in (3.25). There is, in fact, a considerable literature (e.g. Fournet 1957; Beeman, Kaesberg, Anderegg & Webb 1957) concerning small-angle X-ray diffraction from dispersions of small 'particles', such as colloidal suspensions. In such cases,  $S(q)$  is taken to be unity for all values

of  $q$ , whilst the scattered intensity is governed by the factor  $|u(q)|^2$ , now redefined as the diffraction factor of a whole 'particle'. If this object happens to be more or less spherical, then the formula for Rayleigh scattering would be appropriate, i.e.

$$|u(q)|^2 \propto \left[ \frac{\sin qD - qD \cos qD}{q^3 D^3} \right]^2. \quad (4.30)$$

Such observations are often analysed in terms of the *Guinier approximation* whereby the dependence of the scattering on  $q$  for small values of  $q$  is written

$$|u(q)|^2 \propto \exp\{-\frac{1}{3}q^2 D^2\}, \quad (4.31)$$

where  $D$  may be defined more explicitly as the radius of gyration of each particle. But the fact that an observed diffraction pattern happens to fit such a formula does not prove that the system actually consists of sharply defined, approximately spherical objects distributed at random in a statistically uniform matrix. This point is important in the interpretation of small-angle diffraction from, say, a glass; density or concentration fluctuations with a spectrum like (4.31) might equally well be suspected (cf. Seward & Uhlmann 1972).

#### 4.5 Diffraction by a mixture

The formula for diffraction by a mixture of various atomic species (e.g. a liquid alloy) is an elementary extension of (4.7). Let us assume, as in (4.6), that the scattering potential can be written as a superposition

$$\mathcal{U}(\mathbf{R}) = \sum_{\alpha} \sum_{i(\alpha)} u_{\alpha}(\mathbf{R} - \mathbf{R}_{i(\alpha)}) \quad (4.32)$$

where the atom at  $\mathbf{R}_{i(\alpha)}$  has potential  $u_{\alpha}$ . The Fourier transform (4.2) can be manipulated as in (4.7) into the general formula

$$I(\mathbf{q}) = N^{-2} \sum_{\alpha, \beta} \sum_{i(\alpha), j(\beta)} \exp\{-i\mathbf{q} \cdot (\mathbf{R}_{i(\alpha)} - \mathbf{R}_{j(\beta)})\} u_{\alpha}^*(\mathbf{q}) u_{\beta}(\mathbf{q}). \quad (4.33)$$

In this expression we segregate the terms for which  $\alpha = \beta$  and  $i(\alpha) = j(\beta)$ : these contribute a structure-independent term, weighted according to the relative concentrations  $c_{\alpha}$  of the components, i.e.

$$\begin{aligned} I_0(\mathbf{q}) &= N^{-1} \sum_{\alpha} c_{\alpha} |u_{\alpha}(\mathbf{q})|^2 \\ &= N^{-1} \left\{ |\vec{u}(\mathbf{q})|^2 + \sum_{\alpha} c_{\alpha} |\Delta u_{\alpha}(\mathbf{q})|^2 \right\} \end{aligned} \quad (4.34)$$

## Guinier-Porod Fits

"old" Guinier function (1934 Book: x-ray diffraction in crystals, imperfect crystals and amorphous bodies)

for spheres & ellipsoids : axes:  $a, a, v \cdot a$  (sphere:  $v=1 \Rightarrow \text{radius } a$ )

Radius of gyration:  $R = \sqrt{\frac{2+v^2}{5}} \cdot a$  (sphere:  $R = \sqrt{\frac{3}{5}} \cdot a$ )

$$I(Q) \approx e^{-\frac{4\pi^2 Q^2 R^2}{3}}$$

Taking the quadratic average on both sides,

$$R^2 = R_D^2 + R_U^2 + R_V^2,$$

where the quantity  $R$ , defined by

$$R^2 = \frac{\int r^2 dv}{V},$$

is the *radius of gyration* of the particle with respect to its center of gravity, and  $R_D, R_U, R_V$  are the inertial distances with respect to the three coordinate planes. Now if these coordinate planes are rotated about the origin,  $R^2$  remains constant and the three averages  $R_D^2, R_U^2, R_V^2$  are equal, so  $3\overline{R^2} = R^2$ . Thus the average scattering power particle in the case of random orientations is given by

$$I(s) = n^2 \exp\left(-\frac{4\pi^2 s^2 R^2}{3}\right) = n^2 \exp\left(-\frac{4\pi^2 R^2}{3\lambda^2} \epsilon^2\right), \quad (10.16)$$

where  $\epsilon$  is the scattering angle.

For a particle of known shape, the radius of gyration is easily calculated. In the case of a sphere of radius  $a$ ,  $R = (3/5)^{1/2}a$ ; for an ellipsoid of revolution with axes  $a, a, v \cdot a$ ,  $R = [(2+v^2)/5]^{1/2}a$ .

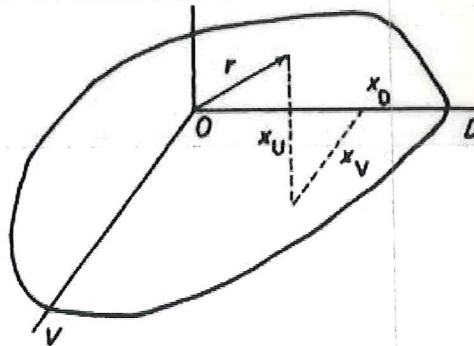


FIGURE 10.9. Calculation of the quadratic average of the inertial distance  $R_n$ .

"new" Guinier function (2010 Hammonda: A new Guinier-Porod Model)

for spheres & cylindrical objects : axes:  $a, a, v \cdot a$  (to keep notation from above)

$$R_g = \begin{cases} a \cdot \sqrt{\frac{1}{2}} \\ a \cdot v \cdot \sqrt{\frac{1}{2}} \end{cases}$$

rod  
disk

Radius of gyration

$$I(Q) \approx \frac{1}{Q^s} \cdot e^{-\frac{Q^2 R_g^2}{3-s}}$$

$\Rightarrow$  different functions  $\Rightarrow$  not comparable

22.03.2017]

Guinier - Diffuse - Interface fits:

The GP fits hardly work for the deposition data & crash whenever I slightly change the limits of the fit range.

⇒ Try diffuse interface fit instead of Porod.

$$I(Q) = GDI_1(Q) + GDI_2(Q), \quad A_1 + A_2 = 2\pi(\sigma g)^2 \text{ SSA}$$

$$GDI_i(Q) = \begin{cases} \frac{G_i}{Q^{s_i}} \cdot e^{-\frac{Q^2 R_{g_i}^2}{3-s_i}}, & Q \leq Q_i \quad \leftarrow Gf_i(Q) \\ A_i \cdot Q^{-4} \cdot e^{-\frac{Q^2 t^2}{3-s_i}}, & Q_i < Q \quad \leftarrow Df_i(Q) \end{cases}$$

derivatives:

$$\frac{dGf_1(Q)}{dQ} = G_1 \cdot Q^{-s_1} \cdot e^{-\frac{Q^2 R_{g_1}^2}{3-s_1}} \cdot \left( -s_1 \cdot Q^{-1} - 2 \cdot \frac{Q R_{g_1}^2}{3-s_1} \right)$$

$$\frac{dDf_1(Q)}{dQ} = A_1 \cdot Q^{-5} \cdot e^{-\frac{Q^2 t^2}{3-s_1}} \cdot \left( -4 \cdot Q^{-5} - 2 \cdot Q \cdot t^2 \right)$$

 $I(Q)$  continuous at  $Q_1$ :

$$\frac{G_1}{Q_1^{s_1}} \cdot e^{-\frac{Q_1^2 R_{g_1}^2}{3-s_1}} = A_1 \cdot Q_1^{-4} \cdot e^{-\frac{Q_1^2 t^2}{3-s_1}} \quad (1)$$

 $\frac{dI(Q)}{dQ}$  continuous at  $Q_1$ :

$$\frac{G_1}{Q_1^{s_1}} \cdot e^{-\frac{Q_1^2 R_{g_1}^2}{3-s_1}} \cdot \left( -s_1 \cdot Q_1^{-1} - 2 \cdot \frac{Q_1 R_{g_1}^2}{3-s_1} \right) = A_1 Q_1^{-5} \cdot e^{-\frac{Q_1^2 t^2}{3-s_1}} \cdot \left( -4 \cdot Q_1^{-1} - 2 \cdot Q_1 \cdot t^2 \right) \quad (2)$$

(1) in (2):

$$A_1 \cdot Q_1^{-4} \cdot e^{-\frac{Q_1^2 t^2}{3-s_1}} \left( -s_1 Q_1^{-1} - 2 \cdot \frac{Q_1 R_{g_1}^2}{3-s_1} \right) = A_1 Q_1^{-4} e^{-\frac{Q_1^2 t^2}{3-s_1}} \cdot \left( -4 Q_1^{-1} - 2 Q_1 \cdot t^2 \right)$$

23.03.2017

$$\Rightarrow (4-s) Q_1^{-1} + \left( 2t^2 - \frac{2R_g^2}{3-s} \right) Q_1 = 0$$

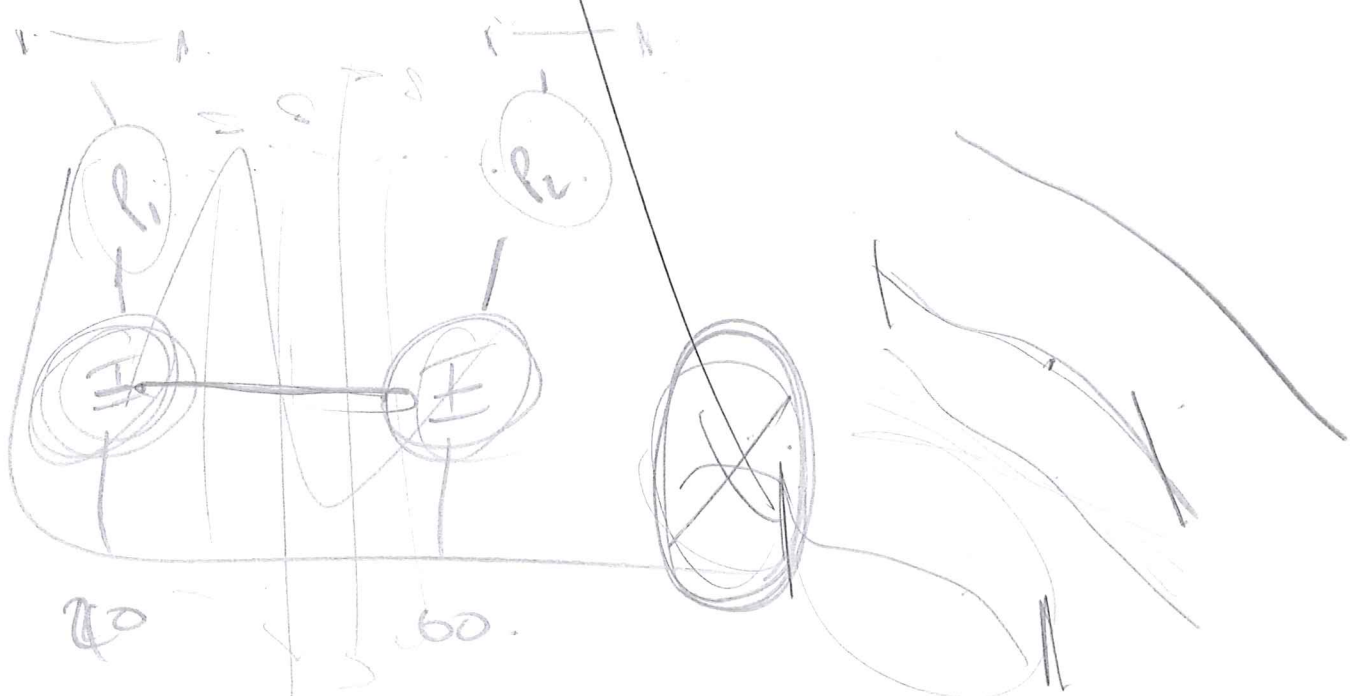
$$\Rightarrow Q_1^2 \left[ -2t^2 + \frac{2R_g^2}{3-s} \right] = 4-s \Rightarrow Q_1^2 = \frac{(4-s) \cdot (3-s)}{2R_g^2 - 2t^2(3-s)}$$

## Summary

- Park the larger scattering objects for now (require experiments on another instrument).
- Upcoming paper will focus on the micropores and the SSA of ASW.
  - Pores at low deposition T: disks, small  $R_g$
  - Pores at high deposition T: rods, larger  $R_g$
  - Heating: rods  $\rightarrow$  disks,  $R_g$  reaches minimum
  - $T > \sim 120$  K: no pores detectable, but diffuse interface
  - SSA: linear decrease below 120 K, exponential decrease above 120 K
  - SSA depends mostly on sample T, rather than deposition T
- Separate 20 K (18 K) sample from the others for now and compare the different 20 K depositions we had across various runs at another point.

## To Do

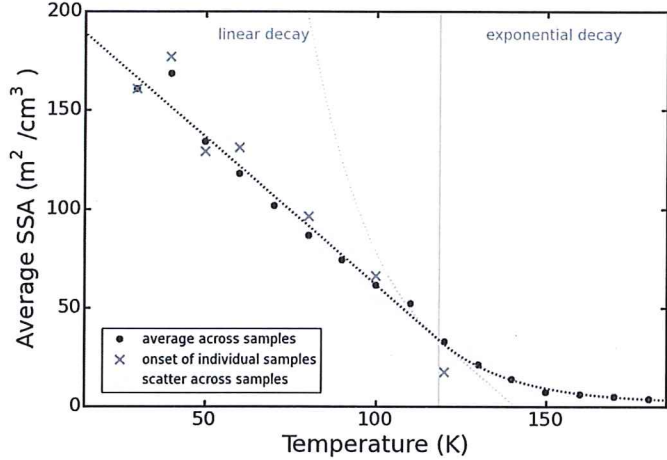
Name	Action	Status
Sabrina	Work out pore dimensions from s-parameter & $R_g$ results	No definition of s-parameter available
	Estimate pore density from SSA (how many pores of the given size would we need to create the observed surface area?)	Assume pores to be spheres of given $R_g$ ? No Linear Scale S
	Plot $I(Q)$ at fixed low-Q value vs sample T & send to Tom (to identify how much scattering stuff we have in the beam)	done
	try Ornstein-Zernike model on data between 90 and 130 K	not suitable for our data
	analyse deposition data	GP fits tricky
	analyse individual scans during heating	GP fits tricky
Helen	Work on picture of the ice that matches all our findings	?
Tom	Look for model to fit the transition region 100 – 130 K (pores difficult to fit, onset of diffuse interface)	maybe next week (27.03. – 31.03.)
	try fitting some cylinder models to the data	maybe next week
	look for definition of s-parameter	maybe next week



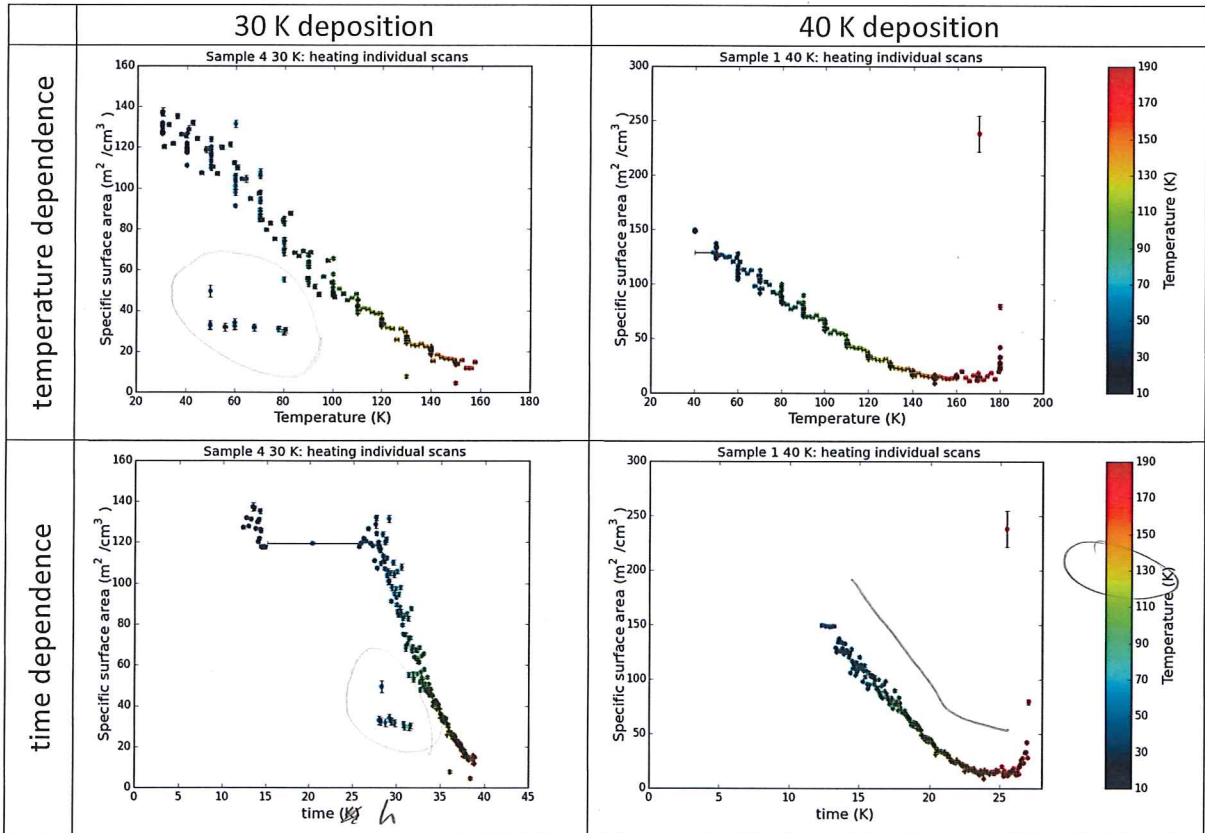
## Results

### SSA

#### Isothermal Steps



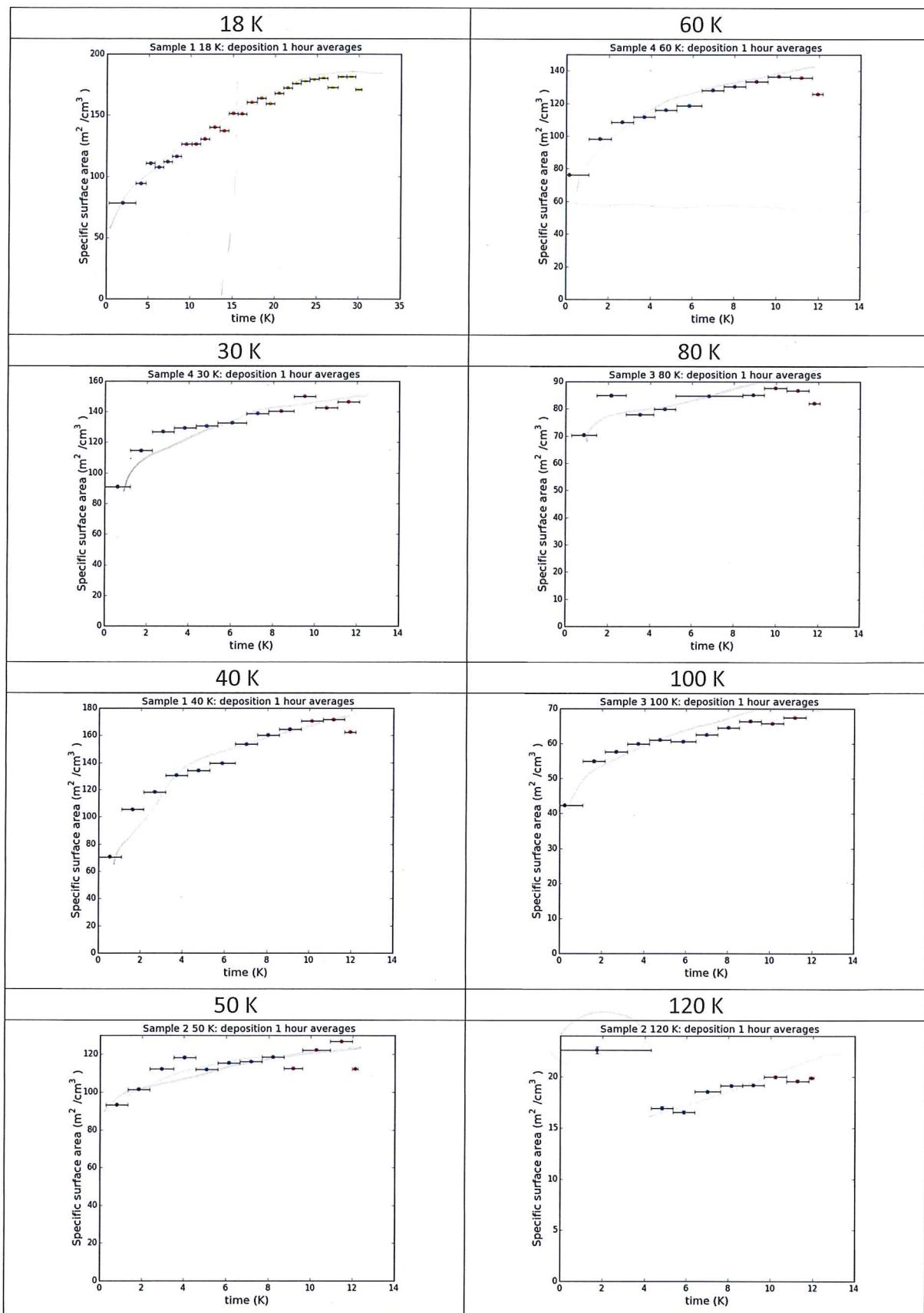
#### Individual Scans



Increase towards the end is probably artefact of fitting on poor statistics => diffuse interface fit might work better.

We might be able to get a temperature dependent rate coefficient (for the time dependence) out of the SSA data.

## Deposition

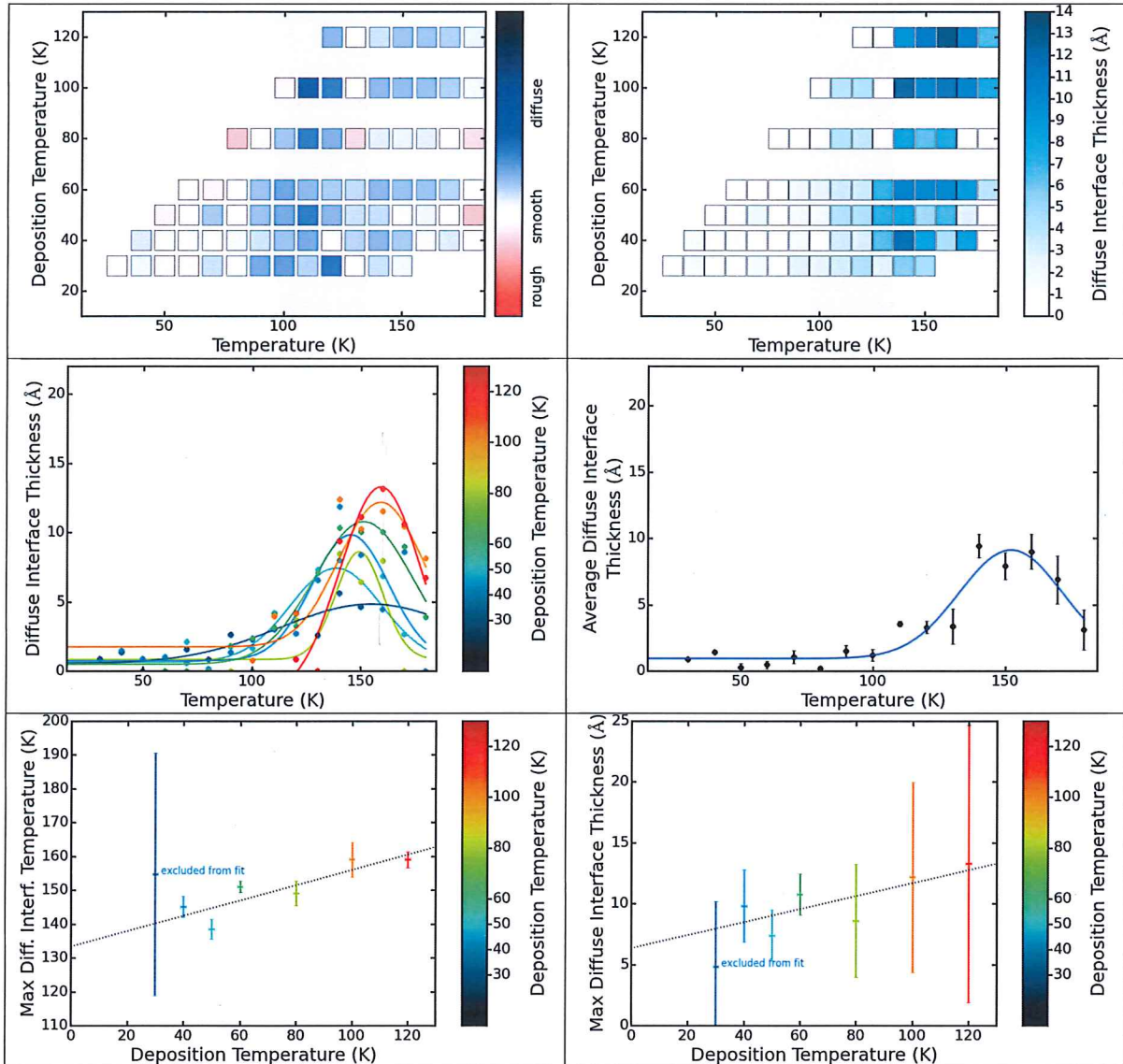


Note: the last data point, which tends to be a bit lower than the others usually has less data (can be seen from the time range the error bar spans).

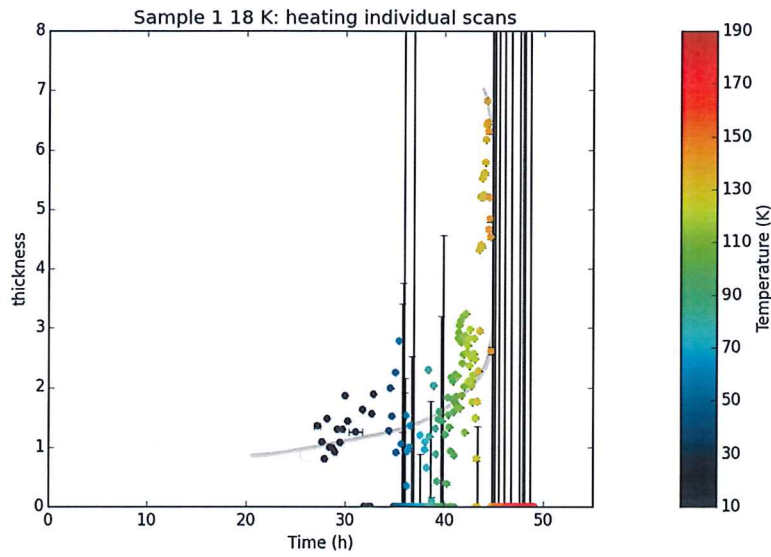
*future paper: fit exp & plot parameters vs dep. T*

## Diffuse Interface

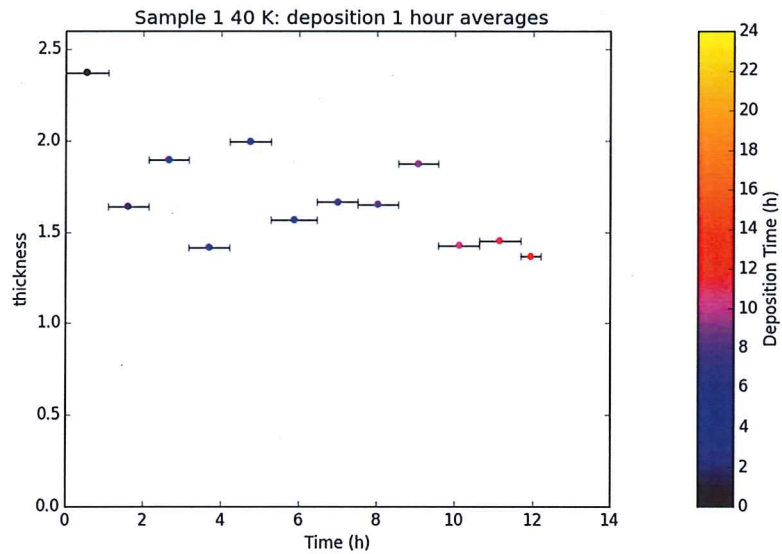
### Isothermal Steps



## Individual Scans



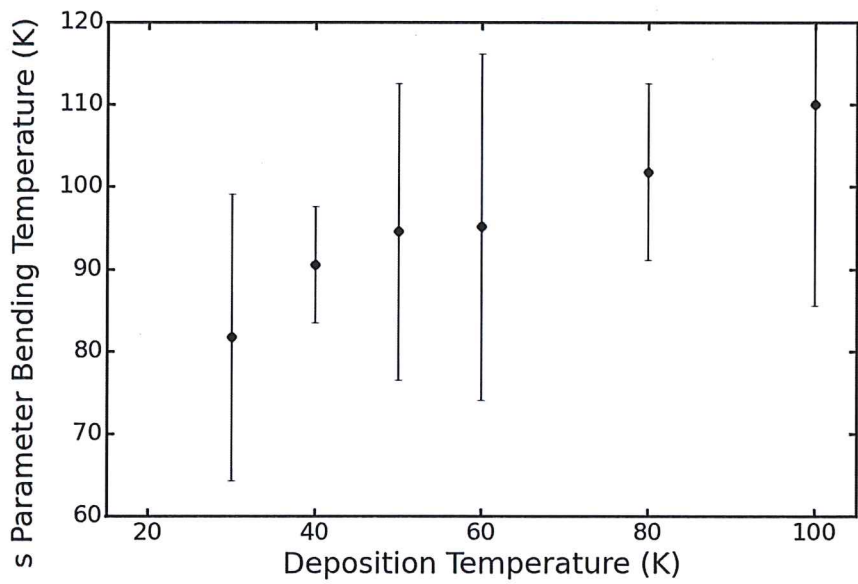
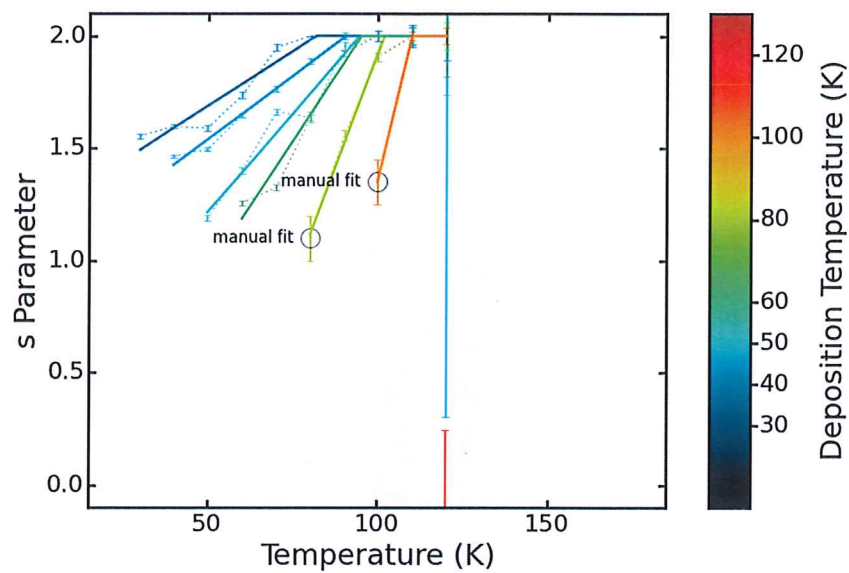
## Deposition



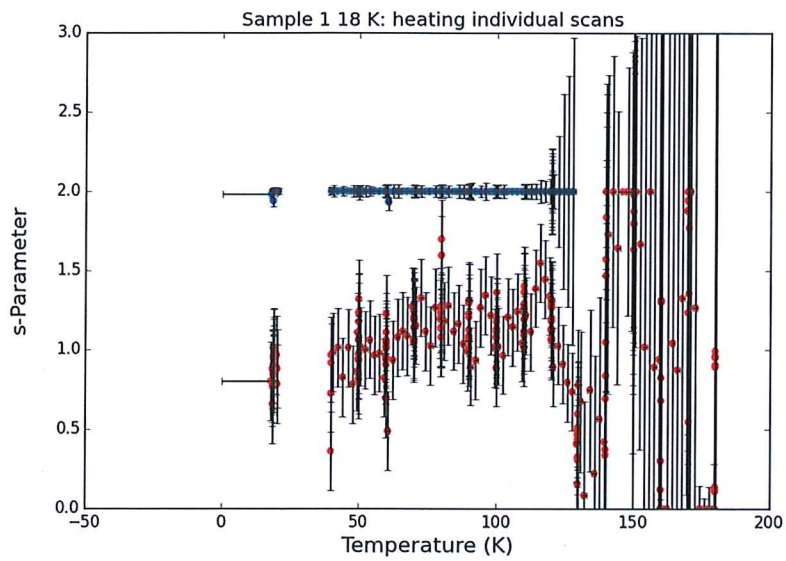
Diffuse interface fit not performed on all samples, because it requires output from Guinier-Porod fit, which barely works on deposition & individual scans (probably because poorer signal to noise).

## Pore Shape

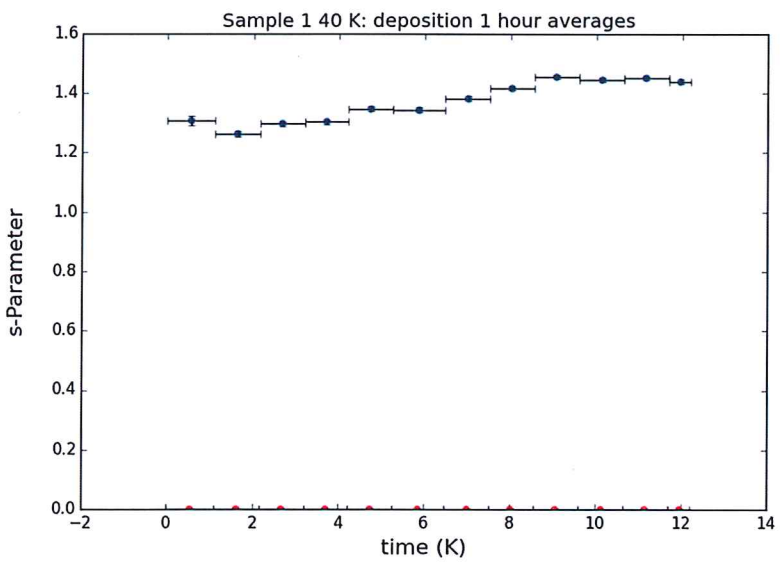
### Isothermal Steps



## Individual Scans

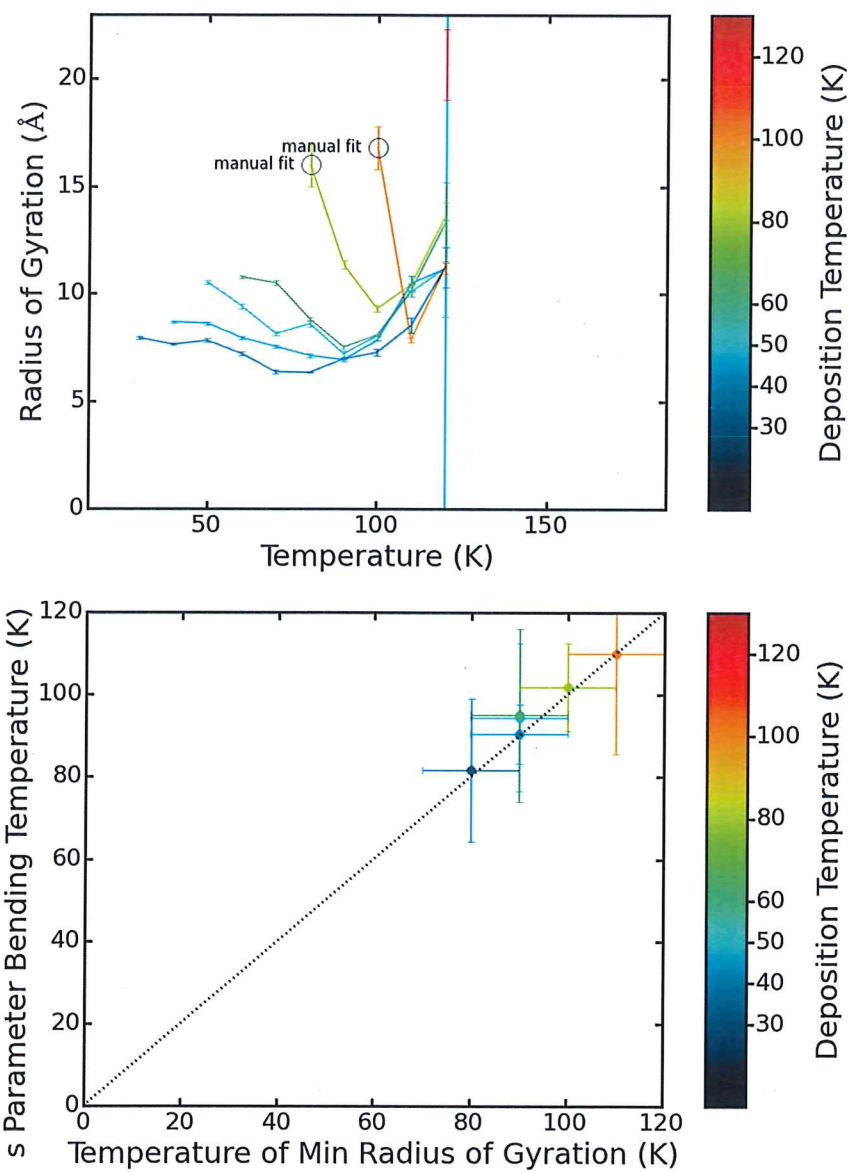


## Deposition

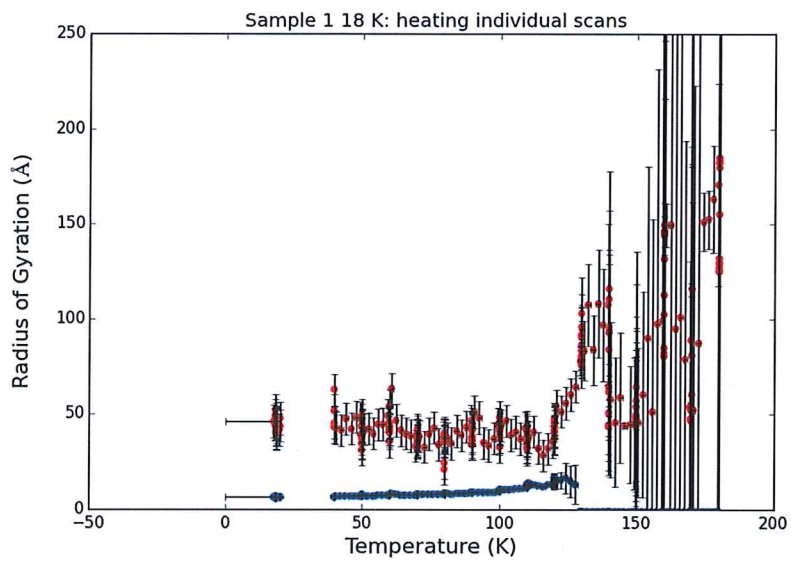


## Pore Size

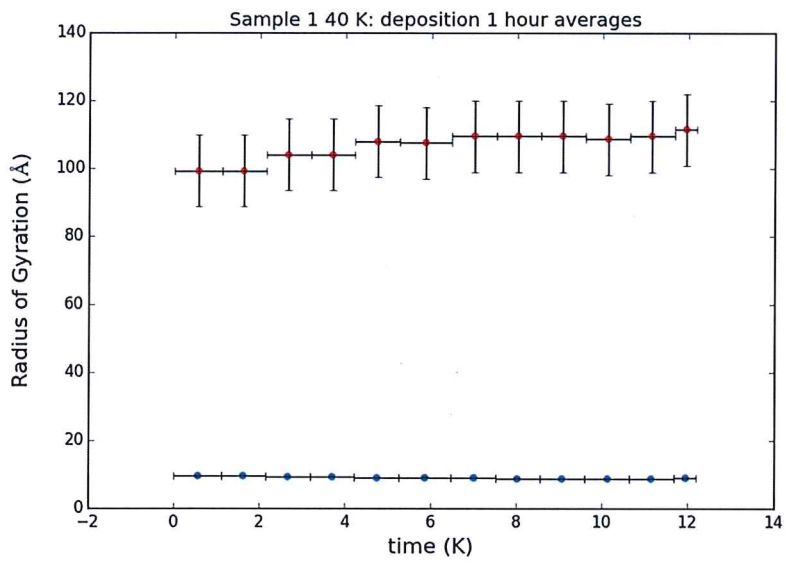
### Isothermal Steps



## Individual Scans



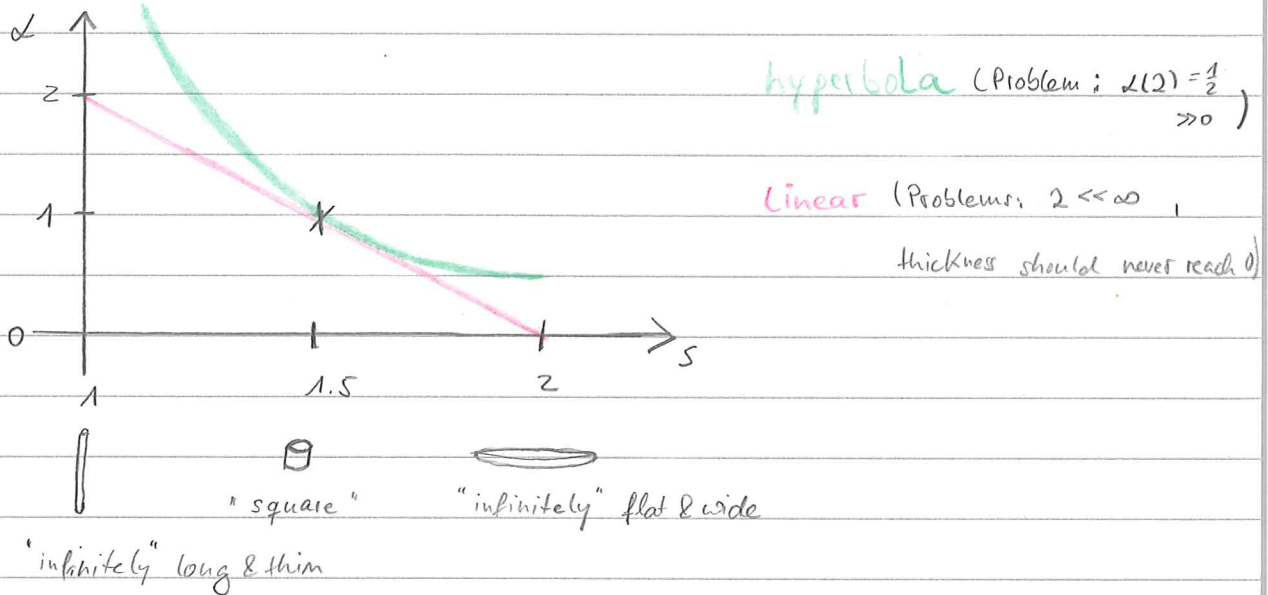
## Deposition



$$\Rightarrow Q_i = \sqrt{\frac{(4-s_i) \cdot (3-s_i)}{2Rg_i^2 - 2t^2(3-s_i)}}$$

$$(1) : A_i = G_i Q_i e^{4-s_i} Q_i^2 \left( t^2 - \frac{Rg_i^2}{3-s_i} \right)$$

Continue with Pore Dimensions:



Problem:  $Rg = 0$  for  $R=0$  or  $L=0 \Rightarrow$  can't be infinitely thin / flat

Try:  $L(s) = \frac{1}{(s-1)} \cdot \frac{1}{2}$  (hyperbola)

$$L(1) = \infty, L(1.5) = \frac{1}{\frac{1}{2}} \cdot \frac{1}{2} = 1, L(2) = \frac{1}{1} \cdot \frac{1}{2} = \frac{1}{2} \gg 0$$

~ not good

Try: exponential:  $L(s) = e^{-(s-\frac{3}{2})}$

$$L(1.5) = 1, L(2) = e^{-\frac{1}{2}} = \frac{1}{\sqrt{e}} \approx 0.6 \gg 0 \sim \text{not good}$$

Need a function that has  $\lim_{s \rightarrow 1} = \infty$ ,  $\lim_{s \rightarrow 2} = 0$ ,  $L(\frac{3}{2}) = 1$  but  $L(2) \neq 0$   
 $\Downarrow$  can be solved  
 $\Downarrow$   
can't think of any

look at pore volume for random cylinders with radius  $R$  & height  $\alpha R$

$$V = \pi \cdot R^2 \cdot \alpha R = \pi \cdot \alpha R^3$$

$$A = 2\pi R \cdot \alpha R = 2\pi \alpha R^2$$

$$R = R_g \cdot \frac{1}{\alpha(2-s)\sqrt{\frac{1}{12}} + (s-1)\sqrt{\frac{1}{2}}}$$

$$= 2\pi R_g^2 \cdot \frac{\alpha}{[\alpha(2-s)\sqrt{\frac{1}{12}} + (s-1)\sqrt{\frac{1}{2}}]^2}$$

$$\Rightarrow V = \pi R_g^3 \cdot \frac{\alpha}{[\alpha(2-s)\sqrt{\frac{1}{12}} + (s-1)\sqrt{\frac{1}{2}}]^3}$$

$$\text{Taylor series for } \alpha \approx 0: V(\alpha) = \pi R_g^3 \cdot \left[ \alpha + \frac{1}{2}\alpha^2 \cdot \frac{(\alpha(2-s)\sqrt{\frac{1}{12}} + (s-1)\sqrt{\frac{1}{2}})^3 - \alpha \cdot 3(2-s)\sqrt{\frac{1}{12}} \cdot (\alpha(2-s)\sqrt{\frac{1}{12}})^2}{1 \dots} \right]$$

$$\approx \pi R_g^3 \cdot \left( \alpha + \frac{1}{2}\alpha^2 \cdot \frac{(s-1)\sqrt{\frac{1}{2}})^3 - 0}{((s-1)\sqrt{\frac{1}{2}})^6} \right)$$

$$= \pi R_g^3 \cdot \left( \alpha + \frac{1}{2}\alpha^2 \cdot \frac{1}{((s-1)\sqrt{\frac{1}{2}})^3} \right) \quad | s=2 \text{ where } \alpha=0$$

$$= \pi R_g^3 \cdot \left( \alpha + \frac{1}{2}\alpha^2 \cdot 2\sqrt{2} \right) = \pi R_g^3 \cdot (\alpha + \sqrt{2}\alpha^2)$$

$\Rightarrow V$  will strongly depend on the values I choose for  $\alpha$

If I use that to work out pore volumes / surfaces & get pore number densities based on SSA, the results will mainly reflect the "random" choices I made for the values of  $\alpha(s)$ .

$\hookrightarrow$  continue 3.8.17

## Temperature & Time Dependence of SSA:

temperature dependence of individual scans looks like stairs ↑  
 but when sitting still at low T for  $\approx 12$  h, the change is comparable to that of 1 h steps.

Idea: each temperature has an "equilibrium" SSA that is approached with exponential time dependence

$$\text{Equilibrium SSA: } \text{ssa}(T) = A + (1 - e^{-\frac{T}{\Theta}}) \cdot (B - A)$$

$\uparrow$  lowT SSA       $\uparrow$  highT SSA

$$\text{time dependence: } \text{SSA}(t) = C + (1 - e^{-\frac{t}{\tau(T)}}) \cdot (\text{ssa}(T) - C)$$

$\uparrow$  SSA at  $t_0$        $\uparrow$

~~$$\text{derivatives: } \frac{\partial}{\partial t} \text{ssa}(T) = -B \cdot e^{-\frac{T}{\Theta}} \left( \frac{1}{\Theta} \right) = \frac{B}{\Theta} \cdot e^{-\frac{T}{\Theta}}$$

$$\frac{\partial}{\partial t} \text{SSA}(t) = \frac{C}{\tau(T)} \cdot e^{-\frac{t}{\tau(T)}}$$~~

"Fitting" the data requires numerical simulation of thermal history, including knowledge of  $T(t)$ .

Each data point can be calculated from the previous data point based on the new temperature and the time elapsed since the previous point

$$\text{SSA}(T_0, 0) = A + (1 - e^{-\frac{T_0}{\Theta}}) \cdot (B - A)$$

$$\text{SSA}(T_1, t_1) = A + (1 - e^{-\frac{T_0}{\Theta}}) \cdot (B - A) + (1 - e^{-\frac{t_1}{\tau(T_1)}}) \cdot [A + (1 - e^{-\frac{T_0}{\Theta}}) \cdot (B - A) - (A + (1 - e^{-\frac{T_0}{\Theta}}) \cdot (B - A))]$$

$$= A + (1 - e^{-\frac{T_0}{\Theta}}) \cdot (B - A) + (1 - e^{-\frac{t_1}{\tau(T_1)}}) \cdot (B - A) \cdot (e^{-\frac{T_0}{\Theta}} - e^{-\frac{T_1}{\Theta}})$$

$$\text{SSA}(T_2, t_2) = \text{SSA}(t_1) + (1 - e^{-\frac{t_2 - t_1}{\tau(T_2)}}) \cdot [A + (1 - e^{-\frac{T_2}{\Theta}}) \cdot (B - A) - \text{SSA}(t_1)]$$

$$\boxed{\text{SSA}(T_{i+1}, t_{i+1}) = \text{SSA}(t_i, t_i) + [\text{ssa}(T_{i+1}) - \text{SSA}(t_i, t_i)] \cdot (1 - e^{-\frac{t_{i+1} - t_i}{\tau(T_{i+1})}})}$$

$$\boxed{\text{test: } \text{ssa}(T) = A + (B - A) \cdot (1 - e^{-\frac{T}{\Theta}}) \quad , \quad \tilde{\tau}(T) = \tilde{\tau} \text{ (const)}}$$

Use  $T(t)$  from individual scans.

That yields results very similar to our data, but change in slope not regularized.

To reproduce change of rate coefficient by:  $\tau = \begin{cases} \bar{\tau}_1 & \bar{T} \leq T_1 \\ \bar{\tau}_2 & \bar{T} > T_1 \end{cases}$

$\Rightarrow$  that is getting more like the data, but doesn't match high  $T$  values (too high)

$\Rightarrow$  one of the rates  $\stackrel{(0, \tau)}{\text{must speed up towards higher } T}$

$$\Theta(T) = \frac{(273 K)^2 - T^2}{(220 K)^2} \cdot 65 K \quad \text{seems to help}$$

07.04.2017

Try to model deposition SSA to get a better starting point for the heating SSA evolution.

Idea: - initial SSA of freshly deposited ASW is a constant ( $T$ -independent)  
 $\Rightarrow D$

- from this value SSA develops with time towards  $T$ -dependent equilibrium  
 $\Rightarrow SSA(t) = D + (1 - e^{-\frac{t}{\tau_{dep}}}) \cdot (SSA(T) - D)$

- concurrently there is new material deposited with initial SSA  $D$   
- assume constant deposition rate:

material deposited between  $t_i$  and  $t_{i+1}$  is fraction  $\frac{t_{i+1} - t_i}{t_{i+1}}$  of all material deposited in total deposition time  $t_{i+1}$  so far

$$\Rightarrow SSA(\bar{T}_{dep}, t_{i+1}) = \left\{ SSA(\bar{T}_{dep}, t_i) + \left(1 - e^{-\frac{t_{i+1} - t_i}{\tau_{dep}}}\right) \cdot [SSA(T_{dep}) - SSA(\bar{T}_{dep}, t_i)] \right\} \cdot \frac{t_i}{t_{i+1}} + \frac{t_{i+1} - t_i}{t_{i+1}} \cdot D$$

this produces the right shape of SSA deposition curves, but the initial value  $D$  needs to decrease somewhat with increasing deposition temperature

- Problem:
- When SSA has not reached equilibrium during deposition, it keeps increasing during begin of heating phase with the above assumptions. Data do not show this trend
  - Why would molecules at low T move to increase SSA?  
→ unphysical

Try instead: - SSA increasing with deposited amount of sample

- this increase is counteracted by SSA changing with time to reach T-dependent equilibrium.

$$\text{increase: } \text{SSA}(t) = D + (1 - e^{-\frac{t}{\tau_{\text{dep}}}}) \cdot (E - D)$$

$\uparrow$                                      $\uparrow$   
 SSA of initial layer                    SSA of whole deposition  
 in equilibrium

$$\text{decrease: } \text{SSA}(t) = \text{SSA}(t_0) + (1 - e^{-\frac{t-t_0}{\tau(T)}}) \cdot (\text{ss}_a(T_{\text{dep}}) - \text{SSA}(t_0))$$

total:

$$\begin{aligned} \text{SSA}(T_{\text{dep}}, t_{i+1}) &= \text{SSA}(T_{\text{dep}}, t_i) + (1 - e^{-\frac{t_{i+1}-t_i}{\tau_{\text{dep}}}}) \cdot (E - \text{SSA}(T_{\text{dep}}, t_i)) \\ &\quad + (1 - e^{-\frac{t_{i+1}-t_i}{\tau(T)}}) \cdot [\text{ss}_a(T_{\text{dep}}) - (1 - e^{-\frac{t_{i+1}-t_i}{\tau_{\text{dep}}}}) \cdot \{E - \text{SSA}(T_{\text{dep}}, t_i)\} - \text{SSA}(T_{\text{dep}}, t_i)] \end{aligned}$$

test:  $e^{-\frac{t_{i+1}-t_i}{\tau_{\text{dep}}}} \approx 0 \Rightarrow \text{SSA} \approx \text{SSA}(T_{\text{dep}}, t_i) + E - \text{SSA}(T_{\text{dep}}, t_i) + (1 - e^{-\frac{t_{i+1}-t_i}{\tau(T)}}) \cdot [\text{ss}_a(T_{\text{dep}}) - (E - \text{SSA}(T_{\text{dep}}, t_i))]$

$$= E + (1 - e^{-\frac{t_{i+1}-t_i}{\tau(T)}}) \cdot [\text{ss}_a(T_{\text{dep}}) - E] \quad \checkmark$$

$e^{-\frac{t_{i+1}-t_i}{\tau(T)}} \approx 0 \Rightarrow \text{SSA} \approx \text{SSA}(T_{\text{dep}}, t_i) + (1 - e^{-\frac{t_{i+1}-t_i}{\tau_{\text{dep}}}}) \cdot (E - \text{SSA}(T_{\text{dep}}, t_i))$

$$+ [\text{ss}_a(T_{\text{dep}}) - (1 - e^{-\frac{t_{i+1}-t_i}{\tau_{\text{dep}}}}) \cdot (E - \text{SSA}(T_{\text{dep}}, t_i)) - \text{SSA}(T_{\text{dep}}, t_i)]$$

$$= \text{ss}_a(T_{\text{dep}}) \quad \checkmark$$

$e^{-\frac{t_{i+1}-t_i}{\tau_{\text{dep}}}} \approx 1 \Rightarrow \text{SSA} \approx \text{SSA}(T_{\text{dep}}, t_i) + (1 - e^{-\frac{t_{i+1}-t_i}{\tau(T)}}) \cdot [\text{ss}_a(T_{\text{dep}}) - \text{SSA}(T_{\text{dep}}, t_i)]$

$e^{-\frac{t_{i+1}-t_i}{\tau(T)}} \approx 1 \Rightarrow \text{SSA} \approx \text{SSA}(T_{\text{dep}}, t_i) + (1 - e^{-\frac{t_{i+1}-t_i}{\tau_{\text{dep}}}}) (E - \text{SSA}(T_{\text{dep}}, t_i)) \quad \checkmark$

$\Rightarrow$  works in theory

10.04.2017

Problem: this does only produce the right shape of deposition curves, when I choose very long timescales for the SSA annealing rate coefficient  $\tau$  ( $\approx 24h$ ) which are far too long to reproduce the annealing change of SSA during heating

04.07.2017

## Re-run Budrun:

Deposition 1 h averages: Use tweak factors derived from porosity literature for each deposition temperature.  
Fit sample thickness based on DCS.

06.07.2017

Deposition individual scans: Read out tweak factors & thicknesses from 1 h average results. Fit thickness data as linear growth and calculate thickness based on individual scan's growth time. Use same tweak factor (constant) throughout each sample.  $\Rightarrow$  No fitting of tweak or thickness based on DCS levels obtained by BudrunN

Heating isothermal steps: Read out thickness from final deposition data point. Use that (constant) throughout each sample.  
Fit tweak factor based on DCS.

Heating individual scans: Read out thicknesses & tweak factors from isothermal steps results. Use same (constant) thickness throughout each sample. Interpolate tweak factor between two data points based on sample temperature.  
 $\Rightarrow$  No fitting of tweak or thickness based on DCS.

Note: ~~check that first tweak factor in results file is correct,~~

 ~~for some reason that is not always replaced in budrun-dcs.dat  
 $\rightarrow$  haven't found the cause of this bug yet.~~

~~The same bug applies to the sample thickness.~~

Solved: Python was saving the next parameters in the loop, not the current ones. Renamed them to solve that.

 This bug was there in all scripts so far!

## Start again with SSA modelling:

- Basic ideas: Deposition:
- Onset of SSA at  $t=0$  might depend on deposition  $T$  (or other conditions like rate, but should be varied for each sample)
  - SSA will evolve towards  $T$ -dependent deposition equilibrium, while freshly deposited material has onset value

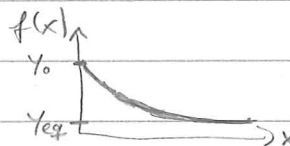
Annealing:

- SSA should always evolve towards final equilibrium value of 0.

- The timeconstant for this evolution will depend on sample  $T$  and activation energy for SSA change
- SSA change activation energy might vary for different ice phases ( $T$  regimes)

Get time constant  $\tau$  from SSA data:

$$f(x) = Y_0 + (1 - e^{-\frac{x-x_0}{\tau}}) \cdot (Y_{eq} - Y_0)$$



$$\Rightarrow f(x) - Y_0 = (1 - e^{-\frac{x-x_0}{\tau}}) \cdot (Y_{eq} - Y_0) \quad \Downarrow \quad f'(x) = (Y_{eq} - Y_0) \cdot \left(-\frac{1}{\tau}\right) e^{-\frac{x-x_0}{\tau}}$$

$$\Rightarrow \frac{f(x) - Y_0}{Y_{eq} - Y_0} = 1 - e^{-\frac{x-x_0}{\tau}}$$

$$= -\frac{Y_{eq} - Y_0}{\tau} e^{-\frac{x-x_0}{\tau}}$$

$$\Rightarrow e^{-\frac{x-x_0}{\tau}} = 1 - \frac{f(x) - Y_0}{Y_{eq} - Y_0} = \frac{Y_{eq} - f(x)}{Y_{eq} - Y_0}$$

$$\Rightarrow \ln(f'(x)) = \ln(Y_0 - Y_{eq}) - \ln(\tau) - \frac{x-x_0}{\tau} \hat{=} a \cdot x + b$$

$$\Rightarrow -\frac{x-x_0}{\tau} = \ln(Y_{eq} - f(x)) - \ln(Y_{eq} - Y_0)$$

$$\Rightarrow \boxed{a = -\frac{1}{\tau}}, \quad b = \ln(Y_0 - Y_{eq}) - \ln(\tau) + \frac{X_0}{\tau}$$

$\Rightarrow$  not helpful

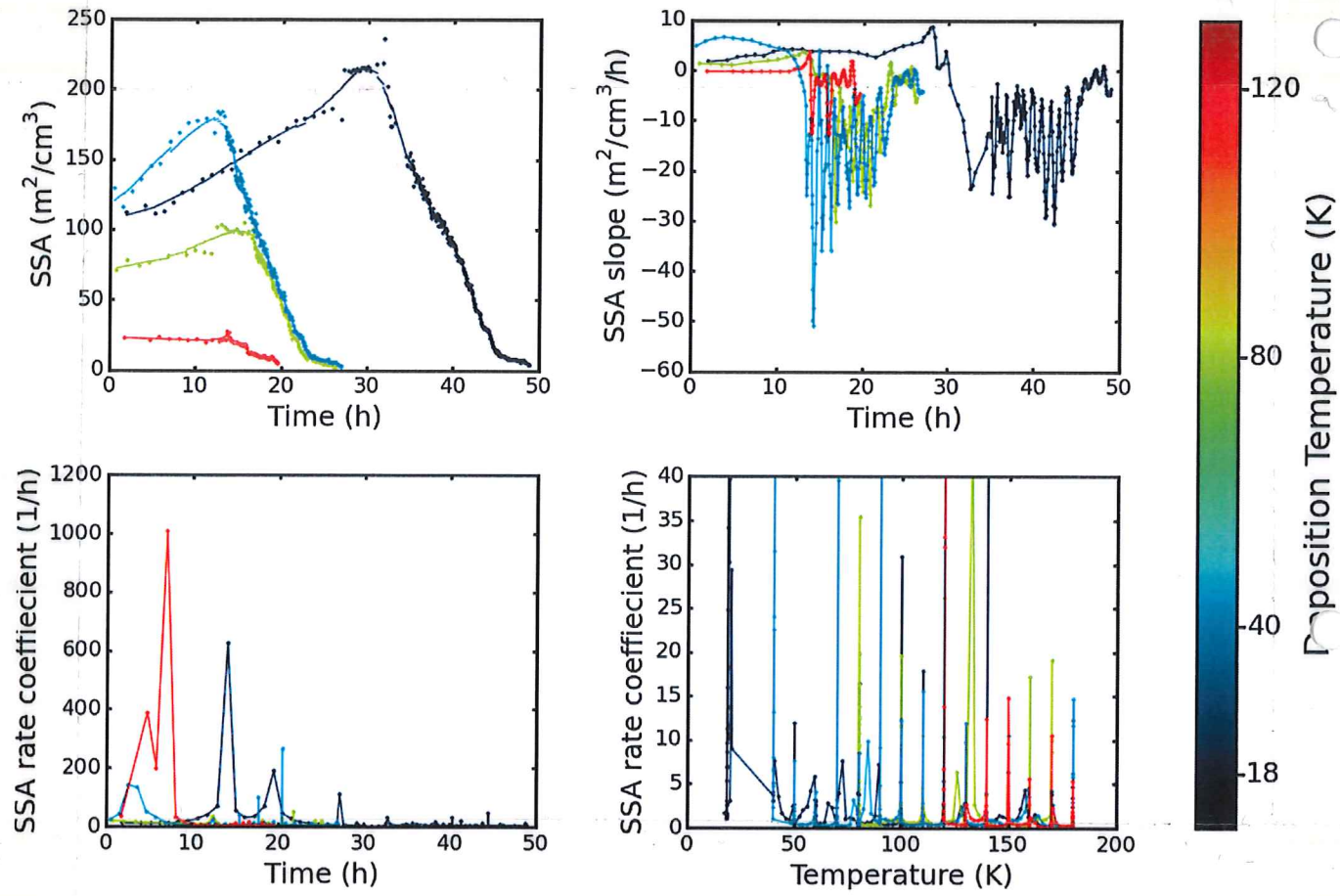
$$\text{assume } Y_{eq}=0 : b = \ln(Y_0) - \ln(\tau) + \frac{X_0}{\tau}$$

\* try fitting straight lines to a few ( $\approx 5$ ) datapoints to obtain "smoothed" values for  $f'(x)$  ( $\hat{=} \text{SSA}(t)$ )

\* do the same for  $\ln(f'(x))$  to obtain  $\tilde{\tau}$

\* plot  $\tilde{\tau}$  vs  $T$  to see if there are correlations

28.07.2017



Split data into deposition, heating ramp, and isothermal annealing steps and run SSA analysis on annealing data again (spikes in  $k$  appear every 10 K, which is distance between annealing steps).

Fit every piece of data with  $f(x) = Y_0 + (1 - e^{-\frac{x-x_0}{\tau}}) \cdot (Y_{eq} - Y_0)$

Data is not sufficient to do this  $\Rightarrow$  try linear fit & Taylor series

$$\begin{aligned}
 f(x) &\approx Y_0 + (1 - e^{-\frac{x-x_0}{\tau}}) \cdot (Y_{eq} - Y_0) + (x - x_0) \cdot \left( -\frac{Y_0 - Y_{eq}}{\tau} \right) \cdot e^{-\frac{x-x_0}{\tau}} \\
 &= \frac{-Y_0 + Y_{eq}}{\tau} \cdot e^{-\frac{x-x_0}{\tau}} \cdot x + Y_0 - Y_0 + Y_{eq} - e^{-\frac{x-x_0}{\tau}} \cdot (Y_{eq} - Y_0 - \frac{x_0 - x_1}{\tau} (Y_0 - Y_{eq})) \\
 &= \frac{-Y_0 + Y_{eq}}{\tau} \cdot e^{-\frac{x-x_0}{\tau}} \cdot x + Y_{eq} - e^{-\frac{x-x_0}{\tau}} \cdot \left( 1 + \frac{x_0 - x_1}{\tau} \right) \cdot (Y_{eq} - Y_0)
 \end{aligned}$$

$$\hat{y} = a \cdot x + b$$

$$a = -\frac{Y_0 - Y_{eq}}{\tau} \cdot e^{-\frac{x_0 - x}{\tau}}$$

$$b = Y_{eq} + (Y_0 - Y_{eq}) \cdot (1 + \frac{x_0}{\tau}) \cdot e^{-\frac{x_0 - x}{\tau}}$$

$$x_0 = x_0 \Rightarrow a = -\frac{Y_0 - Y_{eq}}{\tau}, \quad b = Y_{eq} + (Y_0 - Y_{eq}) \cdot (1 + \frac{x_0}{\tau})$$

$\uparrow$   
(take first x data point of data piece as  $x_0$ )

$$\text{assume } Y_{eq} = 0 \Rightarrow a = -\frac{Y_0}{\tau}, \quad b = Y_0 \cdot (1 + \frac{x_0}{\tau})$$

$$\Rightarrow \tau = -\frac{Y_0}{a}, \quad b = Y_0 \cdot (1 + \frac{x_0 \cdot a}{Y_0}) = Y_0 + x_0 \cdot a$$

$$\Rightarrow \tau = -\frac{b - x_0 \cdot a}{a}, \quad Y_0 = b - x_0 \cdot a$$

$$\Rightarrow \tau = -\frac{b}{a} + x_0, \quad Y_0 = b - x_0 \cdot a$$

31.07.2017

$$\hookrightarrow f(x) \approx -\frac{Y_0}{\tau} \cdot x + Y_0 \cdot (1 + \frac{x_0}{\tau}) = \frac{Y_0}{\tau} \cdot (\tau + x_0 - x)$$

01.08.2017

This approach works reasonably well. ( $x_0$  = first time in sus set)

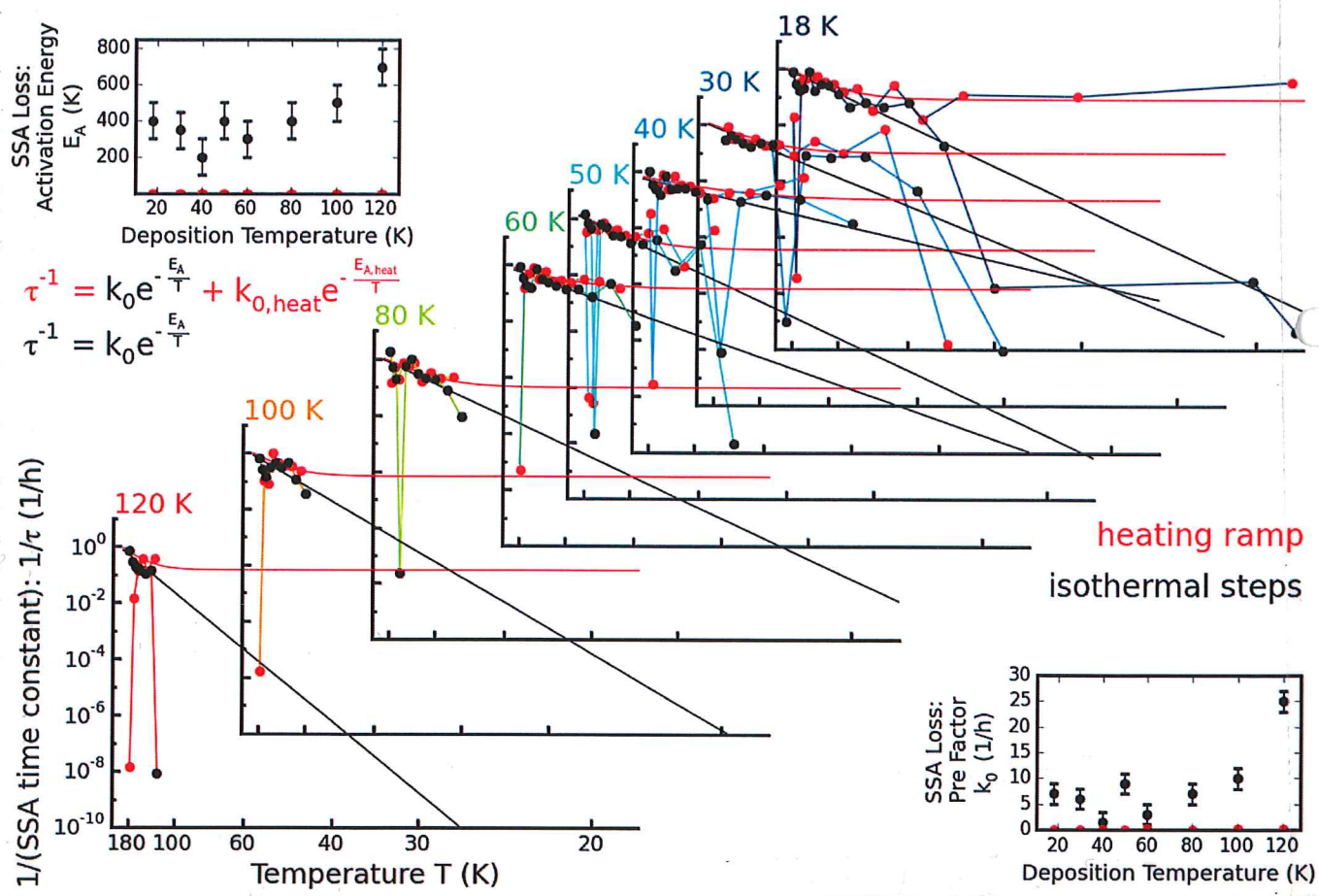
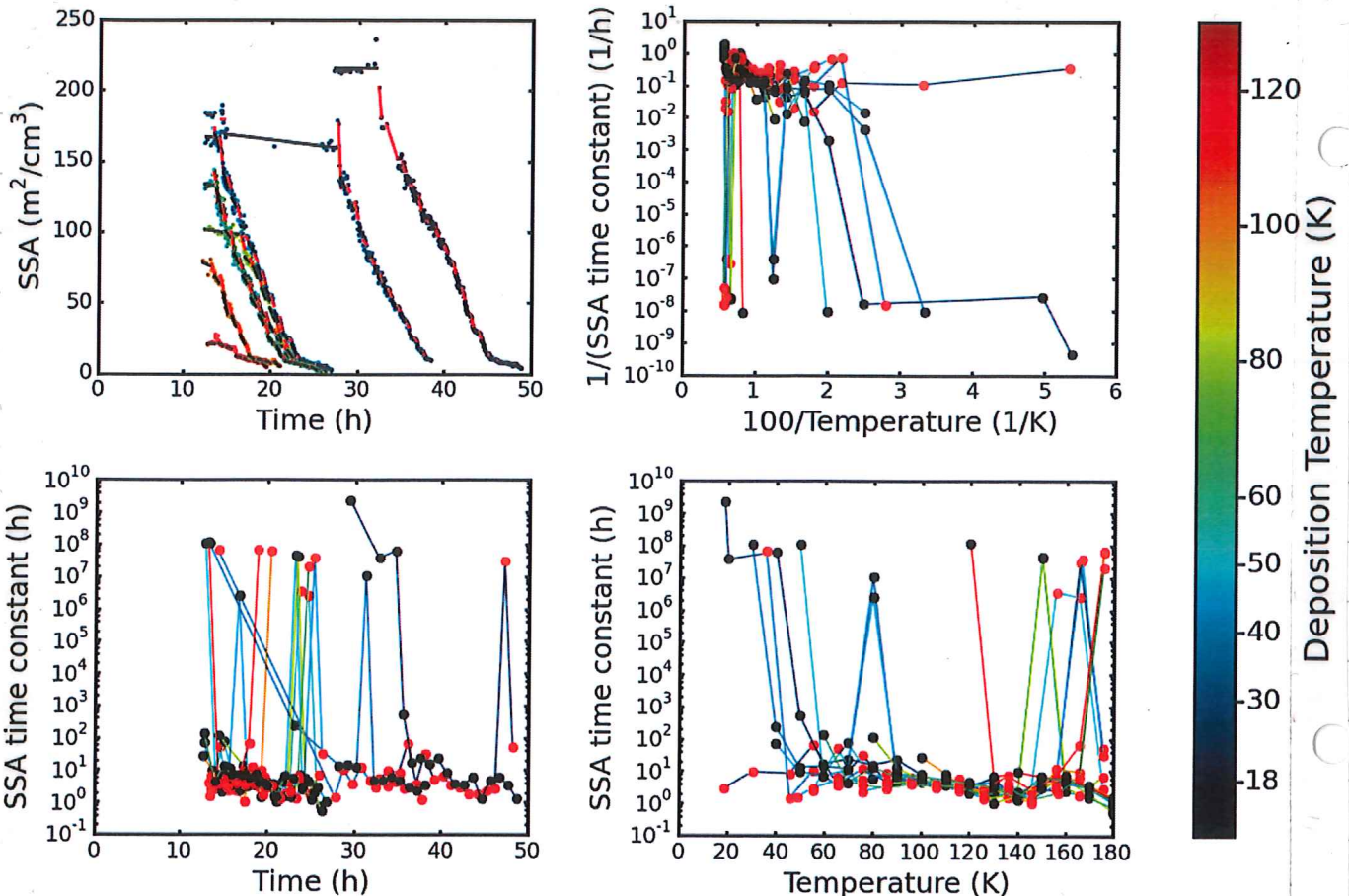
Caveat: a few sub sets of data of only 2 data points!

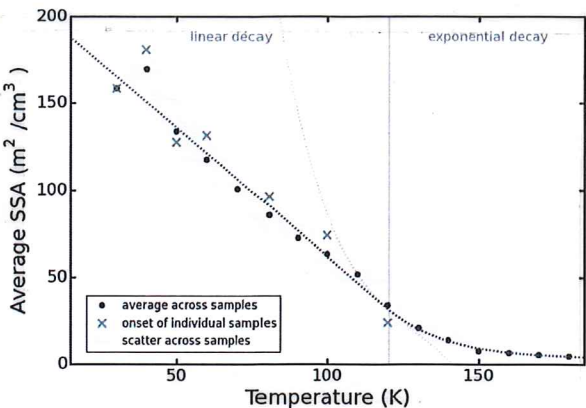
Results plotted on next page. Outlier occur where SSA is increasing on the start of a heating ramp and then decreasing again. These are mostly the last annealing points within each sample. 30 & 40 K depositions show such an outlier at 80 K isothermal. 80 K deposition shows one at 150 K. 50 & 120 K depositions have unusually slow onset of SSA decrease (first isothermal point). 30 K deposition has unusually low initial heating ramp change (before beam-off).

Arrhenius plots: treat  $\frac{1}{T}$  as rate coefficient  $\Rightarrow$  plot  $\ln(\frac{1}{T})$  vs  $\frac{1}{T}$ .

Fit: Natural SSA decay:  $\frac{1}{T} = k_0 e^{-\frac{E_A}{T}}$ ,  $E_A$  = activation energy in kJ (isothermal)

heating ramp SSA decay:  $\frac{1}{T} = k_0 e^{-\frac{E_A}{T}} + k_{0,\text{heat}} e^{-\frac{E_{A,\text{heat}}}{T}}$ ,  $E_{A,\text{heat}} = 0$  (from fit)





Maybe the competition between desorption and pore loss, which must be causing the SSA rate of change outliers at high T, is responsible for the change from linear to exponential decay at  $\approx 120$  K on the averaged SSA?

Although exponential decay is what sounds more "physical", linear decay can't continue forever. Also, the model on the previous pages is based on exponential decay. So the question is: Why does the decay look linear below 120 K?

$\Rightarrow$  I am varying the time constant with temperature. These changes are larger at low T than at high T  $\Rightarrow$  it probably can be approximated as linear decay at low T and exponential decay at high T.

$$SSA(t, T) = SSA(t_0) + (1 - e^{-\frac{t-t_0}{\tau(T)}}) \cdot (0 - SSA(t_0))$$

$$= SSA(t_0) \cdot e^{-\frac{t-t_0}{\tau(T)}}$$

$$\frac{1}{\tau(T)} = k_0 e^{-\frac{E_A}{T}} + x \cdot k_{0, \text{heat}}, \quad T(t) = a \cdot t + b \Rightarrow t = \frac{T-b}{a}$$

$$\Rightarrow SSA(T) = SSA(t_0) \cdot e^{-\frac{T-b}{a} \cdot (k_0 e^{-\frac{E_A}{T}} + x k_{0, \text{heat}})} \quad (*)$$

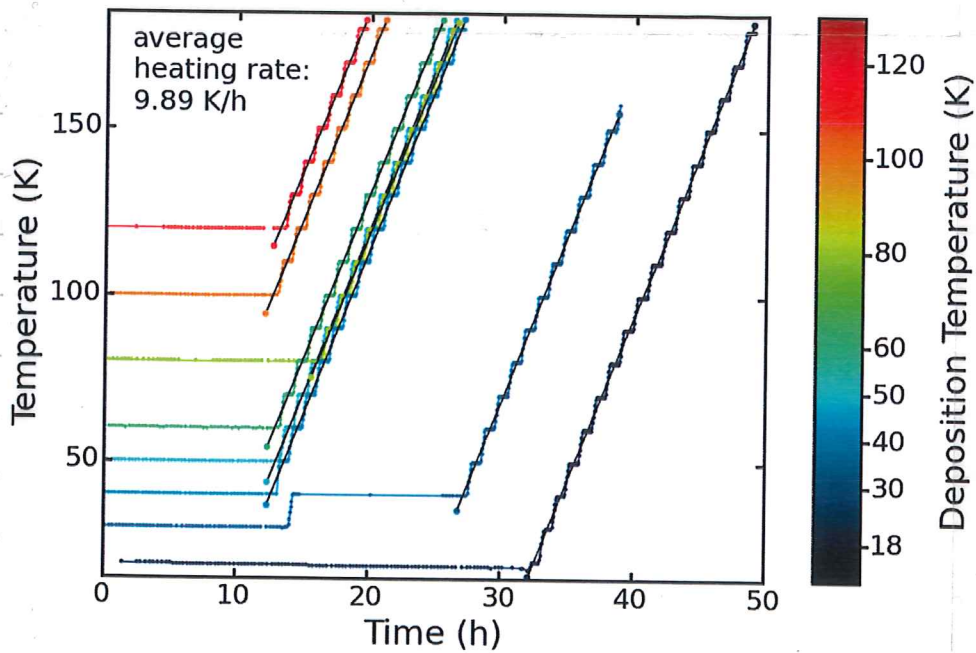
$$= SSA(t_0) \cdot e^{-\frac{k_0 \cdot (T-b)}{a} e^{-\frac{E_A}{T}}} \cdot e^{-\frac{x \cdot k_{0, \text{heat}} (T-b)}{a}}$$

02.08.2017

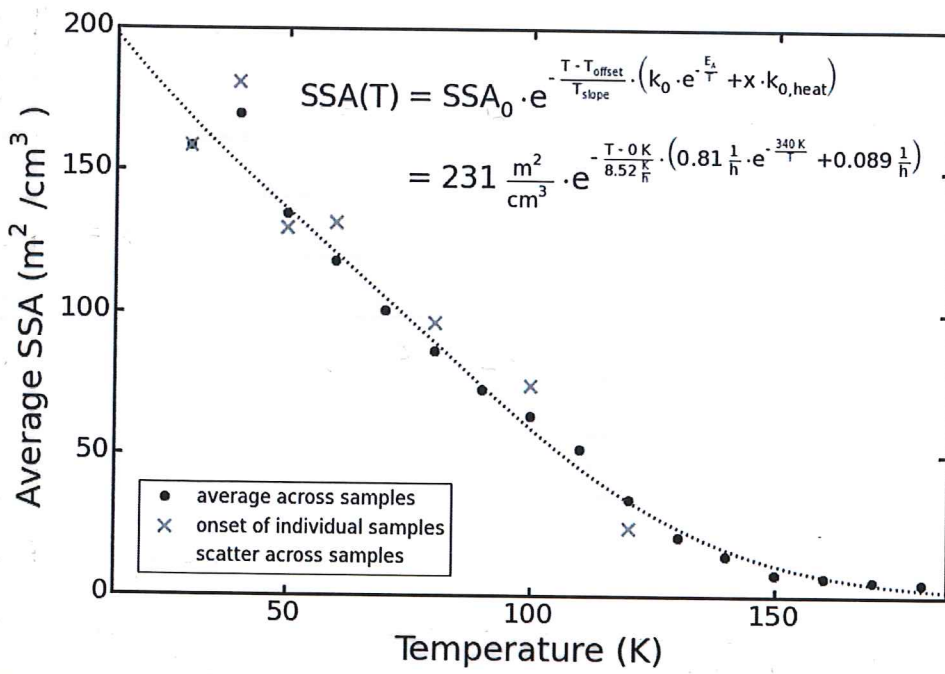
$$E_A \approx 400 \text{ K}, a \approx 10 \frac{\text{K}}{\text{h}}, b \approx 0 \text{ K}, k_0 \approx 10 \frac{1}{\text{h}}, k_{0, \text{heat}} = 0.1 \frac{1}{\text{h}}, x \in [0, 1]$$

$$\Rightarrow SSA(T) \approx SSA(t_0) \cdot e^{-\frac{10 \frac{1}{\text{h}}}{10 \frac{1}{\text{h}}} \cdot T \cdot e^{-\frac{400 \text{ K}}{T}}} \cdot e^{-\frac{x \cdot 10 \frac{1}{\text{h}}}{10 \frac{1}{\text{h}}} \cdot T}$$

$$= SSA(t_0) \cdot e^{-\frac{T}{1 \text{ K}} \cdot e^{-\frac{400 \text{ K}}{T}}} \cdot e^{-\frac{x \cdot T}{100 \text{ K}}} = SSA(t_0) \cdot e^{-\frac{T}{1 \text{ K}} \left( e^{-\frac{400 \text{ K}}{T}} + \frac{x}{100} \right)}$$



← Note:  
 onset of heating  
 ramp manually  
 shifted for  
 18, 30, 80 K  
 depositions  
 (all from first  
 run), because  
 onset of actual  
 heating ramp  
 delayed for  
 various reasons



← Note:  
 18 K deposition  
 not plotted  
 (as agreed  
 earlier)

fitting function (\*) works quite well, but gives slightly different results than individual scan analysis so far

individual	averaged
heat rate ( $\frac{\text{K}}{\text{h}}$ )	9.89
$E_A$ (K)	average 406
$k_0 (\frac{1}{\text{h}})$	$\approx 10$
$k_{0,\text{heat}} (\frac{1}{\text{h}})$	$\approx 0.01$
	2.52
	340
	0.8
	$0.09 (k_{0,\text{heat}} \cdot x)$

Sadchenko 2000 b state:

barriers to diffusion:

- molecule rotation to increase

coordination no. from 2 → 3

$5 \pm 1 \text{ kcal/mol} \hat{=} 2500 \text{ K}$

- molecule diffusion (coord. 3 → 4)

$9 \pm 2 \text{ kcal/mol} \hat{=} 4500 \text{ K}$

Return to pore dimensions:

$$\text{See 15.02.2017: cylinder (radius } R, s=1) : R_g = R \cdot \sqrt{\frac{1}{2}}$$

$$\text{lamella (thickness } T, s=2) : R_g = T \cdot \sqrt{\frac{1}{12}}$$

assume random cylinder (radius  $R$ , height  $\alpha \cdot R$ ,  $s \in [1,2]$ ):

$$R_g = x \cdot R \sqrt{\frac{1}{2}} + y \cdot T \sqrt{\frac{1}{12}}$$

$$\text{requirements: cylinder } (s=1) : x=1, y=0$$

$$\text{lamella } (s=2) : x=0, y=1$$

$$x = a \cdot s + b \Rightarrow a+s = 1 \wedge 2a+b = 0$$

$$\Rightarrow a = 1-b \wedge 2-2b+b = 0$$

$$\Rightarrow a = -1 \wedge b = 2 \Rightarrow x = 2-s$$

$$y = a \cdot s + b \Rightarrow a+b = 0 \wedge 2a+b = 1$$

$$\Rightarrow a = -b \wedge -2b+b = 1$$

$$\Rightarrow a = 1 \wedge b = -1 \Rightarrow y = s-1$$

$$R_g = (2-s) R \sqrt{\frac{1}{2}} + (s-1) \alpha R \sqrt{\frac{1}{12}} = R \cdot \left( \frac{2-s}{\sqrt{2}} + \alpha \frac{s-1}{\sqrt{12}} \right)$$

Back to original question: What should  $\alpha(s)$  look like?

Volumes & surfaces:

$$\text{sample volume} = V_s, \text{ total pore volume} = V_p = N_p \cdot v_p$$

$$\text{total number of pores} = N_p, \text{ volume of individual pore} = v_p$$

$$\text{surface of individual pore} = a_p, \text{ surface of all pores} = A_p = a_p \cdot N_p$$

$$\text{SSA of sample} \approx \frac{A_p}{V_i}, \text{ ice volume} = V_i = V_s - V_p$$

$$(\text{surface of compact ice negligible}) \quad \text{tweak factor} = t = \frac{V_s}{V_i}$$

$$t = \frac{V_i + V_p}{V_i} = 1 + \frac{V_p}{V_i} = 1 + \frac{N_p}{V_i} \cdot v_p = 1 + m_p \cdot v_p, m_p = \frac{N_p}{V_i} = \text{number density of pores}$$

$$\Rightarrow m_p = \frac{t-1}{v_p}$$

$$SSA = \frac{A_p}{V_i} = \frac{a_p \cdot N_p}{V_i} = n_p \cdot a_p = (t-1) \cdot \frac{a_p}{n_p}$$

Volume of random cylinder (radius  $R$ , height  $d \cdot R$ ): (see 23.3.17)

$$n_p = \pi d R^3 \quad , \quad \text{surface: } a_p = 2\pi d R^2$$

$$\Rightarrow SSA = (t-1) \cdot \frac{2\pi d R^2}{\pi d R^3} = (t-1) \cdot \frac{2}{R} \quad \left| R = R_g \cdot \left( \frac{2-s}{\sqrt{2}} + d \frac{s-1}{\sqrt{2}} \right)^{-1} \right.$$

$$\Rightarrow SSA = (t-1) \cdot \frac{2}{R_g} \cdot \left( \frac{2-s}{\sqrt{2}} + d \frac{s-1}{\sqrt{2}} \right)$$

What does  $\lambda(s)$  look like?

$$s=1 \Rightarrow \lambda \gg 1 \quad ("^\infty") \quad , \quad s=2 \Rightarrow 0 < \lambda \ll 1 \quad ("0")$$

$$s=1.5 \Rightarrow \lambda = 1$$

$$\text{try } \lambda(s) = a \cdot e^{-\frac{s-b}{c}} \Rightarrow a \cdot e^{-\frac{1.5-b}{c}} = 1 \Rightarrow \frac{1.5-b}{c} = \ln(a)$$

$$a \cdot e^{-\frac{2-b}{c}} \ll 1 \Rightarrow e^{+\frac{1.5-b}{c}} \cdot e^{-\frac{2-b}{c}} \ll 1 \Rightarrow \frac{1.5-2+b+5}{c} \ll 0 \Rightarrow -\frac{0.5}{c} \ll 0$$

$$a \cdot e^{-\frac{1-b}{c}} \gg 1 \Rightarrow e^{\frac{1.5-b}{c}} \cdot e^{-\frac{1-b}{c}} \gg 1 \Rightarrow \frac{1.5-1-b+5}{c} \gg 0 \Rightarrow \frac{0.5}{c} \gg 0$$

$$\text{try } a=1, b=1.5 \Rightarrow \lambda(s) = e^{-\frac{s-1.5}{c}}$$

$$\lambda(1.5) = e^0 = 1 \quad \checkmark \quad \lambda(1) = e^{\frac{1}{2c}} \gg 1$$

$$\lambda(2) = e^{-\frac{1}{2c}} \ll 1 \quad , \quad e^{\frac{1}{2}} = 1.65 \quad , \quad e^{-\frac{1}{2}} = 0.61$$

$$\lambda(1) = (1.65)^{\frac{1}{c}} \quad , \quad \lambda(2) = (0.61)^{\frac{1}{c}} \quad , \quad \frac{1}{c} = d \quad (\text{simpler notation})$$

$$\Rightarrow SSA = (t-1) \cdot \frac{2}{R_g} \cdot \left( \frac{2-s}{\sqrt{2}} + e^{-d \cdot (s-1.5)} \cdot \frac{s-1}{\sqrt{2}} \right)$$

→ that's not leading anywhere

$$SSA = (t-1) \cdot \frac{2}{R_g} \cdot \left( \frac{2-s}{\sqrt{2}} + \alpha \frac{s-1}{\sqrt{2}} \right)$$

$$\Rightarrow \alpha \frac{s-1}{\sqrt{2}} \cdot (t-1) \cdot \frac{2}{R_g} = SSA - (t-1) \cdot \frac{2}{R_g} \cdot \frac{2-s}{\sqrt{2}}$$

$$\Rightarrow \alpha = \frac{SSA}{t-1} \cdot \frac{R_g}{2} \cdot \frac{\sqrt{2}}{s-1} - \frac{2-s}{s-1} \cdot \frac{\sqrt{2}}{2} = \frac{SSA}{t-1} \cdot \frac{R_g}{s-1} \cdot \frac{\sqrt{3}}{2} - \frac{2-s}{s-1} \cdot \frac{\sqrt{6}}{2} \quad (*)$$

$$\alpha(s=2) = \frac{SSA}{t-1} \cdot R_g \cdot \frac{\sqrt{3}}{1} - 0 = \sqrt{3} \frac{SSA}{t-1} \cdot R_g$$

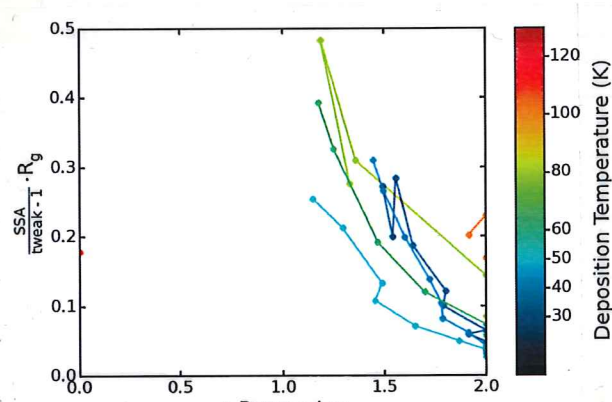
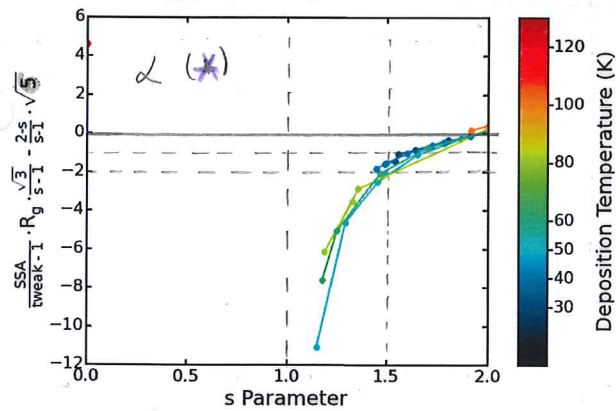
$$\alpha(s=1) = \frac{1}{0} \text{ undefined } \rightarrow \infty$$

$$\frac{SSA}{t-1} \cdot R_g = \sqrt{2}(2-s) + \alpha \frac{(s-1)}{\sqrt{3}} = 2\sqrt{2} - \sqrt{2}s + \frac{\alpha}{\sqrt{3}}s - \frac{\alpha}{\sqrt{3}} = \left(\frac{\alpha}{\sqrt{3}} - \sqrt{2}\right)s + 2\sqrt{2} - \frac{\alpha}{\sqrt{3}}$$

try plotting  $\frac{SSA}{t-1} \cdot R_g$  against  $s$ .

$\Rightarrow$  that's not very helpful

$\Rightarrow$  plot  $\alpha (*)$  vs  $s$  instead.



that shows a clear trend, but it comes out negative.  
Per definition ( $\alpha = \frac{I}{R}$ ) it should be positive!

$$t > 1 \Rightarrow t-1 > 0, s \in [1, 2] \Rightarrow s-1 > 0 \wedge 2-s > 0$$

$$\alpha < 0 \Rightarrow \frac{SSA}{t-1} \cdot R_g \cdot \sqrt{3} < (2-s) \cdot \sqrt{6} \Rightarrow \frac{SSA}{t-1} \cdot R_g \cdot \frac{1}{\sqrt{2}} - 2 < -s$$

$$\Rightarrow s < 2 - \underbrace{\frac{SSA}{t-1} \cdot R_g \cdot \frac{1}{\sqrt{2}}}_{\in [0, \frac{1}{2}]} \Rightarrow s \in [2 - \frac{1}{2} \cdot \frac{1}{\sqrt{2}}, 2] \text{ seems right}$$

but why is  $\alpha < 0$ ?

09.08.2017

Radius of gyration:

$$\text{Random cylinder : } R_g = \sqrt{\frac{R^2}{2} + \frac{L^2}{12}} \quad \begin{array}{l} \text{(from Tom, citing Feigin & Svergun 1987, Book)} \\ \text{cylinder } (s=1) : R_g = \frac{R}{\sqrt{2}} \\ \text{lamella } (s=2) : R_g = \frac{L}{\sqrt{12}} \end{array}$$

Hammond et al 2010:  
A new Guinier-Porod model

Extreme cases of random cylinder:

$$R \ll L : R_g \approx \frac{L}{\sqrt{12}} \quad (\text{cylinder (rod)})$$

$$R \gg L : R_g \approx \frac{R}{\sqrt{2}} \quad (\text{lamella / platelet})$$

24.08.2017

SAS View fitting: Lamellar + Gaussian

$$\text{Lamellar Model : } I(q) = \frac{2\pi}{\delta q^2} P(q), \quad s = \text{bilayer thickness}$$

$$\text{form factor : } P(q) = \frac{2\Delta S^2}{q^2} (1 - \cos(qS))$$

$$\Rightarrow I(q) = \frac{4\pi}{q^4} \cdot \frac{\Delta S^2}{s} \cdot (1 - \cos(qS))$$

returned value is in  $\text{cm}^{-1}$  on absolute scale $\Rightarrow$  convert input intensity to  $\text{cm}^{-1}$ !

Scale : volume fraction of the scatterer

$$\text{Peak Gauss Model : } I(q) = \text{scale} \cdot e^{-\frac{(q-q_0)^2}{2B^2}} + \text{background}$$

A Gaussian not normalised.

What does scale mean for this model?

$\frac{dt}{dT}$ 

## SSA

I've given up on modelling the SSA evolution and went back to analytical functions. I will only focus on the annealing data for now.

At any time  $t$  (and temperature  $T(t)$ ), the SSA should evolve from a starting value  $SSA_0$  at  $t_0$  towards the equilibrium value, which is assumed to be  $SSA_{eq} = 0 \text{ m}^2/\text{cm}^3$ , following an exponential decay:

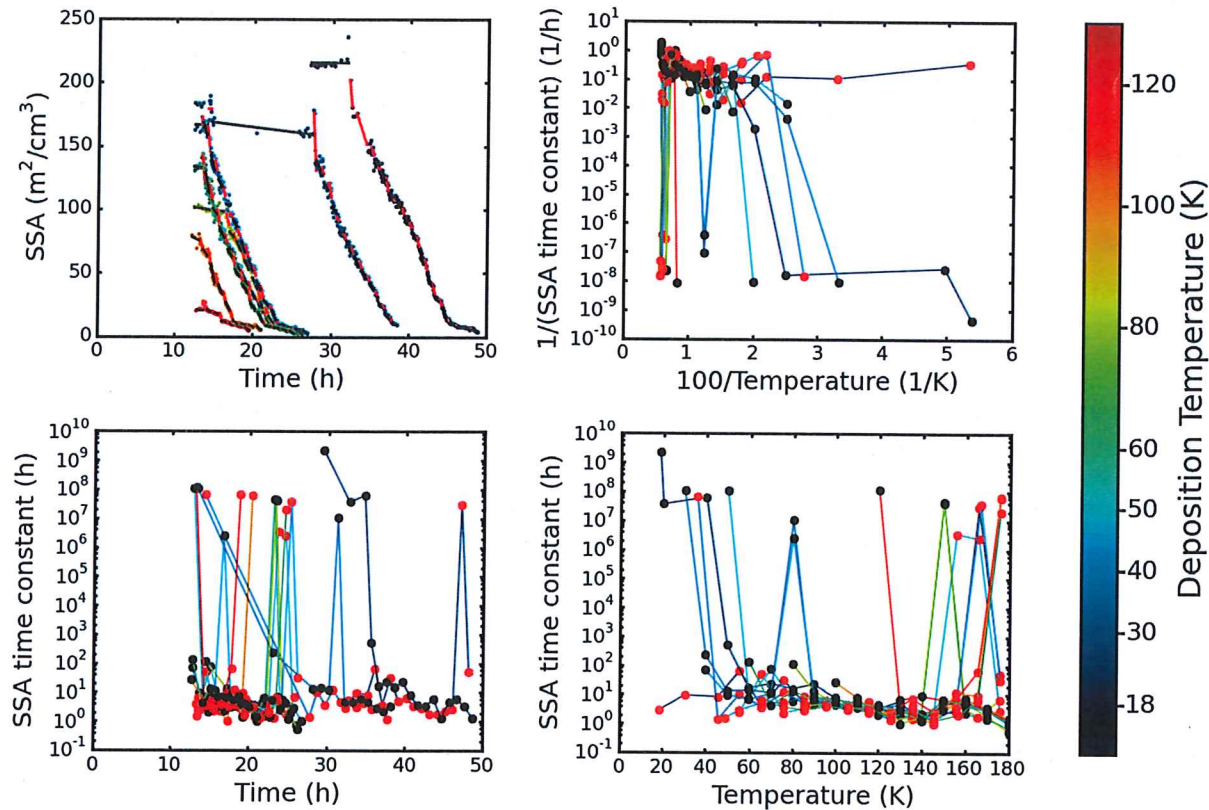
$$SSA(t, T) = SSA_0 + \left(1 - e^{-\frac{t-t_0}{\tau(T)}}\right) \cdot (SSA_{eq} - SSA_0)$$

$\int \frac{dSSA}{dt} = SSA_0 \cdot e^{-\frac{t-t_0}{\tau(T)}}$ 
(1)

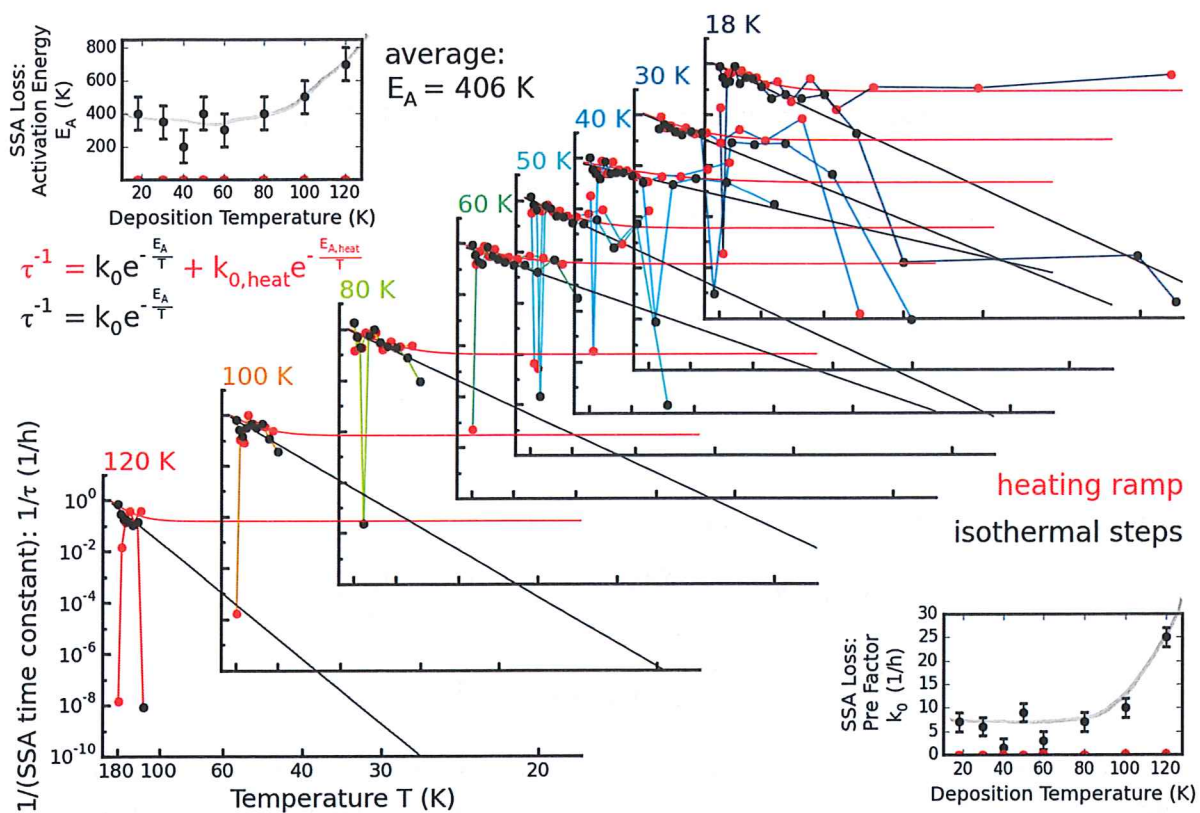
For short times ( $T \approx \text{const.}$ ) this can be approximated by (Taylor expansion):

$$\begin{aligned} SSA(t, T) &\approx -\frac{SSA_0}{\tau(T)} \cdot t + SSA_0 \cdot \left(1 + \frac{t_0}{\tau(T)}\right) \\ &= \frac{SSA_0}{\tau(T)} \cdot [\tau(T) + t_0 - t] \end{aligned}$$

I have fitted the individual scans from each isothermal step and from each heating ramp in between isothermal steps individually with this linear function to derive the temperature dependent time constants  $\tau(T)$ . Plots below show isothermal data in black, heating ramp data in red.



The upper right shows an Arrhenius type plot, treating  $1/\tau$  as a rate coefficient and therefore plotting  $\ln(1/\tau)$  against  $1/T$ . The figure below shows the same plots but offset by deposition temperature.



The isothermal  $\tau$  results scatter around a straight line in this plot, while the heating ramp results follow the same trend only at high T (left end of x-axis) and level off towards low T (right end of x-axis).

These data can be fitted with the two functions stated in the above figure (LHS). They represent a one (two) state system with activation energies  $E_A$  (&  $E_{A,heat}$ ). That is, on a heating ramp, the SSA behaves as if part of the sample is in an excited state and therefore requires a lower (zero in this case) activation energy to undergo change.

#### Notes:

- The above  $1/\tau$  fits were done manually, as python couldn't find a good fit. This is probably due to the outliers (especially at very high T).
- A close look on these outliers shows that on these heating ramps the SSA initially is increasing, going through a maximum and then decreasing again, so the overall slope looks very shallow. This is probably due to sample desorption, which must compete with molecular restructuring.

The temperature dependence of  $\tau$  can now be inserted in Eq. (1) and the time dependence of the temperature T can be approximated by the average heating ramp:

$$T(t) = a \cdot (t - t_0) + b$$

$$\Rightarrow t - t_0 = \frac{T - b}{a}$$

This transforms Eq. (1) to:

$$SSA(T) = SSA_0 \cdot e^{-\frac{T-b}{a} \cdot \left( k_0 \cdot e^{-\frac{E_A}{T}} + x \cdot k_{0,heat} \right)}$$

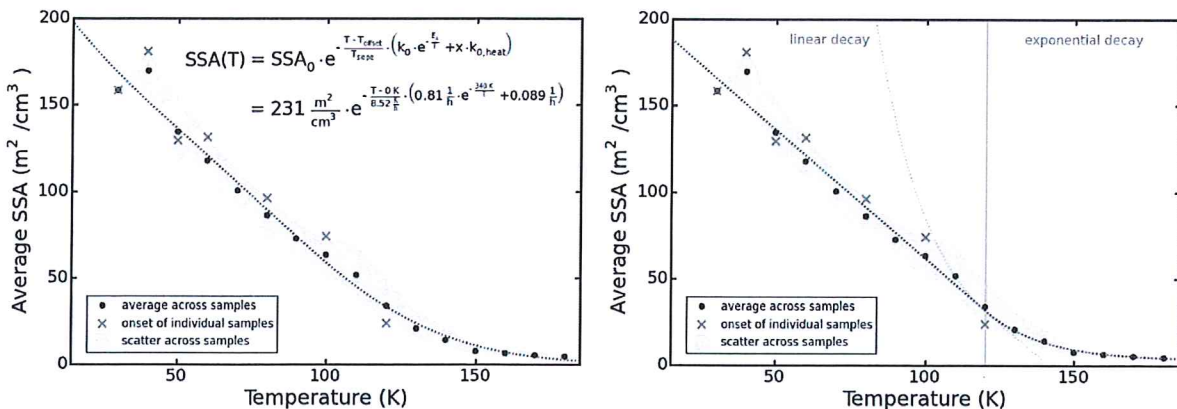


With the factor x accounting for the average influence the second term (with no activation energy) might have.

Rate  $\frac{d[A]}{dt} = (A)^x \cdot k \cdot R = A e^{-\frac{E_A}{RT}}$

$$\theta \quad \beta \left( \frac{\partial T}{\partial t} \right) \sqrt{t}$$

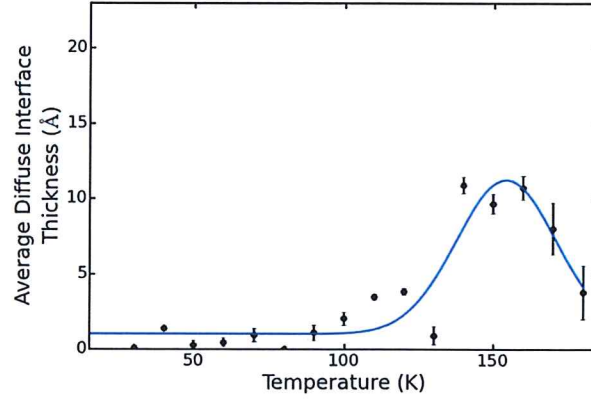
I have used that function to fit the averaged SSA data from all samples. The fit results come out a bit differently to those from the individual scans, but overall the fit works and looks very similar to the linear & exponential decay piece-wise fit that I have done before. See plots below.



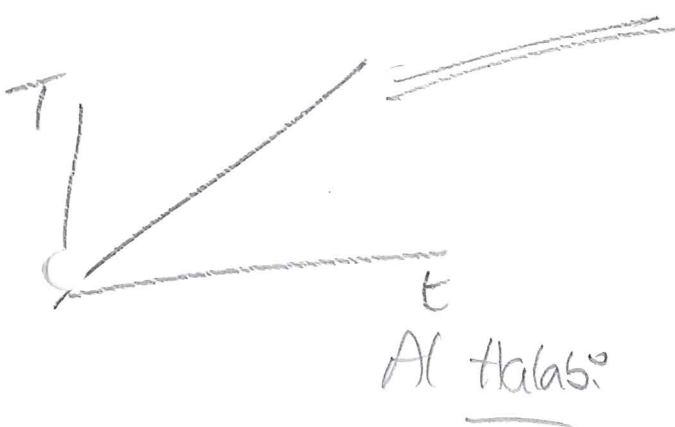
Parameters:	individual scans	averaged across all samples	Literature:
heating rate $a$ (K/h)	9.89	8.52	rotation to increase coord. 2 $\rightarrow$ 3
activation energy $E_A$ (K)	406	340	$(5 \pm 1)$ kcal/mol (2500 K)
pre factor isoth. $k_0$ (1/h)	$\approx 10$	0.81	diffusion to increase coord. 3 $\rightarrow$ 4
pre factor heat. $k_{0,\text{heat}}$ (1/h)	$\approx 0.01$	0.089 ( $x \cdot k$ )	$(9 \pm 2)$ kcal/mol (4500 K)

I'm not sure what to make of the rather low activation energy for the SSA change. I would have expected this to be of the same order as breaking at least one hydrogen bond (i.e.  $\approx 2500$  K). How could molecules move without breaking their bonds? Could they "stretch" the bonds to diffuse into the pores?

Also, why do we see SSA loss (which must mean molecular mobility and probably pore loss in some way) at all temperatures, but the diffuse layer starts to increase only around 100 – 110 K?

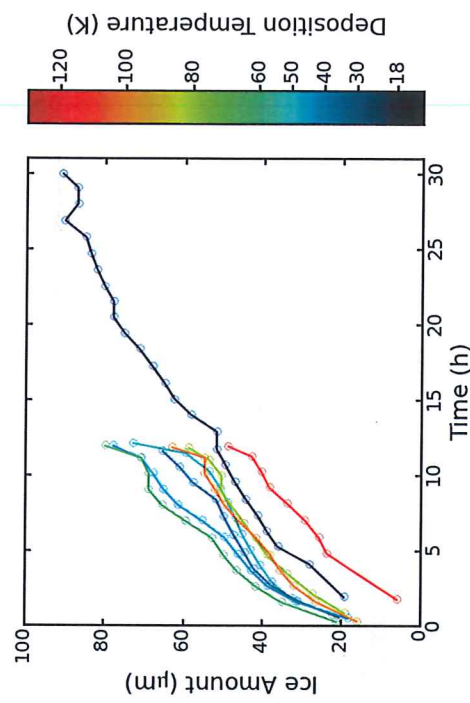


$$\frac{dt}{dT} = \frac{dL}{dT} \times \frac{1}{\frac{d(L)}{dt}}$$



## Gudrun Data Processing

Action	Analysis	tweak factor	sample thickness
Deposition	1 hour averages	derived from porosity literature (different for each deposition temperature)	fitted based on DCS level at high Q
	individual scans	Read out tweak factors & thickness from 1 hour average results.	
Annealing	isothermal averages	Use same tweak factor (constant) throughout each sample (different between samples).	Fit thickness data as linear growth (forced to start at 0 at $t_0$ ). Calculate thickness of individual scan based on its growth time.
		fitted based on DCS level at high Q	Read out thickness form final deposition data point (1 hour averages). Use that (constant) throughout each sample (different between samples).
	individual scans	Read out tweak factors & thickness from isothermal average results.	
		Interpolate tweak factor between two data points based on sample temperature (extrapolate at the ends).	Use same (constant) thickness throughout each sample (different between samples).



Ice growth is not linear. I think, we can see the changes in deposition pressure from the changing slopes. The double bump structure would then be explained by the refilling of the dosing line.  
Assuming linear growth is therefore a rather crude approximation, but I don't think that a proper fit to the ice growth is required for our purposes, so I'll leave it at that with a caveat to the SSA interpretation.

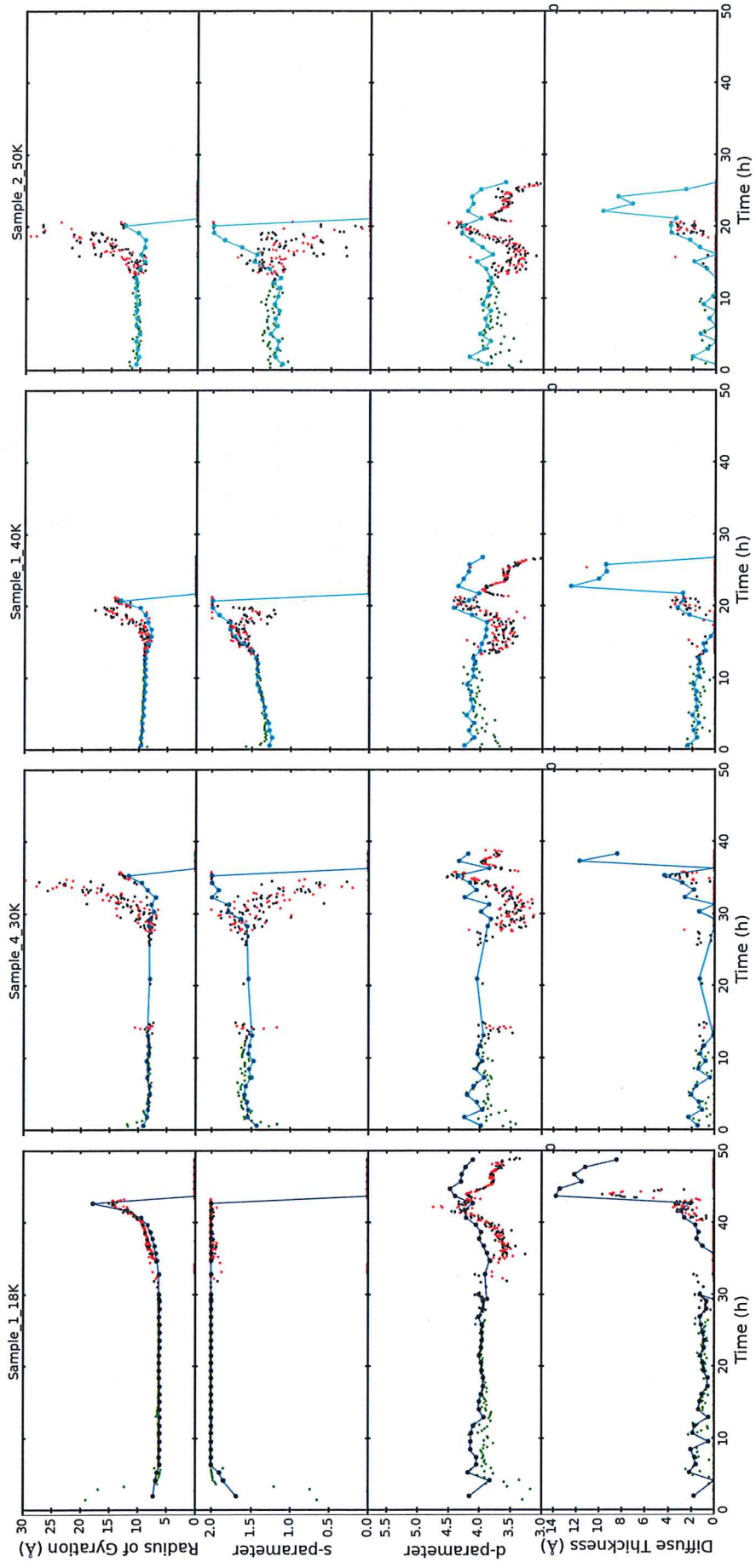
## Compare individual scans and 1 hour averages

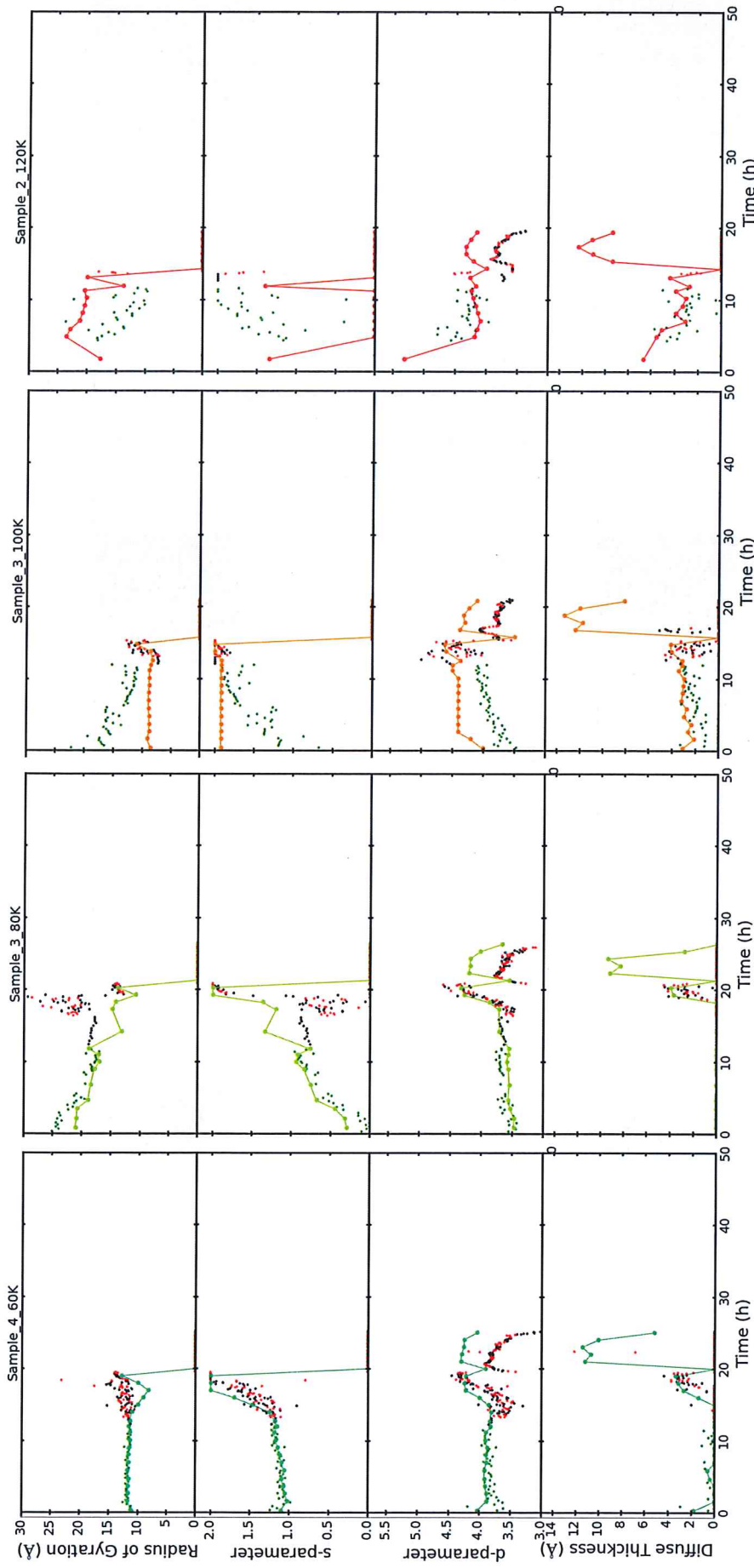
### Guinier-Porod and diffuse interface

individual scans: ● 1 hour averages during deposition / isothermal steps during annealing (colour code)

- deposition ● heating ramp ● isothermal

Deposition Temperature (K)





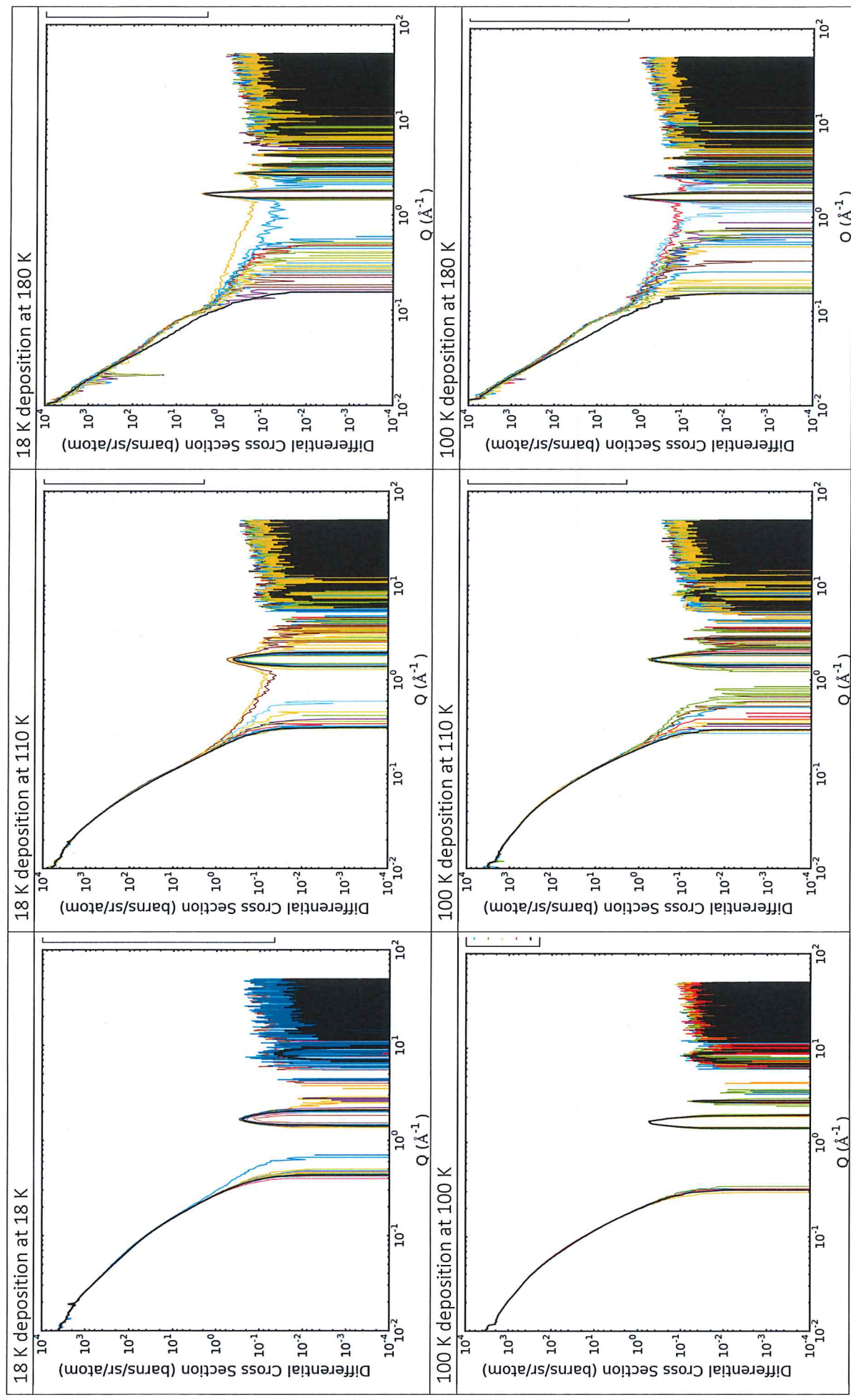
### Summary

Note: I have now fitted the same double Guinier-Porod model to all data (individual & averaged) for  $T \leq 120$  K.

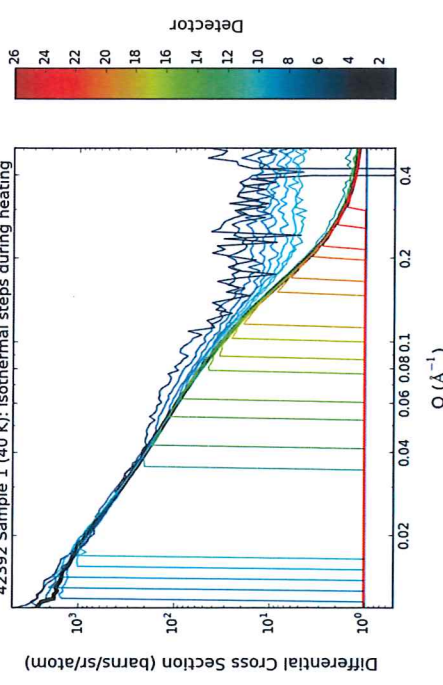
$R_g$  tends to come out larger for individual scans,  $s$ - and  $d$ -parameters (and because of  $d$  the diffuse interface thickness) tend to come out smaller for individual scans.

For most samples these discrepancies set on during the annealing, higher temperature depositions (80, 100, 120 K) show deviations also during deposition.

Part of this might be caused by different slopes. When  $d$  needs to be smaller to match a flatter slope in the high-Q end, an increase in  $R_g$  and decrease in  $s$  is required to keep the "bump" shape and position the same. The  $d$ -issue could be due to less reliable background correction for individual scans.



Comparison of the mint results (plots above) tells a somewhat different story: at the end of deposition individual scans (colour) and 1 hour averages (black) match closely. With increasing  $T$ , the high- $Q$  slopes (high- $Q$  meaning the right end of the Porod slope at a few  $10^{-1} \text{ Å}^{-1}$ ) start to flatten, but the bump stays the same. Around  $120 - 130 \text{ K}$  the individual scans start showing a pronounced bump around  $8 \times 10^{-1} \text{ Å}^{-1}$ , which isn't there in the isothermal averages. This bump appears at the end of the range where double Guinier-Porod fits are not working very well anyways as the small scattering objects (pores?) disappear (in the  $R_g$  &  $s$  plots above that is where  $R_g$  and  $s$  drop to zero). As the bump becomes more pronounced it affects the slope that is fitted in the high temperature Guinier-Porod fits, making it flat again.



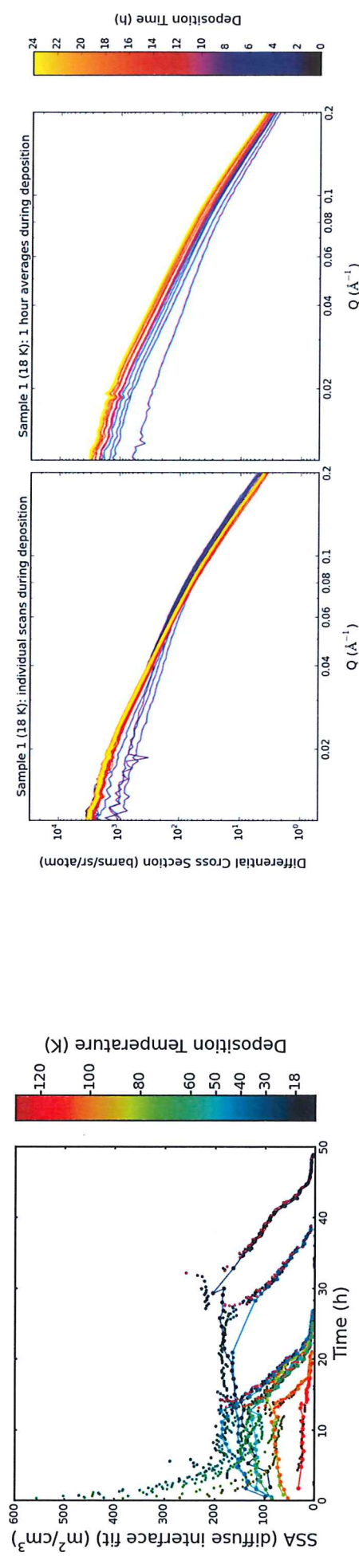
I'm happy to believe that the slope at the high- $Q$  end is affected by background subtraction issues when working with poor statistics.

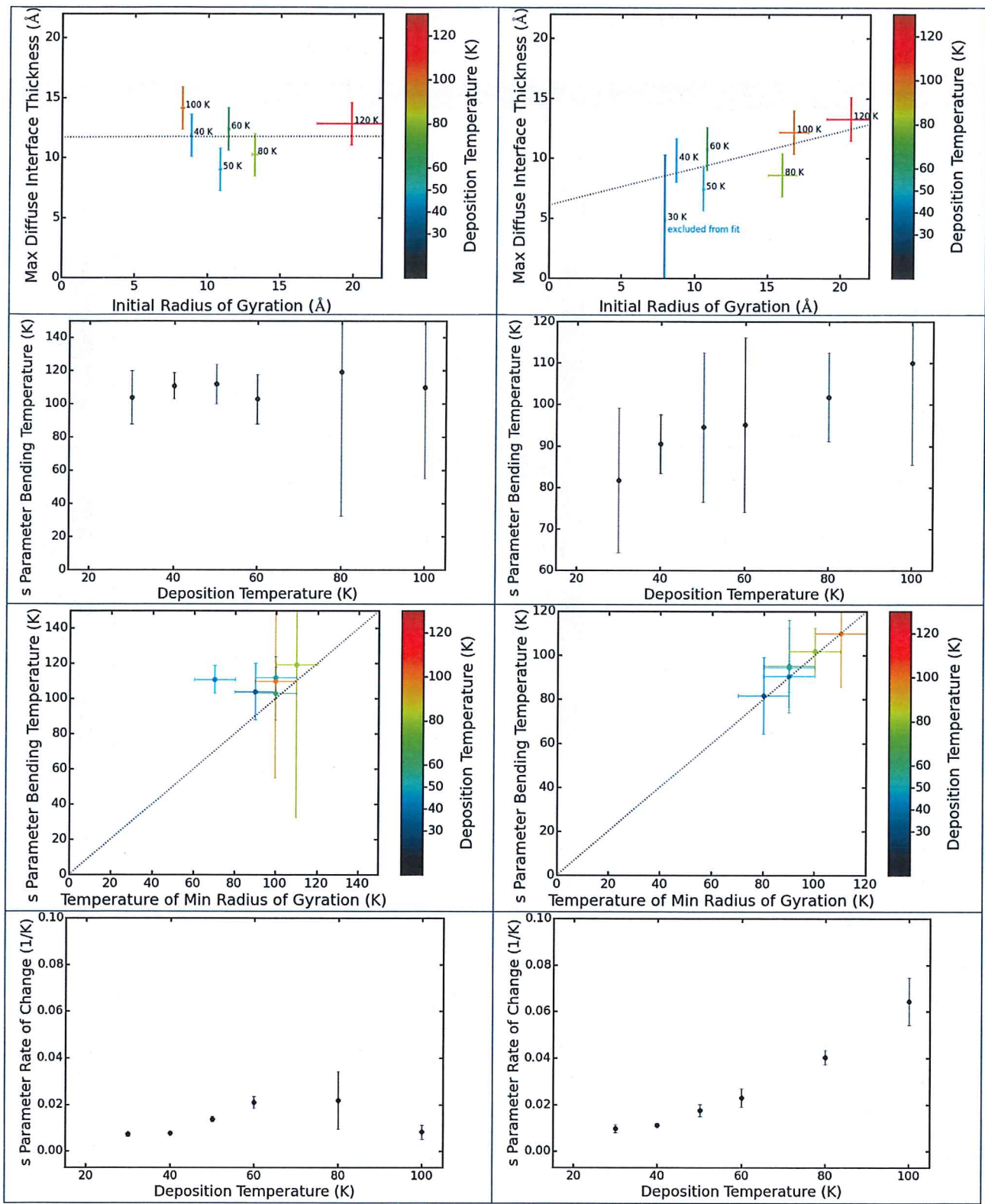
What about the high temperature data? The odd bump is two orders of magnitude above the background noise level. But it is where weird bumps appear in the isothermal data as well, when splitting them up into the different detectors (see plot to the right). So it probably is statistics issues as well, just of another type.

**The consequence of both would be to trust the Guinier-Porod and diffuse interface results from 1 hour averaged data and ignore those from individual scans.**

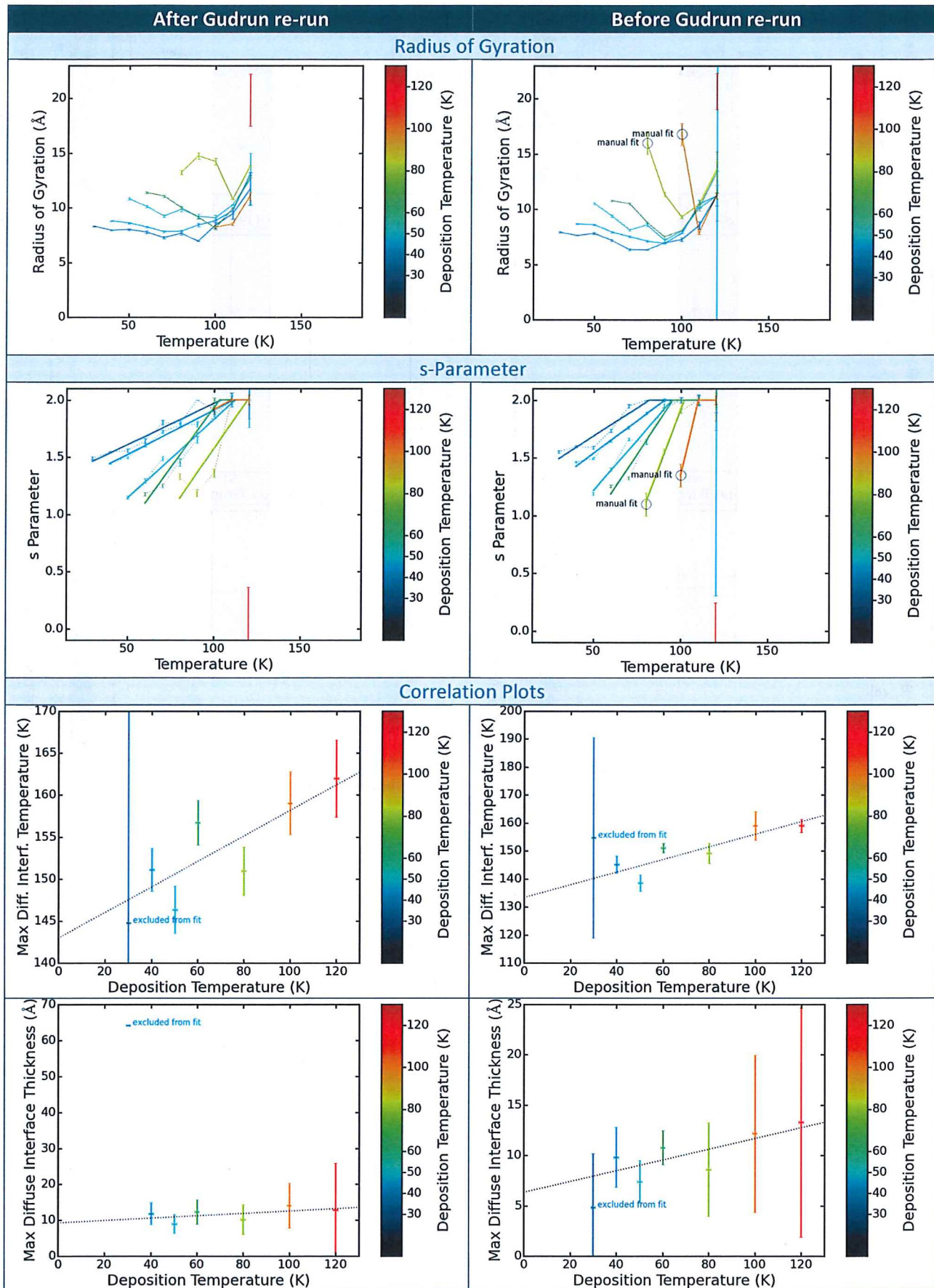
### SSA

The SSA during annealing closely matches for individual scans and isothermal averages. The deposition SSA starts off way too high and with time comes down to the 1 hour average results (symbols and colour code as in Guinier-Porod result plots above). This can be explained by the way I constrained sample thickness and tweak factor in the Gudrun processing.

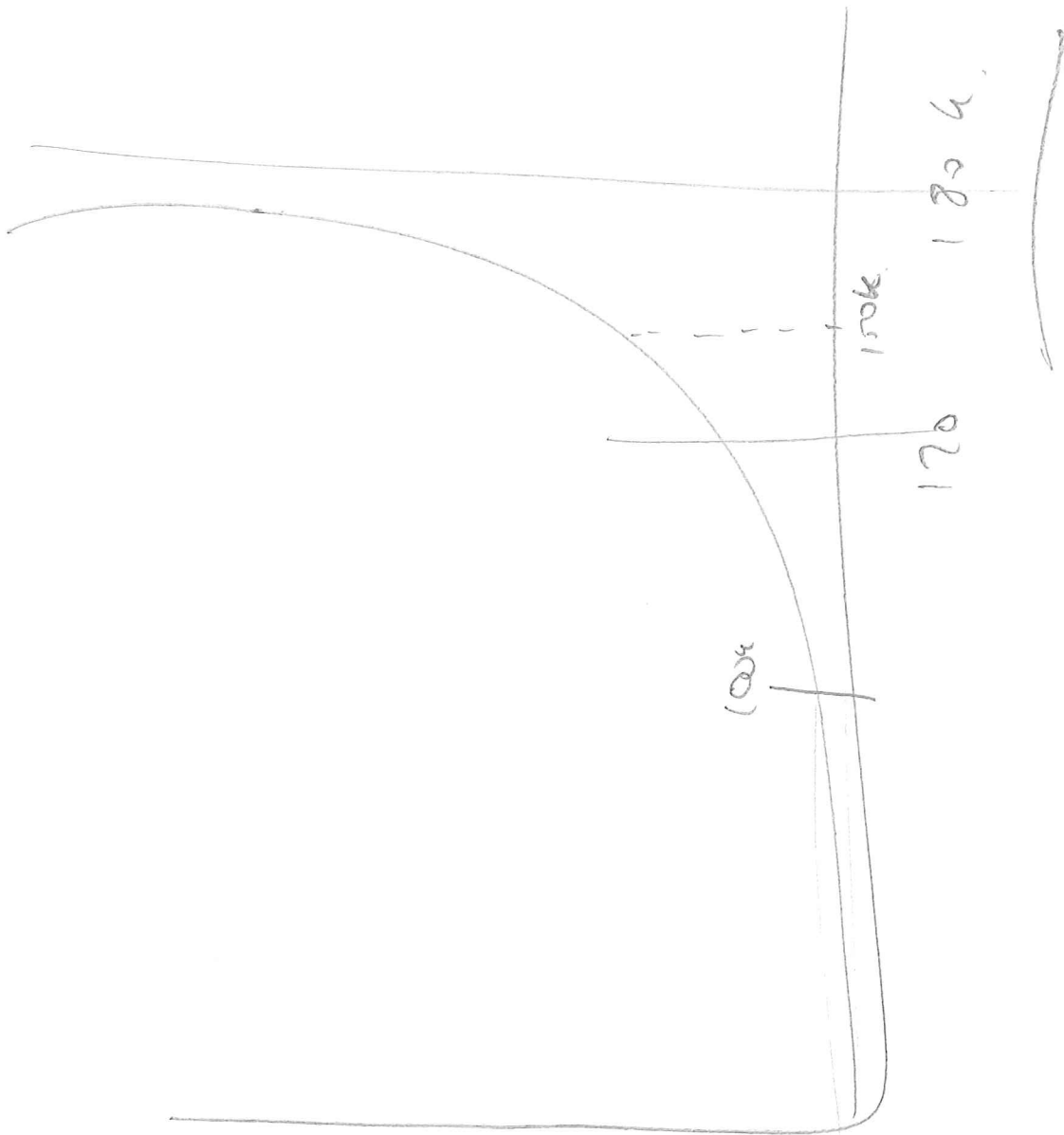




Some of the correlations between deposition temperature and changes in  $s$ ,  $R_g$ , and diffuse interface thickness are less clear after re-running Gudrun. We need to discuss to what degree we can interpret those.



24.08.2017



$$\alpha = 0.94 \text{ fm}$$



$$\frac{1}{T_x} \approx 1/\nu$$

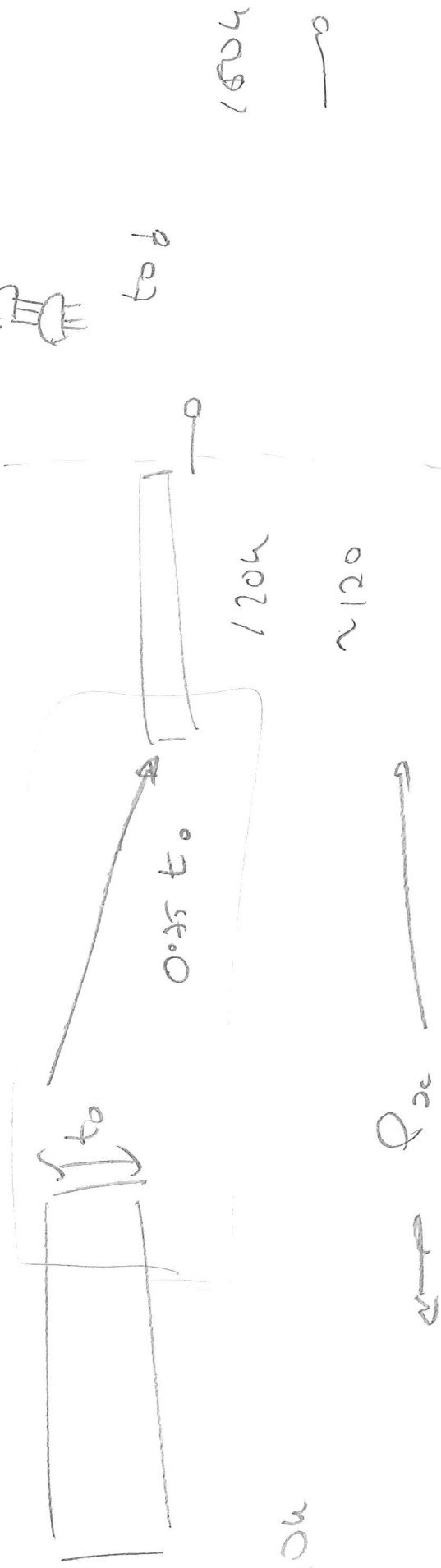


(long) waves - standing

Peak dist.

unif.

Box



100k

Osc.  $t_0$

~120

~180k

to b

100k

120k

$T_x$

## Porosity & Pore Dimensions

### Radius of Gyration:

Guinier-Porod model:

infinitely long cylinder (rod)	radius R	$s = 1$	$R_g = \frac{R}{\sqrt{2}}$	per definition
lamella (infinitely thin disk)	thickness T	$s = 2$	$R_g = \frac{T}{\sqrt{12}}$	per definition
random cylinder	radius R thickness T = $\alpha \cdot R$	$s \in [1,2]$	$R_g = R \cdot \left( \frac{2-s}{\sqrt{2}} - \alpha \cdot \frac{s-1}{\sqrt{12}} \right)$	I made that up (to match both extreme cases)

### Volumes & Surfaces

volume of individual pore	$v_p$	total number of pores	$N_p$	total pore volume	$V_p = N_p \cdot v_p$
ice volume (excluding pores)	$V_i$	number density of pores	$n_p = \frac{N_p}{V_i}$	sample volume (including pores)	$V_s = V_i + V_p$
tweak factor	$t = \frac{V_s}{V_i}$	surface area of individual pore	$a_p$	total surface area of all pores	$A_p = N_p \cdot a_p$

$$t = \frac{V_i + V_p}{V_i} = 1 + n_p \cdot v_p \quad \Rightarrow \quad n_p = \frac{t-1}{v_p}$$

Assume that sample surface is negligible compared to pore surface:

$$SSA = \frac{A_p}{V_i} = n_p \cdot a_p = (t-1) \cdot \frac{a_p}{v_p}$$

Go back to random cylinder from above:

$$\begin{aligned} v_p &= \pi \cdot \alpha \cdot R^3 \quad \wedge \quad a_p = 2\pi \cdot \alpha \cdot R^2 \\ \Rightarrow SSA &= (t-1) \cdot \frac{2}{R} = (t-1) \cdot \frac{2}{R_g} \cdot \left( \frac{2-s}{\sqrt{2}} + \alpha \cdot \frac{s-1}{\sqrt{12}} \right) \\ \Rightarrow \alpha &= \frac{SSA \cdot R_g \cdot \sqrt{3}}{(t-1) \cdot (s-1)} - \frac{2-s}{s-1} \cdot \sqrt{6} \end{aligned}$$

Plot  $\alpha$  against  $s$ :

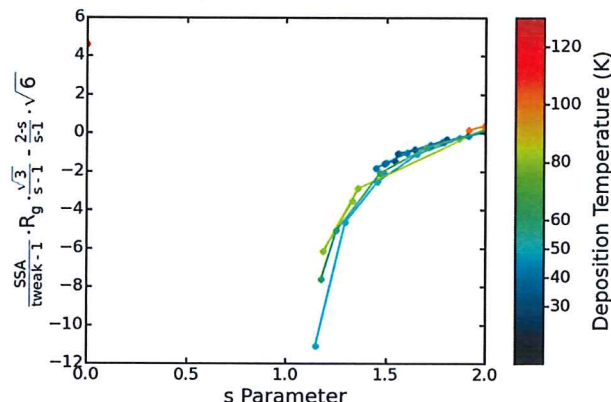
That shows a clear trend, but comes out negative.

Per definition it should be positive ( $\alpha = T/R$ ).

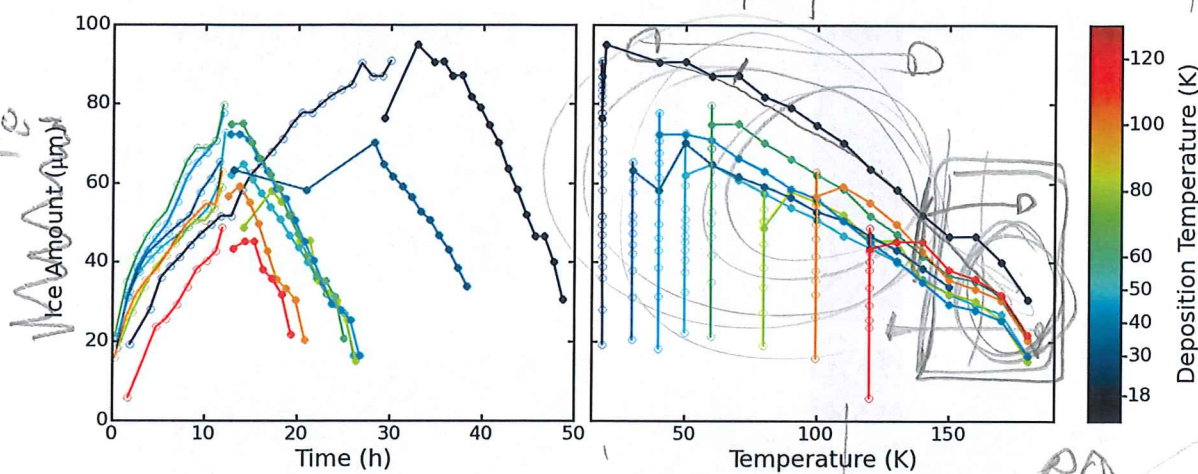
I would expect:

$$\alpha \rightarrow \infty \text{ for } s \rightarrow 1 \quad \text{and} \quad \alpha \rightarrow 0 \text{ for } s \rightarrow 2$$

Is  $\alpha < 0$  because the assumption that only pores contribute to SSA is completely wrong for our (probably granular) samples? Or should  $n_p$  be  $N_p/V_s$ ? Or are tweak factors and  $V_s$  rubbish (desorption)?



## Ice Amount



Empty circles: deposition, filled circles: annealing

Ice amount is corrected for tweak factor (i.e. total thickness used in Gudrun divided by tweak factor used in Gudrun).

Deposition:  $I_c$  growth seems to slow down with deposition time (except for 120 K deposition).

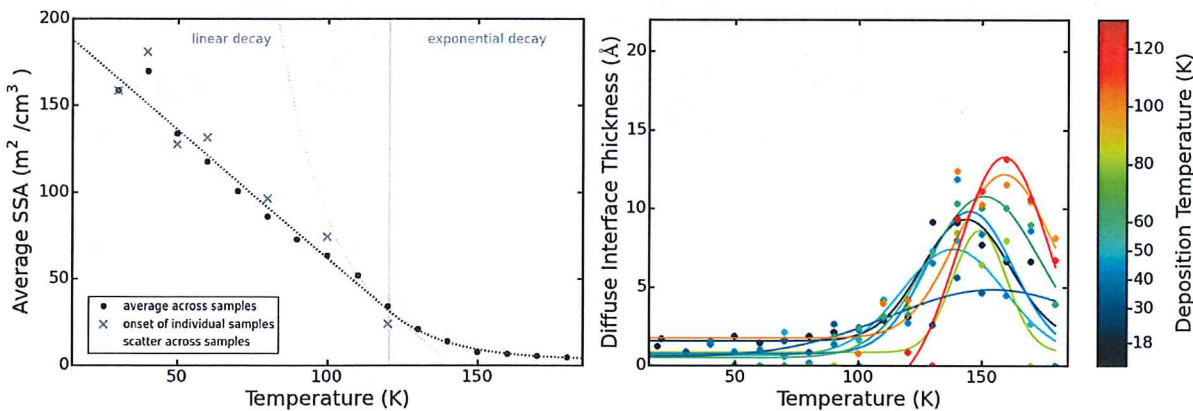
⇒ Thermal conductivity issues with increasing ice thickness?

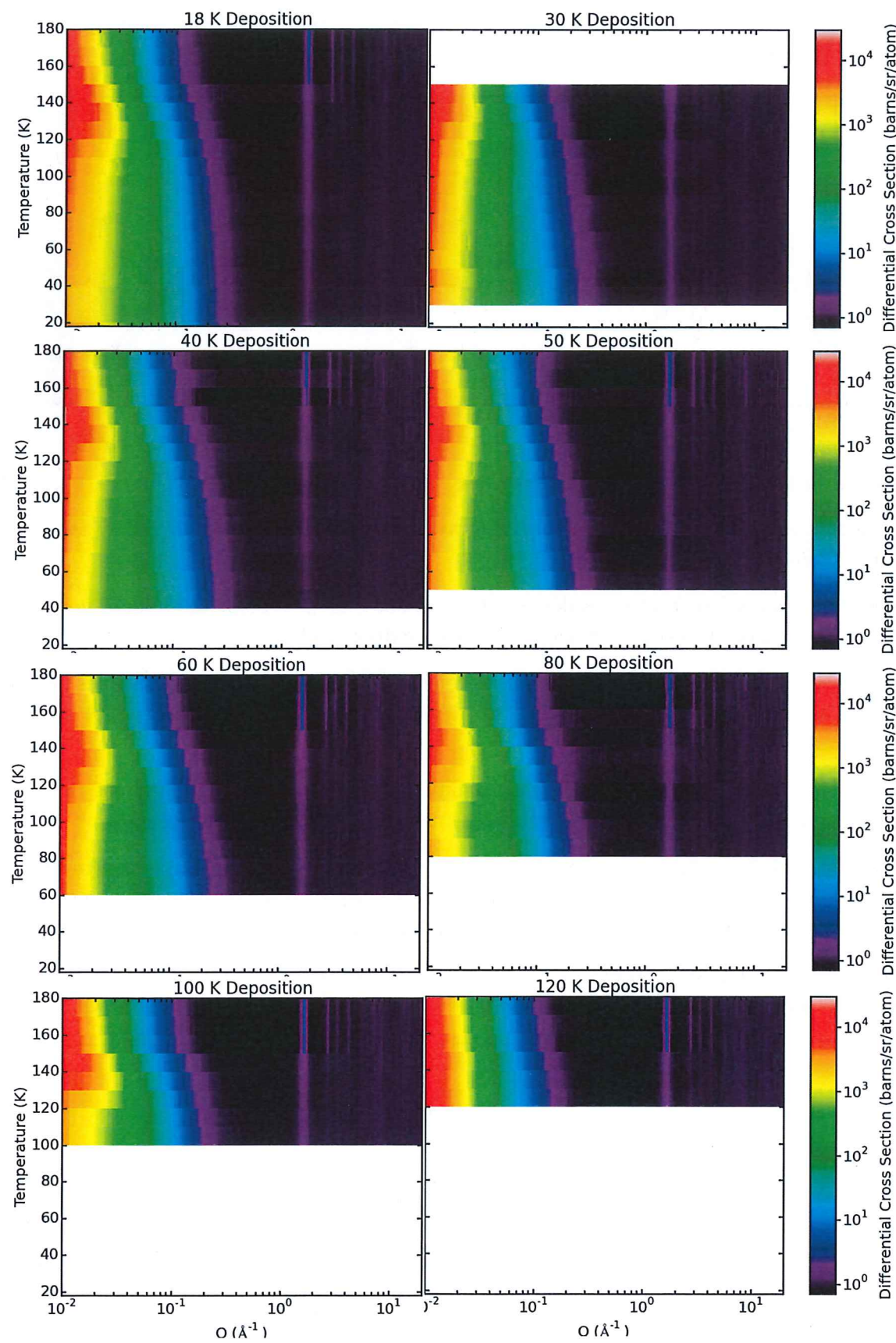
Ice amount decreases with increasing annealing temperature. Slopes for different samples very nicely line up. Slopes suddenly change (less steep) for all samples at 150 K, then go back (steep) around 160 – 170 K.

This matches the crystallisation temperature and the maximum of the diffuse interface thickness. It does not match the point where we see changes in SSA behaviour! (See pictures below.)

Therefore, I conclude that as we are heating the sample, we are using some of this energy to evaporate material. At the crystallisation point, most of the energy is used for molecular re-orientation (crystallisation and diffuse surface increase). When that is done, the evaporation rate goes back up.

I don't think it is neutron statistics issues, which would reflect the behaviour of the SSA (if too many neutrons were scattered to small angles so we were left with "wrong" numbers at high Q).





Conversion between  $\frac{1}{\text{cm}}$  & barn/sr/atom intensity units:

(Gudrun manual)  
equation 3.1  
page 51

Differential cross section:

$$\frac{d\sigma}{d\Omega}(\lambda, 2\theta) = \frac{\text{CNT}(\lambda, 2\theta)}{N \langle \Phi(\lambda, t) \rangle_t \Delta \Omega(2\theta) \Delta t}$$

N: number of atoms

$\Delta\lambda$ : wavelength range  $\lambda, \lambda + \Delta\lambda$  (neutron wavelength)

$\Delta t$ : time interval

$\Delta\Omega(2\theta)$ : solid angle in the direction  $2\theta$

$\langle \Phi(\lambda, t) \rangle_t = \frac{\int_0^t \Phi(\lambda, t') dt'}{\Delta t}$  : average number of impinging particles  
(per unit area, time & wavelength)

CNT( $\lambda, 2\theta$ ): number of neutrons scattered in  $\Delta t$ ,  $\Delta\lambda$  &  $\Delta\Omega(2\theta)$

$\Rightarrow$  differential cross section =  $\frac{\text{detected scattered neutrons}}{\text{scattering atoms} \cdot \text{incident neutrons} \cdot \Delta t, \Delta\lambda, \Delta\Omega(2\theta)}$

units:  $[DCS] = \frac{1}{\text{s} \cdot \text{m} \cdot \text{sr} \cdot \text{atom}}$

That doesn't make sense.

To convert from  $\frac{10^{-28} \text{ m}^2}{\text{sr} \cdot \text{atom}}$  to  $\frac{1}{\text{cm}}$ , I would have to multiply by  $\frac{\text{sr} \cdot \text{atoms}}{\text{m}^3}$ .

$$I = \Omega \cdot m \cdot DCS \Rightarrow [I] = \frac{10^{-28}}{m} = \frac{10^{-28}}{10^2 \text{ cm}} = \frac{10^{-30}}{\text{cm}}$$

solid angle  
number density  
of scatterers

08.09.2017

SasView assumes units of  $\frac{1}{\text{cm} \cdot \text{sr}}$ . Conversion requires only the number density

$$I = m \cdot DCS, m = 0.094 \frac{\text{atoms}}{\text{A}^3} \Rightarrow [I] = \frac{10^{-28} \text{ m}^2}{\text{sr} \cdot \text{A}^3} = \frac{10^{-28}}{10^{-30}} \frac{1}{\text{sr} \cdot \text{m}} = \frac{1}{10^2 \text{ m} \cdot \text{sr}}$$

07.09.2017

## Interpretation of SasView results:

$$p_2 \text{ peak position (Gaussian)} = \frac{2\pi}{\text{lamella spacing}} \Rightarrow \text{pos} = \frac{2\pi}{s}$$

$$\Rightarrow s = \frac{2\pi}{\text{pos}} \Rightarrow \Delta s = \frac{2\pi \Delta \text{pos}}{\text{pos}^2} = s \cdot \frac{\Delta \text{pos}}{\text{pos}}$$

scale: SasView fits  $I(q) = \text{scale} \cdot \text{function}(q)$

I provided  $\text{DCS} = \frac{I}{m}$  instead of  $I \Rightarrow \frac{I}{m} = \frac{\text{scale}}{m} \cdot \text{function}$

$$\Rightarrow \text{scale}_{\text{DCS}} = \frac{\text{scale}}{m} \Rightarrow \text{scale} = m \cdot \text{scale}_{\text{DCS}}$$

scale is the volume fraction of scatterers (voids):

$$V = V_{\text{sample}} + V_{\text{void}} \Rightarrow 1 = \frac{V_{\text{sample}}}{V} + \frac{V_{\text{void}}}{V} = \frac{V_{\text{sample}}}{V} + \text{scale}$$

porosity is volume of pores divided by total volume  $\Rightarrow \text{porosity} = \text{scale}$

## Theory about surface changes:

(Kolasinski 2002, Surface Science - Book from Helen)

For a uniform potential, surface diffusion is governed by an Arrhenius form:  
(eq. 3.1, page 87)

$$D = D_0 e^{-\frac{E_{\text{diff}}}{RT}}$$

,  $E_{\text{diff}}$  = activation energy for diffusion

$R$  = gas constant,  $T$  = temperature (surface)

This equation does not work for:

a) very light adsorbates (e.g. H) at very low temperatures

→ tunneling → diffusion  $T$ -independent

b) high temperatures:  $RT \gg E_{\text{diff}}$

→ Brownian motion, only bound perpendicular to surface → 2D gas

Surface structure: if surface has rows or other defects, molecules have preferential diffusion directions, dictated by surface structure

08.09.2017

Surface coverages:  $\Theta \rightarrow$  w.r.t. number of surface atoms

$\delta \rightarrow$  fractional coverage w.r.t. number of adsorption sites

(Definitions: table 4.1, page 166)

Rate of desorption (Polanyi-Wigner equation 4.25, page 173):

$$\dot{\Gamma}_{\text{des}} = -\frac{\partial \Theta}{\partial t} = v_n \Theta^m e^{-\frac{E_{\text{des}}}{RT}}$$

,  $v_n$ : pre-exponential factor

(in ML/s)

$m$ : order of the chemical process

First order desorption:

$$\dot{\Gamma}_{\text{des}} = \Theta k_{\text{des}}$$

,  $k_{\text{des}}$ : rate constant

$$k_{\text{des}} = A e^{-\frac{E_{\text{des}}}{RT}}$$

,  $A$ : pre-exponential factor

often  $A$  and  $E_{\text{des}}$  vary with coverage  $\Rightarrow A = A(\Theta)$ ,  $E_{\text{des}} = E_{\text{des}}(\Theta)$

often they vary in concert:  $A(\Theta) = c \cdot e^{\frac{E_{\text{des}}(\Theta)}{RT\Theta}}$ ,  $T_\Theta$ : isokinetic temp.

$$\Rightarrow k_{\text{des}} = c \cdot e^{\frac{E_{\text{des}}(\Theta)}{RT\Theta}} e^{\frac{E_{\text{des}}(\Theta)}{RT}} = c \cdot e^{\frac{E_{\text{des}}}{RT\Theta} \cdot (T_\Theta + T)} = c \cdot e^{\frac{E_{\text{des}}}{RT} \cdot (1 + \frac{T}{T_\Theta})}$$

the above relation is called compensation effect, it results from:

- heterogeneous surfaces (range of binding energies)
- lateral interactions (can cause coverage dependent phase changes of adsorbate)
  - \* direct interaction due to wavefunction overlap (upto chemical bonds)
  - \* indirect interaction: binding of adsorbate shifts states of neighbouring sites
- \* elastic interaction: local lattice distortion in vicinity of adsorbate
  - ⇒ repulsive interaction with neighbouring adsorbates
- \* nonlocal electrostatic effects: dipole-dipole (or multipole-multipole) Van-der-Waals forces between adsorbates
  - repulsive or attractive depending on dipole orientation
- adsorbate induced changes in substrate structure

11.09.2017

Temperature Programmed Desorption: (pages 193 onwards)

temperature ramp:  $T_s = T_0 + \beta t$ ,  $T_s$  = surface temperature,  
 $\beta$  = heating rate,  $t$  = time,  $T_0$  = base temperature

change in the number of gas phase molecules:  $V$  = chamber volume

$$V \frac{dc_g}{dt} = A_s \tau_{des}(t) + L - c_g S$$

$c_g$  = gas density

$A_s$  = sample surface area

$S$  = pumping speed

assumptions:  $S$  &  $L$  constant

$L$  = desorption rate from walls

( $\rightarrow$  sample holder not warming up and pressure rise not high enough to affect pumping speed)

steady state solution:  $L = c_g S$

$$\Rightarrow \text{steady state pressure: } p_s = \frac{k_B T_g c_g}{S} \quad T_g = \text{gas temperature}$$

pressure change caused by desorption:  $\Delta p = p - p_s$

$$\Rightarrow \Delta p = k_B T_g c_g - k_B T_g \frac{L}{S} = k_B T_g \left( c_g - \frac{L}{S} \right)$$

$$\Rightarrow c_g = \frac{\Delta p}{k_B T_g} + \frac{L}{S}$$

$$\Rightarrow V \frac{dp}{dt} \left( \frac{\Delta p}{k_B T_g} + \frac{L}{S} \right) = A_s \tau_{des}(t) + L - \left( \frac{\Delta p}{k_B T_g} + \frac{L}{S} \right) \cdot S \quad | T_g \text{ const.}$$

$$\Rightarrow V \frac{dp}{dt} \Delta p = k_B T_g \cdot (A_s \tau_{des}(t) + L - \frac{\Delta p S}{k_B T_g} - \frac{L}{S} \cdot S - \frac{d(L)}{dt} \cdot S) \cdot V$$

$$\Rightarrow V \frac{d\Delta p}{dt} = k_B T_g (A_s \dot{r}_{des}(t) - 0 \cdot V) - \Delta p S$$

$$\Rightarrow V \frac{d\Delta p}{dt} + \Delta p S = k_B T_g A_s \dot{r}_{des}(t)$$

For high pumping speed  $\frac{d\Delta p}{dt} \approx 0 \Rightarrow \Delta p = \frac{k_B T_g A_s}{S} \dot{r}_{des}(t)$

→ the measured pressure change is directly proportional to the desorption rate

Questions: \* How reasonable is the assumption that the temperature of the gas is not changing as the sample is heated?

\* How reasonable are then the assumptions that pumping speed and wall-desorption are not changing during heating?

\* The assumption  $\frac{d\Delta p}{dt} = 0$  means  $\frac{d^2}{dt^2} p = 0$ , right?

So only linear pressure changes. This clearly does not hold true, as TPD curves usually show pressure peaks. ⇒ How can they be interpreted based on oversimplified equations?

Back to Polanyi-Wigner equation for desorption:

$$-\frac{\partial \theta}{\partial t} = r_{des}(t) = V_m \theta^m e^{-\frac{E_{des}}{RT_s}} \quad \text{set } R=1 \text{ for easier math}$$

$$= V_m \theta^m e^{-\frac{E_{des}}{T_0 + \beta t}}$$

assume  $V_m \& E_{des}$  to be  $\theta$ -independent

Desorption maximum occurs where  $\frac{dr_{des}}{dt} = 0$  and  $\frac{d^2 r_{des}}{dt^2} < 0$

$$\frac{d}{dt} r_{des}(t) = V_m m \cdot \theta^{m-1} \cdot \frac{\partial}{\partial t} \theta \cdot e^{-\frac{E_{des}}{T_0 + \beta t}} + V_m \cdot \theta^m \cdot e^{-\frac{E_{des}}{T_0 + \beta t}} \cdot \frac{\partial}{\partial t} \left( -\frac{E_{des}}{T_0 + \beta t} \right)$$

$$= V_m \cdot m \cdot \theta^{m-1} \cdot (-r_{des}(t)) \cdot e^{-\frac{E_{des}}{T_0 + \beta t}} + V_m \theta^m \cdot e^{-\frac{E_{des}}{T_0 + \beta t}} \cdot \left( -\frac{E_{des}}{(T_0 + \beta t)^2} \right) \cdot (-\beta)$$

$$= V_m \cdot m \theta^{m-1} \cdot e^{-\frac{E_{des}}{T_0 + \beta t}} \cdot (-r_{des}(t)) + \theta/m \frac{E_{des}}{(T_0 + \beta t)^2} \cdot \beta \stackrel{!}{=} 0$$

$$\Rightarrow r_{des}(t) = \frac{\theta \cdot \beta}{m} \frac{E_{des}}{(T_0 + \beta t)^2} \Rightarrow V_m \theta^m e^{-\frac{E_{des}}{T_0 + \beta t}} = \frac{\theta \cdot \beta}{m} \frac{E_{des}}{(T_0 + \beta t)^2}$$

$$\text{temperature of desorption maximum: } T_p \Rightarrow \frac{E_{des}}{T_p^2} = V_m \cdot \frac{m}{\beta} \theta^{m-1} e^{-\frac{E_{des}}{T_p}}$$

11.09.2017

## ASW: Understand Porosity & Surface Changes

### SSA:

Assumption 1: Sample is formed by square blocks of ice, separated by thin layers of vacuum ("streets of New York" picture).  
 Blocks & sample are infinitely high. (sample thickness  $\approx 70 \mu\text{m} = 7 \cdot 10^5 \text{\AA}$ , blocks & gaps will be  $\approx 2 \cdot 10^2 \text{\AA}$ )

$$\text{Volume of block: } V_b = b^2 \cdot h \quad b = \text{block width}, h = \text{height}$$

$$\text{Volume of sample: } V_s = N \cdot V_b = N \cdot b^2 \cdot h \quad N = \text{number of blocks} \quad (\text{intrinsic volume})$$

$$\text{Surface of block: } S_b = 4 \cdot b \cdot h + 2 \underbrace{b^2}_{\text{ignore when sample infinitely high}}$$

$$\text{Surface of Sample: } S_s = N \cdot S_b \approx 4 \cdot b \cdot h \cdot N$$

$$\Rightarrow \text{SSA} = \frac{S_s}{V_s} = \frac{4 b h N}{b^2 h N} = \frac{4}{b} \quad \Rightarrow \quad b = \frac{4}{\text{SSA}}$$

$$\text{Examples: } \text{SSA}_{20K} \approx 160 \frac{\text{m}^2}{\text{cm}^3} = 160 \cdot 10^{-4} \frac{1}{\text{\AA}} = 16 \cdot 10^{-3} \frac{1}{\text{\AA}}$$

$$\Rightarrow b_{20K} \approx \frac{4}{16} \cdot 10^3 \text{\AA} = \frac{1}{4} \cdot 10^3 \text{\AA} = 250 \text{\AA}$$

$$\text{SSA}_{180K} \approx 6 \frac{\text{m}^2}{\text{cm}^3} = 6 \cdot 10^{-4} \frac{1}{\text{\AA}}$$

$$\Rightarrow b_{180K} \approx \frac{4}{6} \cdot 10^4 \text{\AA} = \frac{2}{3} 10^4 \text{\AA} \approx 6,7 \cdot 10^3 \text{\AA}$$

} These numbers  
are larger than  
the SasView  
results

Assumption 2: Sample is formed by cubic blocks of ice, separated by thin layers

$$V_b = b^3, V_s = N \cdot b^3, S_b = 6 \cdot b^2, S_s = N \cdot 6 \cdot b^2$$

$$\Rightarrow \text{SSA} = \frac{6}{b} \quad \Rightarrow \quad b = \frac{6}{\text{SSA}} \quad \rightarrow \text{Even larger numbers for } b$$

Assumption 3: Sample is formed by infinitely long blocks with thin gaps (valleys)

$$V_b = b \cdot L \cdot h, V_s = N \cdot b \cdot L \cdot h, S_b = 2L \cdot h + 2b \cdot h + 2L \cdot b, S_s = N \cdot S_b$$

$$\Rightarrow \text{SSA} = 2 \frac{Lh + bh + Lb}{bLh} = \frac{2}{b} + \frac{2}{L} + \frac{2}{h} \approx \frac{2}{b} \quad \text{if } L \approx h \approx \infty \quad \Rightarrow \quad b \approx \frac{2}{\text{SSA}}$$

$$\Rightarrow b_{20K} \approx 125 \text{ \AA} ; b_{180K} \approx 3.3 \cdot 10^3 \text{ \AA}$$

The low T value is similar to the results obtained from SasView.

However, the SasView position for the Gaussian peak does not change significantly with T, while the SSA does.

If the Gaussian peak position really is the spacing between pores (i.e. width of ice blocks) it should change, as the pore width is changing. 160 \AA thick pores cannot be 100 \AA apart. Maybe the issue is just caused by unreliable results for the Gaussian position.

### Porosity:

Assumption 3:

$$\rho = \frac{N \cdot V_p}{N \cdot V_p + V_s}$$

$$V_p = p \cdot L \cdot h \quad p = \text{pore width}$$

$$= \frac{N \cdot p \cdot L \cdot h}{N \cdot p \cdot L \cdot h + N \cdot b \cdot L \cdot h} \quad \text{assume number of pores = number of blocks}$$

$$\Rightarrow \rho = \frac{p}{p+b} \approx \frac{p}{p+\frac{b}{SSA}}$$

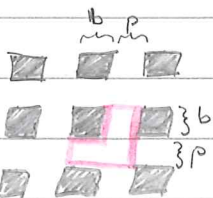
$$\Rightarrow \rho \cdot p + \frac{\rho \cdot 2}{SSA} = p \Rightarrow p \cdot (1-\rho) = \frac{2\rho}{SSA} \Rightarrow p = \frac{\rho}{1-\rho} \cdot \frac{2}{SSA}$$

$$\text{Examples: } P_{20K} \approx 11 \cdot 10^{-2} \Rightarrow p_{20K} \approx 1.5 \cdot 10^3 \cdot 10^4 \text{ \AA} = 15 \text{ \AA}$$

$$P_{180K} \approx 3 \cdot 10^{-2} \Rightarrow p_{180K} \approx 1 \cdot 10^{-2} \cdot 10^4 \text{ \AA} = 100 \text{ \AA}$$

These numbers are very close to the actual fit results from SasView (18 and 160 \AA)

$$\text{Assumption 1: } V_p = h \cdot (p \cdot b \cdot 2 + p^2), \quad N_p = N_b = N$$



$$\rho = \frac{N \cdot h \cdot (2pb + p^2)}{Nh(2pb + p^2) + Nh \cdot b^2} = \frac{2pb + p^2}{2pb + p^2 + b^2}$$

$$\Rightarrow p^2 + 2pb - \rho p^2 - \rho 2pb - \rho b^2 = 0 \Rightarrow p^2(1-\rho) + 2pb(1-\rho) - \rho b^2 = 0$$

$$\Rightarrow p^2 + 2pb + b^2 - b^2 - \frac{p}{1-p} b^2 = 0 \Rightarrow (p+b)^2 = \frac{1-p+p}{1-p} b^2$$

$$\Rightarrow p+b = \sqrt{\frac{1}{1-p}} b \Rightarrow p = b \cdot \left( \sqrt{\frac{1}{1-p}} - 1 \right) = \frac{b}{SSA} \cdot \left( \sqrt{\frac{1}{1-p}} - 1 \right)$$

Examples:  $p_{20K} \approx 1.5 \cdot 10^{-3} \cdot 10^4 \text{ Å} = 15 \text{ Å}$ ,  $p_{180K} \approx 10^{-2} \cdot 10^4 \text{ Å} = 100 \text{ Å}$

Differences between the two assumptions are negligible w.r.t. results for pore dimensions.

Pore spacings (i.e. ice block widths) seem to be closest to Gaussian peak position for assumption 3 (valleys & mountain chains), but Gaussian position is not reliable enough to hang a model on.

Changes with annealing: Pores and ice blocks become wider.

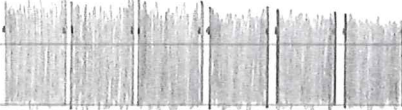
based on porosity & SSA changes, blocks grow by a factor of

$$\frac{1}{3} \cdot 10^3 \cdot \left( \frac{1}{8} \cdot 10^3 \right)^{-1} = \frac{8}{3}, \text{ pores grow by } \frac{100}{15} = \frac{20}{3} \quad (\text{or } \frac{160}{18} = \frac{80}{9} \approx \frac{27}{3})$$

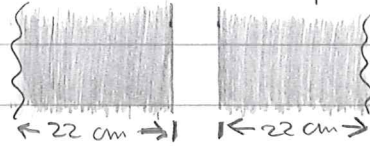
$\Rightarrow$  Pore width grows  $\approx$  factor 3 more than ice block width.

What mechanism could cause such changes?

$$20K: 125 \text{ Å blocks} \quad \left. \begin{matrix} \\ \end{matrix} \right\} \approx 8:1 \quad 15 \text{ Å pores}$$



$$180K: 3333 \text{ Å blocks} \quad \left. \begin{matrix} \\ \end{matrix} \right\} \approx 33:1 \quad 100 \text{ Å pores}$$



Sample amounts:  $V_{Si} = N_i \cdot b_i \cdot L_i \cdot h_i$ ,  $i = 20K$  (initial)

$$V_{Sf} = N_f \cdot b_f \cdot L_f \cdot h_f \quad , f = 180K \text{ (final)}$$

etc.

total volume

$$\Rightarrow V_{ti,i} = V_{Si} + V_{Pi,i} = N_i (b_i + p_i) L_i h_i = N_i l_i h_i b_i (x_i + 1), b_i/f = x_i p_i/f$$

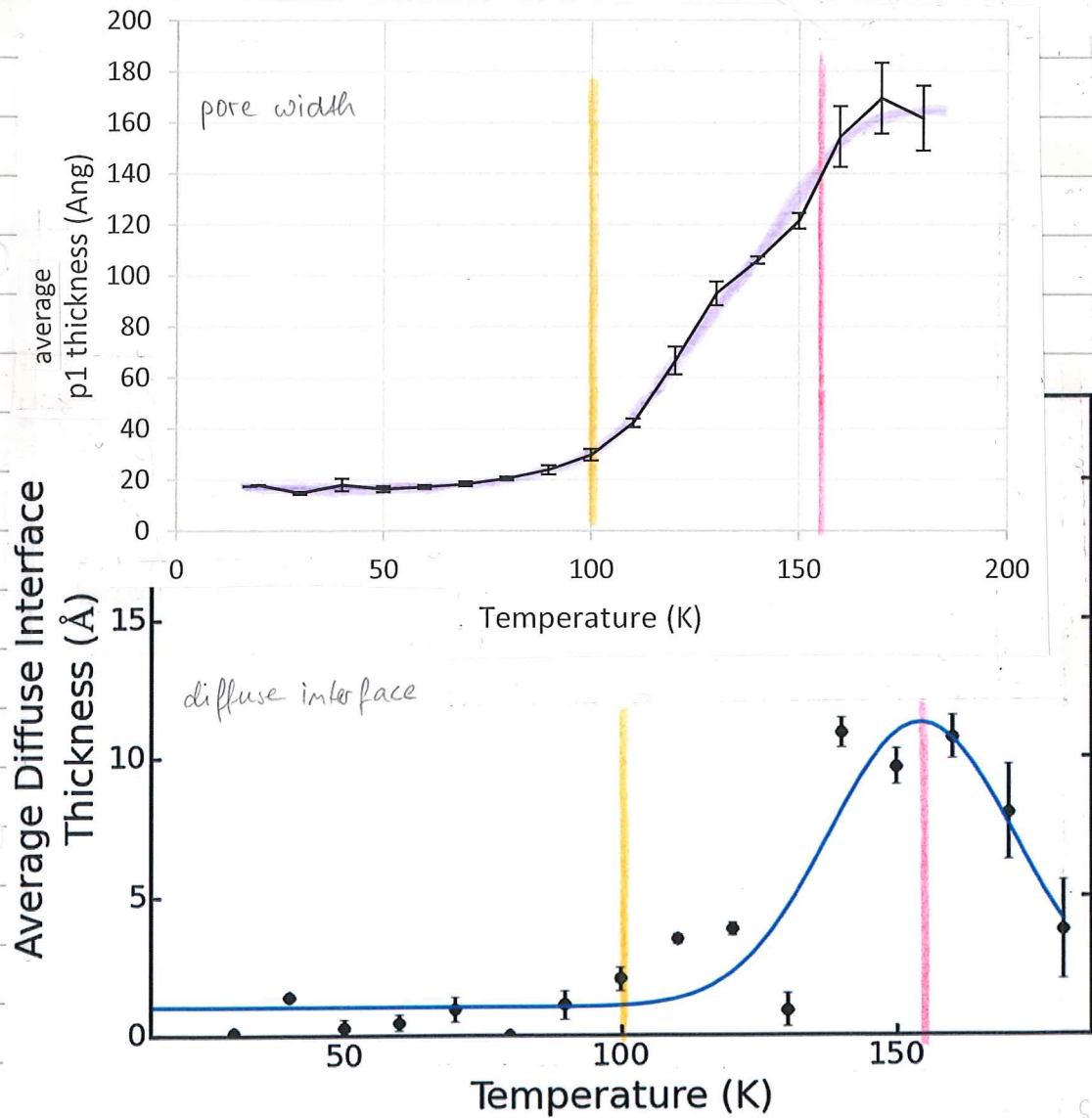
$$V_{tf,f} = V_{Sf} + V_{Pf,f} = N_f (b_f + p_f) L_f h_f = N_f l_f h_f b_f (x_f + 1)$$

$$\Rightarrow \text{Volume change: } \frac{V_{tf}}{V_{ti}} = \frac{N_f l_f h_f b_f (x_f + 1)}{N_i l_i h_i b_i (x_i + 1)}$$

assume total volume ( $l, h$  & width) do not change:  $N_f b_f (x_f + 1) = N_i b_i (x_i + 1)$

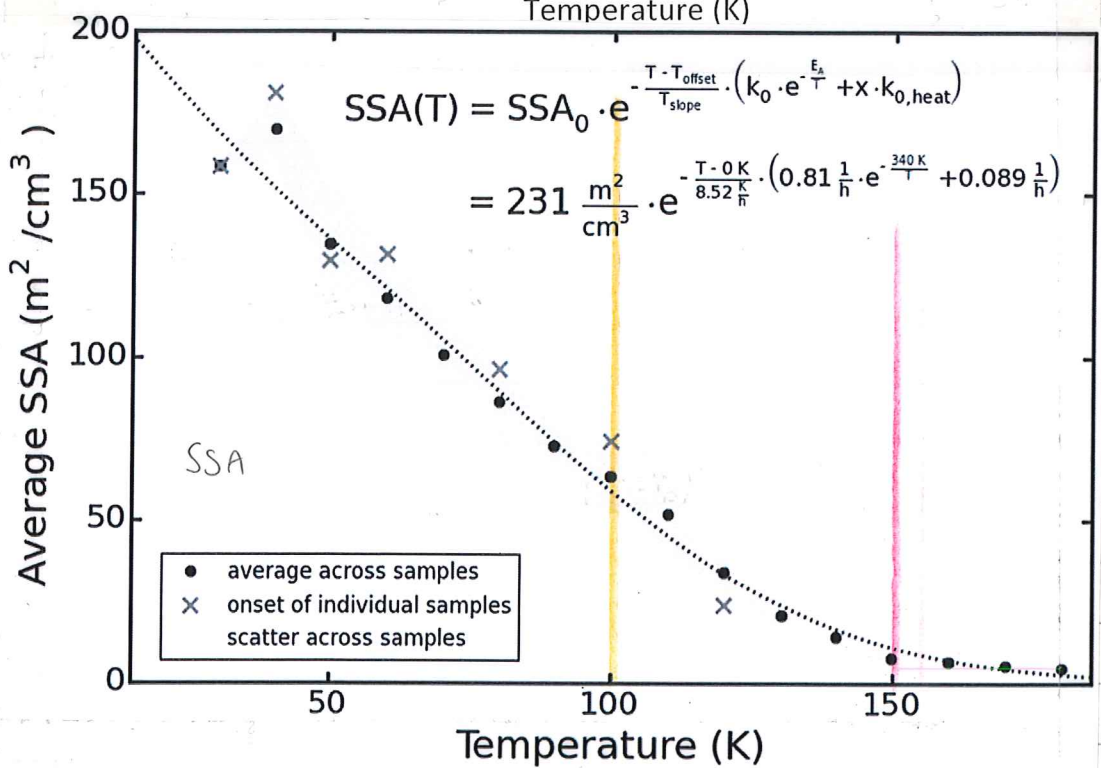
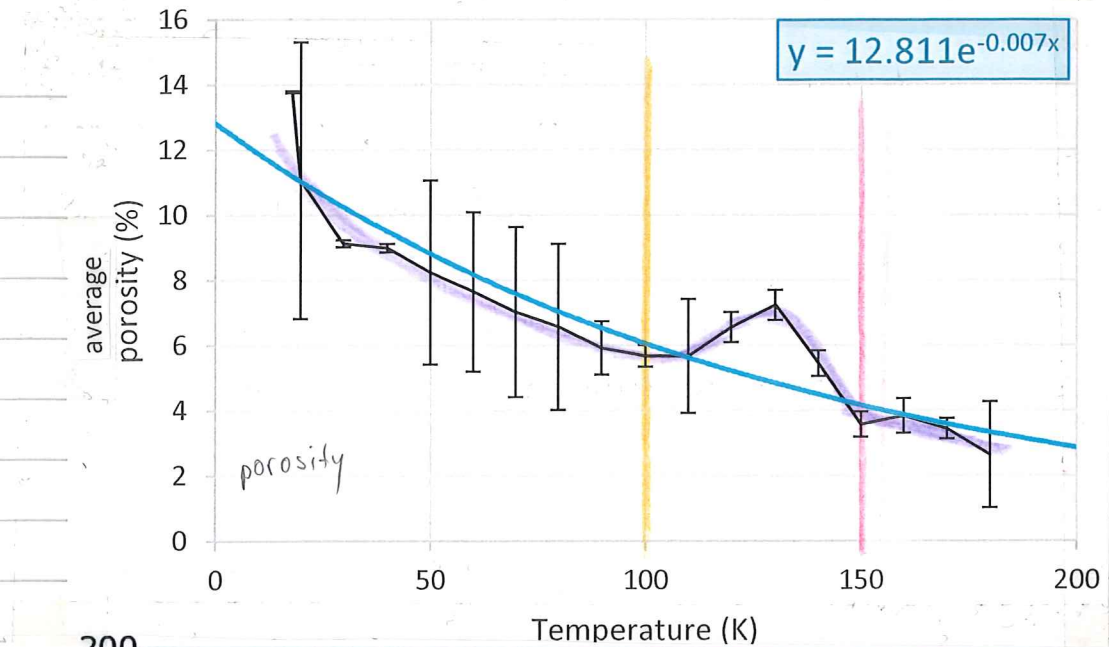
$$\Rightarrow \frac{N_f b_f}{N_i b_i} = \frac{x_i + 1}{x_f + 1} \Rightarrow x_f = \frac{N_i b_i}{N_f b_f} (x_i + 1) - 1$$

That's not going anywhere. Also, we know that total volume is changing as pores are lost  $\Rightarrow$  stupid assumption



Change in the pore width sets in at the same temperature where the thickness of the diffuse interface starts to increase.

Most drastic changes in pore width are in the T-regime, where the diffuse interface is increasing in thickness.



Porosity & SSA are lost over the whole temperature range.

Porosity shows a bump in the temperature range, where the diffuse interface thickness is increasing; SSA doesn't show this bump.

How can the width of the ice blocks increase without changing the pore width in between them, while simultaneously porosity & SSA are lost.

If molecules were diffusing in to fill the pores, shouldn't we see a diffuse surface layer increase at low temperatures? Why would only some pores fill, but not others?

Some new ideas:

re-adsorption might be directed by potential differences between ice blocks of different sizes  $\Rightarrow$  some grow at the expense of others, but gaps stay of same width (difficult for molecules to escape from really deep pores  $\rightarrow$  old mining cave collapsed)

mechanisms: desorption & re-adsorption (partially)

at low T this will be hit-and-stick, at

higher T some molecular rearrangement will happen

$\sim$  formation of diffuse interface to increase molecular coordination numbers at surface ( $\sim$  gradual loss of dangling bonds above  $\approx 100$  K)

$\sim$  crystallisation at  $\approx 150$  K

towards higher T, diffusion will add to loss of SSA & porosity

analysis: fit - SSA (continuous double exponential)

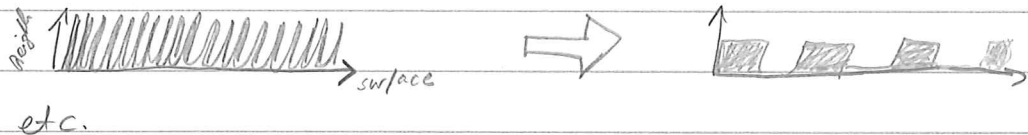
- porosity (exponential decay + Gaussian bump @ 130 K)

- ice amount (some sort of exponential decay + Gaussian bump @ 150 K)

from these fit results calculate pore width, ice block width

& actual sample height as function of T and

plot cross sections through sample at each T



Sample height:

Assume infinitely long & wide sample with finite height.

Sample formed by blocks of width  $b$  (infinitely long) with gaps of width  $p$

Intrinsic height:  $H$  = height if sample was compact.

Actual height:  $h$

$$V_t = N \cdot H \cdot (b + p) \cdot l, P = \frac{p}{p+b} \Rightarrow p = \frac{P}{1-P} \cdot b$$

$$= N \cdot h \cdot l \cdot b \cdot \left(1 + \frac{P}{1-P}\right) = N \cdot h \cdot l \cdot b \left(\frac{1-\beta+\beta}{1-\beta}\right)$$

$$= N \cdot h \cdot l \cdot b \left(\frac{1}{1-\beta}\right), \text{ SSA} = \frac{\frac{2}{6}}{b} + \frac{\frac{2}{6}}{b} + \frac{\frac{2}{6}}{b} \Rightarrow \frac{2}{b} = \text{SSA} - \frac{2}{6} - \frac{2}{6}$$

~~$$= N \cdot h \cdot l^2 \left(\frac{1}{1-\beta}\right) \cdot \frac{2}{b \cdot \text{SSA} - \frac{2}{6} - \frac{2}{6}}$$~~

$$V_s = N \cdot b \cdot H \cdot l = N \cdot (b+p) \cdot H \cdot l \Rightarrow h = H \cdot \frac{b+p}{b} = H \cdot \frac{1 + \frac{P}{1-P}}{1}$$

$$\Rightarrow h = H \cdot \left(1 + \frac{P}{1-P}\right) = H \cdot \frac{1}{1-\beta} \Leftrightarrow H = h \cdot (1-\beta)$$

$$\Leftrightarrow \frac{H}{h} = 1 - \beta \Leftrightarrow \beta = 1 - \frac{H}{h} = \frac{h-H}{h} = \frac{\text{height caused by pores}}{\text{total height}} \checkmark$$

$$\text{Summary: } h = \frac{H}{1-\delta}, b = \frac{2h}{SSA \cdot h - 2} \quad (l=\infty), p = \frac{P}{1-\delta} \cdot b$$

$$1 \frac{\text{m}^2}{\text{cm}^3} = 10^{-4} \frac{1}{\text{A}}$$

Ice amounts ( $H$ ): they vary between samples. to average in a useful way:

1. Normalise each data set to the 130 K data point (they all have that one).

(2) Average across data sets.

3. Average all data points at 130 K.

4. Multiply normalised <sup>data</sup> average by that.

Fit porosity:

$$P(T) = P_0 \left( 1 - e^{-\frac{E_a}{kT}} \right) + \frac{I}{\sqrt{2\pi\sigma^2}} e^{-\frac{(T-T_p)^2}{2\sigma^2}}$$

$T_p$  = peak position

Fit ice amount:

$$H(T) = a + b \cdot T + c \cdot T^2 + \frac{I}{\sqrt{2\pi\sigma^2}} e^{-\frac{(T-T_p)^2}{2\sigma^2}}$$

quadratic decay is not working

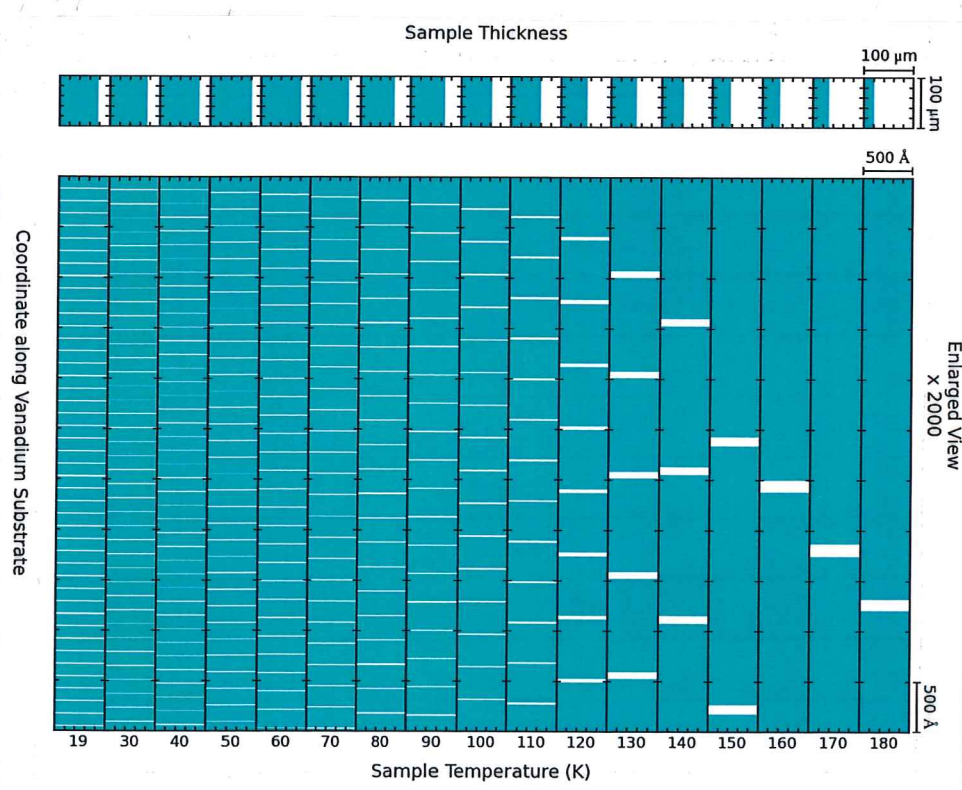
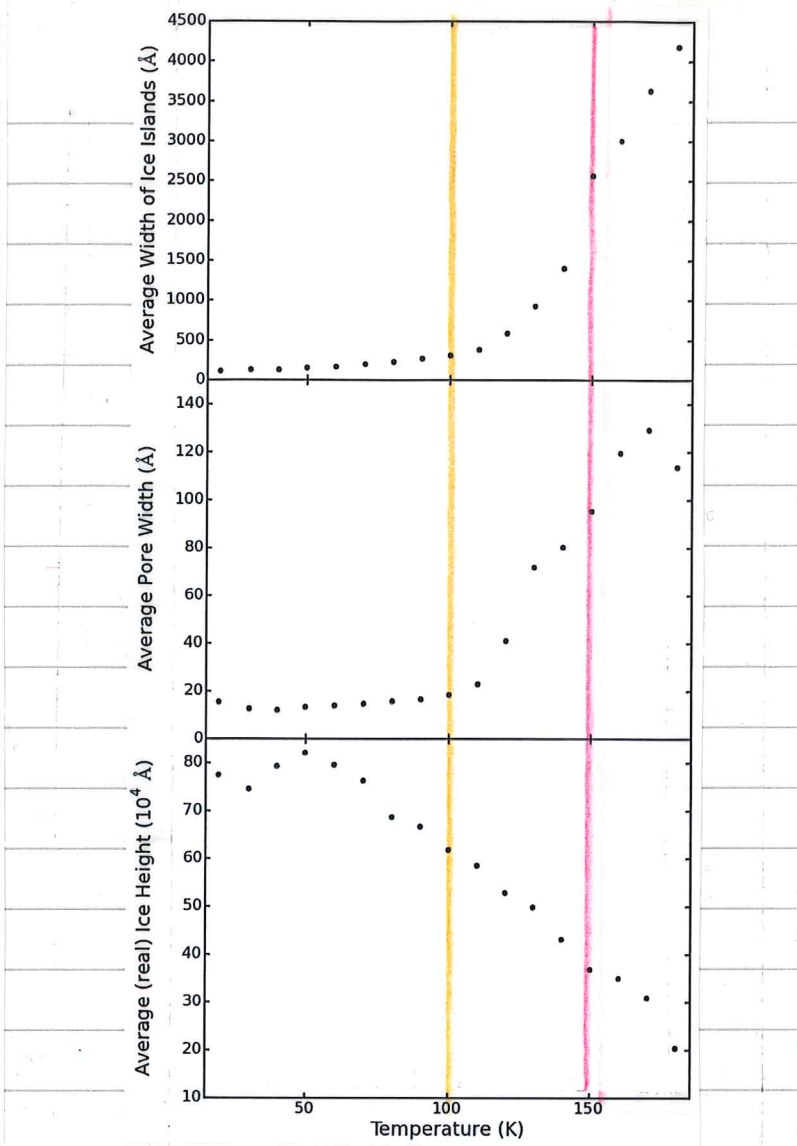
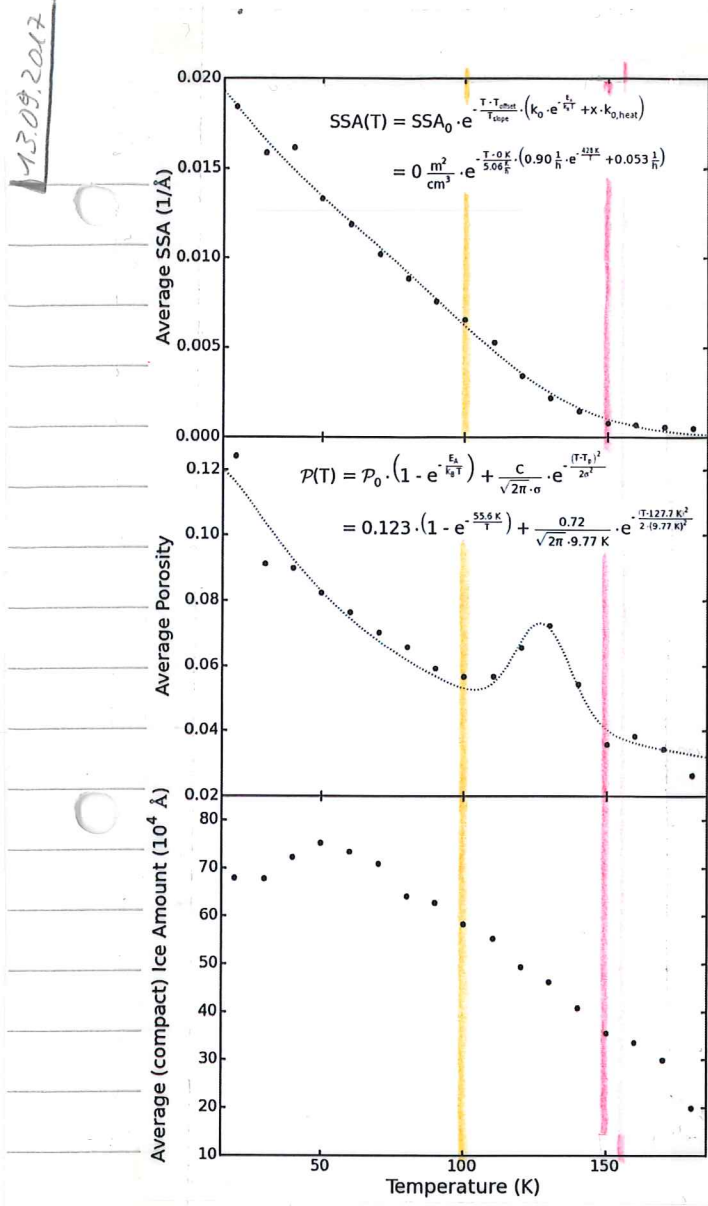
linear decay is better, but not ideal as well

Problem: the first one or two data points on each sample are scattering a lot, the first one is always too low.

→ Use actual averaged data rather than fit to move on.

13.09.2017]

The pore widths calculated based on porosity, SSA & sample amount came out very close to and follow the same trend as those derived by SasView directly. (compare plots on next page and from 11.09.2017, 3 pages ago.)



18.09.2017

Assume SSA & porosity changes go via desorption & re-adsorption:

$$\left| P = \frac{P}{P+b} \right|, \text{SSA} = \frac{2}{b} + \frac{2}{h} \quad (\text{infinitely long sample}, l=\infty)$$

$$h = H \cdot \frac{b+p}{b} \Rightarrow \boxed{\text{SSA} = \frac{2}{b} + \frac{2b}{H(b+p)}}$$

H changes by desorption which is not followed by re-adsorption  
 p and b change by desorption followed by re-adsorption and by desorption only

Problem: When molecule re-adsorbs in the same pore it originally desorbed from, the average pore and ice widths do not change. They only change, when I take into account that the smallest ice blocks are "eaten" up by the larger ones.



How to describe that mathematically?

SasView suggests, that we have a size distribution: probability W

$$W(p) = \frac{1}{\sqrt{2\pi}\sigma} e^{-\frac{(p-p_0)^2}{2\sigma^2}} = \frac{1}{\sqrt{2\pi}\sigma p_0} e^{-\frac{(p-p_0)^2}{2\sigma^2 p_0^2}}$$

where  $\sigma$  is  $\approx$  constant and  $p_0$  changes with time (temperature)

The best guess is that the same description works for the ice width b.

$\leadsto p_0 \hat{=} p$ ,  $b_0 \hat{=} b$  in the simplified model

Number of Molecules in ice effective thickness H:  $X = x \cdot H$

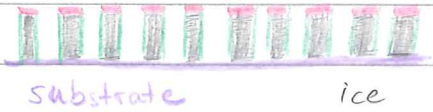
Assume that relocation of X molecules via des-ads changes pore and ice width by 1 ML  $\Rightarrow b = \frac{B}{x} \Rightarrow \frac{B+1}{x} = b + \frac{1}{x}$ ,  $p \rightarrow p + \frac{1}{x}$  ( $B=HL$  in ice block)

Desorption only will change  $b \rightarrow b - \frac{1}{x}$ ,  $p \rightarrow p + \frac{1}{x}$

Problem: with these assumptions  $p$  is changing faster than  $b$ .

Assume that relocation of  $X$  molecules changes  $b \rightarrow b + \frac{1}{X}$ ,  $p \rightarrow p + \frac{\alpha}{X}$   
 $(\alpha \in [0, 1])$

Assume that desorption only processes do occur only on the top layer  
and affect only the sample's effective height  $H$ .



desorption only

desorption & re-adsorption

$$-\frac{d}{dt} H = A \cdot e^{-\frac{E_{des}}{k_B T}} = A e^{-\frac{E_{des}}{k_B (T_0 + \beta t)}}$$

, heating ramp:  $T = T_0 + \beta t$

relocation of 1 molecule:  $b \rightarrow b + \frac{1}{X} \cdot X$ ,  $X = x \cdot H$

$$= b + \frac{1}{Hx^2}, \quad p \rightarrow p + \frac{\alpha}{Hx^2}$$

$$\frac{\partial}{\partial t} b = \frac{1}{Hx^2} \tilde{A} e^{-\frac{E_{des}}{k_B (T_0 + \beta t)}}, \quad \frac{\partial}{\partial t} p = \frac{d}{Hx^2} \tilde{A} e^{-\frac{E_{des}}{k_B (T_0 + \beta t)}}$$

$$\frac{d}{dt} p = \frac{\left( \frac{d}{dt} p \right) \cdot (p+b) - p \cdot \frac{d}{dt} (p+b)}{(p+b)^2} = \frac{\left( \frac{d}{dt} p \right) \cdot b - p \cdot \frac{d}{dt} b}{(p+b)^2}$$

$$= \frac{\tilde{A}}{Hx^2} e^{-\frac{E}{k_B (T_0 + \beta t)}} \cdot \left( \frac{d}{dt} H \right) \cdot (2b - p) \cdot (p+b)^{-2} = \frac{\tilde{A} \cdot A}{Hx^2} \cdot e^{-\frac{2E_{des}}{k_B (T_0 + \beta t)}} \cdot \frac{p - 2b}{(p+b)^2}$$

Note:  $H, p, b$  are  $t$ -dependent

$$\begin{aligned} \frac{d}{dt} SSA &= -\frac{2}{b^2} \cdot \left( \frac{d}{dt} b \right) + \frac{2 \left( \frac{d}{dt} b \right) \cdot (H(b+p)) - 2b \frac{d}{dt} (H(b+p))}{(H(b+p))^2} \\ &= \frac{\tilde{A}}{Hx^2} e^{-\frac{E_{des}}{k_B (T_0 + \beta t)}} \cdot \left( \frac{d}{dt} H \right) \left( \frac{2}{H(b+p)} - \frac{2}{b^2} \right) - \frac{2b \cdot \left( \frac{d}{dt} H \right) \cdot (b+p) + 2bH \frac{d}{dt} (b+p)}{(H(b+p))^2} \\ &= \frac{\tilde{A} \cdot A}{Hx^2} e^{-\frac{2E_{des}}{k_B (T_0 + \beta t)}} \cdot \left( \frac{2}{H(b+p)} - \frac{2}{b^2} \right) - e^{-\frac{E_{des}}{k_B (T_0 + \beta t)}} \cdot \frac{2b}{(H(b+p))^2} \cdot \left( A(b+p) + H \cdot \frac{\tilde{A}}{Hx^2}(1+\lambda) \right) \\ &= e^{-\frac{2E_{des}}{k_B (T_0 + \beta t)}} \cdot \frac{2AA}{Hx^2} \cdot \frac{b^2 - H(b+p)}{b^2 + H(b+p)} - e^{-\frac{E_{des}}{k_B (T_0 + \beta t)}} \cdot \frac{2b}{(H(b+p))^2} \cdot \left( A(b+p) + \frac{\tilde{A}}{X}(1+\lambda) \right) \end{aligned}$$

These equations are not really helpful, but they have in common with my SSA fit function that the rate of change is described by  $e^{-\frac{EA}{k_B T}}$ .

Approach the problem the other way around:

$$SSA(T) = SSA_0 \cdot e^{-\frac{T-T_0}{\beta} \cdot (k_0 e^{-\frac{E_A}{k_B(T_0+\beta t)}} + k_{0,heat})}$$

$$T = T_0 + \beta t$$

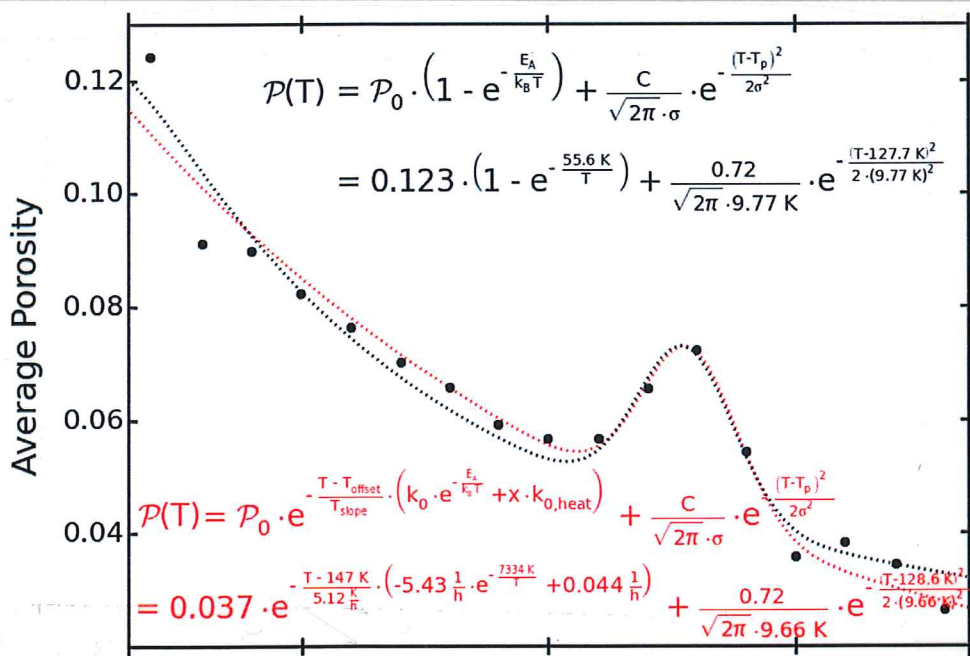
$$\Rightarrow SSA(t) = SSA_0 \cdot e^{-t \cdot (k_0 e^{-\frac{E_A}{k_B(T_0+\beta t)}} + k_{0,heat})}$$

$$\frac{d}{dt} SSA(t) = SSA_0 \cdot e^{-t \cdot (k_0 e^{-\frac{E_A}{k_B(T_0+\beta t)}} + k_{0,heat})} \left[ (-1) \cdot (k_0 e^{-\frac{E_A}{k_B(T_0+\beta t)}} + k_{0,heat}) - t \cdot k_0 e^{-\frac{E_A}{k_B(T_0+\beta t)}} \right]$$

$$= -SSA(t) \cdot \left[ k_0 e^{-\frac{E_A}{k_B(T_0+\beta t)}} + k_{0,heat} - t \cdot \frac{k_0 \beta E_A}{(k_B(T_0+\beta t))^2} e^{-\frac{E_A}{k_B(T_0+\beta t)}} \right]$$

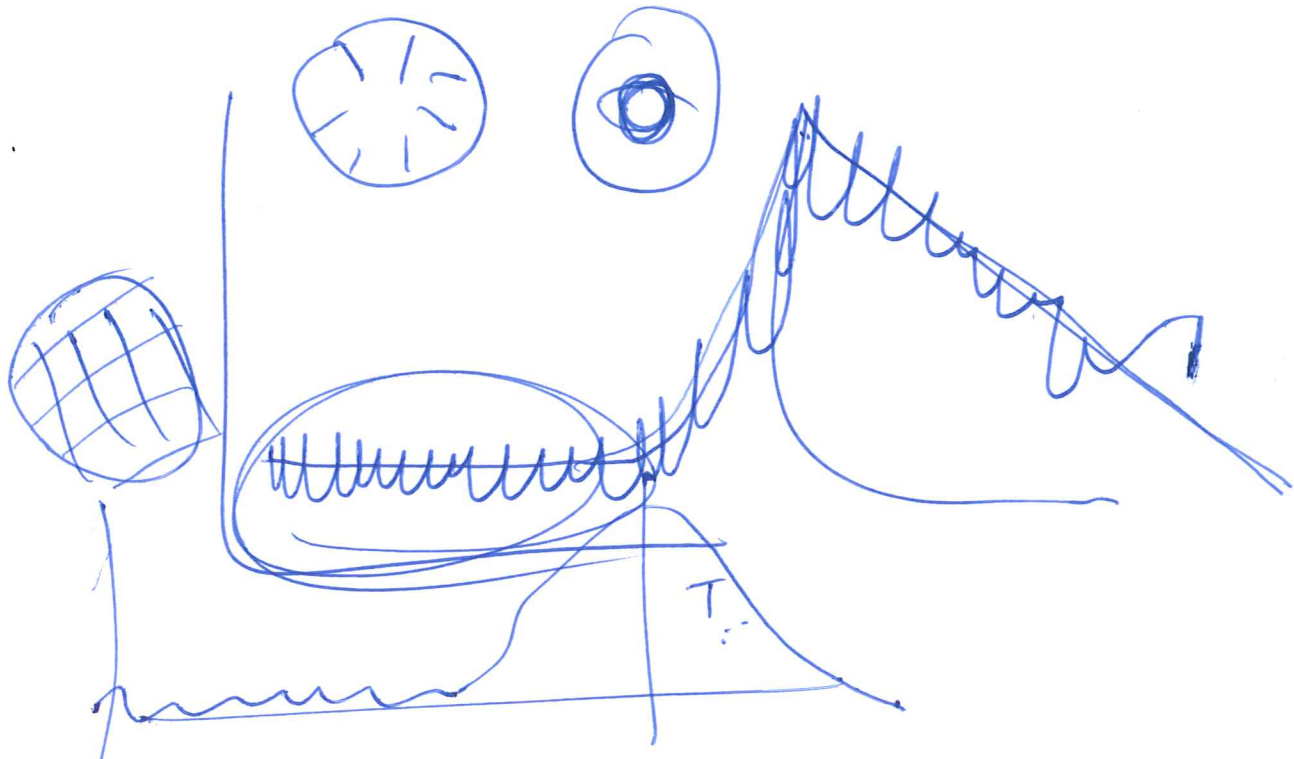
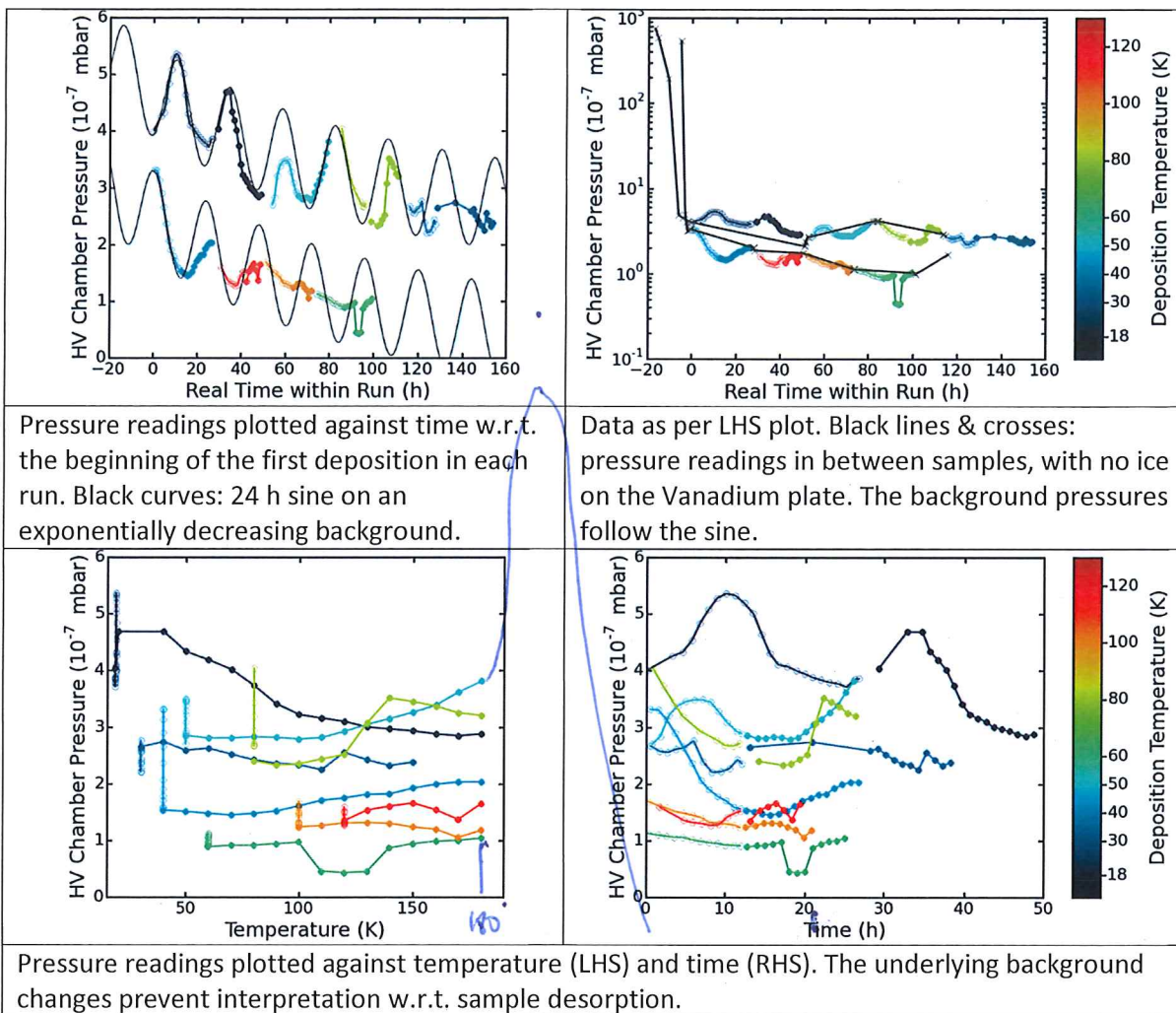
$$= -SSA(t) \cdot \left[ e^{-\frac{E_A}{k_B(T_0+\beta t)}} \cdot k_0 \cdot \left( 1 - \frac{E_A \beta t}{(k_B(T_0+\beta t))^2} \right) + k_{0,heat} \right]$$

The most obvious difference to the model based equation (4) is the term  $k_{0,heat}$ , a rate of change contribution, which requires no activation energy.



## HV Chamber Pressures

The pressure readings seem to be more sensitive to environmental changes than to ice desorption rates. There is a 24 h sinusoidal dominating the pressure changes, but other (unknown) influences prevent a suitable baseline fit and subtraction.



# Do pores in vapour deposited ASW collapse?

## Journal

PCCP

## Key Questions

### Porosity

How does growth T affect pore sizes & shapes?

What is the mechanism behind pore loss with increasing T (collapse, clustering, ...)?

How do pore sizes & shapes change with annealing T?

Are the pores open (i.e. interconnected) or closed?

How is pore collapse affected by growth T?

### SSA

How does SSA change with temperature & time?

Is SSA loss directly linked to pore loss?

### Ice Phase

Are there clear phase transitions between different amorphous forms of ice?

Are changes in SSA or pores linked to ice phase changes?

## Introduction

ASW metastable material:

- Activation energy for conversion to  $I_c$ : 0.4 eV (i.e.  $\approx 4600$  K), activation energy for molecular rotation to increase coordination number of surface molecules  $\approx 2500$  K (Sadchenko 2000b).
- ASW will change with a temperature dependent rate => heating rate influences observed onset temperatures for crystallisation (& pore loss)

### Ice phase

T (K)		phase
deposition	heating	
< 10 – 20		High-density ASW phase (high intrinsic density, but very porous)
	114	Transforms to low-density ASW

10 – 20 to 38 – 68		p-ASW (lower intrinsic density, higher global density than low-T ASW)
38 – 68 to 110 – 130		lacking long range crystalline order while keeping local tetrahedral ordering  some papers distinguish between ranges, some don't  upper/lower limits vary
		ASW sublimes two orders of magnitude faster than $I_c$
	30 – 80	Potential amorphous – amorphous phase transition
	136	Glass transition
	136 – 160	Crystallisation to $I_c$
	166	Desorption of $I_c$
135 to 190		$I_c$
	160 – 200	Converts to $I_h$
	172	Desorption of $I_h$
> 190		$I_h$

## Porosity

Depends on growth conditions:

- Temperature:
- Deposition rate:
- Deposition angle: porosity increases with incident angle (normal deposition => no pores)
- Contamination/Mixing: when too high amounts of other gases are co-deposited, the ASW structure changes (e.g. > 10 % N<sub>2</sub>)

Proposed origins of porosity:

- Hit & stick
- incoming molecules attach preferentially to dangling bonds (sticking out of surface) => form increasingly long surface protrusions

Methods to determine porosity:

- IR reflectance spectra ( $3.1\text{ }\mu\text{m}$  O-H stretch band widened by proton-disorder & O-H vibrational stretch in dangling bonds => sharp absorption at  $2.71\text{ }\mu\text{m}$ )
- Ice film density (intrinsic density derived from O-O distances (X-ray diffraction), optical measurements yield global density (including pores))
- Refraction index
- Gas absorption in pores (TPD/spectroscopy):
  - closed pores invisible, absorbed gases yield surface area => this is mostly pore surface unless film is ultra-thin or very rough
  - size of probe molecule influences diffusion into pores, indirect measure
- modelling

Pore dimensions: a few to  $30\text{ \AA}$ )

### Pore collapse

Most works on background deposited ASW observe end of pore loss between 120 and 150 K (varies between methods), stated mechanisms for pore loss vary.

Clustering: modelling (Cazaux 2015) & positron annihilation on thin film (Wu 2010)

Collapse: positron annihilation on thick film (Wu 2010/2011) & X-ray absorption & scattering (Parent 2002)

Unspecified: TPD & isothermal desorption with  $\text{CCl}_4$  (Sadtchenko 2000a,b), electron scanning-tunneling microscopy & 2 photon photo-emission spectroscopy (Stähler 2007), positron annihilation (Eldrup 1985) & FTIR & interferometry (Bossa 2012 & Isokoski 2014).

Temperatures: Experiments ending at 120 K: Isokoski, Bossa, Stähler (claiming ice to be compact), Cazaux. Wu 2010 states pore loss complete at 135 K, Wu 2011 state essentially complete pore loss at 120 K, but near surface pores remaining until 150 K, Sadtchenko states complete pore loss at 140 K (100 K deposition starts to lose pores at 100 K, 118 K deposition starts to lose pores at 127 K). Parent state complete pore loss at 150 K, but a change from collapse to sintering as underlying mechanism at 130 K.

### Surface

Up to several  $100\text{ m}^2/\text{g}$  (density  $\approx 1\text{ g/cm}^3$ )

Surface area determined from IR spectra

- IR bands produced by surfaces of nanopores are indicative of the nature of surface sites
- surface molecule bands for p-ASW are broader & less well defined => only d-H ( $3697\text{ cm}^{-1}$ ) & d-O ( $3570\text{ cm}^{-1}$ ) bands shift visibly when coated with weak adsorbate
- pore collapse visible in spectrum when annealing 12 - 120 K
- onset of rotational diffusion of surface water molecules: 60 K
  - identified from spectra of  $\text{H}_2\text{O} / \text{D}_2\text{O}$  mixed ices => defect movement converts them to HDO

### Simulations

- of large ASW cluster growth indicate highly convoluted surfaces with incipient pore structure, range of water ring sizes & coordination numbers, bent H bonds, high intrinsic density
- revealed three types of surface sites in nanopores:
  - dangling-O (2-coordinated O), dangling-H, s-4 (surface 4-coordinated O)

Simulations & spectra identified exceptionally large surface area for p-ASW grown @  $T < 30$  K, characterized by both 2 & 3-coordinated dangling H molecules

- 2-coordinated sites decrease when warming in 30 - 60 K range
- 3-coordinated sites decrease when warming in 60 - 120 K range
- 4-coordinated surface molecules have IR bands shifted w.r.t. 4-coordinated bulk molecules ( $2500\text{ cm}^{-1}$  w.r.t.  $2400\text{ cm}^{-1}$ )

## Contamination

- depends on ambient conditions
  - lab: contamination proportional to  $P \cdot t / d$  ( $P$  = pressure,  $t$  = exposure time,  $d$  = ice thickness) => e<sup>-</sup>-microscopy, X-ray & neutron diffraction very susceptible to contamination (thin films)
- often not analysed (or mentioned) in literature
- can affect properties (ice phase/porosity) of ASW deposits

Why do it with neutrons what unique information do we get with neutrons which we don't get elsewhere?

E.g. structural information on different length scales at the same time with the same technique... (see degree crystallinity with the evolution on nanoscale – up to 60 nm)

e.g. TPD – probe molecules give SSA – "same" as can be extracted from neutron data – comparator between our data and others..

What's the advantage of neutron scattering SSA versus using a probe molecule in TPD? Direct measure not indirect with additional potential constraints...

I.e. no desorption diffusion trapping ... volcano effects...

Key focus Neutron scattering from low Q

SSA

Surface roughness ( $\beta$ ) – Porod

Pores exit yes or no – shape and size of pores

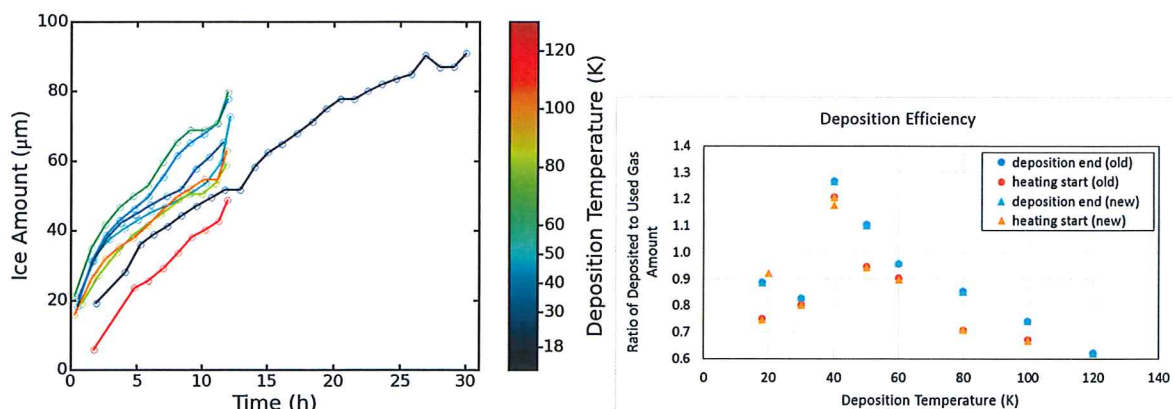
## Experimental

Need add quite a lot detail and explain what we did and why?

Can you have a bash at writing this bit up and adding as many figures as you think might be needed...?

Vapour deposited D<sub>2</sub>O (better neutron scattering properties than H<sub>2</sub>O). No discernible effect on results presented here.

Vapour deposition rate, pressure, time, estimated amount of sample.



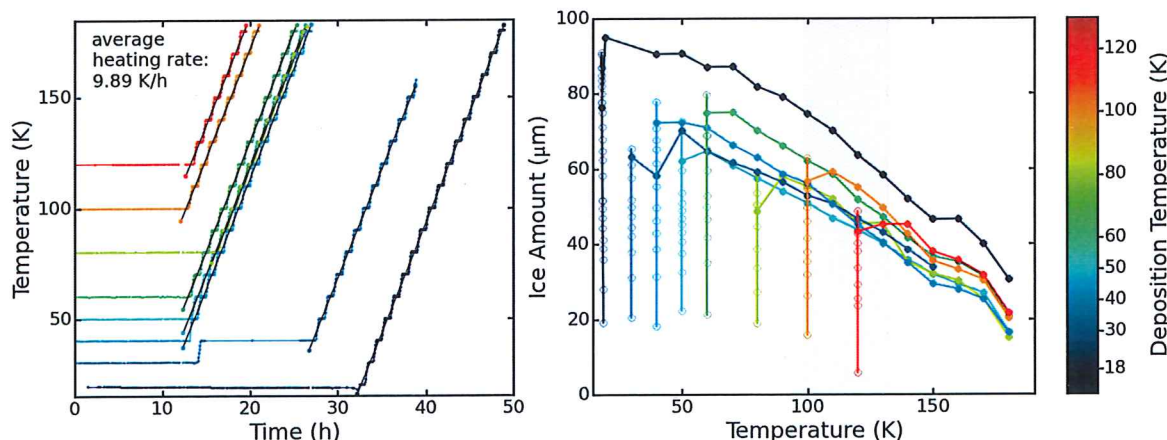
Figures: LHS ice growth. RHS deposition efficiency (make simpler version: only end of deposition data points & normalise to 40 K being 100 %)

background pressure (mbar)	3.5E-05 ± 1.0E-06	deposition temperatures
deposition total pressure (mbar)	4.7E-05 ± 2.0E-06	06/2015: 18, 30, 50, 80 K
deposition partial pressure (mbar)	1.2E-05 ± 2.2E-06	04/2016: 40, 60, 100, 120 K

deposition T (K)	18	30	40	50	60	80	100	120
deposition rate (ML/s)	86.4	147.6	170.5	152.5	176.3	123.9	138.5	105.8

Deposited at 8 different temperatures: 18, 30, 40, 50, 60, 80, 100, and 120 K.

Heating profile: 30 min isothermal scan @ deposition T, heating (heating rate 10 K in 30 min) with isothermal scans for 30 min every 10 K up to 180 K.

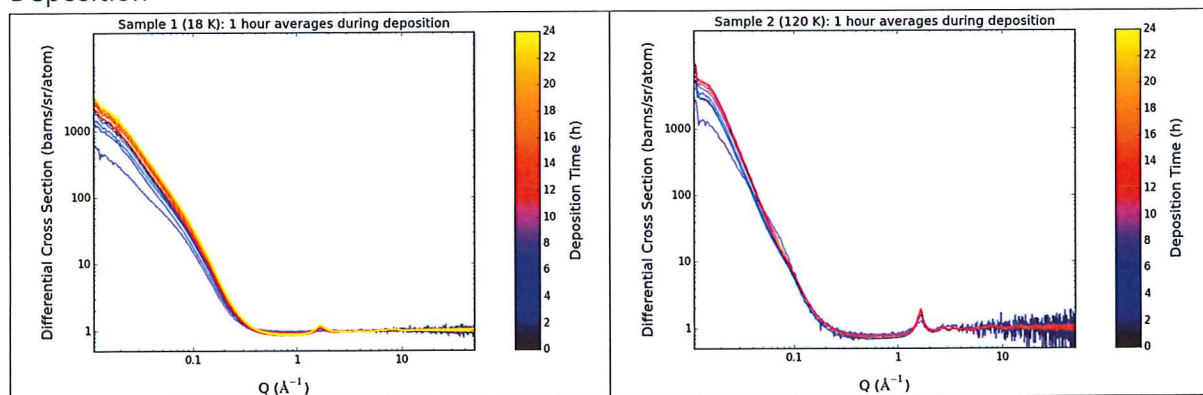


Figures: LHS Temperature profile (remove fits), RHS annealing (remove deposition data points from that plot).

## Raw data

What figures are really needed here and what science points do they justify? How might they lead through the story...

## Deposition



In the first hours of deposition, intensity increasing (=> SSA of sample increasing). Only minor changes after first 10 hours => further samples deposited for 12 hours only.

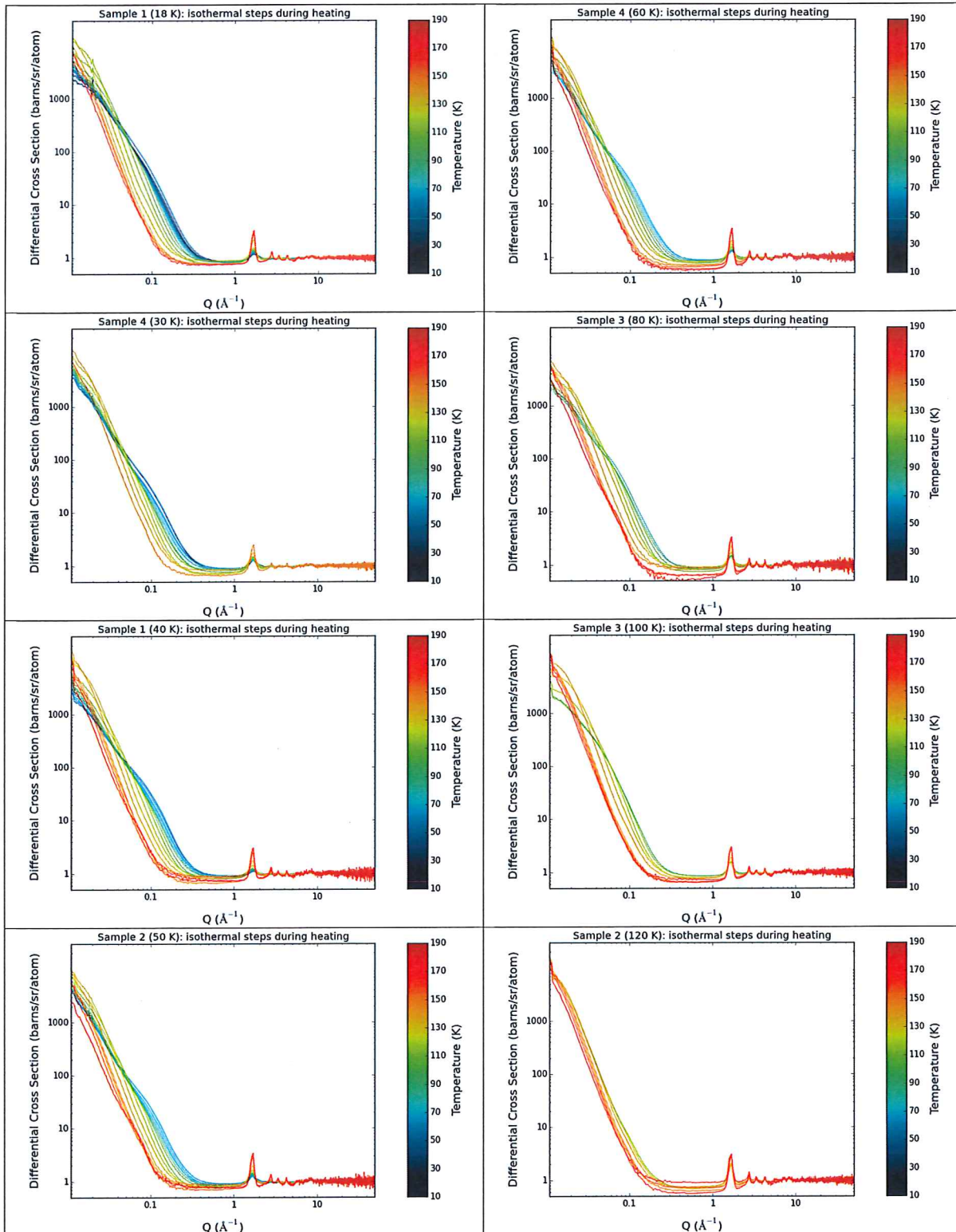
Low Q:

18 K deposition: No change in bump structure with deposition time => no restructuring (pore loss)  
120 K deposition: change in bump structure with deposition time => ice is porous upon deposition, but restructures (pore loss) as we continue depositing

High-Q peaks:

18 K deposition: slight increase in intensity with longer deposition => no crystallisation at low T  
120 K deposition: increase in intensity concurrently with decrease in width => crystallisation during deposition at high T => restructuring

## Heating of the individual samples



Temperature evolution within each sample looks similar.

Low T (blueish):

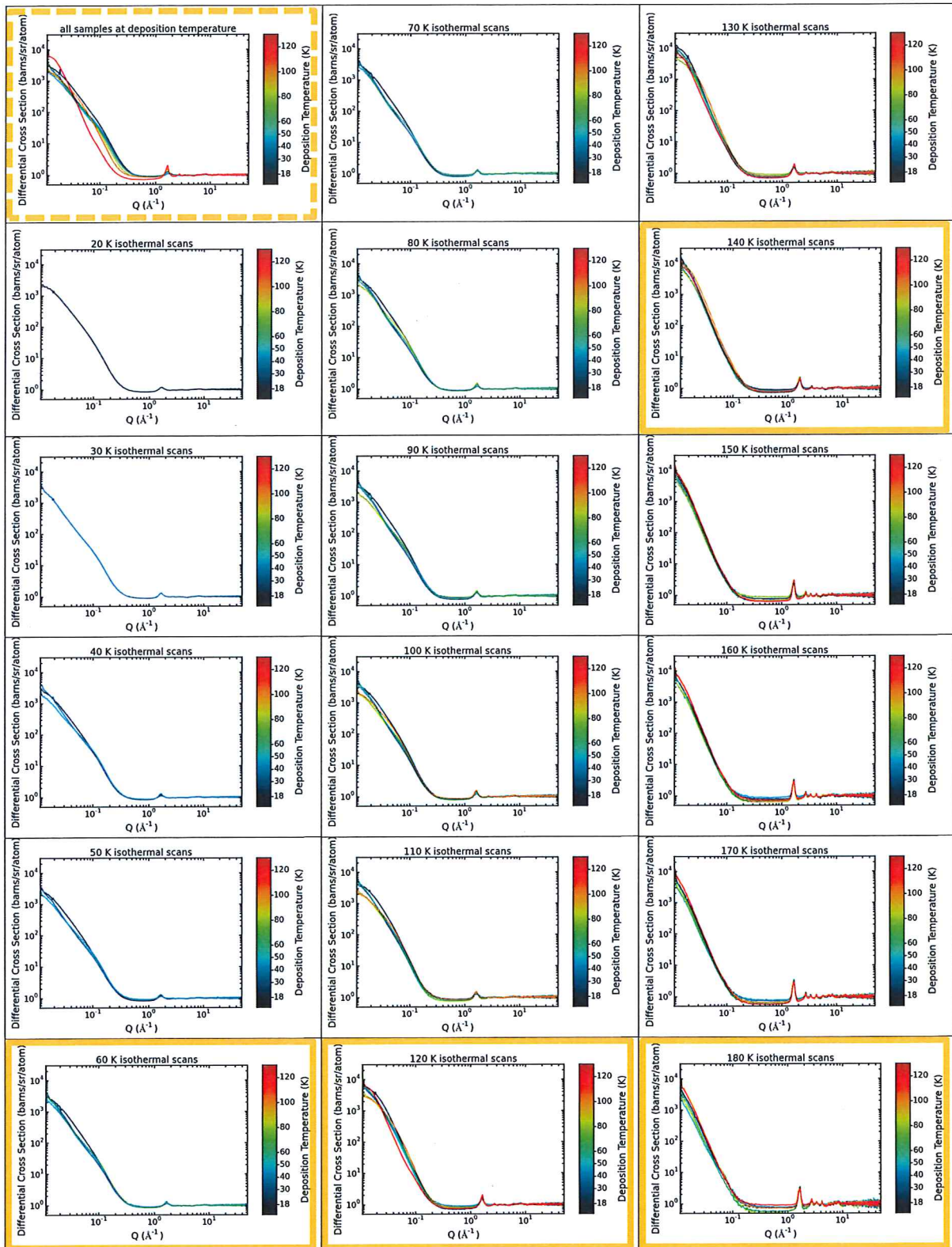
Low Q: Slope = granular, bumps = porous, High Q: Broad peak @  $1.7 \text{ 1/\AA}$  = amorphous

High T (reddish):

Low Q: Slope = granular, no bumps = non-porous, High Q: Sharp peaks @ 1.7, 2.8, 3.4, 4.3  
1/ $\text{\AA}$  = cubic crystalline

Onset of crystallisation: 40 – 50 K, Peak intensities still increasing at 180 K (indicates continued growth of crystallites). At this stage we will not quantify crystallinity.

Compare different samples at same T



The samples deposited at different temperatures look different at each temperature step up to 130 K (path-dependent ice). From 140 K on, they all look very similar (evolve to the same type of ice beyond glass transition).

120 K deposition shows more crystallinity than amorphous samples heated to 120 K.

Think of better way to point out differences between them (e.g. 3D plots as in Catherine's thesis).

## Theory (Fit Functions)

We would break up a paper by having theory section.... Need to have within results... and maybe discuss multiple models and approaches... might need to justify why we used what... might be good idea to know what we did before Catherine's thesis – PCCP / ice particles PRL... also what others have done... literature review of SANS high q data on ASW// LDA – HAD..ILL (Joh Dore?) x-rays? Loerting ...

Pores

Two approaches: Guinier-Porod and SasView model (lamellar pores plus Gaussian peak).

*Guinier-Porod*

T ≤ 120 K:

$$GP_i(Q) = \begin{cases} G_i Q^{-s_i} e^{-\frac{Q^2 R_{gi}^2}{3-s_i}} & , Q \leq Q_i \\ A_i Q^{-d} & , Q_i < Q \end{cases} \quad | \quad Q_i = \frac{1}{R_{gi}} \sqrt{\frac{(d - s_i)(3 - s_i)}{2}}$$

$$I(Q) = GP_1(Q) + GP_2(Q)$$

120 K < T ≤ 180 K:

$$I(Q) = GP(Q)$$

Fit procedure within each sample: split Q-range (around 0.04 Å⁻¹, but varying for each data point) and fit GP to low-Q half, starting at highest T. Then keep R<sub>g1</sub> & s<sub>1</sub> fixed, varying only G<sub>1</sub> and fit full range (up to around 0.15 Å⁻¹, but varying for each data point) with double GP to determine d, G<sub>2</sub>, R<sub>g2</sub> & s<sub>2</sub>, starting at lowest T.

*SasView model: lamellar + Gaussian*

$$I(Q) = \mathcal{P} \frac{4\pi}{Q^4} \frac{\Delta\rho^2}{\delta} (1 - \cos(\delta Q)) + \mathcal{S} e^{-\frac{(Q-Q_0)^2}{2B^2}}$$

lamellar scale factor $\mathcal{P}$ = $\frac{\text{pore volume}}{\text{total volume}}$ (= porosity)	Gaussian scale factor $\mathcal{S}$
scattering length density difference $\Delta\rho = 5.995 \times 10^{-6} \text{ \AA}^{-1}$	mean spacing of lamellae (pores) $\frac{2\pi}{Q_0}$ (= ice island width)
bilayer thickness $\delta$ (= pore width) (follows Gaussian size distribution with relative width $\sigma$ )	relative width of ice size distribution $\frac{B}{Q_0}$

Surface

Two approaches: Porod & diffuse interface

*Porod*

Fit constant K to  $I(Q) * Q^4$ . => SSA =  $K/(2\pi(\Delta\rho)^2)$

*Diffuse Interface*

(From icy particles paper: -> rephrase) Values of d > 4 indicate that no surface roughness on nm length scales is introduced by the freezing process, but that the surfaces are diffuse, i.e. showing a density

gradient (e.g. Strey et al. 1991; Su et al. 1998). However, in the case of diffuse interfaces the particle surface density cannot be validly modeled by a step function (as in the Porod analysis) but is best described by convoluting a Gaussian with said step function. The width of this Gaussian indicates the thickness of the diffuse interface,  $t$ . The resulting fit-function for the background corrected low-Q data is (Strey et al. 1991):

$$I(Q) = 2\pi(\Delta\rho)^2 \text{SSA} Q^{-4} e^{-Q^2 t^2},$$

where SSA is the specific surface area, and  $\Delta\rho = 5.995 \times 10^{-6} \text{ \AA}^{-1}$  is the scattering length density difference. Under our specific experimental conditions, this is the scattering length density of D<sub>2</sub>O, since no other material is present that has not already been corrected for by the calibration scans.

### SSA

Average results from Porod & diffuse interface analyses.

the annealing data for now.

At any time  $t$  (and temperature  $T(t)$ ), the SSA should evolve from a starting value  $\text{SSA}_0$  at  $t_0$  towards the equilibrium value, which is assumed to be  $\text{SSA}_{eq} = 0 \text{ m}^2/\text{cm}^3$ , following an exponential decay:

$$\begin{aligned} \text{SSA}(t, T) &= \text{SSA}_0 + \left(1 - e^{-\frac{t-t_0}{\tau(T)}}\right) \cdot (\text{SSA}_{eq} - \text{SSA}_0) \\ &= \text{SSA}_0 \cdot e^{-\frac{t-t_0}{\tau(T)}} \end{aligned} \quad (1)$$

For short times ( $T \approx \text{const.}$ ) this can be approximated by (Taylor expansion):

$$\begin{aligned} \text{SSA}(t, T) &\approx -\frac{\text{SSA}_0}{\tau(T)} \cdot t + \text{SSA}_0 \cdot \left(1 + \frac{t_0}{\tau(T)}\right) \\ &= \frac{\text{SSA}_0}{\tau(T)} \cdot [\tau(T) + t_0 - t] \end{aligned}$$

Derive temperature dependence of  $\tau$  from individual scans on heating ramp / isothermal step.

$$\begin{array}{ll} \text{isothermal step} & \frac{1}{\tau(T)} = k_0 \cdot e^{-\frac{E_A}{T}} \\ \text{heating ramp} & \frac{1}{\tau(T)} = k_0 \cdot e^{-\frac{E_A}{T}} + k_{0,heat} \cdot e^{-\frac{E_{A,heat}}{T}} \end{array}$$

The temperature dependence of  $\tau$  can then be inserted in Eq. (1) and the time dependence of the temperature  $T$  can be approximated by the average heating ramp:

$$\begin{aligned} T(t) &= a \cdot (t - t_0) + b \\ \Rightarrow t - t_0 &= \frac{T - b}{a} \end{aligned}$$

This transforms Eq. (1) to:

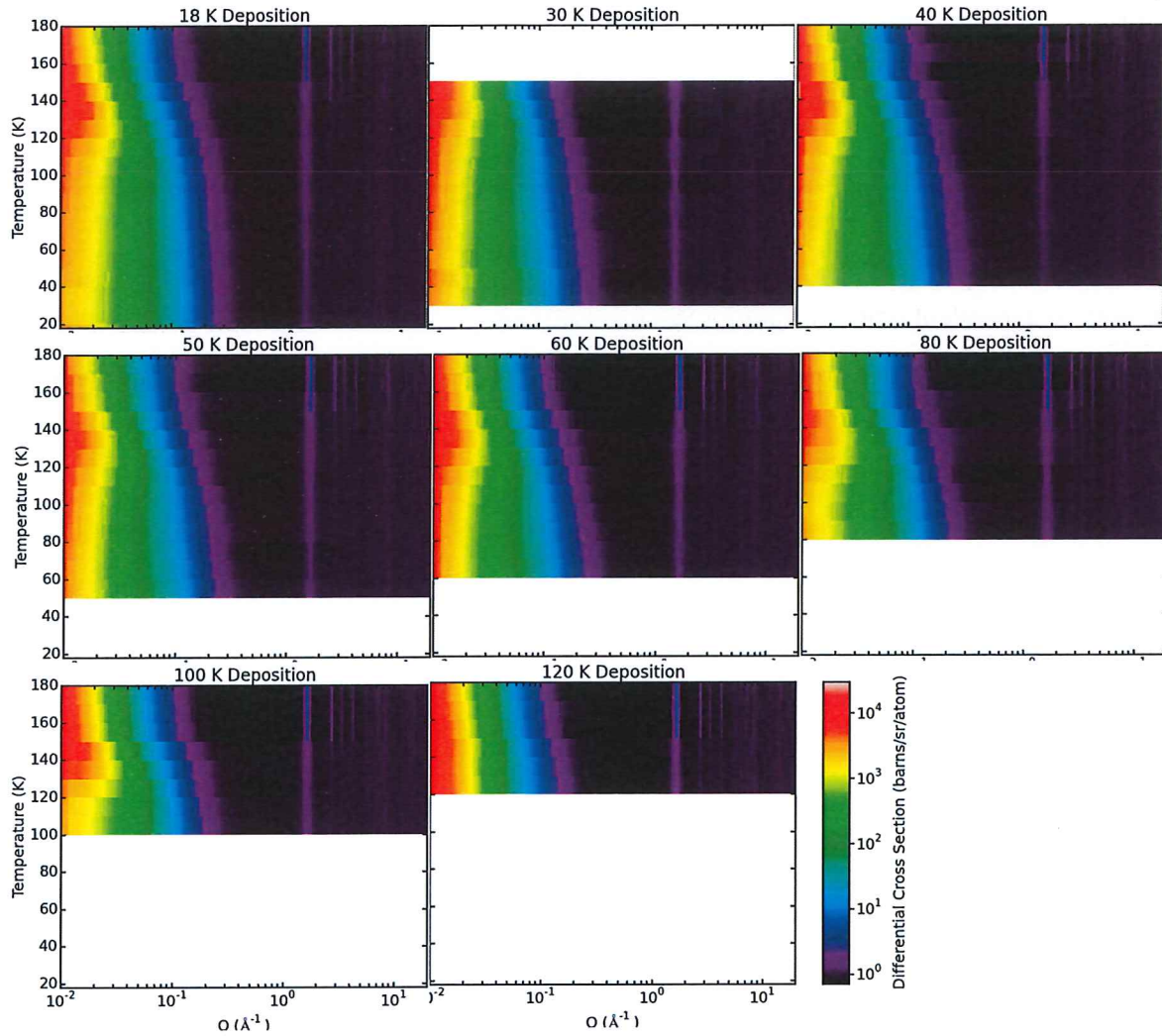
$$\text{SSA}(T) = \text{SSA}_0 \cdot e^{-\frac{T-b}{a} \left( k_0 \cdot e^{-\frac{E_A}{T}} + x \cdot k_{0,heat} \cdot e^{-\frac{E_{A,heat}}{T}} \right)}$$

With the factor  $x$  accounting for the average influence the second term (heating ramp) might have.

## Results & Discussion

### Ice phase

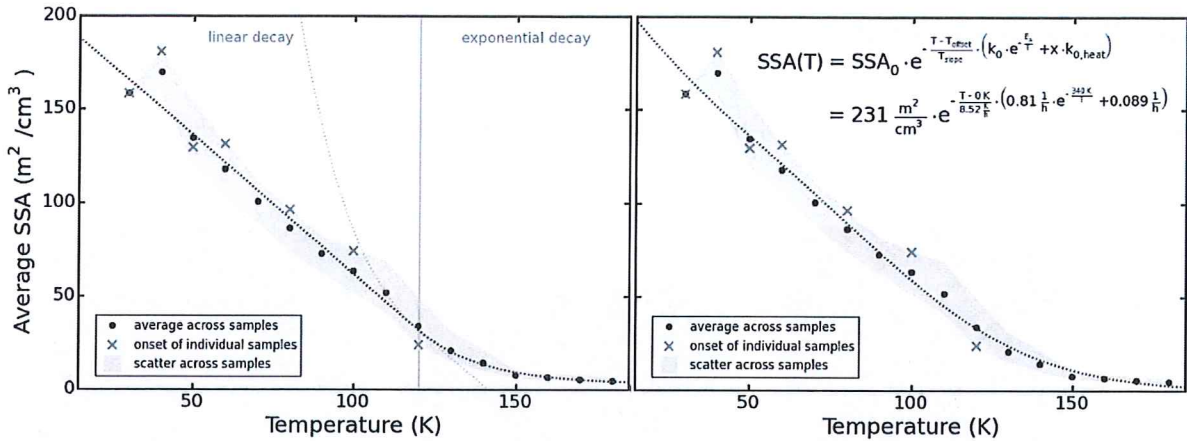
Our crystallisation T compares well with other experiments at similar heating rates (150 K, e.g. Isokoski 2014, Maté 2012).



### SSA

Our results in same order of magnitude as literature results.

SSA decreasing with increasing sample T. Individual samples very similar but not perfectly overlapping. No trend with deposition T evident (SSA starts roughly on average curve for sample T).



Figures: SSA averaged across samples. LHS simple fits (linear & exponential), RHS fit based on temperature dependent time constant for SSA loss (see below).

Note: SSA does not show transition at 60-70 K (porous – compact ASW, reported from other methods => open/closed pore issue).

SSA loss almost linear with increasing T until 140 – 150 K, then slows down.

We know from He-thickness measurements (literature) that ASW thickness decreases by factor of 5 upon heating.

Can we somehow determine the pore density? (Probably depends on model we eventually choose.)

Whatever model we use eventually, check what Porod-exponent does in 60-70 K range (can we see a transition from open to closed pores in the surface roughness?).

Catherine's PRL:

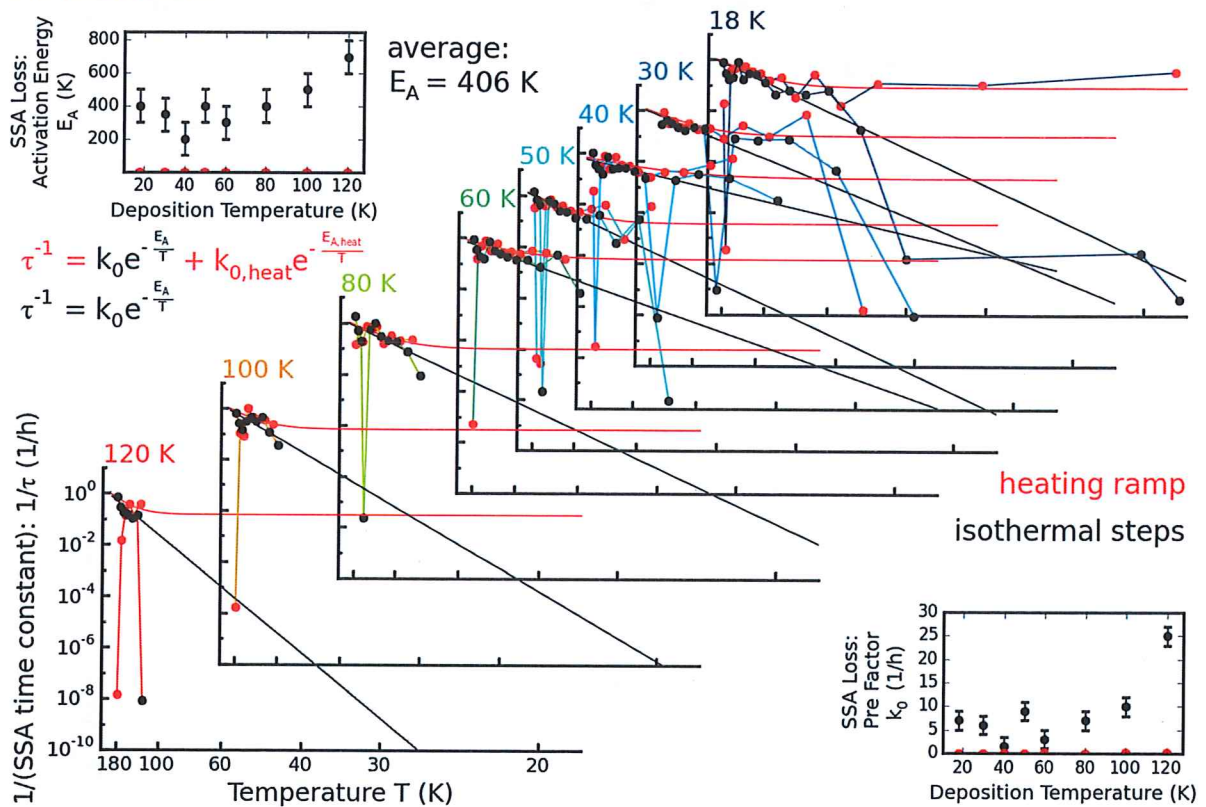
- $d_{\text{GP}}$ : internal surface of pores ( $0.045 - 0.2 \text{ \AA}^{-1}$ ), 3 = rough, 4 = smooth
- $\beta$ : surface roughness ( $0.02 - 0.03 \text{ \AA}^{-1}$ ), size & shape of granular material

Models:

Be careful with bump in very low-Q region. Data at  $Q < 0.02 \text{ \AA}^{-1}$  is not reliable enough to hang a whole model on.

Lower limit for analysis:  $Q = 0.15 \text{ \AA}^{-1}$ .

### Individual scans



Arrhenius plots for rate coefficient ( $1/\tau$ ), i.e.  $\log(1/\tau)$  against  $1/T$ . Isothermal data characteristic for 1-state system. Heating ramp data characteristic for 2-state system. Excited state requires 0 energy to enable SSA loss. Activation energy of "ground" state varies between samples, but no clear trend evident (large uncertainties).

Based on these results: Fit function to averaged SSA data:

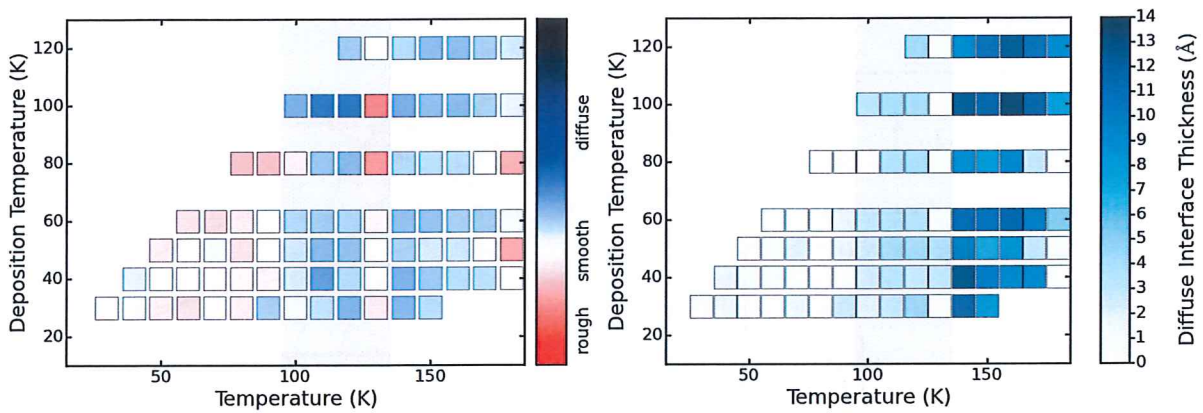
$$SSA(T) = SSA_0 \cdot e^{-\frac{T-b}{a} \left( k_0 \cdot e^{-\frac{E_A}{T}} + x \cdot k_{0,heat} \right)}$$

Parameters:		individual scans	averaged across all samples	Literature: barriers to diffusion (Sadchenko 2000b)
heating rate	a (K/h)	9.89	8.52	rotation to increase coord. 2 $\rightarrow$ 3
activation energy	$E_A$ (K)	406	340	$(5 \pm 1)$ kcal/mol (2500 K)
pre factor isoth.	$k_0$ (1/h)	$\approx 10$	0.81	diffusion to increase coord. 3 $\rightarrow$ 4
pre factor heat.	$k_{0,heat}$ (1/h)	$\approx 0.01$	0.089 (x·k)	$(9 \pm 2)$ kcal/mol (4500 K)

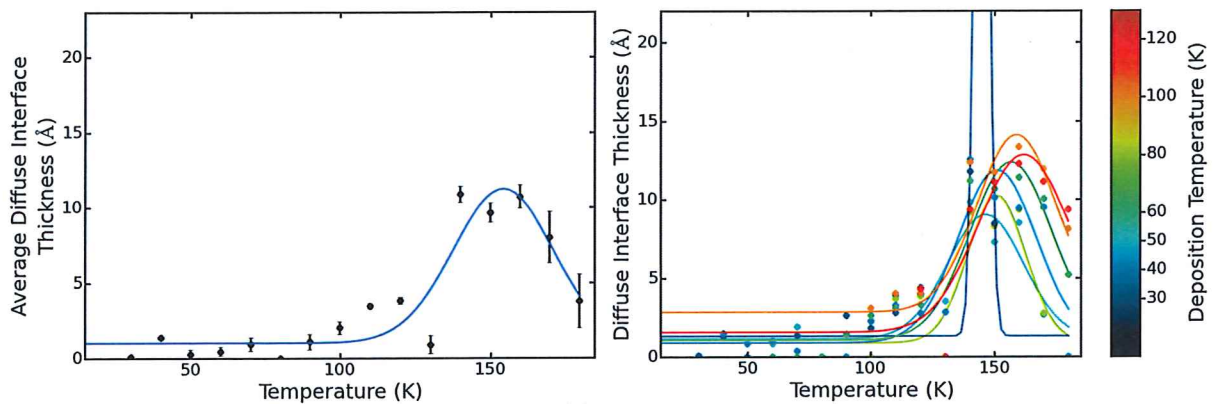
### Surface

At the end of deposition most samples have slightly rough surface. Roughness increasing with increasing deposition temperature (deeper red in plot below).

Annealing: at 100 K surfaces start to become diffuse. Values jump at 130 K. Maximum thickness of diffuse interface reached around 150 – 160 K (varying between samples). In general diffuse interface seems to become thicker for higher deposition temperatures, but data scatter.



Figures: LHS surface roughness, colour scale: Porod exponent  $d$  (deep red:  $d = 3$ , deep blue:  $d = 6$ ). RHS thickness of diffuse interface. Both: greyed area shows transition region (100 – 130 K), where neither double nor normal Guinier-Porod model fits the data well.



Figures: LHS averaged thickness of diffuse interface (averaged across samples), fitted with Gaussian (add grey area). RHS individual samples, each fitted with Gaussian (note: 30 K deposition only annealed to 150 K (end of beam time) => remove fit function, add note).

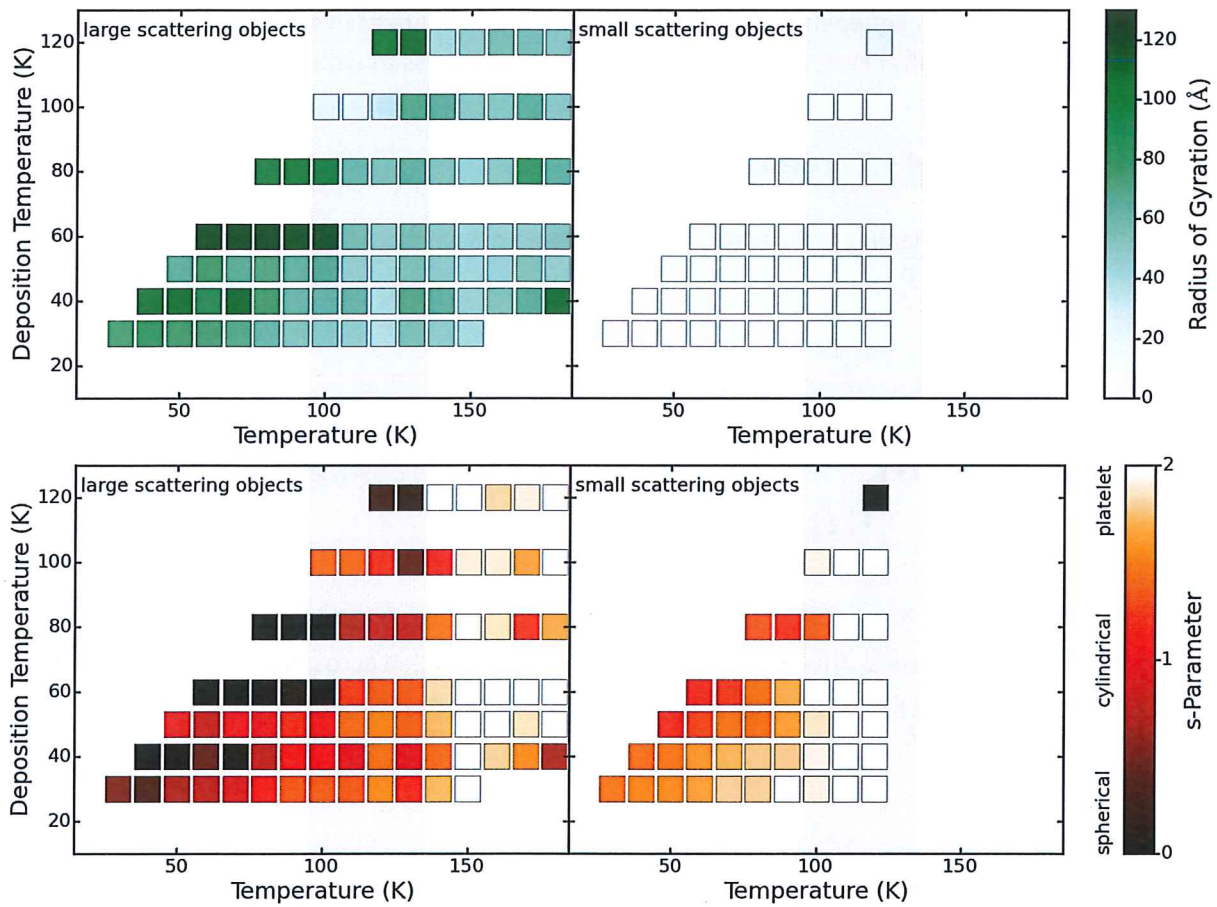
Possible interpretation: low T: open pores  $\rightarrow$  rough surface, increasing T: molecules rearrange, pores close, but surface develops density gradient/gets less ordered, high T: formation of crystal grains  $\rightarrow$  surface gets more ordered, rough structure due to grains

Would fit in with literature

### Pores

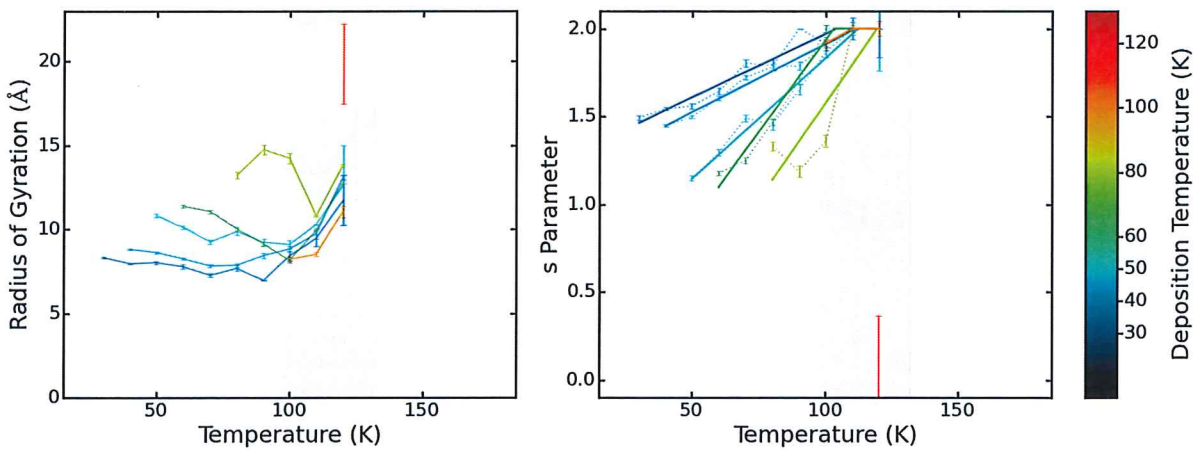
#### Double Guinier-Porod fits

Two types of scattering objects for  $T \leq 120$  K.



Overall s tends to increase with increasing T. Large  $R_g$ : Onset of pore shape between spherical and cylindrical but no clear trend with increasing dep-T. Pores collapsing to platelets via cylinders.

Large scattering objects (size range 35 - 120 Å, but some scatter) are on the edge of the instrument Q-range => can give indications for future experiments, but are not sufficient for quantitative interpretation. Focus only on the small scattering objects in this work.

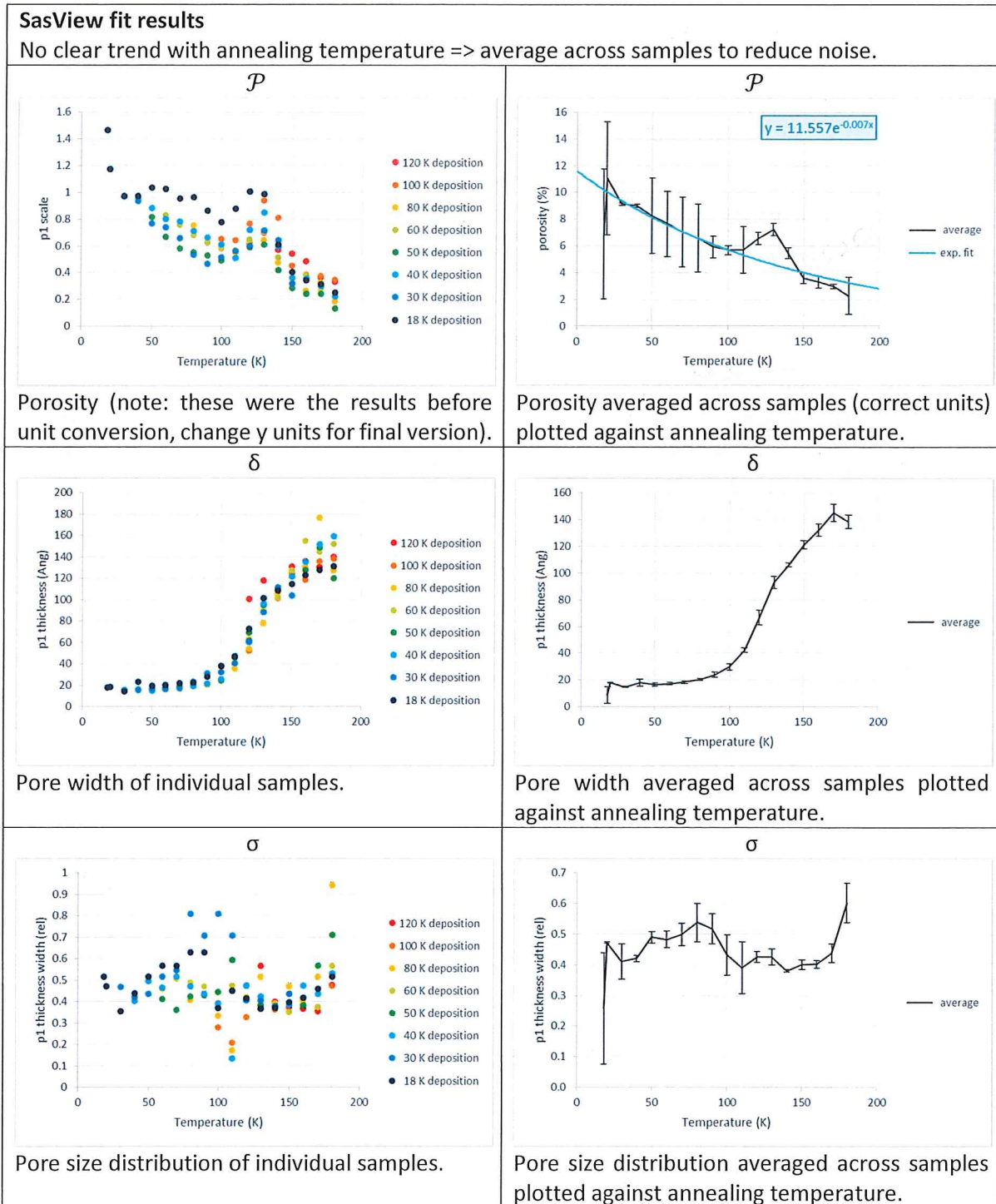


Small  $R_g$ :  $\approx 10 - 15 \text{ \AA}$ , onset increasing with increasing deposition T, pore size decreasing to minimum around 90 K (that's where other papers report pores to be closed). Then size increasing with annealing T (trend very similar between samples). Can be fitted up to 120 K, but fits difficult for  $T \geq 100 \text{ K}$ .

Onset of pore shape increasingly cylindrical with increasing dep-T. Pores collapsing to platelets on annealing. Rate of collapse seems to increase with dep-T.

Some of the correlations between deposition temperature and changes in  $s$ ,  $R_g$ , and diffuse interface thickness are less clear after re-running Gudrun. We need to discuss to what degree we can interpret those.

### SasView lamellar model + Gaussian



Fit results of the Gaussian peak (scale factor  $\mathcal{S}$ , mean ice island width  $\frac{2\pi}{Q_0}$ , and size ice distribution  $\frac{B}{Q_0}$ ) scatter a lot and are probably not very reliable, although the Gaussian peak improves the fit w.r.t. lamellae alone.

## Discussion

### Simplified Ice & Pore Model

SasView assumes randomly oriented lamellae. To make it easier to visualise the ice structure, assume the following:

Sample is formed by infinitely long blocks of ice with thin gaps (valleys) between them. These are the lamellar pores.

### Parameters

To describe ice model			
ice block width $b$	pore width $p$	real sample height $h$	sample length $l$ (infinite)
from SasView	from Porod/DI analysis	from GudrunN settings	
porosity $\mathcal{P}$	specific surface area SSA	effective sample height $H$ (if sample was compact)	

### Equations

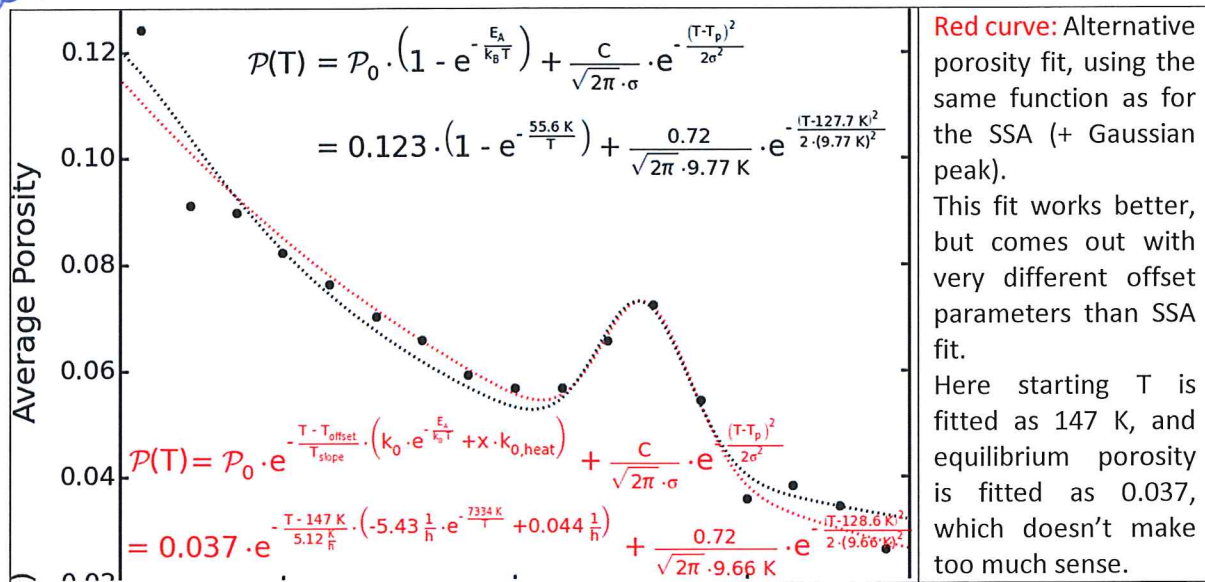
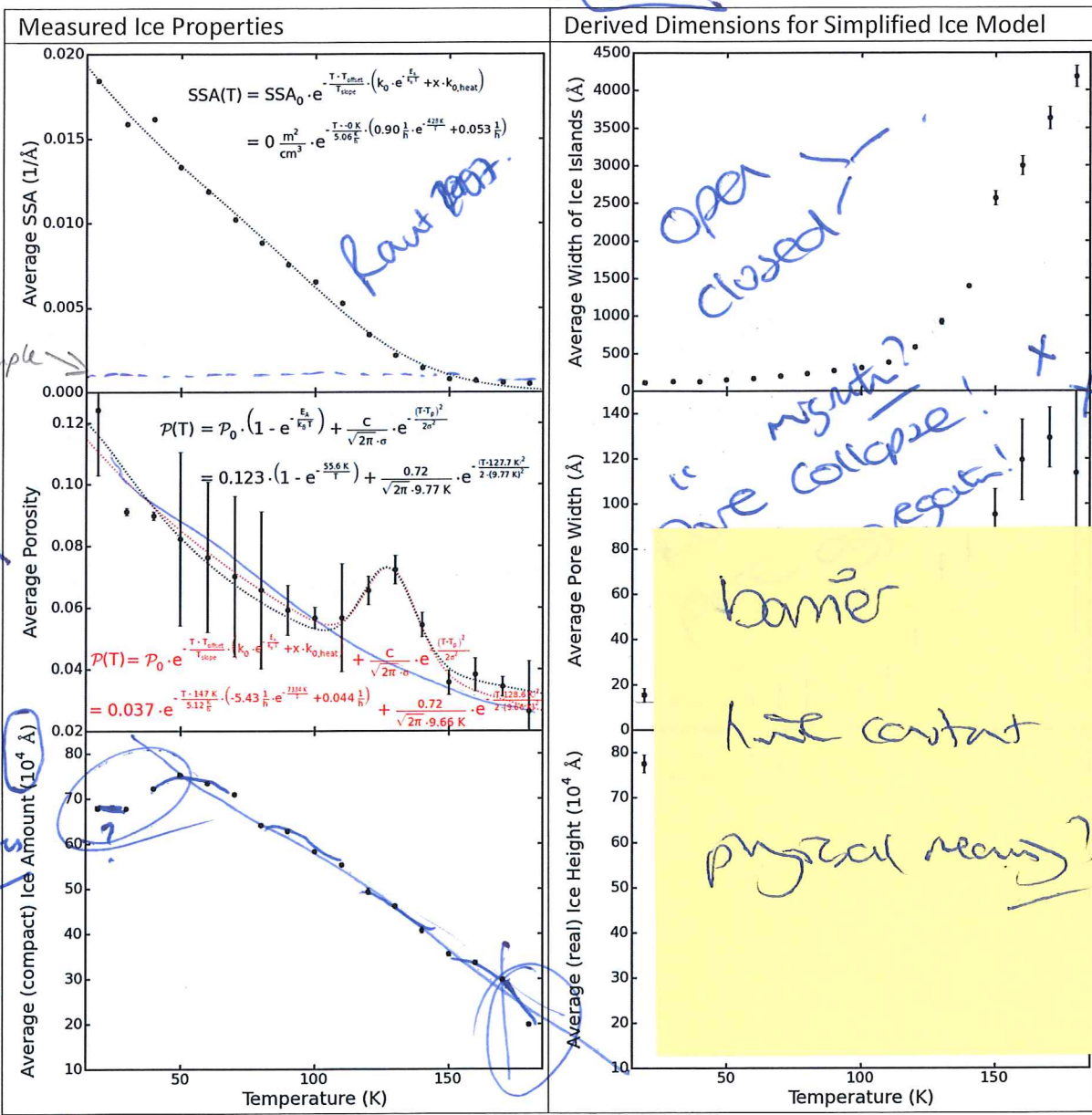
	Individual ice block	Whole Sample (N ice blocks)
Volume	$V_b = b \cdot l \cdot h$	$V_s = N \cdot blh = N \cdot (p + b) \cdot H \cdot l$
Surface	$S_b = 2lh + 2bh + 2bl$	$S_s = N \cdot (2lh + 2bh + 2bl)$
Specific Surface Area		$SSA = \frac{S_s}{V_s} = \frac{2}{b} + \frac{2}{h} + \frac{2}{l} \approx \frac{2}{b} + \frac{2}{h}$ (for infinite $l$ )
Pore Volume	$V_p = p \cdot l \cdot h$	$V_p = N \cdot plh$
Porosity		$\mathcal{P} = \frac{V_p}{V_p + V_s} = \frac{p}{p + b}$
Real Sample Height		$h = H \cdot \frac{p + b}{b} = \frac{H}{1 - \mathcal{P}}$
Ice Block Width		$b = \frac{2}{SSA - \frac{2}{h}} = \frac{2h}{SSA \cdot h - 2}$ (for infinite $l$ )
Pore Width		$p = \frac{\mathcal{P}}{1 - \mathcal{P}} \cdot b$

### Results

SSA and porosity have been averaged across samples. The deposited ice amounts varied between samples, therefore the effective sample height  $H$  has been normalised to the average sample height at an intermediate temperature before averaging across samples. (Not all temperature points are covered at all samples, which would introduce systematic errors without normalisation.)

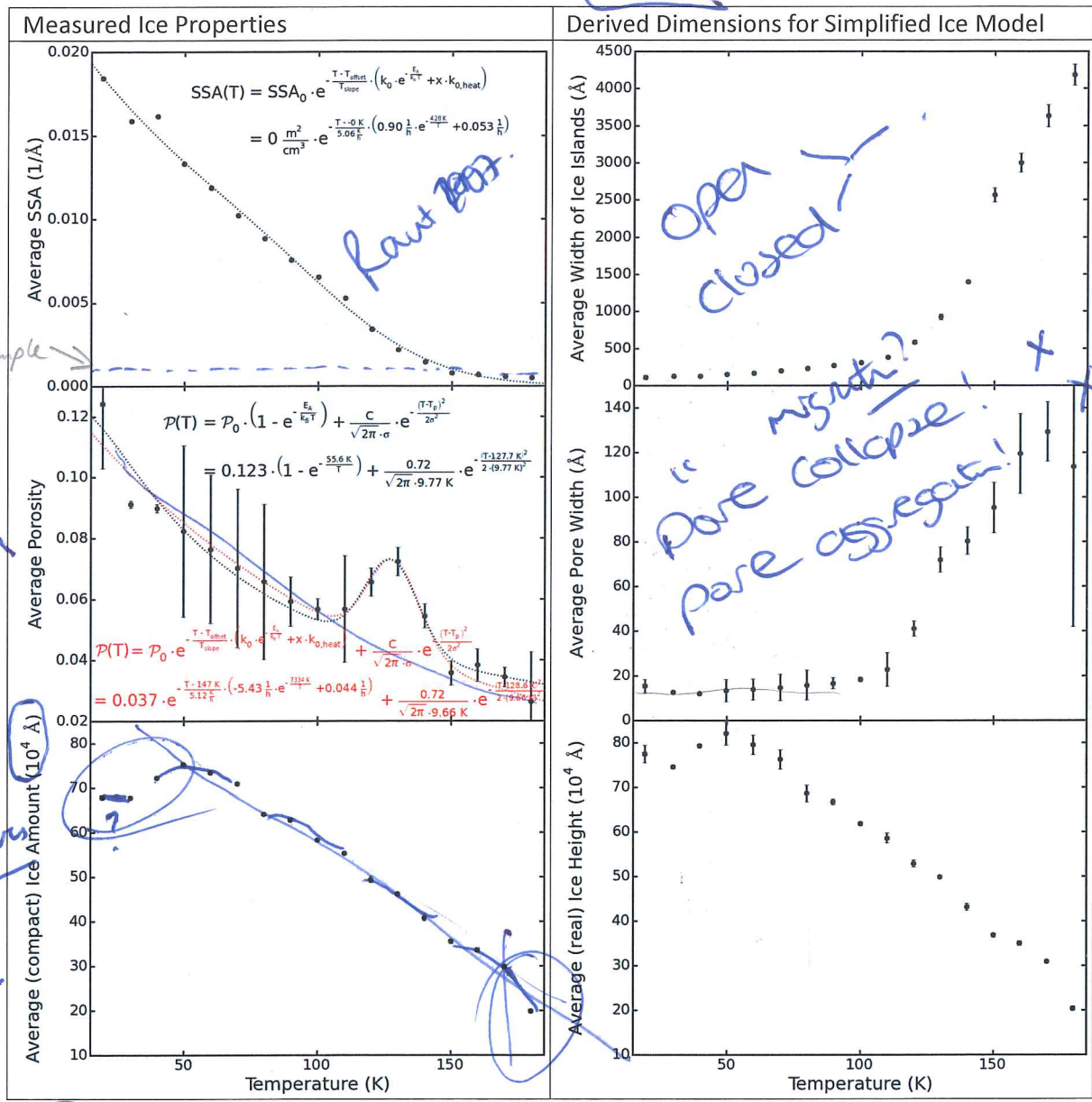
100

20/09/2017

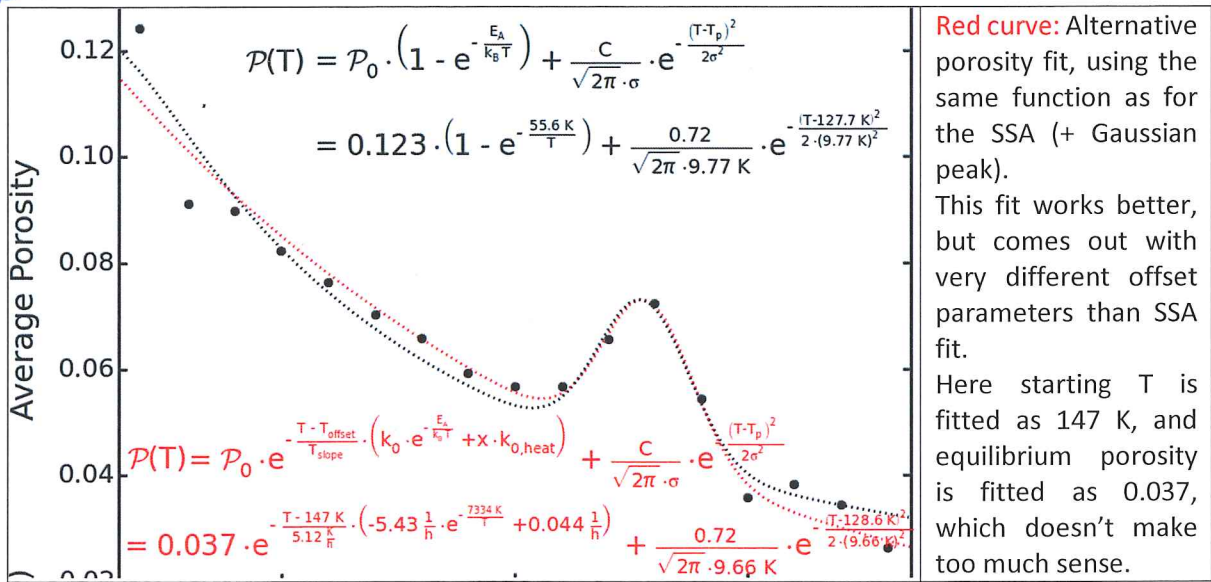


100

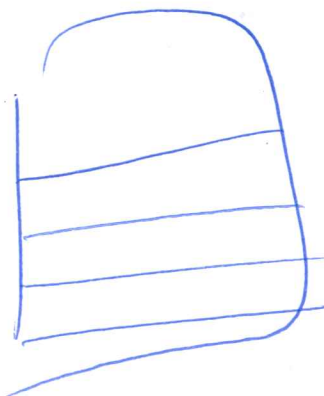
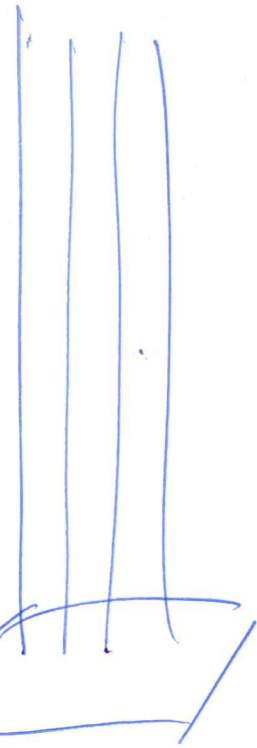
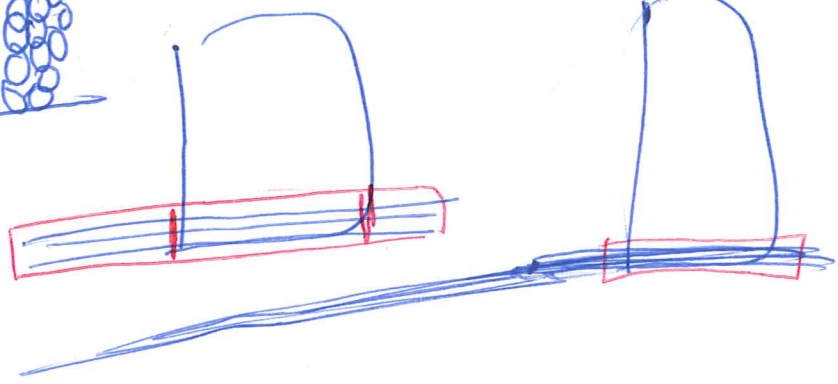
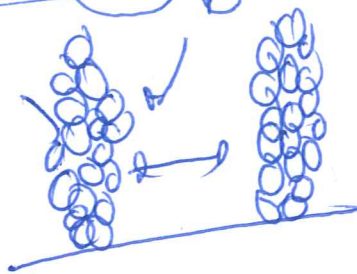
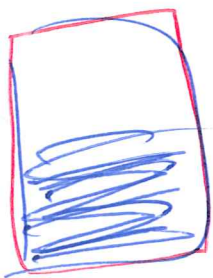
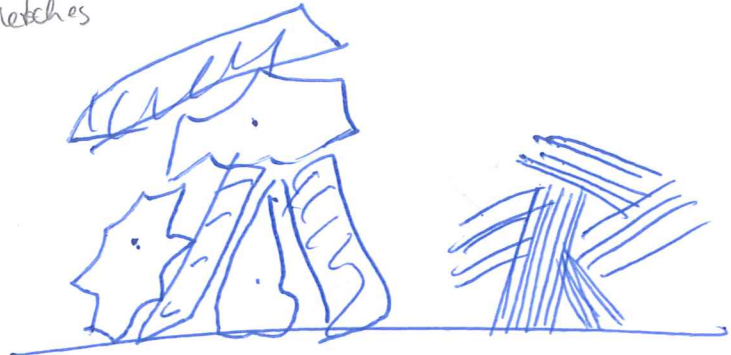
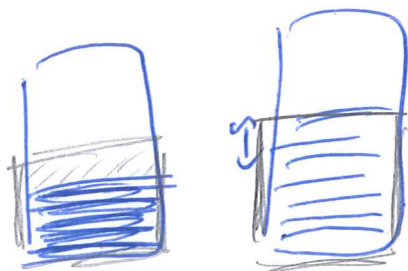
20/09/2017



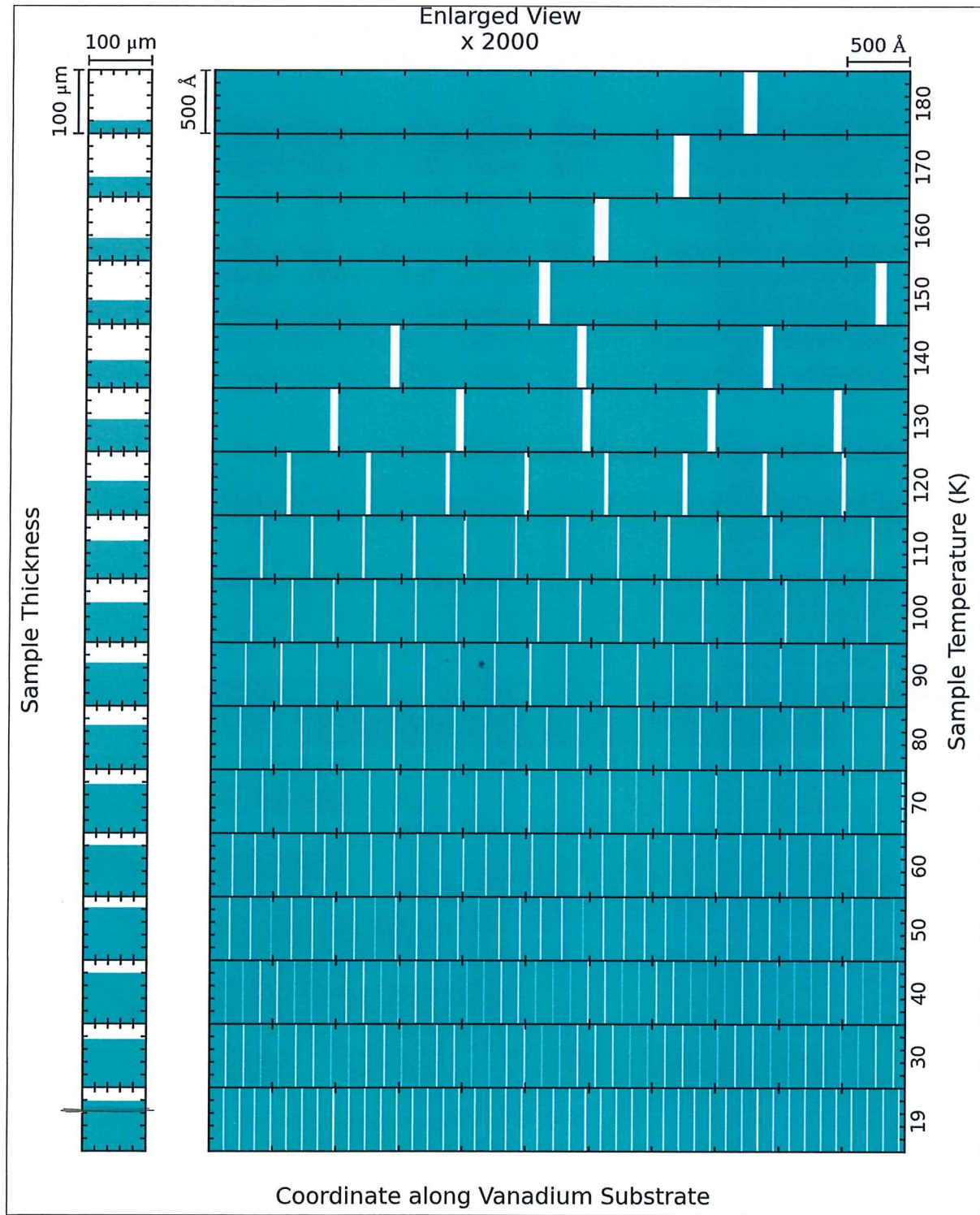
6000000



Jacob







#### *Mechanism for Pore Loss*

Changes in the ice structure will be mainly driven by desorption and re-adsorption. At the lowest temperature (20 K), the pore width is  $\approx 15 \text{ \AA}$ , the sample thickness is  $\approx 7.5 \times 10^5 \text{ \AA}$ , i.e.  $5 \times 10^4$  times the pore width. Although the system is constantly pumped, this will make it very unlikely for any desorbed molecule to escape the ice sample before being re-adsorbed at another place.

Initial variations in the width of the ice blocks, may lead to differences in the potential energy and thereby influence the probability of adsorption in different sites. This could allow larger ice blocks to

grow at the expense of smaller ones, eventually increasing the average width of the blocks as well as that of the pores. (Similar to the way old mining tunnels move towards the surface, by repeated ceiling collapses.)

As the results show, the width of the blocks is growing faster than the width of the pores. Thereby the sample is losing porosity and the real sample height is decreasing faster than the effective sample height (which is only changed by deposition or desorption of material).

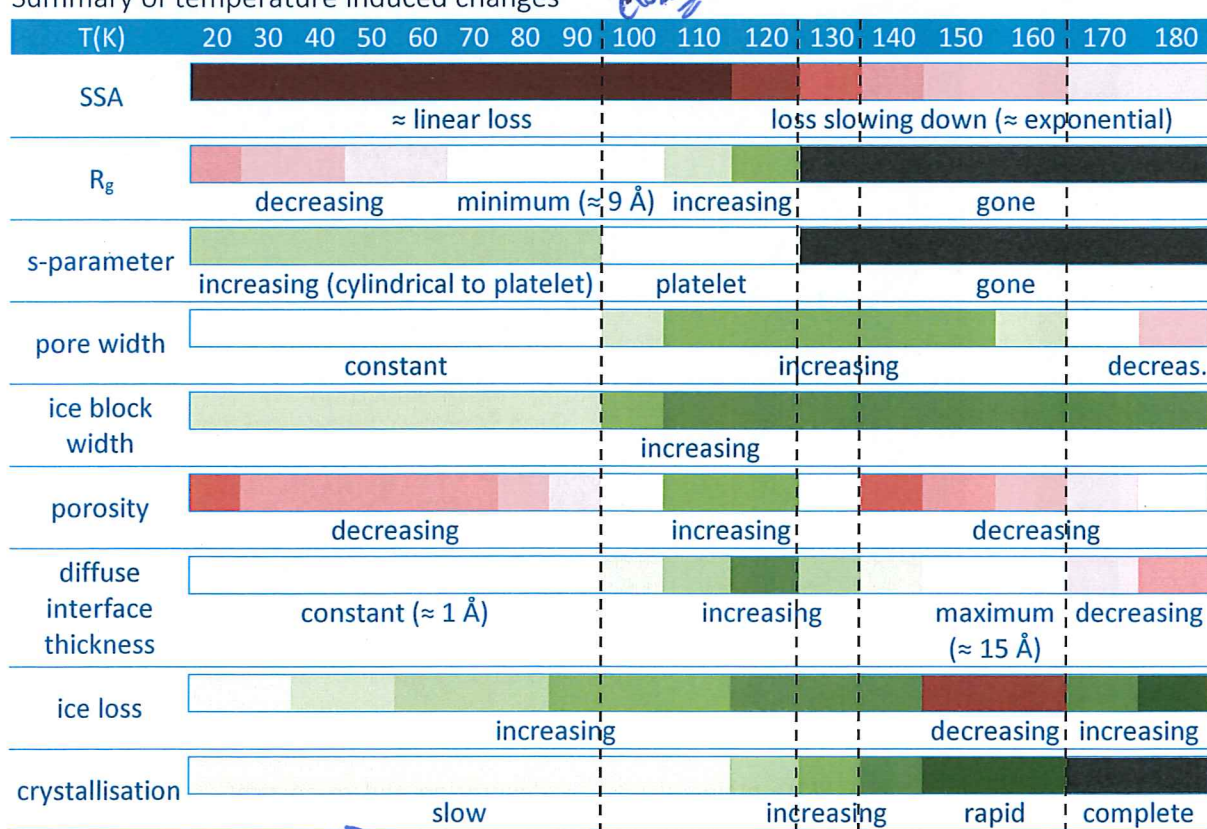
The re-adsorption at low temperatures will be hit-and-stick, as during deposition, therefore not changing the ice phase or average surface morphology. Towards higher temperatures, the molecule gain mobility, first allowing the formation of a thick diffuse interface (molecular re-orientation to increase their coordination number, this is where loss of dangling bonds is seen above  $\approx 100$  K). At  $\approx 150$  K crystallisation happens and thickness of diffuse interface decreases again. (Not sure why, need to discuss this.)

Towards higher T, diffusion might add to loss of SSA & porosity.

Interesting: formation of diffuse interface seems to temporarily increase porosity (see peak in porosity fit). (Not sure why, need to discuss this.)

Need to discuss, why diffuse interface thickness increases to initial pore width at max. Pore width at 100 K has already increased a bit ( $\approx 20$  Å), pore width at DI maximum ( $\approx 150$  K) is  $\approx 95$  Å.

Summary of temperature induced changes



SSA loss changes when micropores are gone. Diffuse Interface thickness starts to increase in final stages of micropore change. Crystallisation becomes significant when diffuse interface starts to increase. When crystallisation is complete, diffuse interface decreases again.

There seem to be two types of molecular mobility:

1. (activation energy  $\approx 340 - 406$  K): restructuring of pores and loss of SSA  $\rightarrow$  dominant at low T
2. (activation energy  $\approx 4000$  K (look up good reference)): restructuring of surface (more to diffuse to increase molecular coordination) and crystallisation  $\rightarrow$  dominant at high T

Sadtchenko split this up in two stages: first rotation to increase surface coordination from 2 to 3, then diffusion to increase surface coordination from 3 to 4

I'm not sure what to make of the rather low activation energy for the SSA change. I would have expected this to be of the same order as breaking at least one hydrogen bond (i.e.  $\approx 2500$  K).

Cartoon and point to be made about Ic...clear comment about 14- > range 15o specifically..Ic forms crystalline grains not a thin film...

Can we compare to TPD probe data and SSA values? Does probe size affect the result?

Why doesn't it matter for SSA whether we grew the ice or warmed it?

What things in lit can we compare to – e.g. height loss in Bossa? SSA in probes TPD?

Is SSA changing due to porosity or is changing just because the ice losing surface area? Smoothing of external surface? From SSA can't see pASW to cASW transition... might be an issue of pores open or closed to vacuum...

## Conclusions

### Porosity

How does growth T affect pore sizes & shapes?

Guinier-Porod	SasView
<p><i>Initial <math>R_g</math></i> increases from <math>\approx 8</math> Å at 30 K to <math>\approx 15</math> Å at 80 K  <math>\Rightarrow</math> Larger pores</p> <p><i>Initial s-parameter</i> decreases from <math>\approx 1.5</math> at 30 K to <math>\approx 1.1</math> at 80 K  <math>\Rightarrow</math> Pores more cylindrical (fits too unreliable for higher T)</p>	<p><i>Initial pore width</i> increases from <math>\approx 15</math> Å at 30 K to <math>\approx 20</math> Å at 80 K  <math>\Rightarrow</math> Larger pores</p> <p><i>Shape model</i> lamellae fit best at all temperatures, but 100-130 K data shows higher deviations</p>

How do pore sizes & shapes change with annealing T? How is pore collapse affected by growth T?

Guinier-Porod	SasView
<p><math>R_g</math> values first decrease, go through minimum (around 100 K), and become more similar between samples, then increase: <math>\approx 12</math> Å at 120 K</p> <p><i>s-parameter</i> Approximately linear increase to 2 (lamellae), transition to lamellae faster for higher deposition T (model not suitable above 120 K)</p>	<p><i>Initial pore width</i> more or less constant below 100 K (maybe small dip around 30 – 40 K), then rapid increase (<math>\approx 70</math> Å at 120 K)</p> <p><i>Shape model</i> lamellae fit best at all temperatures, but 100-130 K data shows higher deviations</p>

Are the pores open (i.e. interconnected) or closed?

I don't think we can tell that from our data.

What is the mechanism behind pore loss with increasing T (collapse, clustering, ...)?

Simplified model suggests that pore clustering combined with pore propagation is the mechanism behind the pore loss. While larger ice blocks grow at the expense of small ones, the pores are shifted, initially changing very little in size. This is similar to the way old mining caves move upwards by repeated ceiling collapses.

As molecular mobility increases with increasing temperature (above 100 K), the pores start to grow dramatically in size, transforming to macropores.

Add something about diffuse interface.

## SSA

How does SSA change with temperature & time?

The rate of isothermal SSA change follows an Arrhenius behaviour. For our samples, which were annealed with an average heating ramp of 10 K per hour, the change is best described by assuming the same Arrhenius behaviour but applied to a system which only partially requires activation energy. Part of the system can be treated as excited state, undergoing the change without thermal energy input (as the energy is put in via the heater).

Is SSA loss directly linked to pore loss?

Below 100 K the ratio of porosity to SSA is approximately constant. Then it starts to increase, as porosity is increasing when the diffuse layer becomes thicker, while loss of SSA continues. The plot (not shown) of this ratio in fact looks very similar to the plot of pore width vs T, because for small porosities and thick samples:  $b \approx \frac{2}{SSA}$  and  $\approx \mathcal{P}b \approx \frac{2\mathcal{P}}{SSA}$ .

In other words, almost complete loss of SSA at high temperatures does not guarantee a non-porous ice. Macroporosity remains up to 180 K, but large ice lumps separated by macropores contribute very little to the sample's total surface area.

## Ice Phase

Are there clear phase transitions between different amorphous forms of ice?

No

Are changes in SSA or pores linked to ice phase changes?

SSA loss slows down around crystallisation, but this can be described by continuous function and does not require a phase transition to be modelled into the SSA change.

Porosity is clearly linked to the formation of the thick diffuse interface, which partially overlaps with the Glass Transition of ASW, but sets in earlier (100 K vs 120-130 K). Porosity peaks around the GT-Temp and then decreases. The width of the Gaussian peak used in the description of porosity is such, that the peak significant contribution of the peak to the curve sets in at 100 K and ends at 150 K (crystallisation).

## Uncertainties for ice parameters (height, pore width, ice block width)

$$\text{height } h = \frac{H}{1-\beta}$$

$$\Delta h = \sqrt{\left(\frac{\Delta H}{1-\beta}\right)^2 + \left(\frac{H \Delta \beta}{(1-\beta)^2}\right)^2}$$

$$= h \cdot \sqrt{\left(\frac{\Delta H}{h}\right)^2 + \left(\frac{\Delta \beta}{1-\beta}\right)^2}$$

H is derived from the initial GudrunN settings (thickness & tweak factor)

variation of the GudrunN processing leads on average to a relative uncertainty of  $4.4 \cdot 10^{-3} = 0.44\%$

I have included those into the uncertainties of the H results averaged across samples

$$\text{ice block width: } b = \frac{2}{SSA - \frac{2}{h}}$$

$$\Delta b = \sqrt{\left(\frac{2 \Delta SSA}{(SSA - \frac{2}{h})^2}\right)^2 + \left(\frac{2 \Delta \beta \cdot \frac{2}{h^2}}{(SSA - \frac{2}{h})^2}\right)^2} = b \cdot \sqrt{\left(\frac{\Delta SSA}{SSA - \frac{2}{h}}\right)^2 + \left(\frac{\Delta h \cdot 2}{(SSA - \frac{2}{h}) \cdot h^2}\right)^2}$$

$$= b \cdot \sqrt{\left(\frac{\Delta SSA}{SSA - \frac{2}{h}}\right)^2 + \left(\frac{2 \Delta h}{h^2 SSA - 2h}\right)^2}$$

$$\text{pore width: } p = \frac{\rho}{1-\beta} \cdot b$$

$$\Delta p = \sqrt{\left(\Delta b \cdot \frac{\rho}{1-\beta}\right)^2 + \left(b \cdot \Delta \beta \cdot \frac{(1-\beta) - \beta \cdot (-1)}{(1-\beta)^2}\right)^2} = p \cdot \sqrt{\left(\frac{\Delta b}{b}\right)^2 + \left(\frac{\Delta \beta}{\beta} \cdot \frac{1-\beta+\beta}{1-\beta}\right)^2}$$

$$= p \cdot \sqrt{\left(\frac{\Delta b}{b}\right)^2 + \left(\frac{\Delta \beta}{\beta(1-\beta)}\right)^2}$$

### To Do:

Activation energies for SSA change: look up rotational level spacing from spectroscopy to get idea of low-midi energy rotation of 1-coordinated molecule would require

Porosity Fit: - try fits without 20 K data point.

- does change of reaction order help to get more useful fit parameters out of double exponential (based on heating ramp)?

Check Wendy Brown & Francois Dulieu Papers for plots of TPD vs different axes

21.09.2017

Burke &amp; Brown 2010 (review):

adsorbate coverage  $\theta$ , TPD trace  $I(T)$ 

$$I(T) \propto v_m^\alpha \theta^m e^{-\frac{E_{des}}{RT}} \Rightarrow \ln(I(T)) \propto m \ln(\theta) + \ln(v_m) - \frac{E_{des}}{RT}$$

$\Rightarrow$  plot  $\ln I(84K)$  against  $\ln \theta|_{84K}$  to obtain straight line with slope

Problem:  $I(T) \propto \frac{d\theta}{dt}$ , so I would have to plot

$\ln\left(\frac{dP}{dt}\right)$  against  $\ln P$  at constant  $T$  for different porosities  $P$   
(analogous for SSA)

At a given  $T$ , we always have only one data point  $(P, T)$  and  
we have no good data for the rate of change  $\frac{dP}{dt}|_T$ .

Different approach: Use fit results from SSA fit for  $P$  function  
and modify only  $P_0$ .  $\Rightarrow$  very good description of the  $P$  trend,  
but offset by  $\approx 0.025$ . What if  $P_{eq}$  (equilibrium at high  $T$ )  
is not 0 (as for SSA)?

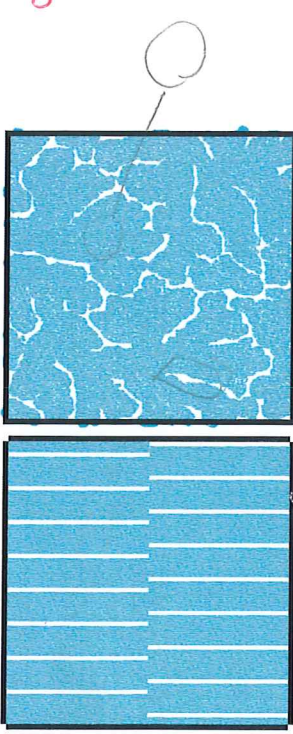
$$\begin{aligned} P(t, T) &= P_0 + (1 - e^{-\frac{t-t_0}{\tau(T)}}) \cdot (P_{eq} - P_0) \\ &= P_0 \cdot e^{-\frac{t-t_0}{\tau(T)}} + P_{eq} \cdot (1 - e^{-\frac{t-t_0}{\tau(T)}}) \\ &= (P_0 - P_{eq}) \cdot e^{-\frac{t-t_0}{\tau(T)}} + P_{eq} \end{aligned}$$

After inserting heating ramp, this yields:

$$P(T) = (P_0 - P_{eq}) \cdot e^{-\frac{T-t_0}{\alpha} \cdot (k_0 e^{-\frac{E_A}{T}} + k_{heat})} + P_{eq}$$

Meeting with Helen - discuss schematic for ASW paper

28.09.2017



110 Å  
15 Å  
1000 Å

Sketch indicating how much porosity we have (just for my own reference, not to be part of the final sketch)

